1-1-2012

The Role of Notch Signaling in the Pathogenesis of Acute Promyelocytic Leukemia

Nicole Grieselhuber
Washington University in St. Louis

WASHINGTON UNIVERSITY IN ST. LOUIS

Division of Biology and Biomedical Sciences

Immunology

Dissertation Examination Committee:
Timothy Ley, Chair
Daniel Link
Jeffrey Milbrandt
Barry Sleckman
Michael Tomasson
Matthew Walter

The Role of Notch Signaling in the Pathogenesis of Acute Promyelocytic Leukemia

by

Nicole Renée Grieselhuber

A dissertation presented to the
Graduate School of Arts and Sciences
of Washington University in
partial fulfillment of the
requirements for the degree
of Doctor of Philosophy

May 2012

Saint Louis, Missouri

ABSTRACT OF THE DISSERTATION

The Role of Notch Signaling in the Pathogenesis of Acute Promyelocytic Leukemia

by

Nicole Renée Grieselhuber

Doctor of Philosophy in Biology and Biomedical Sciences
(Immunology)

Washington University in St. Louis, 2012

Professor Timothy Ley, Chairperson

The t(15;17) translocation is found in nearly 98% of acute promyelocytic leukemia (APL, FAB subtype M3) cases and results in the fusion of the promyelocytic leukemia (PML) gene with the retinoic acid receptor alpha (RARA) gene. The fusion product, PML-RARA, encodes a functionally altered transcription factor that is the initiating event in APL. To better understand the transcriptional changes associated with APL pathogenesis, we compared the gene expression profiles of APL samples to those of other acute myeloid leukemia FAB subtypes and of enriched normal human promyelocytes. We identified a signature of genes that are specifically dysregulated in APL relative to other AML subtypes and normal promyelocytes. We found that most dysregulated genes are not direct targets of PML-RARA, but are rather distal events in pathogenesis. In contrast, the APL signature was enriched in leukemia cells derived from a mouse model of APL, demonstrating that common leukemogenic pathways exist in mouse and human cells.

We then observed that human APL overexpresses the Notch ligand Jagged-1 (*JAG1*) compared to other AML and normal promyelocytes. Unlike many APL signature

genes, overexpression of *JAG1* is also found in human APL cell lines and in murine APL. We hypothesized that Notch signaling, which has known roles in proliferation and survival, may be important in leukemogenesis. Inhibition of Notch signaling by pharmacological and genetic approaches resulted in a loss of serial replating by marrow cells from young non-leukemic mCG-PML-RARA animals. In contrast, colony formation by wildtype marrow is unaffected by Notch inhibition, suggesting that PML-RARA expressing cells are uniquely dependent upon Notch signaling for increased self renewal. Growth of primary murine APL cells in vitro was variably reduced by pharmacological inhibition of Notch signaling (6/9 samples), demonstrating that while Notch signaling is required for early events in leukemogenesis, in some cases it is dispensible for the fully transformed tumor. However, inhibition of Notch signaling in four tumor samples tested did not result in reduced tumor burdens *in vivo*. In conclusion, we have demonstrated a previously unappreciated role for the Notch signaling pathway in the development of acute promyelocytic leukemia.

ACKNOWLEDGEMENTS

During the past 5 years, I have had the privilege of undertaking graduate studies at the Washington University School of Medicine. I have received much help along the way, and hope to convey my appreciation in these few pages. My first thanks go to my advisor, Dr. Timothy Ley. As a mentor, Dr. Ley has created a collegial and intellectually stimulating environment in which science is done with rigor, and ideas, information, and expertise are freely shared amongst colleagues. I am especially appreciative of the opportunity to forge a new path of research within the Ley laboratory; it was not always easy but I have learned much from it. The bar has been set very high indeed in looking for post-doctoral research opportunities and perhaps in establishing my own research laboratory someday. I am also grateful to have had a committee composed of talented and wise scientists to guide me. Dr. Daniel Link deserves special recognition for agreeing to serve as the chair of my committee. Like Dr. Ley, he is a wonderful role model of a physician scientist, and I have sincerely enjoyed our discussions. Drs. Jeffry Milbrandt, Barry Sleckman, Michael Tomasson, and Matthew Walter have also provided excellent advice during my journey. I additionally want to thank Dr. James Hsieh, who was a valued member of my committee until his recent departure from the university; I wish him all the best when he begins his new appointment at the Memorial Sloan-Kettering Cancer Center.

The Ley laboratory is composed of many talented individuals with whom I have had the pleasure of working during years in graduate school. In particular, I thank John Welch, Lukas Wartman and Sheng Cai for helpful discussions and Jackie Payton for her invaluable expertise in data analysis. Additional thanks go to Mieke Hoock, Dan George

and Nick Protopsaltis for their excellent animal husbandry assistance and Erin Wehmeyer for technical assistance. The core facilities of the Siteman Cancer Center, including the High Speed Cell Sorter Core, Bioinformatics Core, Laboratory of Clinical Genomics, Molecular Imaging Core and Tissue Procurement Core, which were instrumental in carrying out my research, and I thank their directors and staff for their skill and dedication. At various times during my graduate school career, the National Institutes of Health, the Barnes-Jewish Hospital Foundation and the Medical Scientist Training Program provided financial support for either my stipend or research endeavors.

I also thank everyone in the section of Stem Cell Biology for making the sixth floor of the Southwest Tower a warm and friendly place in which to work. I will especially miss Adam Greenbaum, Kilannin Krysiak, Ghada Kunter and Maria Trissal, and have fond memories of several people whose graduations preceded mine, including Jennifer Cain, Kyle Eash, David Grenda and Julie O'Neal. I appreciate the Washington University Medical Scientist Training Program for skillfully handling all the details inherent in pursuing two degrees, leaving students free to concentrate on their studies.

Finally, I must acknowledge a group of people who are, and will remain, anonymous to me, but without whom none of my research would be possible: the AML patients of Washington University who agreed to participate in our tumor banking program. On what was surely one of the worst days of their lives, these patients and their families decided to contribute to science, and for that I offer my sincerest thanks and gratitude.

On a personal level, I have made many friends and happy memories during my years at Washington University. My classmates are some of the brightest, most hard-

working and kindest individuals I have met, and I look forward to seeing what paths we all take in the coming years. And although it is perhaps not traditional, I thank my 4-legged friends Missy, Pixie, Belle, Nora and Heidi, for providing the quiet equine and feline companionship that kept me sane and balanced. Outside of my work in the laboratory, nothing has taught me more about persistence, flexibility and patience than my feisty little chestnut mare Pixie. I am definitely a better scientist and a better person for being so challenged.

My path through graduate school would have been much more difficult without my family to cheer me on. I thank my sisters, Leslie and Teresa, and my aunt, Doris Emich, for their love, laughter and support over the years, and am sincerely glad they can join me in this momentous occasion. Although age and poor health prevent my grandparents, Otto and Esther Emich, from making the journey to St. Louis to see my thesis defense, I know that they are with me in my heart, and in the lessons they have taught me. I also wish to thank them for having the foresight to buy me savings bonds for my birthdays when I was young and probably would have rather received another toy. All of my various proposals, grants, updates, data analyses and presentations over these past 5 years have been crafted on the computer I bought with those “boring” savings bonds!

Finally, my greatest thanks go to my parents, Rene and Caroline, who have been my biggest cheerleaders. I thank my father for introducing me to science with PBS documentaries, for his steadfast belief in me and for his dedicated care of my beloved first horse Missy in her retirement. I thank my mother for her patience and encouragement when I had moments of doubt, for her sensible advice and for teaching

me to cook (despite my initial lack of interest), which became not just a means of survival but a stress relieving hobby. Mom and Dad, I offer you my heartfelt appreciation for your love and support and dedicate this thesis to you.

TABLE OF CONTENTS

LIST OF FIGURES

Chapter 2 - Definition of the APL dysregulome

Chapter 3- Notch signaling has a role in leukemogenesis in a mouse model of acute promyelocytic leukemia (APL).

LIST OF TABLES

Chapter 2 - Definition of the APL dysregulome

Chapter 3- Notch signaling has a role in leukemogenesis in a mouse model of acute promyelocytic leukemia (APL).

"A disease that, starting from an insignificant injury, can attack a person in perfect health, in the full vigor of early maturity, and in some insidious, mysterious way, within a few months, destroy life, is surely a subject important enough to demand our best thought and continued study." – Dr. William Coley, from an address to the New York Academy of Medicine on April 27, 1891

Chapter 1

Introduction

1.1. Acute Myeloid Lekemia and Acute Promyelocytic Leukemia

Acute myeloid leukemia (AML) is a hematopoietic malignancy characterized by a block in the differentiation of progenitor cells and an accumulation of immature cells in the bone marrow and blood (1). Rather than a single disorder, AML represents a collection of related malignancies. The French-American-British (FAB) classification recognizes 8 major subtypes of AML, based on cellular morphology and cytochemical staining (2). Approximately 10,000 new cases of AML are diagnosed in the United States each year (3). However, a substantial minority of patients, approximately 25 percent, carry recurrent chromosomal translocations that result in the fusions of the coding regions of specific genes (4). One such example is the t(15;17) (q21;q22) translocation found in over 98% of acute promyelocytic leukemia (APL, FAB subtype M3) cases (3). The translocation results in the fusion of the promyelocytic leukemia (PML) gene on chromosome 15 with the retinoic acid receptor alpha (RARA) gene on chromosome 17 (5-7). The fusion product, PML-RARA, encodes a functionally altered transcription factor that is the initiating event in APL leukemogenesis. As such, it represents a unique opportunity for modeling the development of leukemia.

1.2. Identification of the t(15;17) translocation and the PML-RARA fusion protein

Hillestad first identified APL as a distinct subtype of AML in 1957, based upon its distinct morphology, the accumulation of promyelocytes, the associated syndrome of disseminated intravascular coagulation (DIC) and a poor clinical course that progressed to lethal disease within a few weeks of presentation (8). Twenty years later, Rowley et al described three APL patients with the t(15;17) in their blasts (9). Subsequent reports

showed that the translocation is present in nearly all APL cases (10, 11). The RARA gene maps to 17q21, close to the breakpoint in the t(15;17) translocation. At the time, it was known that retinoic acid could induce differentiation of APL cells and some leukemic cell lines (12, 13). Based on these observations, several groups investigated the role of the RARA gene in the t(15;17) translocation (14-16) and simultaneously reported in 1991 that RARA was fused to an unknown locus, initially named myl (6, 7, 17). de The et al subsequently renamed the transcript promyelocytic leukemia (PML) and reported the sequences of both the native PML and PML-RARA fusion transcripts (5).

The reported length of the PML-RARA transcript varied in early reports (5, 6, 7, 17, 18). An analysis of the breakpoints in a collection of APL patients demonstrated that while the chromosome 17 breakpoint is always found within intron 2 of the RARA gene, the chromosome 15 breakpoint can occur in at least 3 different locations within the PML gene (19). The most common breakpoint, termed bcr1, occurs in intron 6 of PML, and joins PML exon 6 to RARA exon 3, resulting in the long isoform of PML-RARA. The bcr 3 breakpoint occurs within PML intron 3, creating a short isoform that joins PML exon 3 to RARA exon 3. Bcr2, which occurs within PML exon 6, is relatively rare. Since the breakpoint invariably occurs within RARA intron 2, the bcr1, bcr2 and bcr3 isoforms of PML-RARA all contain the same RARA domains: the N terminal AF-1 domain is lost but the ligand binding domain, DNA binding domain and AF-2 transactivation domains remain intact (20). The PML sequences that are retained in the fusion vary amongst the different breakpoints; however, all contain the RBCC motif (21). The bcr1 isoform additionally retains the NLS present in PML exon 6. The bcr3 PML-RARA isoform lacks the NLS, since it only preserves the first three exons of PML.

Together, bcr 1 and bcr3 account for 95% of APL patients (20). The relative frequencies of bcr1 and bcr3 are known to vary in different ethnic groups (22-24) and in pediatric populations (25). There is some evidence that patients harboring the bcr3 rearrangement have a worse prognosis (26), perhaps because of that isoform's lower affinity for ATRA (27). To date, the majority of studies, including our own, have focused on the bcr1 isoform, so the differences in the functions of the isoforms is not well studied. Additionally, multiple isoforms of PML-RARA can occur within the same cell, due to alternative splicing of both the PML and RARA portion of the fusion gene (19). Since the bcr1 cDNA is sufficient for leukemogenesis in multiple mouse models (28-30), the functional role of alternatively spliced isoforms is unclear.

1.3. Treatment of APL with all trans-retinoic acid (ATRA)

Prior to the development of targeted therapies, the prognosis of APL was among the worst of all AML subtypes, with a 5 year survival of only 25-30 percent (31). Death occurred in up to 15 percent of patients undergoing induction chemotherapy, most often due to DIC, and those who achieved a complete remission invariably relapsed within 2 years (32). However, in the mid 1980s, based on the observation that retinoic acid could induce differentiation of APL cells *in vitro*, Huang et al performed a small trial of all trans-retinoic acid (ATRA) alone or in combination with traditional chemotherapy in 24 APL patients (33). The success of this study and subsequent trials (34-36) led to the adoption of ATRA therapy in combination with anthracycline based chemotherapy as the standard treatment for APL. Currently, the 5-year disease free survival of APL patients treated with combination chemotherapy and ATRA is approximately 75 percent (37).

This development was all the more remarkable, in that ATRA was investigated before the realization that RARA itself is involved in APL-associated translocations. Once the t(15;17) breakpoints were characterized, it was apparent that ATRA targets the very molecule that is mutated in nearly all APL cases.

Despite the success of ATRA therapy of APL, many challenges remain in the treatment of APL patients. APL patients have a propensity to develop coagulation and bleeding disorders, and are at particular risk for early death during the initiation of chemotherapy due to DIC (38). Patients commonly develop "ATRA syndrome," characterized by leukocyte activation, fever, respiratory difficulties, pleural or pericardial effusions and renal failure (38). ATRA syndrome can be treated successfully with corticosteroids, but nevertheless is a potentially life threatening complication. In addition, up to 30 percent of APL patients will eventually experience a relapse of their leukemia despite ATRA and chemotherapy treatment (37). Relapsed APL is frequently resistant to ATRA (39). Relapsed or refractory APL may be treated with chemotherapy in combination with arsenic trioxide, histone deacetylase (HDAC) inhibitors, hematopoeitic stem cell transplantation and various experimental drugs currently in clinical trials (31, 35, 37). Despite these advances, approximately 40-50 percent of patients will die within 2 years of relapse (40). These facts underscore the need for a better understanding of PML-RARA mediated leukemogenesis.

1.4. Mouse models of APL

Mouse models have been critical in establishing that PML-RARA is the initiating event in APL, as well as in demonstrating the importance of targeting expression to the

correct cellular compartment and the correct developmental stage to initiate disease. Several early attempts to create a transgenic mouse model of APL failed because transgene expression was directed to the incorrect developmental stage. When PML-RARA was expressed under the control of the CD11b promoter, which is activated at the myelocyte stage (a later stage than promyelocytes), no mice were observed to develop leukemia despite robust expression of the transgene (41). Similarly, when PML-RARA was directed to early myeloid progenitors under the control of the c-fes promoter, no leukemia developed (42). Attempts were made to create a transgenic line with a β-actin promoter driving PML-RARA, but no viable animals were born, suggesting that widespread PML-RARA expression is incompatible with life (43).

The Ley laboratory created the first successful transgenic APL mouse model. PML-RARA bcr-1 was expressed under the control of human cathepsin G regulatory sequences previously shown to target transgene expression to the promyelocyte compartment (29). All of these hCG-PR mice exhibited myeloproliferation without a block in differentiation. As the mice aged, 15 percent of the mice developed leukemia characterized by promyelocyte expansion, anemia, thrombocytopenia and splenomegaly, with an average latency of approximately 220 days. A second group later created a transgenic line with the same PML-RARA isoform expressed under the control of the same hCG region and obtained similar results (43). Around the same time, a third group published a report describing the MRP8-PML-RARA transgenic mouse, in which PML-RARA was expressed under the control of a human MRP8 promoter fragment, which is activated at the promyelocyte stage, with persistent expression to mature neutrophils (28). These mice also developed leukemia, but a complete analysis was hampered leaky

expression in keratinocytes, leading to the development of fatal PML-RARA induced skin lesions. Bone marrow transplants into lethally irradiated syngeneic hosts allowed further study of this murine APL.

The penetrance of APL development could be increased in transgenic PML-RARA mice by coexpressing additional oncogenes, including bcr-3 RARA-PML (44), an activated FLT3 allele (45), Bcl2 (46), or activated K-ras (47), and also by crossing PML-RARA transgenic mice with PML knockout mice (48) or PU.1 haploinsufficient animals (49). However, a high penetrance model remained elusive until our laboratory developed a mouse in which the PML-RARA cDNA is knocked into the endogenous murine cathepsin G locus ($mCG^{+/PR}$ mice) (30). It had been noted that transgene expression in hCG-PR mice was unexpectedly low, and it was initially hypothesized that the endogenous CG promoter might lead to increased expression and therefore increased penetrance. While the mCG-PR mice did develop APL with a penetrance of greater than 90%, PML-RARA expression was unexpectedly nearly 50 fold lower than in the hCG-PR mice. These observations provided evidence for the "gain-of-function" hypothesis of PML-RARA function, discussed in more detail below. In addition, because virtually all mice are "preleukemic," the high penetrance model allowed for the performance of valuable studies of hematopoietic perterbations in preleukemic mice (58). These studies would be impossible in strains in which a substantial proportion of the mice never develop overt leukemia. A study published by our lab investigated the gene expression profiles of APL tumors derived from mCG-PR mice and of cells from wildtype and preleukemic mice undergoing *in vitro* myeloid differentiation (50). Many of the genes that were dysregulated in the APL tumors were expressed normally in preleukemic

myeloid cells, indicating that perhaps the vast majority of dysregulated genes represent late events in pathogenesis. In addition, leukemic cells isolated from APL mice have recurrant chromosomal abnormalities (51). Collectively, these results suggest that additional 'progression hits' are required for the development of frank leukemia from the preleukemic state.

Recently, the Ley lab has developed a conditional PML-RARA knockin model. A PML-RARA cDNA preceeded by a Lox-Stop-Lox cassette was knocked into the 5'UTR of the murine PML locus (52). PML-RARA is only expressed upon Cre mediated excision of the Lox-Stop-Lox. Importantly, PML-RARA expression is controlled by the native PML promoter, allowing for dose appropriate expression. In addition, PML-RARA expression is somatically acquired in only a few cells, which more accurately models the human disease than mice in which PML-RARA is expressed in all myeloid cells for the entire lifespan of the animal. Unexpectedly, leukemia development in the conditional knockin mice is an uncommon event. When PML-PR^{flox} mice are crossed with LysM-Cre mice, only rare leukemias develop. In a second experiment, PML-PR^{flox} mice were bred to ERT2-Cre mice expressing a tamoxifen inducible Cre. Tamoxifen treatment results an expansion of the floxed (PML-RARA expressing) cells, but no overt leukemias. These results suggest that many cooperating downstream events are necessary for leukemogenesis, and that PML-RARA expression by itself is insufficient for development of disease.

1.5. Cellular effects of PML-RARA expression

In all mouse models of APL, leukemogenesis proceeds slowly, requiring months and secondary events. In hCG-PR transgenic and mCG-PR knockin mice, young animals do not have overt signs of disease and have normal peripheral blood counts (29, 30). However, there are subtle alterations in hematopoeisis that indicate that expression of PML-RARA by itself alters hematopoeisis. In hCG-PR mice, there is a small but significant increase in the percentage of myeloid cells in the peripheral blood, and an increase in promyelocytes and myelocytes in the marrow (29). Myeloid colony forming units in the spleen and bone marrow are increased as well compared to wildtype animals (49). In addition, an abnormal Gr-1^+, c-kit^+ population is found in the spleens of transgenic animals. Similarly, preleukemic mCG-PR knockin mice have normal peripheral blood counts, but Gr-1^+, $CD34^+$ cells are significantly increased in the spleen (30). When cells from the marrow of mCG-PR animals are subjected to G-CSF induced in vitro differentiation, they expand more rapidly and have an increased fraction of morphologically immature cells compared to wildtype marrow cultures (53). In addition, mCG-PR marrow has increased colony formation and will serially replate in methylcellulose cultures for up to one month, in contrast to wildtype cells which do not form colonies after the second week in culture (54). When marrow PML-PR^{flox} x ERT2-CRE mice is treated with tamoxifen in vitro, serial replating is similarly observed (52). In competitive repopulation assays with wildtype marrow, expansions of mCG-PR cells were observed not just in the Gr-1^+ myeloid cells as expected, but also in the $B220^+$ and $CD3^+$ lymphoid lineage cells, suggesting that PML-RARA may act at a multipotent progenitor cell, and not at a myeloid committed stage as previously proposed (55). Similarly, after a single tamoxifen treatment, the percentage of floxed (PML-RARA

expressing) cells in the marrow of PML-PR^{flox} x ERT2-Cre mice increases from 5% to over 40%, suggesting clonal expansion is occurring (52). Collectively, these results from multiple mouse models suggest that PML-RARA acts in a multipotent progenitor to increase self renewal and partially block myeloid differentiation. The molecular pathways that are activated or repressed to create these phenomena remain largely unknown, as are the secondary cooperating events responsible for the development of leukemia, but remain an area of active investigation in the Ley laboratory.

1.6. Normal RARA Functions

1.6.1. Protein structure of RARA

RARA is a member of the nuclear receptor superfamily of ligand-dependent transcription factors. While nuclear receptors were originally recognized for their role in steroid hormone signaling, it was later appreciated that other family members respond to fat soluble vitamins, thyroid hormone, lipids, or inflammatory mediators (56). A large sub-family of orphan receptors responds to no known ligand (57). The nuclear receptors share a common protein structure consisting of four major domains. The AF-1 and AF-2 transactivation domains are located at the N and C termini, respectively, while the zinc finger DNA binding domain (DBD) and ligand binding domain (LBD) are located centrally(56). The LBD consists of 11 alpha helices which form a pocket that varies in size and shape to recognize specific ligands (58, 59). In the absence of ligand, the LBD is blocked by helix 12 of the AF-2 domain. In this conformation, helices 3 and 4 bind the corepressors NCOR1 (nuclear corepressor 1) and silencing mediator for retinoid and thyroid hormone receptor (SMRT) (60, 61). NCOR1 and SMRT recruit histone

deacetylases (HDACs), which silence genes by closing chromatin. In the presence of ligand, helix 12 is repositioned so that it no longer covers the LBD pocket, but instead disrupts the interaction of corepressors with helices 3 and 4 (58). At the same time, helices 3,4, and 12 form a new binding motif recognized by coactivators, including p300, histone acetyl transferases (HATs), chromatin remodeling proteins, and RNA polymerases (56).

RARA recognizes both all-trans retinoic acid (ATRA) and 9-cis retinoic acid (62). However, the normal physiologic role of the 9-cis isomer is controversial and ATRA is regarded as the major native ligand. RARA function requires heterodimerization with the promiscuous rexinoid X receptor (RXR) (63, 64). RXR also partners with vitamin D receptors (VDRs), thyroid hormone receptor (TR), peroxisome proliferator activated receptors (PPAR) and various lipid responsive receptors (63). Dimerization with RXR increases DNA binding efficiency, but the consensus site binding specificity is provided by the specific nuclear receptor (65). RAR-RXR heterodimers recognize retinoic acid response elements (RAREs) consisting of direct repeats of the 6 base pair half site (A/G)G(G/T)TCA separated by either 2 or 5 base pairs (62, 66, 67). These sites are termed DR2 and DR 5 sites respectively. RAR-RXR heterodimers can also bind DR1 sites, but evidence suggests that they are unable to activate transcription even in the presence of ligand (62). In general, RXR binds the 5' half site, while RARA recognizes the 3' half site (68, 69, 70). As described above, in the absence of retinoic acid, RARA recruits corepressors, leading to transcriptional repression. Retinoic acid induces the dissociation of the corepressor complex and the formation of a coactivator complex.

RXR is incapable of binding corepressors and only weakly binds coactivators, so the switch from repression to activation of transcription is dependent upon RARA.

1.6.2. RARA and Hematopoeisis

The *in vivo* role of RARA in hematopoeisis remains unclear. RARA is not absolutely required for granulopoiesis, since RARA-/- animals have normal numbers of peripheral neutrophils and Gr-1^{+}Mac-1^{+} cells in the bone marrow (71-74). Hematopoetic cells also express retinoic acid receptor gamma (RARG), yet double knockout RARA-/- x RARG-/- mice have no detectable defects in fetal hematopoeisis (75). The double knockout cells have no ability to respond to retinoids, indicating that retinoic acid signaling is not required for the production of mature neutrophils. However, several lines of experimental evidence support RARA as a modulator of granulopoiesis. First, exogenous retinoic acid enhances the formation of CFU-GM colonies in cultured hematopoietic precursors (76). Secondly, mice fed a vitamin A deficient diet develop an expansion of mature neutrophils that reverses upon ATRA supplementation (77). Similarly, mice treated with a pan-RAR antagonist also exhibit myeloid expansion, but with an increase in immature forms (75). Furthermore, mouse marrow cells that are retrovirally transduced with a dominant negative RARA containing a mutated ligand binding domain cannot terminally differentiate, and are blocked at the promyelocyte stage (78). However, these cells are not fully transformed and cannot induce leukemia when transplanted to a secondary host. It is believed that RARA promotes the terminal differentiation and death of granulocytes, accounting for the myeloid expansion in animals in which retinoic acid signaling is inhibited or deficient (76).

1.7. Normal PML Functions

PML is a ubiquitously expressed RING finger domain protein that characteristically localizes to discrete sub-nuclear protein aggregates variously termed PML oncogenic domains (PODs), also known as nuclear bodies (NBs) (79, 80). When the PML cDNA was identified, de The et al initially noted that the predicted protein sequence contained a proline rich N-terminus and three cysteine rich regions (5). The first cysteine cluster was later shown to reside within a zinc binding domain known as a RING finger motif, while the others are part of two B box domains which can also bind zinc. The B box domains are followed by a coiled-coil domain composed of two alpha helices. Together, the RING domain, B boxes and coiled-coil domain form a RBCC motif, a conserved structure that defines a large family of proteins (21). The PML RBCC motif serves largely to allow homo- and heterodimeric protein-protein interactions, and is critical in establishing sub-cellular localization to PODs (81). While the RBCC motif is present in all PML isoforms, the C terminus of PML varies considerably due to alternative splicing (81). Most isoforms contain a C terminal nuclear localization signal (NLS), but several appear to be cytoplasmic (82). One isoform, designated PML-I, contains C terminal nuclear export signal (NES) in addition to the NLS, suggesting that it may shuttle between the cytoplasm and nucleus (83). Additionally, the C terminal domains can confer isoform-specific protein interactions. For example, the PML-IV isoform can interact with the tumor suppressor p53 (84) and histone deacetylases (HDACs) (85), properties not shared by PML-RARA or other PML isoforms.

PML has known roles in cell growth, apoptosis, tumor suppression, transcriptional activation, and antiviral responses. Much of this knowledge was obtained from studies of PML deficient mice. Despite the ubiquitous expression of PML and its involvement in diverse cellular processes, PML-/- mice are viable and grossly normal in appearance and fertile; however, they are susceptible to fatal *Botryomycosis* infections (86). They do not develop leukemia or any other spontaneous malignancy. PML-/- mice have reduced circulating granulocytes and a decreased ability to terminally differentiate myeloid cells. PML deficient mice were more susceptible to chemical carcinogen-induced skin papillomas and lymphomas. In addition, while overexpression of PML in mouse embryonic fibroblasts (MEFs) (87) can inhibit growth, PML deficient MEFs exhibited increased growth, as did PML negative splenic lymphocytes undergoing concanavalin A activation. When PML-/- mice were crossed with hCG-PR transgenic mice, the incidence of disease increased and latency decreased in a dose dependent fashion (48). These results support the idea that PML functions as a tumor suppressor with growth suppressive properties. PML was found to be required for several apoptotic pathways. Cells from PML deficient mice are resistant to irradiation, Fas, TNF, IFN, and ceramide-induced apoptosis, and the majority of PML -/- mice can survive γ-radiation doses equivalent to the LD50 for wildtype mice (88). However, not all apoptotic pathways are attenuated in PML -/- mice, since complete suppression of apoptosis is generally incompatible with life. PML is therefore best regarded as a modulator of apoptosis. Additionally, PML has been shown to interact with several proteins involved in the DNA damage response, including the checkpoint kinase Chk2 and TopBP1, a protein involved in the repair of double strand DNA breaks (89). PML's tumor

suppressor properties likely are due to a combination of effects on both the DNA damage response and apoptosis.

1.8. DNA Binding Properties of PML-RARA

1.8.1. PML-RARA as a Dominant Negative RARA

After demonstrating that t(15;17) results in the fusion of RARA to the previously unknown myl (PML) locus, de The et al speculated that such a fusion could result in a dominant negative RARA that inhibited the transcription of normal RARA target genes (6). In a follow up study, the same group showed that PML-RARA could repress RA dependent luciferase expression from a reporter vector containing three tandem DR5 sites from the RARβ gene (5). The same result was observed when a reporter construct with an optimized palindromic thyroid hormone response element (TRE) was used. However, these studies were performed in HepG2 cells; other groups obtained different results using different cell lines. For example, Kakizuka et al found that in CV-1 and K562 cells, PML-RARA could constitutively activate TRE and RARβ driven reporters in the absence of RA (17). When RA was added, PML-RARA could enhance activation beyond that observed with wildtype RARA. Oddly, they also observed PML-RARA superactivation in HepG2 cells, the same cell line in which de The et al saw PML-RARA driven repression. In HL60 cells, PML-RARA could suppress basal transcription of RARA targets, but exhibited superactivation in the presence of RA. Kastner et al also demonstrated that the degree of PML-RARA mediated repression or activation varied with different promoters, RAREs, and cell lines (18). It was later found that PML-RARA could also induce transcription from promoters containing PPAR response elements

(PPRE) in the presence in RA, but repressed transcription in the presence of PPAR ligands (90). Similarly, PML-RARA can inhibit vitamin D response elements (VDRE) (91). Inhibition of PPAR and VDR mediated transcription was purported to be a result of PML-RARA sequestering RXR, a common heterodimerization partner for RARA, PPAR and VDR, as opposed to PML-RARA directly binding to the response elements. While PML-RARA can bind RXR (91), definitive evidence that PML-RARA competes with other nuclear receptors for heterodimerization partners is still lacking.

Many of these early studies on PML-RARA's DNA binding and transactivation properties had substantial limitations. First, as evidenced by the varied results obtained using different promoters, reporter constructs and cell lines, PML-RARA function is highly dependent upon its cellular context. It is difficult to say what relevance experiments performed in non-myeloid cell lines such as Cos and HeLa cells have for PML-RARA functions in a promyelocyte. Secondly, all of these studies exhibited intrinsic bias, in that the RAREs and other response elements were chosen by investigators without considerating the possibility that PML-RARA may well bind additional consensus sites besides canonical RAREs. Third, many of these early studies relied exclusively upon luciferase or chloramphenicol acetyl-transferase reporter assays, and did not directly investigate whether PML-RARA physically interacted with the various response elements. Nevertheless, despite these limitations, PML-RARA came to be considered primarily a dominant negative RARA with "super-repressor" properties, a paradigm that would direct APL research for over a decade after the discovery of PML-RARA.

1.8.2. PML-RARA Specific Consensus Sites

However, two studies of PML-RARA's *in vitro* DNA binding specificity provided early evidence that PML-RARA was not merely a dominant negative RARA, but had its own unique binding properties. Perez et al investigated the binding of RARA and PML-RARA in *in vitro* gel shift assays to DR1-5 elements containing either GGGTCA(n_{1-5})AGGTCA or GGTTCA(n_{1-5})AGTTCA half sites, termed DRnG and DRnT sites respectively (91). While RARA/RXR bound equally well to DRnG and DRnT DR2 and DR5 probes, PML-RARA showed a marked preference for the DRnG probes. However, in light of the fact that the RARβ DR5 site used as the prototypical PML-RARA binding site is a DRnT site, it remains unclear what effect, if any, these preferences would have in the proper cellular context. Additionally, PML-RARA bound DR2 probes as well as DR3 probes, unlike RARA/RXR homodimers, which bind DR2 and DR5 sites most strongly. This study was the first evidence that PML-RARA has an extended binding repertoire compared to RARA. A subsequent study by Hauksdottir and Privalsky examined the binding of RARA and PML-RARA to a canonical AG**AGGTCA**ACGAG**AGGTCA** DR5 site when half site residues or preceeding residues were systematically mutated (92). PML-RARA proved less sensitive than RARA to changes in the base immediately preceeding a half site, and to changes in the third residue of a half site. The presence of RXR further enhanced PML-RARA binding to less favorable sites *in vitro*. However, the correlation of binding with activation was imperfect. While PML-RARA alone could activate mutated DR5 sites better than RARA/RXR in reporter assays, the presence of RXR reversed this trend. PML-

RARA/RXR transactivation was less than that seen with RARA/RXR, suggesting that repression by PML-RARA may be dependent upon RXR.

A 2004 study by Kamashev et al provided the first unbiased screen of PML-RARA consensus sites (93). PML-RARA protein was incubated with 25 base pair random DNA duplexes, and bound sequences were selected by gel shifts and amplified. After six rounds of selection and amplification, the duplexes were cloned and sequenced. The identified binding sites contained not only canonical DR2, DR3, DR4 and DR5 RAREs, but also widely spaced RAREs containing up to 13 base pair spacers between half sites. Inverted repeats, most commonly IR0 sites, and everted repeat sites (most often ER8 sites) were also identified. The addition of RXR to gel shift assays extended the binding of PML-RARA to RARES with up to 20 residues separating half sites (DR20 sites). Interestingly, transgenic mice expressing PML-RARA which cannot bind RXRA do not develop leukemia (94), suggesting that the role of RXR in DNA binding may also be relevant in vivo. Kamashev et al demonstrated that IR0, ER8 and DR sites with more than 5 base pair spacers are minimally activated by RARA in the presence of RA, but are strongly induced by PML-RARA. The relaxed binding specificity of PML-RARA is a clear gain-of-function above basal RARA functions; PML-RARA can no longer be considered to be solely a dominant negative RARA. Accordingly, in other studies, when APL blasts or NB4 cells are treated with ATRA, many of the induced or repressed genes do not contain known RAREs in their promoters (95). These relaxed binding sites provide a potential mechanism by which PML-RARA can alter expression of genes other than RARA targets.

However, the study by Kamashev et al did not examine whether PML-RARA binds altered RAREs in a chromosomal context, instead relying upon gel shift and luciferase reporter assays. In recent years, several chromatin immunoprecipitation studies have been published which have validated non-canonical RAREs as bona fide PML-RARA binding sites, as well as demonstrating new motifs. Hoemme et al reported a ChIP-chip study of PR9 cells, which contain a zinc inducible PML-RARA construct (96). Only 40% of the identified PML-RARA targets contained classical RAREs, and many of the remaining genomic regions contained altered RAREs. While this study was limited by the design of the arrays used, which contained only 12,000 known promoter regions and 12,000 CpG islands, it did demonstrate that PML-RARA had altered DNA properties in a chromosomal context. Two later reports expanded upon these observations. Martens et al performed chromatin precipitation coupled to high throughput next-generation DNA sequencing (ChIP-seq), using PR9 cells, NB4 cells and primary APL patient samples (97). Nearly all possible combinations of half sites were found within PML-RARA binding regions, including DR elements with up to 13 nucleotide spacers and half sites in everted or inverted orientation. Wang et al reported a separate study ChIP-chip study (98) at the same time as the Martens study. This study represented an improvement over the previous ChIP-chip study because of improved array design (probes covering over 25,500 promoters versus only 12,000 promoters) and advances in bioinformatic identification of binding regions and potential motif sequences. Consistent with previous reports, binding regions with various orientations of RARE half sites were identified. However, bioinformatic motif discovery approaches demonstrated that RARE half sites frequently appeared near PU.1 consensus sites. A separate ChIP-

chip experiment demonstrated that PU.1 protein was in fact occupying the consensus sites near RARE half sites. PML-RARA selectively binds RARE half sites in proximity to occupied PU.1 consensus sites, via both coiled-coiled domain dependent protein-protein interactions with PU.1 and DNA binding to the half site. Formation of this PML-RARA-PU.1 complex leads to repression of PU.1 transcriptional targets.

1.9. Protein-protein interactions of PML-RARA

1.9.1. Interactions Which Produce Gene Repression

PML-RARA has domains that allow protein-protein interactions in both the RARA and PML portions. Like wildtype RARA, PML-RARA can recruit the NCor/SMRT/HDAC corepressor complex (99-102). Histone deacetylation causes chromatin to adopt a "closed" conformation that is less accessible to the transcriptional machinery, therefore silencing gene expression. In contrast to RARA, PML-RARA does not dissociate from the corepressor complex in the presence of physiological concentrations of RA, but requires pharmacological doses to relieve transcriptional repression. PML-RARA, unlike RARA, can self-dimerize and form higher order oligomers; it has been suggested that oligomerization allows for increased corepressor binding (103). Along with the data from transient transfections, this biochemical evidence is the primary support for the role of PML-RARA as a "super-repressor."

PML-RARA may alter chromatin structure through mechanisms distinct from the NCor/SMRT pathway shared with wild type nuclear receptors. Wildtype PML can bind Daxx through its coiled-coil domain (104); this interaction is dependent upon sumoylation of lysine-160 (105). PML-RARA retains the ability to recruit Daxx through

the same domain. Daxx recruits DNA methyltransferase 1 (DNMT1) in a DNMT associated protein-1 (DMAP1) dependent manner, leading to promoter methylation (106). Additionally, Daxx has also been shown to bind HDAC1 (104). The interaction between PML-RARA and Daxx is essential for leukemogenesis, since transgenic mice expressing a PML-RARA transgene with a mutated sumoylation site do not develop leukemia (107). A recent report demonstrated that PML-RARA can also recruit the polcomb repressor complex 2 (PRC2) to target genes (108). PRC2 includes the proteins EZH2, SUZ12 and histone binding proteins. PRC2 recruitment results in H3K27 histone methylation by EZH2, another epigenetic modification associated with transcriptional repression. It is not yet known whether PRC2 recruitment is essential for PML-RARA induced leukemogenesis or immortalization. Additionally, there is evidence that PML-RARA can recruit histone methyltransferases directly (109). In summary, PML-RARA appears to drive repression through three distinct mechanisms: histone deacetylation, DNA methylation, and histone methylation.

Accordingly, PML-RARA bound regions undergo epigenetic modification, including decreases in histone H3 acetylation and increases in lysine 9 and lysine 9 trimethylation. Upon ATRA treatment, H3 acetylation increases in most PML-RARA bound regions as well as globally (97). The global DNA methylation profile of APL samples is also distinct from that of other AML (110). Since PML-RARA target genes include chromatin modifying enzymes such as JMJD3 (H3K27 demethylation), SETDB1 (H3K9 methylation), and DNMT3a (DNA methylation) (97, 98), it is likely that the global changes reflect both direct recruitment of modifying enzymes by PML-RARA and effects on expression of the enzymes.

1.9.2. Interactions which produce gene activation

Under certain conditions, PML-RARA can act as a transcriptional activator in the absence of RA. Paradoxically, it largely associates with repressor proteins and it has been difficult to explain how PML-RARA could activate transcription. Some have suggested that PML-RARA could indirectly deregulate gene expression by titrating corepressors and RXR away from sites of transcription. However, this mechanism has cannot account for specificity of activation. A report by Reineke et al investigated the interaction of PML-RARA with members of the co-activator complex (111). PML-RARA was able to bind the co-activators ACTR, SRC-1, GRIP1, and p300/CBP in a ligand independent manner, while RARA associates with these proteins only in the presence of RA. These interactions were confirmed in both *in vitro* GST pull-down assays and in co-immunoprecipitation experiments. Surprisingly, the hormone independent interactions of PML-RARA were mediated by the same domains as for wildtype RARA, and deletions of PML domains had no effect on PML-RARA's ability to bind co-activators. The conformational characteristics of PML-RARA that allow it to constituitively bind co-activators remain unknown. The authors presented evidence that in transient transfection assays, the ability of PML-RARA to repress glucocorticoid receptor (GcR) mediated transcription is dependent upon its association with coactivators, suggesting that PML-RARA can indirectly inhibit gene expression by sequestering coactivators. Again, this hypothesis fails to account for specificity, since the transcription of many genes is dependent upon co-activators. We favor the alternative interpretation that PML-RARA can associate both with corepressors and coactivators,

and can therefore act as either a repressor or activator of transcription, depending upon the cellular and molecular context.

1.9.3 Interactions with Transcription Factors

In addition to its direct effects on target genes, PML-RARA may alter gene expression through inhibition of other transcription factors through protein-protein interactions. For example, in the presence of ligand, RARA is known to inhibit activity of the AP-1 transcription factor composed of c-fos/c-jun heterodimers. In contrast, PML-RARA increases AP-1 activity in the presence of physiological concentrations of RA (1-10nM), and this effect is believed to be dependent upon a physical interaction between c-jun and PML-RARA (112). Similarly, PML-RARA inhibits transcription of p53 targets by inducing the Mdm dependent degradation of p53 (113). The PML-IV isoform normally stabilizes p53 by promoting its acetylation. PML-RARA binds PML-IV and recruits HDACs to the PML-p53 complex, leading to deacetylation and destabilization of p53. Similarly, while PML-RARA has long been thought to downregulate the expression of the transcription factor PU.1, recent evidence suggests that it may also inhibit PU.1 protein activity (114). PML IV promotes the formation of a PU.1/p300 complex on the promoter of the CEBPε gene, a transcription factor required for terminal differentiation of granulocytes, leading to enhanced transcription. The CEBPε promoter contains a RARE and it was initially thought that PML-RARA repressed CEBPε by binding this consensus site and then recruiting corepressors to the locus. However, PML-RARA disrupts the PML IV/PU.1/p300 complex and can repress CEBPε even when the RARE in the promoter has been mutated.

Additionally, it has become increasingly apparent that PML-RARA can alter gene expression via disruption of the Sp1 transcription facor. PML-RARA induces the expression of the basic helix-loop-helix (bHLH) transcription factors ID1 and ID2 in the presence of ATRA, and represses expression in the absence of ATRA (115). Surprisingly, neither the ID1 nor the ID2 promoter contain RAREs. Transactivation is dependent upon a CCAAT box and a GC box located within the proximal promoter. These sites are known motifs for the NF-Y and Sp1 transcription factors, respectively. PML-RARA interacts with Sp1, forming a complex with NF-Y and Sp1, and transforming ID1 and ID2 into ATRA responsive genes. These interactions are dependent upon the coiled-coil domain of the PML moiety. Similarly, tissue factor (TF), a known target gene of Sp1 and the AP-1 complex, is overexpressed in APL cells, which may be partly responsible for the high incidence of coagulopathy in APL patients (116). PML-RARA can interact with the TF promoter and induce TF expression only with an intact coiled-coil domain. In contrast, mutants lacking the RARA DNA binding domain are unimpaired. It is believed that through interactions with Sp1, PML-RARA deregulates TF. Finally, PML-RARA, in the absence of ATRA, upregulates Hes1, another bHLH transcription factor and canonical target of Notch signaling (117). Like ID1, ID2 and TF, the regulation of Hes1 by PML-RARA is dependent upon the coiled-coil domain, not the DNA binding domain. Similar to ID1 and ID2, the Hes1 promoter contains NF-Y and Sp1 consensus sites in close proximity.

Collectively, these studies indicate that PML-RARA has both direct and indirect effects on transcription that are more complex than initially recognized. PML-RARA can alter gene expression via at least 4 mechanisms: 1) direct DNA binding to motifs

containing RARE half sites in various orientations, 2) protein-protein interactions with other transcription factors, including Sp1, c-jun and PU.1, 3) simultaneously binding a single RARE and the PU.1 transcription factor occupying a consensus site in the same promoter and 4) disrupting PML-IV complexes with other transcription factors. Notably, all of these mechanisms represent a gain-of-function compared to wildtype RARA. These results also explain the puzzling observation that transgenic mice expressing PML-RARA lacking the DNA binding domain still develop leukemia (118). Through protein-protein interactions, PML-RARA can disrupt the activities of other transcription factors, and this disruption is sufficient to cause leukemogenesis.

1.10. Proposed mechanisms of PML-RARA induced leukemogenesis

The balanced t(15;17) translocation creates 4 genetic changes: 1) generation of the PML-RARA fusion protein 2) generation of the reciprocal RARA-PML fusion in ~80% of cases (119) 3) PML haploinsufficiency and 4) RARA haploinsufficiency. However, PML-RARA was first hypothesized to act as a dominant negative inhibitor of RARA signaling. At the time PML-RARA was identified, it was already known that differentiation of APL cells could be induced by ATRA treatment (12, 13). Several early studies of PML-RARA function demonstrated that it could repress RARA target genes when transfected into various cell lines, and that the repression was lifted with the addition of pharmacological doses of ATRA to the culture medium (5, 6, 17, 18, 92). In addition, vitamin A deficiency and RARA antagonists can produce myeloid expansion, though not frank leukemia, in mice (75-77), suggesting that inhibition of RARA function could alter myelopoiesis. A retrovirus harboring a dominant negative RARA construct

immortalized mouse bone marrow progenitors at the promyelocyte stage; ATRA could induce differentiation in these cells as well (78).

However, several lines of evidence suggest that inhibition of RARA does not completely explain PML-RARA's actions. First of all, many of the transient transfections performed in early studies used non-myeloid cell lines, making it difficult to extend the results to promyelocytes. In some cases, PML-RARA was separately reported as either activating or repressing a promoter, depending in which cell line the experiments were performed. Secondly, while excesses or deficiencies of vitamin A can alter hematopoeisis both *in vitro* and *in vivo*, neither is sufficient to cause leukemia, suggesting that additional pathways must be involved. Third, PML-RARA is expressed at extremely low levels in patients and APL mouse models (30), so high level expression of a dominant negative RARA driven by a retroviral promoter may not accurately reflect the human disease process. Indeed, when self-dimerizing, artificial RARA fusion proteins were expressed in the myeloid cells of transgenic mice, leukemia development was extremely rare (4/164 mice), despite the fact that these artificial fusions do repress RAREs in transient transfection assays (120). Likewise, transgenic mice in which HDAC1 was artificially fused to RARA did not develop leukemia, demonstrating that enforced recruitment of corepressors onto RARA target genes is insufficient for leukemogenesis *in vivo (*121). Recently, an APL patient was identified in which a frameshift mutation created a truncated PML-RARA with no RARA domains, suggesting that APL can develop in the absence of any RARA inhibition (122). It should be noted that it is possible that the frameshift mutation occurred *after* PML-RARA initiated leukemia. Similarly, transgenic mice expressing a PML-RARA cDNA with a mutated

DNA binding domain still develop leukemia (118), indicating that the ability of PML-RARA to directly activate or repress transcription is not essential for leukemogenesis.

PML was an unknown locus when PML-RARA cDNA was initially cloned. After subsequent studies demonstrated that PML overexpression could suppress growth in fibroblasts (87), it was hypothesized that PML-RARA may act as a double dominant negative, inhibiting both PML and RARA. PML-RARA expression disrupts PODs and causes PML to relocalize to hundreds of smaller nuclear foci (18). While PML knockout mice do not spontaneously develop malignancies, they are at increased risk in several cancer models (48, 86), suggesting that PML deficiency could cooperate with other oncogenes to produce cancer. PML is known to interact with several tumor suppressor proteins, including p53 and Rb (89), and PML deficient cells are resistant to inducers of apoptosis including radiation, Fas and TNF (88). Inhibition of PML functions could alter cell cycle properties, priming cells for malignant transformation. When PML +/- mice are crossed with hCG-PML-RARA transgenic mice, the incidence of leukemia in the first year of life increases from 12 to 31 percent, suggesting PML-RARA and PML haploinsufficiency may cooperate (48). However, the presence of rare alternative translocations in APL, leading to other RARA fusions (PLZF-RARA, NPM-RARA, NUMA-RARA and STAT5B-RARA) suggests that PML inhibition is not necessary for APL pathogenesis (20). The other RARA fusions do not disrupt PODs, demonstrating that intact PML function does not prevent leukemogenesis.

Since the evidence does not support dominant negative inhibition of PML, RARA or both PML and RARA as the sole mechanism of PML-RARA action, PML-RARA is now considered to have unique gain-of-function properties in addition to its inhibitory

activities. First of all, overexpression of PML-RARA is toxic in cell lines and primary cells of both hematopoietic and non-hematopoietic origin (53, 123, 124). Neither PML nor RARA deficiency leads to cell death, and PML deficiency has been shown to protect against apoptosis-inducing stimuli (88). Secondly, higher expression of PML-RARA does not lead to increased penetrance in mouse models of APL (30). In a simple dominant negative model, increased dose should result in an increased incidence of disease. The higher incidence of leukemia in our $mCG^{PR/+}$ mice, which have a 50 fold lower expression of PML-RARA compared to hCG-PML-RARA transgenic mice, argues strongly against this model, and suggests that there is an optimal PML-RARA expression level for disease initiation. Even a 2 fold increase in dose in $mCG^{PR/PR}$ mice resulted in decreased penetrance, demonstrating the sensitivity of the system to dose. Biochemical studies of the PML-RARA protein also support the gain-of-function hypothesis. As described above, PML-RARA interacts with a variety of chromatin altering proteins, including some that do not bind wild type RARA (107, 108, 111). Additionally, studies of PML-RARA's DNA binding properties revealed that PML-RARA is capable of binding to widely spaced RAREs that RARA does not recognize (93). It is likely that PML-RARA activities depends upon a combination of gain-of-function, inhibition of endogenous RARA and PML functions, and haploinsufficiency of wildtype RARA and PML.

1.11. The APL dsyregulome

The development of microarray technology allowed for the identification of gene expression signatures from different leukemia subtypes. Several reports have shown that

the expression profile of APL reproducibly clusters separately from other AML. Schoch et al found that principal component analysis could separate t(15;17) cases from those AML samples carrying the t(8;21) or inv(16) rearrangements (125). Furthermore, two different methodologies (weighted voting and multiple tree classification) could reliably predict to which karyotypic class samples belonged. Later studies compared the expression profiles of larger groups of patients, including AML without recurrent chromosomal rearrangements. In these reports, patients with t(15;17) clustered separately in unsupervised analyses (126-128). A similar phenomenon was seen in pediatric APL patients (129). When statistical methods such as Significance Analysis of Microarrays (SAM) were utilized to identify class discriminating genes, a number of genes were consistently reported as characteristically overexpressed in APL, including hepatocyte growth factor (HGF), macrophage stimulating growth factor 1 (MST1) and stabillin-1 (STAB1) (125-129). Collectively, these studies suggest that t(15;17) positive AML cells have a distinct set of genes that is consistently dysregulated, termed the APL dysregulome.

It was initially assumed that downstream targets of PML-RARA would be found within the unique signatures of genes overexpressed or underexpressed in APL. However, early gene expression profiling studies did not compare APL samples to normal myeloid cells, especially normal promyelocytes. Many genes characteristically expressed in CD34+ progenitors are downregulated in promyelocytes as part of a normal developmental program of myelopoiesis. The single published study which did utilize a normal promyelocyte comparison relied upon G-CSF in vitro differentiated CD34+ cells as “promyelocytes,” which may not represent the unmanipulated cells (130). Failure to

compare APL expression patterns to those of normal promyelocytes leads to the misidentification of genes as APL specific when they have the same expression pattern in all promyelocytes, both normal and malignant. We hypothesized that any bona fide PML-RARA transcriptional target must be uniquely expressed or repressed in APL cells compared both to other AML and normal promyelocytes. Genes with similar expression in normal and leukemic myeloid cells, or that are repressed in both APL and normal promyelocytes, are unlikely to represent direct targets of PML-RARA. In order to identify the true APL dysregulome, we compared gene expression profiles of APL samples to those of both other AML and sorted normal human myeloid cells, including CD34+ stem/progenitor cells, promyelocytes and neutrophils (131). The identification of the human APL dysregulome is described in further detail in **Chapter 2.**

We compared the set of genes dysregulated in human APL to our previously published murine APL dysregulome and to two cell line models of APL. We hypothesized that a gene with altered expression in human APL as well as multiple model systems was most likely to be an important player in pathogenesis. We found that the Notch ligand Jagged-1 (*JAG1*) is overexpressed in human APL compared to normal promyelocytes and other AML. *JAG1* is also highly expressed in murine APL cells and in NB-4 cells, an APL cell line. Finally, in the PR-9 cell line, which contains a zinc inducible PML-RARA cassette, *JAG1* mRNA increased upon PML-RARA induction. Since Notch signaling has a known role in self renewal and leukemogenesis, we then conducted in depth studies of the functional role of Notch signaling in APL, as discussed further in **Chapter 3.** A detailed description of Notch signaling and its roles in normal and leukemic hematopoeisis follows below.

1.12. Notch signaling

Notch signaling is highly conserved pathway with critical roles in lineage specification, differentiation, proliferation and cellular survival. The principle components of the notch pathway include the Notch receptors, ligands of Delta/Serrate/LAG (DSL) family, and downstream transcriptional activators such as CSL and Mastermind (132). The core pathway elements are found in all metazoan animal species examined, including sponges, cnidarians, C. elegans, Drosophila and vertebrates, but are absent in plants (133). Notch signaling does not appear to be present in fungi or protists, but some taxa have isolated components, such transcription factors homologous to CSL or genes with unknown function that contain domains homologous to Notch. This suggests that the individual building blocks of the Notch pathway predate the evolution of multicellular animals. Mammalian genomes, including mice and humans, contain 4 Notch receptors, termed Notch1-4, and 5 Notch ligands, Delta-like 1, 3 and 4 and Jagged1-2.

1.12.1. Notch receptors

Notch receptors are synthesized as type I transmembrane proteins (134). The extracellular domain contains numerous tandem EGF repeats which are important for interaction with DSL ligands, while the intracellular domain contains a RAM domain, 6 ankyrin repeats, 2 nuclear location signals, a transactivation domain and a C-terminal PEST domain (135). The RAM domain and ankyrin repeats are thought to mediate protein-protein interactions, while the PEST domain plays an important role in protein

turnover. The extracellular domain is cleaved at the S1 site immediately proximal to the transmembrane domain by furin-like convertases residing the trans-Golgi network. The two resulting fragments associate non-covalently to form the functional Notch heterodimer. Importantly, the C-terminus of the N-terminal extracellular fragment contains a Lin12/Notch (LNR) domain which associates with and protects the transmembrane domain from cleavage in the absence of ligand binding (134). The extracellular domain is further modified by O-linked glycosylation during its transit through the Golgi apparatus; these additions seem to promote proper folding and trafficking (136). Some of the O-fucose residues may be extended via addition of N-acetylglucosamine by Fringe family glycosyltransferases. Fringe mediated glycosylation characteristically occurs O-fucose residues within EGF repeat 12, which is critical for ligand binding (135). Several studies have demonstrated that Fringe modified Notch preferentially binds to Delta family ligands and interacts poorly with Jagged type ligands, representing a mechanism for specificity of ligand-receptor interactions (137, 138).

1.12.2. Notch Ligands

Notch ligands are divided into two families, the Delta and Serrate/Jagged families, based upon structure and sequence homology. Like Notch receptors, Notch ligands are type 1 cell surface proteins with many EGF repeats in the extracellular domain (139). Both Delta and Jagged type ligands contain a conserved N-terminal (NT) and DSL domain, which are required, along with the first two EGF repeats, for ligand/receptor interactions. Jagged ligands contain nearly double the number of EGF repeats of Delta ligands, and also possess a cysteine-rich (CR) region immediately

proximal to the transmembrane domain (140). The role of the additional EGF repeats and CR region in the function of Jagged ligands is not yet clear. The intracellular domain of Notch ligands is less well conserved, but most contain multiple lysine residues which can be ubiquitinated to regulate trafficking and turnover (141). In vertebrates, Jag1, Dll1 and Dll4 have a PDZ ligand motif within the C-terminus of the intracellular domain (139). The PDZ ligand domain of Jag1 interacts with the PDZ domain of afadin-6 (AF6), a Ras target with roles in cellular junctions (142). The PDZL domain has been shown to be required for cellular transformation of rat kidney epithelial (RKE) cells by overexpression of Jag1 (143). These effects are independent of Notch signaling and suggest possible cell intrinsic activities of Notch ligands. Similarly, the PDZL domain of Dll1 interacts with the discs large 1 (Dlg1) and membrane associated guanylate kinases with inverted domains (MAGI) proteins (144). The interaction with Dlg1 seems to regulate cell-cell junctions and reduce cellular migration, while MAGI proteins recruit Dll1 to adherens junctions.

Computational analysis has predicted other domains within the intracellular tails of Notch ligands, such as SH2, SH3 and cyclin binding domains, which could potentially allow for diverse interactions with various signaling proteins. In addition potential O-linked glycosylation sites are found in some Notch ligands. The validity of these sites and their roles in the function of Notch ligands has not yet been investigated.

1.12.3. Canonical Notch signaling

Notch signaling occurs via an ordered sequence of proteolytic processing steps. The first cleavage (S1) occurs within the Golgi apparatus, where furin-like covertases

cleave the Notch precursor protein into N and C terminal fragments that associate to form the mature Notch heterodimeric receptor (145). Once on the cell surface, binding of the DSL domain of a Notch ligand to EGF repeats 11-12 of a Notch receptor results in a conformational change in the LNR domain of the receptor that exposes the S2 proteolytic cleavage site. Notch is cleaved at S2 by metalloproteinases of the ADAM10/TACE family, allowing removal of the Notch extracellular domain (146). The membrane anchored Notch intracellular domain is then cleaved at the S3 site by intramembrane protease γ-secretase (135). Cleavage by γ-secretase is a necessary and rate-limiting step in Notch signaling. The freed intracellular Notch (ICN) fragment then translocates to the cell, where it associates with the CSL transcription factor (also called CBF-1 or RBP-Jκ) and the co-activator Mastermind-like (MAML) (132). In the absence of Notch signaling, CSL functions as a transcriptional repressor through recruitment of NCoR/SMRT co-repressors and histone deacetylases (HDACs) to target gene promoters (147, 148). The formation of the ternary ICN/CSL/MAML complex displaces co-repressors and recruits the histone aceytlase p300 and RNA polymerase II, activating transcription (149). Known Notch target genes include c-myc, Hes-1, Deltex and Cyclin D1 (134). Under normal physiologic conditions, Notch signaling is short-lived due to degradation of ICN. ICN is phosphorylated in the PEST domain by CDK8 (150). Fbxw7 then ubiquitinates phospho-ICN, targeting it for degradation (150, 151).

1.12.4. Non-canonical Notch signaling

Several non-canonical Notch signaling pathways have been described. ICN has been shown to interact with IKKα and promote its activity, resulting in Ikb degradation

and Nf-kb activity (152). This effect is not dependent on the presence of CSL. The hypoxia activated transcription factor HIF1α can associate with ICN and potentiate Notch signaling (153). This interaction may underlie the ability of hypoxia to promote an undifferentiated state in many stem cell populations. Finally, ICN may have functions outside of transcription. In Drosophila, ICN positively regulates axon growth via interactions with the cytoskeletal proteins Disabled and Trio (154). This association has not yet been described in mammalian systems, although Notch signaling does play a role in mammalian axon growth. A second example of non-transcriptional effects of Notch is seen in the interaction of ICN with mTOR and Rictor, resulting in activation of Akt; this mechanism is believed to be important for the anti-apoptotic effects of Notch in both normal tissues and various cancers (155). However, while these CSL independent pathways are intriguing, they appear to be a minor component of Notch signaling. CSL knockout embryos phenocopy Notch deficiency (156), suggesting that the majority of its cellular effects are CSL mediated.

1.12.5. The role of intracellular trafficking in Notch signaling

A number of accessory proteins involved in trafficking of both receptors and ligands are required for Notch signaling. The E3 ubiquitin ligase mindbomb (Mib) ubiquitinates lysine residues in the intracellular tail of Notch ligands (157). The cytoplasmic protein epsin binds these tagged residues and recruits clathrin and other endocytic machinery, resulting in the internalization of the ligand into an endosome compartment (139). This process influences Notch signaling via two distinct mechanisms. First, endocytosis is required for the maintenance of active ligand at the

cell surface (158). Ligands must traffic through recycling endosomes and back to the cell surface in order to be able to activate Notch signaling. Presently it is unclear how ligands become activated, although several attractive mechanisms, including oligomerization of ligands, post-translational modifications and sorting of ligand into lipid rafts, have been proposed. Secondly, during Notch signaling, ligand endocytosis creates a mechanical force on the extracellular domain of Notch, exposing the S2 site and allowing ADAM10/TACE mediated cleavage (159). The ligand/extracellular Notch complex are then endocytosed together. Notch receptors are also thought to be endocytosed following S2 cleavage, and this may promote S3 cleavage (160). The bulk of cellular γ-secretase resides within the endosome compartment (161), and this may provide a mechanism for bringing Notch into contact with high concentrations of secretase, allowing for more efficient generation of ICN.

1.13. Notch signaling and hematopoiesis

1.13.1. Notch and embryonic hematopoiesis

In the embryo, hematopoiesis occurs in two waves, termed the primitive and definitive phases. The primitive phase occurs in the yolk sac in the E7.5 mouse embryo, and gives rise to primitive nucleated erythrocytes expressing embryonic hemoglobin and macrophage progenitors (162). The yolk sac progenitor cells can form colonies in vitro but lack long term repopulating ability when transplanted into a whole animal. Definitive hematopoiesis begins in the aorta-gonadal-mesonephros (AGM) region at E10.5, when clusters of hematopoietic cells appear in the ventral wall of the dorsal aorta. It is currently believed that a bipotent population of hemangioblasts in this region

differentiates into hematopoietic lineage upon appropriate signaling, and becomes endothelium by default in the absence of such signals (163). These cells later seed the fetal liver and bone marrow, and are capable of repopulating the marrow of lethally irradiated recipients. Notch 1 and 4 are expressed in AGM cells and the ligands Jag1, Jag2 and Dll4 are found in the surrounding stroma (163).

Primitive hematopoiesis in the yolk sac is not perturbed by genetic ablation of Notch ligands or receptors, indicating that Notch signaling is dispensable for this process. In contrast, AGM cells from Notch1-/- embryos cannot form colonies and lack expression of hematopoietic genes such as Runx1 and Gata2 (164). Similar results are observed in zebrafish embryos treated with gamma secretase inhibitors (165), and in mindbomb1 (166) and CSL (167) deficient mouse embryos, which also lack Notch signaling. However, these results are complicated by the severe vascular defects in these animals and disruption of arterial identity specification (156). It is currently believed that arterial identity is a prerequisite for proper specification of HSCs within the dorsal aorta. This conundrum was solved by the observation that Jag1-/- embryos, which have a less severe vascular phenotype and intact arterial identity, nonetheless do not form definitive HSCs within the AGM (168). AGM explants can be rescued in vitro by culture with Jag1 expressing fibroblasts, demonstrating that the requirement for Jag1 is non-cell autonomous. Notch signaling in the dorsal aorta hemangioblast induces expression of Gata2, an essential transcription factor in hematopoiesis (169). In contrast, Jag2 (168) and Dll4 deficient animals do not have detectable defects in HSC specification, although the development of the T cell lineage is altered in these mice. Therefore, there is a non-redundant requirement for Notch1/Jag1 signaling to specify definitive hematopoiesis.

1.13.2. Notch and adult hematopoiesis

The role of Notch signaling in adult hematopoiesis is more controversial, and remains an active area of investigation. Notch ligands, including Jag1, Jag2, and Dll1, are expressed on the non-hematopoietic stroma of the bone marrow microenvironment. Both murine KLS and human CD34+ cells express Notch receptors. Furthermore, stem and progenitor cells cultured in the presence of Notch ligand expressing fibroblasts, stroma or artificial ligand monolayers expand, yet retain an immature phenotype, suggesting that Notch signaling promotes self renewal and inhibits differentiation (170-174). A criticism of such experiments is that the concentration of ligand may be higher than in vivo and therefore not physiologically relevant. Conditional knockouts of Notch1 (175), Notch2 (176) and Jag1 (175) under the control of the interferon inducible Mx-Cre have no detectible phenotype on HSCs. Hypothesizing that redundancy of Notch receptors and ligands may explain the lack of a detectable phenotype, Maillard et al generated animals in which Notch signaling is totally ablated by either expression of a dominant negative MAML or conditional knockout of CSL (177). These animals had no HSC defects at rest, and none were apparent even after stringent competitive repopulation assays or serial transplantation experiments, suggesting that canonical Notch signaling is dispensable for steady-state hematopoiesis and after myeloablative radiation. The authors further demonstrated that the expression of many Notch target genes, such as Hes1 and Hey5 are very low in HSCs compared to early T cell progenitors in the thymus, even though expression of Notch receptors is comparable. They hypothesized that Notch signaling is opposed in the bone marrow to prevent ectopic T cell development. The LRF

proto-oncogene is known to inhibit Notch signaling through unknown mechanisms (178), and is strongly expressed in HSCs.

Nevertheless, HSCs appear poised to respond to Notch signaling. The ability of HSCs to expand upon exposure to Notch ligands in vitro is well documented. Similar phenomena occur in vivo in certain settings. For example, exogenous administration of parathyroid hormone leads to increased Jag1 expression on osteoblasts via a cAMP dependent mechanism, and a concurrent expansion of the HSC population (179). In addition, TNFα or LPS, which stimulates its production, can lead to increased Jag1 and Jag2 on marrow endothelium and a similar increase in HSCs and progenitors (180, 181). Osteoblasts and endothelial cells are components of the "stem cell niche," and as such are capable of altering HSC activity. Notch signaling may therefore modulate adult hematopoiesis in times of stress, such as infection, inflammation or bone trauma.

1.13.3. Notch signaling in the bone marrow microenvironment

Notch signaling may also have indirect effects on hematopoiesis through its role in bone biology and the bone marrow microenvironment. Genetic ablation of Notch signaling in osteoblasts results in osteoporosis (182) secondary to an increase in osteoclasts. In mature osteoblasts, Notch positively regulates the transcription of osteoprotegerin, a secreted negative regulator of osteoclastgenesis. In contrast, overexpression of ICN in osteoblasts causes osteosclerosis and marrow cavities filled with trabecular bone (183). In this model, the bone is poorly organized and contains increased immature osteoblasts, suggesting that Notch signaling prevents terminal differentiation into mature osteoblasts. Similarly, conditional knockout of the

presenillins (part of the γ-secretase complex) in mesenychmal stem cells produces animals with increased bone density, due to increased differentiation of MSCs into osteoblasts (182). Confusingly, in certain settings, Notch signaling may also promote differentiation. Activation of bone morphogenic protein (BMP) signaling concordantly with Notch signaling promotes MSC commitment to the osteoblastic lineage (184, 185). Notch signaling therefore appears to have a dual role in bone biology: it both maintains MSCs and immature osteoblasts in an undifferentiated state and drives them to adopt an osteoblastic fate. In addition, Notch signaling in marrow osteoclast precursors inhibits osteoclastgenesis and bone resorption (186). Collectively, these results suggest that caution should be used in interpreting experiments that do not control for the effect of the microenvironment.

Indeed, several mouse models have demonstrated that altered Notch signaling in the non-hematopoietic components of the bone marrow environment can have a profound effect on hematopoietic cells. The conditional deletion of mindbomb-1 (Mib1) results in myeloproliferation dependent on defective Notch signaling in the stroma (187). Mib1 -/- cells transplanted into a wildtype recipient do not produce MPD, while wildtype cells transplanted into a Mib1-/- animal produce highly proliferative granulocytes and granulocytic progenitors. This effect is reversible if a second transplant into a wildtype recipient is performed. Notch signaling within the hematopoietic compartment was intact, but was defective within the stroma. Similarly, presenilin-1 haploinsufficient, presenilin-2 knockout (PS1+/- PS2-/-) animals have reduced Notch signaling and develop a non-transplantable MPD (188), suggesting that a defective microenvironment is also responsible.

1.14. Notch Signaling in Leukemia

1.14.1. Notch Signaling in T-ALL

The human Notch1 gene was originally identified through analysis of the t(7;9) translocation found in a minority of T cell acute lymphoblastic leukemia (T-ALL) patients (189). The breakpoint of this translocation invariably occurs within intron 24 of the Notch1 gene and places exons 24-30 under the control of the TCRβ locus. The resulting truncated transcript, termed TAN1 (truncated activated Notch1), encodes a mutant Notch1 protein which lacks the extracellular EGF repeats and LNR domains, but retains the transmembrane and intracellular domains. TAN1 is constitutively active and causes T-ALL in mice transplanted with retrovirally transduced TAN1 marrow (190). However, t(7;9) is present in only 1-2% of T-ALL cases. Sequencing of the Notch1 gene in human T-ALL cases revealed that 50-60% of cases have mutations in either the heterodimerization domain, the C-terminal PEST domain or both (191). HD domain mutations make the Notch receptor more susceptible to gamma secretase cleavage, while PEST domain mutations prevent ubiquitination of cleaved Notch1 by Fbxw7, and subsequent degradation by the proteosome (192). Interestingly, 10% of T-ALL cases lack Notch mutations or translocations but have inactivating mutations of Fbxw7, which also lead to an inability to degrade cleaved Notch (192).

The mechanism of Notch induced leukemogenesis appears to involve activation of multiple downstream target genes and cross talk with many signaling pathways. In mouse models, Notch1 mutations cooperate with overexpression of c-myc and Pbx3, both of which cause T-ALL with long latency, as well as loss of p53, Ikaros and p27 (134). A

genomic approach comparing Notch ChIP-on-chip and microarray expression analysis of GSI treated T-ALL cell lines identified several upregulated transcriptional targets of activated Notch1 (193), including the pro-proliferative oncogene c-myc, Taspase-1, which promotes cell cycle progression (194, 195), cyclin D3, which promotes G1/S progression (196) and the cold shock domain protein CSDA, which has anti-senescent activities (197). T-ALL associated Notch mutants also appear to activate the PI3K/Akt survival pathway, either directly (155) or through its downstream transcriptional target, Hes1, which represses PTEN expression (198). In addition, Notch signaling induces transcription of Skp2, which has anti-senescent activities via its role in the degradation of the cyclin dependent kinase inhibitor p27 (199). T-ALL associated Notch mutants also activate pro-survival NF-κB signaling both via inducing transcription of RelB and NFKB2 and by direct activation of the IκB kinase complex (200). In summary, the overall effect of Notch signaling in T-ALL seems to be promotion of cellular survival and proliferation.

1.14.2. Notch signaling in myeloid leukemias

Notch mutations are only rarely found in acute myeloid leukemia (AML). These cases belong to the primitive M0 subtype and are characterized by expression of T-cell markers, a mixed lineage immunophenotype and high expression of the Notch target gene TRIB2 (201). However, Notch signaling may still be altered in AML in the absence of Notch mutations. Data from the Ley laboratory shows that Notch receptors are expressed in human AML (131). Gene expression profiling of a large set of AML patients (FAB subtypes M0-M7) revealed that NOTCH1 and NOTCH2 are highly expressed in nearly

all samples. The delta-like ligands are typically either not expressed or expressed at low levels. In contrast, JAG2 expression is detectable across a wide range of FAB subtypes. JAG1 is characteristically overexpressed in APL (see **Chapter 3**), but is also highly expressed in occasional non-M3 cases. In addition, the components of the gamma secretase complex and the mastermind-like coactivators are robustly expressed in nearly all AML, suggesting that AML cells are capable of transducing Notch signals.

Several AML associated fusion proteins ectopically activate Notch signaling in the absence of ligand. Notch signaling is required for the differentiation of megakaryocytes, as demonstrated by the reduction in both mature megakaryocytes and megakaryocyte progenitors in mice transplanted with dominant negative MAML transduced marrow (202). Acute megakaryoblastic leukemia (AMKL, FAB M7) is characterized by a recurrent t(1;22) translocation which results in the fusion protein OTT-MAL. Wildtype OTT binds CSL and causes repression of its transcriptional targets, while wild type MAL functions as a transcriptional activator. The OTT-MAL fusion binds CSL and leads to inappropriate activation of CSL target genes in the absence of Notch signaling (203). In addition, t (1;22) AMKL have increased expression of Notch/CSL target genes such as Hes1 and Hey1 compared to AMKL with GATA1 mutations. A knock-in mouse model of OTT-MAL resulted in hematopoietic abnormalities and frank megakaryoblastic leukemia in 10-15% of the animals. Similarly, the AML-ETO fusion protein produced by the t(8;21) translocation found in M2 AML can cause Notch independent transcription of CSL target genes (204). Wild type ETO is part of the corepressor complex recruited by CSL in the absence of Notch signaling.

Expression of AML-ETO inhibits corepressor recruitment, causing activation of Notch target genes.

PML-RARA appears to alter Notch signaling through at least three possible mechanisms. When PML-RARA expression is induced in the PR-9 cell line, both JAG1 protein and mRNA increase (131, 205). Cotransfection of PML-RARA and a Hes1 promoter reporter construct results in increased luciferase expression, suggesting that PML-RARA expression leads to downstream activation of Notch signaling (205). APL samples characteristically overexpress JAG1 relative to other AML, promyelocytes and CD34+ stem and progenitor cells (128, 130, 131, 205), suggesting that PML-RARA increases JAG1 in primary cells as well as cell lines. It is currently unclear how PML-RARA upregulates JAG1 expression; three genome wide ChIP studies failed to find evidence of PML-RARA binding in the JAG1 promoter, suggesting that the mechanism is not direct transcriptional regulation (96, 97, 98). Concordant with its upregulation of JAG1, PML-RARA may also negatively regulate the glycosyltransferase Lunatic Fringe (LFNG). LFNG mRNA decreases upon PML-RARA induction in PR9 cells (205) and is decreased in APL relative to other AML (128, 131). A genome wide ChIP-seq study of PML-RARA transcriptional targets identified multiple peaks in the LFNG promoter, suggesting that regulation of LFNG by PML-RARA may be direct (97). LFNG modified Notch molecules preferentially signal through Delta-like family ligands and have impaired interactions with Jagged family ligands (137, 138). Therefore, PML-RARA both increases JAG1 and promotes Jagged/Notch signaling via downregulation of LFNG. Finally, the Notch target gene Hes1 may be a transcriptional target of PML-RARA through its interactions with Sp1 and NF-Y (117). Despite these data implicating Notch

signaling in APL, its role in APL pathogenesis is still not defined; this will be addressed further in **Chapter 3.**

Expression of Notch ligands and target genes may be altered in myeloid malignancies in the absence of the fusion proteins described above. For example, expression of the Notch target gene Hes1 has been noted to increase in the accelerated and blast crisis phases of chronic myeloid leukemia (CML) as compared to the chronic phase (206). Retroviral overexpression of Hes1 immortalizes committed myeloid progenitors, and cooperates with BCR-ABL to cause leukemia, suggesting a role for Notch signaling in leukemic transformation (206). A study of expression profiling in human leukemic stem cells by Gal et al. found that JAG2 expression is increased in the CD34+ CD38- putative LSC population as compared to the more mature CD34+ CD38+ population (207). Treatment of primary AML samples with the gamma secretase inhibitor DAPT lead to decreased colony formation and colony size in methylcellulose, suggesting that Notch signaling contributes to self-renewal and proliferation in AML. Collectively these studies indicate that Notch signaling may play a wider role in myeloid malignancies than is commonly recognized.

Inhibition of Notch signaling may also be associated with myeloid malignancies. Recently, an inversion on chromosome 11 which fuses the mixed-lineage leukemia (MLL) gene to the Notch associated coactivator Mastermind-like 2 (MAML2) has been identified in rare cases of myelodysplastic syndrome (MDS), secondary AML and secondary T-ALL (208). The MLL-MAML2 fusion protein lacks the domains necessary for interaction with cleaved Notch and seems to act in a dominant negative fashion to prevent transcription of Notch target genes. Because of the contributions of the N-

terminal MLL domain of the fusion protein, it is difficult to assess the contributions of inhibited Notch signaling to the overall leukemogenic process. In addition, several studies have reported that Delta-like (Dlk1) is overexpressed in myelodysplastic syndrome (MDS) marrow samples and MDS CD34+ cells compared to normal CD34+ cells (209-211). Dlk1 is a secreted homologue of the Dll family Notch ligands that is believed to inhibit Notch signaling. Ectopic expression of Dlk1 results in reduced proliferation and impaired differentiation and colony formation (209). In the setting of MDS, Dlk1 mediated Notch inhibition may be more responsible for the cytopenias associated with the disease than promoting leukemic transformation.

1.15. Summary

In this thesis, we will study the downstream pathways altered in the setting of PML-RARA expression in myeloid cells and how those alterations produce the development of promyelocytic leukemia. We address broad two questions:

(1) How is gene expression altered in primary human APL compared to other forms of AML and normal myeloid cells, and how well do current cell line and animal model systems reflect the gene expression changes associated with the human disease?
(2) What is the role of Jagged/Notch signaling in the pathogenesis of APL, and is that role is the same or different in the pre-leukemic phase versus the fully transformed tumor?

In **Chapter 2**, we will describe the identification of the human APL dysregulome, its validation by high throughput digital mRNA quantification and the comparison between gene expression changes in human APL and those observed in various model systems. **Chapter 3** examines the role of the overexpression of the Notch ligand Jagged-1 (JAG1) in the pathogenesis of APL, especially in the hematopoietic alterations found in young, preleukemic mCG-PR mice. Finally, in **Chapter 4**, we will discuss our cumulative results and investigate future lines of inquiry that could be employed to continue the study of the role of Notch in APL pathogenesis.

1.16. References

1. Estey E, Döhner H. Acute myeloid leukaemia. *The Lancet*. 2006;368:1894-1907.

2. Bennett JM, Catovsky D, Daniel MT, et al. Proposed revised criteria for the classification of acute myeloid leukemia: a report of the French-American-British Cooperative Group. *Annals of Internal Medicine*. 1985;103:620-625.

3. Douer D. The epidemiology of acute promyelocytic leukaemia. *Best Practice & Research Clinical Haematology*. 2003;16:357–367.

4. Vardiman JW, Harris NL, Brunning RD. The World Health Organization (WHO) classification of the myeloid neoplasms. *Blood*. 2002;100:2292-2302.

5. de The H, Lava C, Marchio A, et al. The PML-RARa Fusion mRNA Generated by the t(l5;17) Translocation in Acute Promyelocytic Leukemia Encodes a Functionally Altered RAR. *Cell*. 1991;66:664-675.

6. de The H, Chomienne C, Lanotte M, Degos L, Dejean A. The t(15;17) translocation fuses the retinoic acid receptor alpha gene to a novel transcribed locus. *Nature*. 1990;347(558-561).

7. Pandolfi PP, Grignani F, Alacay M, et al. Structure and origin of the acute promyelocytic leukemia myl/RAR alpha cDNA and characterization of its retinoid binding and transactivation propertives. *Oncogene*. 1991;6:1292-1295.

8. Hillestad LK. Acute promyelocytic leukemia. *Acta Medica Scandinavica*. 1957;159:189-194.

9. Rowley JD, Golomb HM, Dougherty C. 15/17 translocation, a consistent chromosomal change in acute promyelocytic leukemia. *Lancet*. 1977;1:549-550.

10. Golomb HM, Testa JR, Vardiman JW, Butler AE, Rowley JD. Cytogenetic and Ultrastructural Features of De Novo Acute Promyelocytic Leukemia; The University of Chicago Experience (1973-1978). *Cancer Genetics and Cytogenetics*. 1979;1:69-78.

11. Rowley JD, Golomb HM, Vardiman J, et al. Further evidence for a non-random chromosomal abnormality in acute promyelocytic leukemia. *International journal of cancer. Journal international du cancer*. 1977;20(6):869-72.

12. Breitman TR, Collins SJ, Keene BR. Terminal differentiation of human promyelocytic leukemic cells in primary cultures in response to retinoic acid. *Blood*. 1981;57:1000-1004.

13. Breitman TR, Selonick SE, Collins SJ. Induction of differentiation of the human promyelocytic leukemia cell line (HL-60) by retinoic acid. *Proceedings of the National Academy of Sciences of the United States of America*. 1980;77:2936-2940.

14. Alcalay M, Zangrilli D, Pandolfi PP, et al. Translocation breakpoint of acute promyelocytic leukemia lies within the retinoic acid receptor a locus. *Proceedings of the National Academy of Sciences of the United States of America*. 1990;88:1977-1981.

15. Borrow J, Goddard AD, Sheer D, Solomon E. Molecular Analysis of Acute Promyelocytic Leukemia Breakpoint Cluster Region on Chromosome 17. *Science*. 1990;249:1577-1580.

16. Longo L, Pandolfi PP, Biondi A, et al. Rearrangements and Aberrant Expression of the Retinoic Acid Receptor a Gene in Acute Promyelocytic Leukemias. *Journal of Experimental Medicine*. 1990;172:1571-1575.

17. Kakizuka A, W. H. Miller J, Umesono K, et al. Chromosomal Translocation t(l5;17) in Human Acute Promyelocytic Leukemia Fuses RARa with a Novel Putative Transcription Factor, PML. *Cell*. 1991;66:663-674.

18. Kastner P, Perez A, Lutz Y, et al. Structure, localization and transcriptional properties of two classes of retinoic acid receptor a fusion proteins in acute promyelocytic leukemia (APL): structural similarities with a new family of oncoproteins. *EMBO Journal*. 1992;11:629-642.

19. Pandolfi PP, Alcalay M, Fagioli M, et al. Genomic variability and alternative splicing generate multiple PML/RARa transcripts that encode aberrant PML proteins and PML/RARa isoforms in acute promyelocytic leukaemia. *EMBO Journal*. 1992;11:1397-1407.

20. Melnick A, Licht JD. Deconstructing a Disease: RARa, Its Fusion Partners, and Their Roles in the Pathogenesis of Acute Promyelocytic Leukemia. *Blood*. 1999;93:3167-3215.

21. Jensen K, Shiels C, Freemont PS. PML protein isoforms and the RBCC/TRIM motif. *Oncogene*. 2001;20:7223-7233.

22. Douer D, Santillana S, Ramezani L, et al. Acute promyelocytic leukaemia in patients originating in Latin America is associated with an increased frequency of the bcr1 subtype of the PML/RARalpha fusion gene. *British Journal of Haematology*. 2003;122:563-570.

23. Ruiz-Argüelles GJ, Garcés-Eisele J, Reyes-Núñez V, Gómez-Rangel JD, Ruiz-Delgado GJ. More on geographic hematology: the breakpoint cluster regions of the PML/RARalpha fusion gene in Mexican Mestizo patients with promyelocytic leukemia are different from those in Caucasians. *Leukemia and Lymphoma*. 2004;45:1365-1368.

24. Sazawal S, Hasan SK, Dutta P, et al. Over-representation of bcr3 subtype of PML/RARalpha fusion gene in APL in Indian patients. *Annals of hematology*. 2005;84(12):781-4.

25. Kane JR, Head DR, Balazs L, et al. Molecular analysis of the PML/RAR alpha chimeric gene in pediatric acute promyelocytic leukemia. *Leukemia*. 1996;10:1296-1302.

26. Kuchenbauer F, Schoch C, Kern W, et al. Impact of FLT3 mutations and promyelocytic leukaemia-breakpoint on clinical characteristics and prognosis in acute promyelocytic leukaemia. *British Journal of Haematology*. 2005;130:196-202.

27. Benedetti L, Levin AA, Scicchitano BM, et al. Characterization of the Retinoid Binding Properties of the Major Fusion Products Present in Acute Promyelocytic Leukemia Cells. *Blood*. 1997;90:1175-1185.

28. Brown D, Kogan S, Lagasse E, et al. A PMLRARalpha transgene initiates murine acute promyelocytic leukemia. *Proceedings of the National Academy of Sciences of the United States of America*. 1997;94:2551-2556.

29. Grisolano JL, Wesselschmidt RL, Pelicci PG, Ley TJ. Altered myeloid development and acute leukemia in transgenic mice expressing PML-RARa under control of cathepsin G regulatory sequences. *Blood*. 1997;89:376-387.

30. Westervelt P, Lane AA, Pollock JL, et al. High-penetrance mouse model of acute promyelocytic leukemia with very low levels of PML-RARa expression. *Blood*. 2003;102:1857-1865.

31. Soignet SL. Clinical Experience of Arsenic Trioxide in Relapsed Acute Promyelocytic Leukemia. *The Oncologist*. 2001;6(suppl2):11-16.

32. Fenaux P, Wang ZZ, Degos L. Treatment of Acute Promyelocytic Leukemia by Retinoids. *Current Topics in Microbiology and Immunology*. 2007;313:101–128.

33. Huang ME, Ye YC, Chen SR, et al. Use of all-trans retinoic acid in the treatment of acute promyelocytic leukemia. *Blood*. 1988;72:567–572.

34. Castaigne S, Chomienne C, Daniel MT, et al. All-trans retinoic acid as a differentiation therapy for acute promyelocytic leukemia. I. Clinical results. *Blood*. 1990;76:1704–1709.

35. Tallman MS, Andersen JW, Schiffer CA, et al. All-trans-retinoic acid in acute promyelocytic leukemia. *New England Journal of Medicine*. 1997;337:1021-1028.

36. Warrell RP, Frankel SR, Miller MH, et al. Differentiation therapy of acute promyelocytic leukemia with tretinoin (all-trans-retinoic acid). *New England Journal of Medicine*. 1991;324(1385-1393).

37. Tallman MS. Treatment of relapsed or refractory acute promyelocytic leukemia. *Best Practice & Research Clinical Haematology*. 2007;20:57-65.

38. Degos L, Wang ZY. All trans retinoic acid in acute promyelocytic leukemia. *Oncogene*. 2001;20:7140-7145.

39. Gallagher RE. Retinoic acid resistance in acute promyelocytic leukemia. *Leukemia*. 2002;16:1940-1958.

40. Sanz MA. Treatment of Acute Promyelocytic Leukemia. *Hematology*. 2006;1:147-155.

41. Early E, Moore MA, Kakizuka A, et al. Transgenic expression of PML/RARa impairs myelopoiesis. *Proceedings of the National Academy of Sciences of the United States of America*. 1996;93:7900-7904.

42. Westervelt P, Ley TJ. Seed Versus Soil: The Importance of the Target Cell for Transgenic Models of Human Leukemias. *Blood*. 1999;93:2143-2148.

43. He LZ, Tribioli C, Rivi R, et al. Acute leukemia with promyelocytic features in PML/RARa transgenic mice. *Proceedings of the National Academy of Sciences of the United States of America*. 1997;94:2551-2556.

44. Pollock JL, Westervelt P, Kurichety AK, et al. A bcr-3 isoform of RARa-PML potentiates the development of PML-RARa-driven acute promyelocytic leukemia. *Proceedings of the National Academy of Sciences of the United States of America*. 1999;96:11508-15103.

45. Kelly LM, Kutok JL, Williams IR, et al. PML/RARa and FLT3-ITD induce an APL-like disease in a mouse model. *Proceedings of the National Academy of Sciences of the United States of America*. 2002;99:8283-8288.

46. Kogan SC, Brown DE, Schultz DB, et al. BCL-2 cooperates with promyelocytic leukemia retinoic acid receptor a chimeric protein (PMLRARa) to block neutrophil differentiation and initiate acute leukemia. *Journal of Experimental Medicine*. 2001;193:531-543.

47. Gilliland DG, Chang I, Kutok JL, et al. Conditional expression of oncogenic K-ras in mice induces a myeloproliferative disease and cooperates with PML-RARa in development of an acute promyelocytic leukemia-like disease. *Blood*. 2003;102:24a.

48. Rego EM, Wang ZG, Peruzzi D, et al. Role of promyelocytic leukemia (PML) protein in tumor suppression. *Journal of Experimental Medicine*. 2001;193:521-529.

49. Walter MJ, Park JS, Ries RE, et al. Reduced PU.1 expression causes myeloid progenitor expansion and increased leukemia penetrance in mice expressing PML-

RARalpha. *Proceedings of the National Academy of Sciences of the United States of America*. 2005;102(35):12513-8.

50. Yuan W, Payton JE, Holt MS, et al. Commonly dysregulated genes in murine APL cells. *Blood*. 2007;109(3):961-70.

51. Le Beau MM, Davis EM, Patel B, et al. Recurring chromosomal abnormalities in leukemia in PML-RARA transgenic mice identify cooperating events and genetic pathways to acute promyelocytic leukemia. *Blood*. 2003;102:1072-1074.

52. Welch JS, Yuan W, Ley TJ. Expression of PML-RAR by the Murine PML Locus Leads to Myeloid Self-Renewal, Clonal Expansion and Morphologic Promyelocytic Leukemia. *Blood*. 2008;112:932.

53. Lane AA, Lane TJ. Neutrophil elastase is important fopr PML-Retinoic acid receptor a activities in early myeloic cells. *Molecular and Cellular Biology*. 2005;25:23-33.

54. Wojiski S, Guibal FC, Kindler T, et al. PML-RARalpha initiates leukemia by conferring properties of self-renewal to committed promyelocytic progenitors. *Leukemia : official journal of the Leukemia Society of America, Leukemia Research Fund, U.K*. 2009;23(8):1462-71.

55. Uy GL, Payton JE, Ley TJ. Multilineage Expansion of Lymphoid and Myeloid Cells in Mice Expressing PML-RAR under the Control of the Murine Cathepsin G Locus. *Blood*. 2006;108:2051.

56. Gronemeyer H, Gustafsson JA, Laudet V. Principles for modulation of the nuclear receptor superfamily. *Nature Reviews Drug Discovery*. 2004;3:950-962.

57. Benoit G, Cooney A, Giguere V, et al. International Union of Pharmacology. LXVI. Orphan Nuclear Receptors. *Pharmacological Reviews*. 2006;58:798-836.

58. Bourguet W, Germain P, Gronemeyer H. Nuclear receptor ligand-binding domains: 3D stuctures, molecular interactions and pharmacological implications. *Trends in Pharmacological Sciences*. 2000;21:381-388.

59. Wurtz JM, Bourguet W, Renaud JP, et al. A canonical structure for the ligand-binding domain of nuclear receptors. *Nature Structural Biology*. 1996;3(87-94).

60. Chen JD, Evans RM. A transcriptional co-repressor that interacts with nuclear hormone receptors. *Nature*. 1995;377:454-457.

61. Heinzel T, Lavinsky RM, Mullen TM, et al. A complex containing N-CoR, mSin3 and histone deacetylase mediates transcriptional repression. *Nature*. 1997;387:43-48.

62. Germain P, Chambon P, Eichele G, et al. International Union of Pharmacology. LX. Retinoic acid receptors. *Pharmacological Reviews*. 2006;58:712-725.

63. Germain P, Chambon P, Eichele G, et al. International Union of Pharmacology. LXIII. Retinoid X receptors. *Pharmacological Reviews*. 2006;58:760-772.

64. Kastner P, Mark M, Ghyselinck N, et al. Genetic evidence that the retinoid signal is transduced by heterodimeric RXR/RAR functional units during mouse development. *Development*. 1997;(124):313-326.

65. Glass CK. Differential recognition of target genes by nuclear receptor monomers, dimers and heterodimers. *Endocrine Reviews*. 1994;15:391-407.

66. Umesono K, Murakami KK, Thompson CC, Evans RM. Direct repeats as selective response elements for the thyroid hormone, retinoic acid, and vitamin D3 receptors. *Cell*. 1991;65(1255-1266).

67. Zechel C, Shen XQ, Chambon P, Gronemeyer H. Dimerization interfaces formed between the DNA binding domains determine the cooperative binding of RXR/RAR and RXR/TR heterodimers to DR5 and DR4 elements. *EMBO Journal*. 1994;13:1414-1424.

68. Kurokawa R, DiRenzo J, Boehm M, et al. Regulation of retinoid signaling by receptor polarity and allosteric control of ligand binding. *Nature*. 1994;371:528-531.

69. Kurokawa R, Soderstrom M, Horlein A, et al. Polarity-specific activities of retinoic acid receptors determined by a co-repressor. *Nature*. 1995;377:451-454.

70. Rastinejad F, Wagner T, Zhao Q, Khorasanizadeh S. Structure of the RXR-RAR DNA-binding complex on the retinoic acid response element DR1. *EMBO Journal*. 2000;19:1045-1054.

71. Labrecque J, Allan D, Chambon P, et al. Impaired granulocytic differentiation in vitro in hematopoietic cells lacking retinoic acid receptors alpha1 and gamma. *Blood*. 1998;92:607-615.

72. Leroy P, Krust A, Zelent A, et al. Multiple isoforms of the mouse retinoic acid receptor alpha are generated by alternative splicing and differential induction by retinoic acid. *EMBO Journal*. 1991;10:59-69.

73. Li E, Sucov HM, Lee KF, Evans RM, Jaenisch R. Normal development and growth of mice carrying a targeted disruption of the alpha 1 retinoic acid receptor gene. *Proceedings of the National Academy of Sciences of the United States of America*. 1993;90:1590-1594.

74. Luftkin T, Lohnes D, Mark M, et al. High postnatal lethality and testis degeneration in retinoic acid receptor alpha mutant mice. *Proceedings of the National Academy of Sciences of the United States of America*. 1993;90:7225-7229.

75. Kastner P, Lawrence HJ, Waltzinger C, et al. Positive and negative regulation of granulopoiesis by endogenous RARalpha. *Blood*. 2001;97(1314-1320).

76. Collins SJ. The role of retinoids and retinoic acid receptors in normal hematopoiesis. *Leukemia*. 2002;16:1896-1905.

77. Kuwata T, Wang IM, Tamura T, et al. Vitamin A deficiency in mice causes a systemic expansion of myeloid cells. *Blood*. 2000;95:3349–3356.

78. Tsai S, Collins S. A dominant negative retinoic acid receptor blocks neutrophil differentiation at the promyelocyte stage. *Proceedings of the National Academy of Sciences of the United States of America*. 1993;90:7153-7157.

79. Chang KS, Fan YH, Andreef M, Liu J, Mu ZM. The PML gene enodes a phophoprotein associated with the nuclear matrix. *Blood*. 1995;85:3646-3653.

80. Dyck JA, Maul GG, Miller J, et al. A novel macromolecular structure is a target of the promyelocytic-retinoic acid receptor. *Cell*. 1994;76:333-343.

81. Fagioli M, Alacay M, Pandolfi PP, et al. Alternative splicing of PML transcripts predicts coexpression of several carboxy-terminally different protein isoforms. *Oncogene*. 1992;7:1083-1091.

82. Salomoni P, Bellodi C. New insights into the cytoplasmic function of PML. *Histology and Histopathology*. 2007;22:937-946.

83. Condemine W, Takahashi Y, Zhu J, et al. Characterization of endogenous human promyelocytic leukemia isoforms. *Cancer Research*. 2006;66:6192-6198.

84. Fogal V, Gostissa M, Sandy P, et al. Regulation of p53 activity in nuclear bodies by a specific PML isoform. *EMBO Journal*. 2000;19:6185-6195.

85. Wu WS, Vallian S, Seto E, et al. The growth suppressor PML represses transcription by functionally and physically interacting with histone deacetylases. *Molecular and Cellular Biology*. 2001;21:2259-2268.

86. Wang ZG, Delva L, Gaboli M, et al. Role of PML in Cell Growth and the Retinoic Acid Pathway. *Science*. 1998;279:1547-1551.

87. Mu ZM, Chin KV, Liu JH, Lozano G, Chang KS. PML, a growth suppressor disrupted in acute promyelocytic leukemia. *Molecular and Cellular Biology*. 1994;14:6858-6867.

88. Wang ZG, Ruggero D, Ronchetti S, et al. Pml is essential for multiple apoptotic pathways. *Nature Genetics*. 1998;20:266-272.

89. Dellaire G, Bazett-Jones DP. PML nuclear bodies: dynamic sensors of DNA damage and cellular stress. *Bioessays*. 2004;26:963-977.

90. Jansen JH, Mahfoudi A, Rambaud S, et al. Multimeric complexes of the PML-retinoic acid receptor a fusion protein in acute promyelocytic leukemia cells and interferences with retinoic and peroxisome-proliferator signaling pathways. *Proceedings of the National Academy of Sciences of the United States of America*. 1995;92:7401-7405.

91. Perez A, Kastner P, Sethi S, et al. PMLRAR homodimers: distinct DNA binding properties and heterodimeric interactions with RXR. *EMBO Journal*. 1993;12:3171-3182.

92. Hauksdottir H, Privalsky ML. DNA recognition by the aberrant retinoic acid receptors implicated in human acute promyelocytic leukemia. *Cell Growth and Differentiation*. 2001;12:85-98.

93. Kamashev D, Vitoux D, de The H. PML-RARA-RXR oligomers mediate retinoid and rexinoid/cAMP cross-talk in acute promyelocytic leukemia cell differentiation. *Journal of Experimental Medicine*. 2004;199:1163-1174.

94. Zhu J, Nasr R, Peres L, et al. RXR Is an Essential Component of the Oncogenic PML/RARA Complex In Vivo. *Cancer Cell*. 2007;12:23–35.

95. Meani N, Minardi S, Licciulli S, et al. Molecular signature of retinoic acid treatment in acute promyelocytic leukemia. *Oncogene*. 2005;24:3358-3368.

96. Hoemme C, Peerzada A, Behre G, et al. Chromatin modifications induced by PML-RARalpha repress critical targets in leukemogenesis as analyzed by ChIP-Chip. *Blood*. 2008;111(5):2887-95.

97. Martens JH, Brinkman AB, Simmer F, et al. PML-RARalpha/RXR Alters the Epigenetic Landscape in Acute Promyelocytic Leukemia. *Cancer cell*. 2010;17(2):173-85.

98. Wang K, Wang P, Shi J, et al. PML/RARalpha targets promoter regions containing PU.1 consensus and RARE half sites in acute promyelocytic leukemia. *Cancer cell*. 2010;17(2):186-97.

99. Grignani F, De Metteis S, Nervi C, et al. Fusion proteins of the retinoic acid receptor-a recruit histone deacteylase in promyelocytic leukemia. *Nature*. 1998;391:815-818.

100. Guidez F, Ivins S, Zhu J, et al. Reduced retinoic acid-sensitivities of nuclear receptor co-repressor binding to PML- and PLZF-RARa underlie molecular pathogenesis and treatment of acute promyelocytic leukemia. *Blood*. 1998;91:2634-2642.

101. He LZ, Guidez F, Triboli C, et al. Distinct interactions of PML-RARa and PLZF-RARa with co-repressors determine differential responses to RA in APL. *Nature Genetics*. 1998;18:126-135.

102. Lin RJ, Nagy L, Inoue S, et al. Role of the histone deacetylase complex in acute promyelocytic leukemia. *Nature*. 1998;391:811-814.

103. Grignani F, Gelmetti V, Fanelli M, et al. Formation of PML/RARa high molecular weight complexes through the PML coiled-coil region is essential for the PML/RARa-mediated retinoic acid response. *Oncogene*. 1999;18:6313-6321.

104. Li Leo, C., Zhu, J., Wu, X., O'Neil, J., Park, E.J., Chen, J.D. H. Sequestration and inhibition of daxx-mediated transcriptional repression by PML. *Molecular and Cellular Biology*. 2000;20:1784–1796.

105. Ishov Sotnikov, A.G., Negorev, D., Vladimirova, O.V., Neff, N., Kamitani, T., Yeh, E., Strauss, J., Maul, G. AM. PML is critical for ND10 formation and recruits the PML-interacting protein Daxx to this nuclear structure when modified by SUMO-1. *Journal of Cell Biology*. 1999;147:221–234.

106. Muromoto R, Sugiyama K, Takachi A, et al. Physical and Functional Interactions between Daxx and DNA Methyltransferase 1-Associated Protein, DMAP1. *Journal of Immunology*. 2004;172:2985-2993.

107. Zhu J, Zhou J, Peres L, et al. A sumoylation site in PML/RARA is essential for leukemic transformation. *Cancer Cell*. 2005;7:143-153.

108. Villa R, Pasini D, Gutierrez A, et al. Role of the polycomb repressive complex 2 in acute promyelocytic leukemia. *Cancer Cell*. 2007;11:513-525.

109. Carbone R, Botrugno OA, Ronzoni S, et al. Recruitment of the Histone Methyltransferase SUV39H1 and Its Role in the Oncogenic Properties of the Leukemia-Associated PML-Retinoic Acid Receptor Fusion Protein. *Molecular and Cellular Biology*. 2006;26:1288–1296.

110. Figueroa ME, Lugthart S, Li Y, et al. DNA methylation signatures identify biologically distinct subtypes in acute myeloid leukemia. *Cancer cell*. 2010;17(1):13-27. Available at: http://www.ncbi.nlm.nih.gov/pubmed/20060365.

111. Reineke EL, Liu H, Lam M, Liu Y, Kao HY. Aberrant association of promyelocytic leukemia protein-retinoic acid receptor-alpha with coactivators contributes to its ability to regulate gene expression. *Journal of Biological Chemistry*. 2007;282:18584-18596.

112. Doucas V, Brockes JP, Yaniv M, De The H, Dejean A. The PML-retinoic acid receptor a translocation converts the receptor from an inhibitor to a retinoic acid-dependent activator of transcription factor AP-1. *Proceedings of the National Academy of Sciences of the United States of America*. 1993;90:9345-9349.

113. Insinga A, Monestiroli S, Ronzoni S, et al. Impairment of p53 acetylation, stability and function by an oncogenic transcription factor. *EMBO Journal*. 2004;23:1144-1154.

114. Yoshida H, H HI, Tagata Y, et al. PML-RARA inhibits PML IV enhancement of PU.1-induced C/EBP{epsilon} expression in myeloid differentiation. *Molecular and Cellular Biology*. 2007; 27: 5819-5834.

115. van Wageningen S, Breems-de Ridder MC, Nigten J, et al. Gene transactivation without direct DNA binding defines a novel gain-of-function for PML-RARalpha. *Blood*. 2008;111(3):1634-43.

116. Yan J, Wang K, Dong L, et al. PML/RARalpha fusion protein transactivates the tissue factor promoter through a GAGC-containing element without direct DNA association. *Proceedings of the National Academy of Sciences of the United States of America*. 2010;107(8):3716-21.

117. van Wageningen S. Downstream effects of the PML-RARA fusion in acute promyelocytic leukemia. 2008:44-46.

118. Kogan SC, Hong S, Shultz DB, Privalsky ML, Bishop JM. Leukemia initiated by PMLRARa: the PMLdomain plays a critical role while retinoic acid–mediated transactivation is dispensable. *Blood*. 2000;95:1541-1550.

119. Alcalay M, Zangrilli D, Fagioli M, et al. Expression pattern of the RARa-PML fusion gene in acute promyelocytic leukemia. *Proceedings of the National Academy of Sciences of the United States of America*. 1992;89:4840-4844.

120. Sternsdorf T, Phan VT, Maunakea ML, et al. Forced retinoic receptor a homodimers prime mice for APL-like leukemia. *Cancer Cell*. 2006;9:81-94.

121. Matsushita H, Scaglioni PP, Bhaumik M, et al. In vivo analysis of the role of aberrant histone deacetylase recruitment and RAR alpha blockade in the pathogenesis of acute promyelocytic leukemia. *The Journal of experimental medicine*. 2006;203(4):821-8.

122. Zayed A, Couban S, Hayne O, et al. Acute promyelocytic leukemia: a novel PML/RARalpha fusion that generates a frameshift in the RARalpha transcript and ATRA resistance. *Leukemia and Lymphoma*. 2007;48:489-496.

123. Ferrucci PR, Grignani F, Pearson M, et al. Cell death induction by the acute promyelocytic leukemia-specific PML/RARalpha fusion protein. *Proceedings of the National Academy of Sciences of the United States of America*. 1997;94:10901-10906.

124. Lane AA, Ley TJ. Neutrophil elastase cleaves PML-RARa and is important for the development of acute promyelocytic leukemia in mice. *Cell*. 2003;115:305-3018.

125. Schoch C, Kohlmann A, Schnittger S, et al. Acute myeloid leukemias with reciprocal rearrangements can be distinguished by specific gene expression profiles. *Proceedings of the National Academy of Sciences of the United States of America*. 2002;99:10008-100013.

126. Bullinger L, Döhner K, Bair E, et al. Use of gene-expression profiling to identify prognostic subclasses in adult acute myeloid leukemia. *New England Journal of Medicine*. 2004;350:1605-1616.

127. Gutierrez NC, Lopez-Perez R, Hernandez JM, et al. Gene expression profile reveals deregulation of genes with relevant functions in the different subclasses of acute myeloid leukemia. *Leukemia*. 2005;19:402-409.

128. Valk PJ, Verhaak RG, Beijen MA, et al. Prognostically useful gene-expression profiles in acute myeloid leukemia. *New England Journal of Medicine*. 2004;350(1617-1628).

129. Ross ME, Mahfouz R, Onciu M, et al. Gene expression profiling of pediatric acute myelogenous leukemia. *Blood*. 2004;104:3679-3687.

130. Casorelli I, Tenedini E, Tagliafico E, et al. Identification of a molecular signature for leukemic promyelocytes and their normal counterparts: focus on DNA repair genes. *Leukemia*. 2006;20:1978–1988.

131. Payton JE, Grieselhuber NR, Chang L, et al. High throughput digital quantification of mRNA abundance in primary human acute myeloid leukemia samples. *The Journal of clinical investigation*. 2009;119(6):1714-26.

132. Fortini ME. Notch signaling: the core pathway and its posttranslational regulation. *Developmental cell*. 2009;16(5):633-47.

133. Gazave E, Lapébie P, Richards GS, et al. Origin and evolution of the Notch signalling pathway: an overview from eukaryotic genomes. *BMC evolutionary biology*. 2009;9:249.

134. Aster JC, Pear WS, Blacklow SC. Notch Signaling in Leukemia. *Annual Review of Pathology: Mechanisms of Disease*. 2008;3(1):587-613.

135. Kopan R, Ilagan MX. The canonical Notch signaling pathway: unfolding the activation mechanism. *Cell*. 2009;137(2):216-33.

136. Jafar-Nejad H, Leonardi J, Fernandez-Valdivia R. Role of Glycans and Glycosyltransferases in the Regulation of Notch Signaling. *Glycobiology*. 2010.

137. Visan I, Tan JB, Yuan JS, et al. Regulation of T lymphopoiesis by Notch1 and Lunatic fringe-mediated competition for intrathymic niches. *Nature immunology*. 2006;7(6):634-43.

138. Porter RL, Calvi LM. Communications between bone cells and hematopoietic stem cells. *Archives of biochemistry and biophysics*. 2008;473(2):193-200.

139. D'Souza B, Miyamoto A, Weinmaster G. The many facets of Notch ligands. *Oncogene*. 2008;27(38):5148-67.

140. Radtke F, Fasnacht N, Macdonald HR. Notch signaling in the immune system. *Immunity*. 2010;32(1):14-27.

141. Pintar A, De Biasio A, Popovic M, Ivanova N, Pongor S. The intracellular region of Notch ligands: does the tail make the difference? *Biology direct*. 2007;2:19.

142. Hock B, Böhme B, Karn T, et al. PDZ-domain-mediated interaction of the Eph-related receptor tyrosine kinase EphB3 and the ras-binding protein AF6 depends on the kinase activity of the receptor. *Proceedings of the National Academy of Sciences of the United States of America*. 1998;95(17):9779-84.

143. Ascano JM, Beverly LJ, Capobianco AJ. The C-terminal PDZ-ligand of JAGGED1 is essential for cellular transformation. *The Journal of biological chemistry*. 2003;278(10):8771-9.

144. Six EM, Ndiaye D, Sauer G, et al. The notch ligand Delta1 recruits Dlg1 at cell-cell contacts and regulates cell migration. *The Journal of biological chemistry*. 2004;279(53):55818-26.

145. Blaumueller CM, Qi H, Zagouras P, Artavanis-Tsakonas S. Intracellular cleavage of Notch leads to a heterodimeric receptor on the plasma membrane. *Cell*. 1997;90(2):281-91.

146. van Tetering G, van Diest P, Verlaan I, et al. Metalloprotease ADAM10 is required for Notch1 site 2 cleavage. *The Journal of biological chemistry*. 2009;284(45):31018-27.

147. Hsieh JJ, Henkel T, Salmon P, et al. Truncated mammalian Notch1 activates CBF1/RBPJk-repressed genes by a mechanism resembling that of Epstein-Barr virus EBNA2. *Molecular and cellular biology*. 1996;16(3):952-9.

148. Hsieh JJ, Zhou S, Chen L, Young DB, Hayward SD. CIR, a corepressor linking the DNA binding factor CBF1 to the histone deacetylase complex. *Proceedings of the National Academy of Sciences of the United States of America*. 1999;96(1):23-8.

149. Fryer CJ, Lamar E, Turbachova I, Kintner C, Jones KA. Mastermind mediates chromatin-specific transcription and turnover of the Notch enhancer complex. *Genes & development*. 2002;16(11):1397-411.

150. Fryer CJ, White JB, Jones KA. Mastermind recruits CycC:CDK8 to phosphorylate the Notch ICD and coordinate activation with turnover. *Molecular cell*. 2004;16(4):509-20.

151. Tsunematsu R, Nakayama K, Oike Y, et al. Mouse Fbw7/Sel-10/Cdc4 is required for notch degradation during vascular development. *The Journal of biological chemistry*. 2004;279(10):9417-23.

152. Song LL, Peng Y, Yun J, et al. Notch-1 associates with IKKalpha and regulates IKK activity in cervical cancer cells. *Oncogene*. 2008;27(44):5833-44.

153. Gustafsson MV, Zheng X, Pereira T, et al. Hypoxia requires notch signaling to maintain the undifferentiated cell state. *Developmental cell*. 2005;9(5):617-28.

154. Le Gall M, De Mattei C, Giniger E. Molecular separation of two signaling pathways for the receptor, Notch. *Developmental biology*. 2008;313(2):556-67.

155. Sade H, Krishna S, Sarin A. The anti-apoptotic effect of Notch-1 requires p56lck-dependent, Akt/PKB-mediated signaling in T cells. *The Journal of biological chemistry*. 2004;279(4):2937-44.

156. Krebs LT, Shutter JR, Tanigaki K, et al. Haploinsufficient lethality and formation of arteriovenous malformations in Notch pathway mutants. *Genes & development*. 2004;18(20):2469-73.

157. Koo B, Lim H, Song R, et al. Mind bomb 1 is essential for generating functional Notch ligands to activate Notch. *Development (Cambridge, England)*. 2005;132(15):3459-70.

158. Parks AL, Klueg KM, Stout JR, Muskavitch MA. Ligand endocytosis drives receptor dissociation and activation in the Notch pathway. *Development (Cambridge, England)*. 2000;127(7):1373-85.

159. Nichols JT, Miyamoto A, Olsen SL, et al. DSL ligand endocytosis physically dissociates Notch1 heterodimers before activating proteolysis can occur. *The Journal of cell biology*. 2007;176(4):445-58.

160. Le Borgne R, Bardin A, Schweisguth F. The roles of receptor and ligand endocytosis in regulating Notch signaling. *Development (Cambridge, England)*. 2005;132(8):1751-62.

161. Vetrivel KS, Cheng H, Lin W, et al. Association of gamma-secretase with lipid rafts in post-Golgi and endosome membranes. *The Journal of biological chemistry*. 2004;279(43):44945-54.

162. Cumano A, Godin I. Ontogeny of the hematopoietic system. *Annual review of immunology*. 2007;25:745-85.

163. Gering M, Patient R. Notch signalling and haematopoietic stem cell formation during embryogenesis. *Journal of cellular physiology*. 2010;222(1):11-6.

164. Kumano K, Chiba S, Kunisato A, et al. Notch1 but not Notch2 is essential for generating hematopoietic stem cells from endothelial cells. *Immunity*. 2003;18(5):699-711.

165. Bertrand JY, Cisson JL, Stachura DL, Traver D. Notch signaling distinguishes 2 waves of definitive hematopoiesis in the zebrafish embryo. *Blood*. 2010;115(14):2777-83.

166. Yoon M, Koo B, Song R, et al. Mind bomb-1 is essential for intraembryonic hematopoiesis in the aortic endothelium and the subaortic patches. *Molecular and cellular biology*. 2008;28(15):4794-804.

167. Robert-Moreno A, Espinosa L, de la Pompa JL, Bigas A. RBPjkappa-dependent Notch function regulates Gata2 and is essential for the formation of intra-embryonic hematopoietic cells. *Development (Cambridge, England)*. 2005;132(5):1117-26.

168. Robert-Moreno A, Guiu J, Ruiz-Herguido C, et al. Impaired embryonic haematopoiesis yet normal arterial development in the absence of the Notch ligand Jagged1. *The EMBO journal*. 2008;27(13):1886-95.

169. de Pooter RF, Schmitt TM, de la Pompa JL, et al. Notch signaling requires GATA-2 to inhibit myelopoiesis from embryonic stem cells and primary hemopoietic progenitors. *Journal of immunology (Baltimore, Md. : 1950)*. 2006;176(9):5267-75.

170. Karanu FN, Murdoch B, Gallacher L, et al. The notch ligand jagged-1 represents a novel growth factor of human hematopoietic stem cells. *The Journal of experimental medicine*. 2000;192(9):1365-72.

171. Delaney C, Heimfeld S, Brashem-Stein C, et al. Notch-mediated expansion of human cord blood progenitor cells capable of rapid myeloid reconstitution. *Nature medicine*. 2010;16(2):232-6.

172. Suzuki T, Yokoyama Y, Kumano K, et al. Highly efficient ex vivo expansion of human hematopoietic stem cells using Delta1-Fc chimeric protein. *Stem cells (Dayton, Ohio)*. 2006;24(11):2456-65.

173. Varnum-Finney B, Purton LE, Yu M, et al. The Notch ligand, Jagged-1, influences the development of primitive hematopoietic precursor cells. *Blood*. 1998;91(11):4084-91.

174. Varnum-Finney B, Xu L, Brashem-Stein C, et al. Pluripotent, cytokine-dependent, hematopoietic stem cells are immortalized by constitutive Notch1 signaling. *Nature medicine*. 2000;6(11):1278-81.

175. Mancini SJ, Mantei N, Dumortier A, et al. Jagged1-dependent Notch signaling is dispensable for hematopoietic stem cell self-renewal and differentiation. *Blood*. 2005;105(6):2340-2.

176. Saito T, Chiba S, Hirai H. Notch2 deficient bone marrow cells can reconstitute both to lymphoid and myeloid lineages. *Blood*. 2001;98:68a.

177. Maillard I, Koch U, Dumortier A, et al. Canonical notch signaling is dispensable for the maintenance of adult hematopoietic stem cells. *Cell stem cell*. 2008;2(4):356-66.

178. Maeda T, Merghoub T, Hobbs RM, et al. Regulation of B versus T lymphoid lineage fate decision by the proto-oncogene LRF. *Science (New York, N.Y.)*. 2007;316(5826):860-6.

179. Calvi LM, Adams GB, Weibrecht KW, et al. Osteoblastic cells regulate the haematopoietic stem cell niche. *Nature*. 2003;425(6960):841-6.

180. Fernandez L, Rodriguez S, Huang H, et al. Tumor necrosis factor-alpha and endothelial cells modulate Notch signaling in the bone marrow microenvironment during inflammation. *Experimental hematology*. 2008;36(5):545-558.

181. Johnston DA, Dong B, Hughes CC. TNF induction of jagged-1 in endothelial cells is NFkappaB-dependent. *Gene*. 2009;435(1-2):36-44.

182. Hilton MJ, Tu X, Wu X, et al. Notch signaling maintains bone marrow mesenchymal progenitors by suppressing osteoblast differentiation. *Nature medicine*. 2008;14(3):306-14.

183. Engin F, Yao Z, Yang T, et al. Dimorphic effects of Notch signaling in bone homeostasis. *Nature medicine*. 2008;14(3):299-305.

184. Nobta M, Tsukazaki T, Shibata Y, et al. Critical Regulation of Bone Morphogenetic Protein-induced Osteoblastic Differentiation by Delta1/Jagged1-activated Notch1 Signaling. *Journal of Biological Chemistry*. 2005;280(16):15842-48.

185. Tezuka K, Yasuda M, Watanabe N, et al. Stimulation of osteoblastic cell differentiation by Notch. *Journal of bone and mineral research : the official journal of the American Society for Bone and Mineral Research*. 2002;17(2):231-9.

186. Bai S, Kopan R, Zou W, et al. NOTCH1 Regulates Osteoclastogenesis Directly in Osteoclast Precursors and Indirectly via Osteoblast Lineage Cells. *Journal of Biological Chemistry*. 2008;283(10):6509-18.

187. Kim Y, Koo B, Jeong H, et al. Defective Notch activation in microenvironment leads to myeloproliferative disease. *Blood*. 2008;112(12):4628-38.

188. Qyang Y, Chambers SM, Wang P, et al. Myeloproliferative disease in mice with reduced presenilin gene dosage: effect of gamma-secretase blockage. *Biochemistry*. 2004;43(18):5352-9.

189. Ellisen L, Bird J, West DC, et al. TAN-1, the human homolog of the Drosophila Notch gene, is broken by chromosomal translocations in T lymphoblastic neoplasms. *Cell*. 1991;66(4):649-661.

190. Pear WS, Aster JC, Scott ML, et al. Exclusive development of T cell neoplasms in mice transplanted with bone marrow expressing activated Notch alleles. *The Journal of experimental medicine*. 1996;183(5):2283-91.

191. Weng AP, Ferrando AA, Lee W, et al. Activating mutations of NOTCH1 in human T cell acute lymphoblastic leukemia. *Science (New York, N.Y.)*. 2004;306(5694):269-71.

192. O'Neil J, Grim J, Strack P, et al. FBW7 mutations in leukemic cells mediate NOTCH pathway activation and resistance to gamma-secretase inhibitors. *The Journal of experimental medicine*. 2007;204(8):1813-24.

193. Palomero T, Lim WK, Odom DT, et al. NOTCH1 directly regulates c-MYC and activates a feed-forward-loop transcriptional network promoting leukemic cell growth. *Proceedings of the National Academy of Sciences of the United States of America*. 2006;103(48):18261-6.

194. Chen DY, Liu H, Takeda S, et al. Taspase1 functions as a non-oncogene addiction protease that coordinates cancer cell proliferation and apoptosis. *Cancer research*. 2010;70(13):5358-67.

195. Takeda S, Chen DY, Westergard TD, et al. Proteolysis of MLL family proteins is essential for taspase1-orchestrated cell cycle progression. *Genes & development*. 2006;20(17):2397-409.

196. Joshi I, Minter LM, Telfer J, et al. Notch signaling mediates G1/S cell-cycle progression in T cells via cyclin D3 and its dependent kinases. *Blood*. 2009;113(8):1689-98.

197. Lu ZH, Books JT, Ley TJ. Cold shock domain family members YB-1 and MSY4 share essential functions during murine embryogenesis. *Molecular and cellular biology*. 2006;26(22):8410-7.

198. Palomero T, Dominguez M, Ferrando AA. The role of the PTEN/AKT Pathway in NOTCH1-induced leukemia. *Cell cycle (Georgetown, Tex.)*. 2008;7(8):965-70.

199. Sarmento LM, Huang H, Limon A, et al. Notch1 modulates timing of G1-S progression by inducing SKP2 transcription and p27 Kip1 degradation. *The Journal of experimental medicine*. 2005;202(1):157-68.

200. Vilimas T, Mascarenhas J, Palomero T, et al. Targeting the NF-kappaB signaling pathway in Notch1-induced T-cell leukemia. *Nature medicine*. 2007;13(1):70-7.

201. Palomero T, McKenna K, O-Neil J, et al. Activating mutations in NOTCH1 in acute myeloid leukemia and lineage switch leukemias. *Leukemia : official journal of the Leukemia Society of America, Leukemia Research Fund, U.K*. 2006;20(11):1963-6.

202. Mercher T, Cornejo MG, Sears C, et al. Notch signaling specifies megakaryocyte development from hematopoietic stem cells. *Cell stem cell*. 2008;3(3):314-26.

203. Mercher T, Raffel GD, Moore SA, et al. The OTT-MAL fusion oncogene activates RBPJ-mediated transcription and induces acute megakaryoblastic leukemia in a knockin mouse model. *The Journal of clinical investigation*. 2009;119(4):852-64.

204. Salat D, Liefke R, Wiedenmann J, Borggrefe T, Oswald F. ETO, but not leukemogenic fusion protein AML1/ETO, augments RBP-Jkappa/SHARP-mediated repression of notch target genes. *Molecular and cellular biology*. 2008;28(10):3502-12.

205. Alcalay M, Meani N, Gelmetti V, et al. Acute myeloid leukemia fusion proteins deregulate genes involved in stem cell maintenance and DNA repair. *The Journal of clinical investigation*. 2003;112(11):1751-61.

206. Nakahara F, Sakata-Yanagimoto M, Komeno Y, et al. Hes1 immortalizes committed progenitors and plays a role in blast crisis transition in chronic myelogenous leukemia. *Blood*. 2010;115(14):2872-81.

207. Gal H, Amariglio N, Trakhtenbrot L, et al. Gene expression profiles of AML derived stem cells; similarity to hematopoietic stem cells. *Leukemia : official journal of the Leukemia Society of America, Leukemia Research Fund, U.K*. 2006;20(12):2147-54.

208. Nemoto N, Suzukawa K, Shimizu S, et al. Identification of a novel fusion gene MLL-MAML2 in secondary acute myelogenous leukemia and myelodysplastic syndrome with inv(11)(q21q23). *Genes, chromosomes & cancer*. 2007;46(9):813-9.

209. Li L, Forman SJ, Bhatia R. Expression of DLK1 in hematopoietic cells results in inhibition of differentiation and proliferation. *Oncogene*. 2005;24(27):4472-6.

210. Sakajiri S, O'kelly J, Yin D, et al. Dlk1 in normal and abnormal hematopoiesis. *Leukemia : official journal of the Leukemia Society of America, Leukemia Research Fund, U.K*. 2005;19(8):1404-10.

211. Qi X, Chen Z, Liu D, Cen J, Gu M. Expression of Dlk1 gene in myelodysplastic syndrome determined by microarray, and its effects on leukemia cells. *International journal of molecular medicine*. 2008;22(1):61-8.

Chapter 2

Definition of the APL dysregulome

This chapter has been published as:

Payton JE*, **Grieselhuber NR***, Chang LW, Murakami MA, Geiss GK, Link DC, Nagarajan R, Watson MA and Ley TJ. High throughput digital quantification of mRNA abundance in primary human acute myeloid leukemia samples. Journal of Clinical Investigation. 2009. 119: 1714-26.

*** denotes equal contribution**

2.1. Abstract

Acute promyelocytic leukemia (APL) is characterized by the t(15;17) chromosomal translocation, which results in fusion of the retinoic acid receptor α (*RARA*) gene to another gene, most commonly promyelocytic leukemia (*PML*). The resulting fusion protein, PML-RARA, initiates APL, which is a subtype (M3) of acute myeloid leukemia (AML). In this report, we identify a gene expression signature that is specific to M3 samples; it was not found in other AML subtypes and did not simply represent the normal gene expression pattern of primary promyelocytes. To validate this signature for a large number of genes, we tested a recently developed high throughput digital technology (NanoString nCounter). Nearly all of the genes tested demonstrated highly significant concordance with our microarray data ($P < 0.05$). The validated gene signature reliably identified M3 samples in 2 other AML datasets, and the validated genes were substantially enriched in our mouse model of APL, but not in a cell line that inducibly expressed PML-RARA. These results demonstrate that nCounter is a highly reproducible, customizable system for mRNA quantification using limited amounts of clinical material, which provides a valuable tool for biomarker measurement in low-abundance patient samples.

2.2. Introduction

Here we describe what is, to our knowledge, the first use of a high-throughput digital system to assay the expression of a large number of genes in primary clinical samples from patients with acute myeloid leukemia (AML). This technology captures and counts individual mRNA transcripts without enzymatic reactions or bias and is notable for its high levels of sensitivity, linearity, multiplex capability, and digital readout (1). The nCounter system (NanoString) is capable of detecting as little as 0.5 fM of a specific mRNA, making it a valuable tool for expression signature validation, diagnostic testing, and large translational studies, all of which often are limited by the very small amounts of clinical material available.

In this study, our primary clinical focus is on acute promyelocytic leukemia (APL), a subtype (M3) of AML that is unique in its morphology and its defining molecular initiating event. (Throughout this manuscript, we refer to human APL as M3 AML and the mouse models as murine APL.) Morphologically, the leukemic cells are abnormal promyelocytes, which nevertheless retain many of the structural and immunophenotypic characteristics of normal promyelocytes. M3 AML is further characterized by fusion of the retinoic acid receptor α (*RARA*) gene to another gene, most commonly the promyelocytic leukemia (*PML*) gene, through a balanced translocation of chromosomes 17 and 15, respectively. The resulting fusion protein, PML-RARA, has been shown to initiate APL in several mouse models (2–5). Unlike most other AML subtypes, the initiating event of M3 AML is known, making it an attractive model for the study of mechanisms of pathogenesis and progression.

Several recent gene expression profiling studies used microarray technologies to compare subclasses of AML and have reported specific expression signatures for individual morphologic or molecular subtypes (6–18). Although a subset of these studies included normal whole bone marrow or purified myeloid precursor CD34+ cells, none of them included fractionated primary hematopoietic cells from multiple discrete stages of myeloid differentiation (6, 7, 9, 11, 13–15, 17, 18). Because different subtypes of AML represent various arrested developmental stages of hematopoiesis (e.g., M3 versus normal promyelocytes), differences in expression may result from these developmental stages rather than a fundamental difference in pathogenesis or progression. The inclusion of normal, primary fractionated myeloid precursors, including promyelocytes, could mitigate this potential pitfall.

Another shortcoming of many gene expression profiling studies, including the AML studies above, is that only a small number of genes have been validated in a small number of samples, due to limiting amounts of clinical material available and the labor-intensive and costly nature of quantitative RT-PCR–based (qRT-PCR–based) validation. In this study, we have overcome these limitations with a digital RNA quantitation system, which allowed triplicate measurements of the expression levels of 46 genes, using only 100 ng of total RNA (the amount obtained from approximately 40,000 myeloid cells) in a multiplex reaction. Thus, the confidence of our M3-specific signature is substantially increased by such extensive validation.

In the current study, we compare M3 cell expression patterns with those of other AML subtypes and to normal CD34+ cells, promyelocytes, and neutrophils purified from independent healthy human bone marrow samples using high-speed flow cytometry.

Using these data, we define a unique expression signature of M3 malignant promyelocytes, which is distinct both from other subtypes of AML and from normal promyelocytes. A subset of the most highly dysregulated genes in this signature were extensively validated using both conventional (qRT-PCR) and innovative (NanoString nCounter system; ref. 1) methodologies.

We further used gene set enrichment analysis (GSEA) (19, 20) to evaluate our validated gene set in 3 other datasets: a published set of 325 human AML samples (18), a mouse model of APL (5), and the PR-9 cell line (21), which is commonly used in studies of PML-RARA activity. Both the human M3 AML and murine APL samples demonstrated significant enrichment of the validated gene set. However, the PR-9 cells failed to show significant enrichment of this gene set after induction of the PML-RARA transgene.

Importantly, the validated genes reliably identified bona fide M3 samples (PML-RARA fusion gene positive), separating them from other FAB subtypes in 3 independent AML datasets.

2.3. Results

In order to identify genes that are specifically dysregulated in M3 AML cells, we compared the gene expression patterns of M3 samples to those of normal myeloid cells at various stages of differentiation. We collected bone marrow from healthy donors and immediately fractionated it into CD34+ cells, promyelocytes, or neutrophils. CD34+ cells were isolated after incubation with an anti-CD34 antibody and separation on a Miltenyi Biotec MACS column, resulting in greater than 90% purity, as validated by flow

cytometry (data not shown). To ensure a high-quality expression analysis of normal promyelocytes, we refined a previously described flow cytometry–based methodology (22) to obtain a large number of highly enriched cells. After red cell lysis, whole bone marrow was incubated with antibodies to CD9, CD14, CD15, and CD16. Washed cells were sorted and collected on a Dako MoFlo flow cytometer as follows: CD9–, CD14–, CD15+, and CD16lo (for promyelocytes) and CD9–, CD14–, CD15+ and CD16hi for neutrophils. (See Methods for details; Figure 2-1A for flow cytometric plots; and Figure 2-1B for photomicrographs of sorted cells.) Cell purity for all myeloid cell fractions was high: the average promyelocyte purity exceeded 80%, and neutrophil and band purity was greater than 95%, as determined by manual differentials performed on cytospin samples. RNA isolated from purified cells was analyzed on Affymetrix U133+2 microarrays.

To confirm that each myeloid cell fraction contained cells with gene expression patterns consistent with the predominant cell type, we compared the RNA expression levels of several developmentally regulated myeloid genes (Figure 2-1C). The "early" hematopoietic genes (associated with primitive myeloid precursor cells) *CD34*, *FLT3*, and *KIT* demonstrated much higher expression in the CD34+ cell fraction than in the other 2 fractions. Conversely, the "late" genes (associated with neutrophils) *CTSS*, *FPR1*, *IL8RB*, and *NCF2* were most highly expressed in the neutrophil fraction. Most importantly for this study, the "mid-myeloid," promyelocyte-specific azurophil granule genes *CTSG*, *ELA2*, *MPO*, and *PRTN3* displayed very high expression in the promyelocyte fraction, which decreased by an order of magnitude or more in neutrophils. Further analysis identified genes specifically expressed in each of the 3 fractions. The heat map in Figure 2-1D illustrates a progression of gene expression from less

differentiated to terminally differentiated myeloid cells. The patterns of expression described above support the flow cytometric and morphologic data, demonstrating that each fraction is highly enriched for the target population. Collection of these fractions was essential for a robust comparison of malignant promyelocytes with normal myeloid cells at different stages of differentiation.

For this study, we analyzed 77 de novo AML bone marrow samples obtained at diagnosis. The characteristics of the patients from which these samples were obtained are summarized in Table 2-1 and have previously been described (Discovery set, FAB subtypes M0–M4; ref. 23). Of these samples, 15 were diagnosed as M3; only samples with t(15;17) confirmed by cytogenetics and/or FISH were included in the M3 analysis set (24). The remaining 62 samples consisted of FAB subtypes M0, M1, M2, and M4 with 2 or fewer cytogenetic abnormalities (these FAB subtypes were chosen because they represent the most common AML subtypes and because there were insufficient numbers of M5, M6, or M7 patient samples available for analysis). RNA was prepared from snap-frozen cell pellets of the bone marrow cells and analyzed on Affymetrix U133+2 expression microarrays. We did not fractionate the AML samples for the following reasons: (a) the bone marrow blast percentage for all samples, including M3 abnormal promyelocytes, was high (median >70%), (b) we have previously observed that AML bone marrow aspirates subjected to Ficoll separation of mononuclear cells, compared with unfractionated snap-frozen cell pellets, demonstrated no significant differences in expression by microarray analysis (our unpublished observations), and (c) as of yet, there is no standard cell surface marker that can reliably separate malignant AML cells from normal human hematopoietic cells.

2.3.1. Defining the M3-specific dysregulome.

To identify genes specific to M3 AML, we compared M3 samples to other FAB subtypes and to normal myeloid cells at various stages of differentiation. We established a series of criteria for M3-specific genes: significant differences in expression when compared with non-M3 AML or normal promyelocytes, including up- or downregulation, high expression similar to that of CD34+ myeloid precursor cells, and/or high expression of genes that are not expressed in any of the normal myeloid cells tested. We first performed significance analysis of microarrays (25), using a false discovery rate (FDR) cutoff of 0.05. This analysis identified 2,023 annotated genes (3,787 probe sets) whose expression was significantly up- or downregulated in M3 compared with other AML subtypes, as demonstrated by the clear separation of the two groups in the expression heat map (Figure 2-2A). We observed that some of the genes were expressed at similar levels in both normal and transformed (M3) promyelocytes. Therefore, to exclude genes that are simply markers of the normal promyelocyte developmental stage, and conversely to retain genes that represent aberrant expression of developmentally regulated genes, we filtered these genes based on a comparison with the specific expression signatures identified for normal myeloid cells at 3 stages of differentiation (see Methods and Figure 2-3). In addition to showing significant (FDR < 0.05) differences in expression compared with other AML subtypes, these genes, which we call the M3-specific dysregulome, fulfilled one or more of the following criteria: (a) were CD34+ precursor stage specific but persistently expressed at similar levels in M3 cells (M3: CD34+ precursor fraction ratio, ≥1:1), (b) showed significantly different expression (FDR < 0.05)

from that of normal promyelocytes, and/or (c) showed significantly upregulated M3 expression (FDR <0.05; M3/normal cell fraction ratio, >2:1) and were not expressed in any of the normal myeloid cells tested (greater than 75% absent calls, determined by the MAS 5 algorithm in Affymetrix expression analysis software). The normal promyelocyte filter removed approximately 1,800 probe sets, and the remaining criteria each removed approximately equal numbers of probe sets. The heat map in Figure 2-2B demonstrates clear separation of these 510 up- or downregulated genes in malignant versus normal promyelocytes (listed in Table 2-2).

Many of the genes in the M3-specific signature exhibited dramatic differences in expression level when compared with other AML subtypes or normal promyelocytes. A subset of genes with the greatest level of differential expression is shown in Table 2-3. To investigate genes that may be activated or repressed in M3 AML, equal numbers of up- and downregulated genes were selected for further study and validation. Some of these highly dysregulated genes (such as *HGF*, *FGF13*, and *PPARG*) have been documented in previous reports (6–8, 12, 14). There are also many genes in this list that have not been previously reported to be dysregulated in M3, including *BCL2A1*, *TWIST1*, and *TNFRSF1B*. Of the 40 genes selected for further study, 17 have not previously been reported in other M3 AML expression studies (6–8, 12, 14).

2.3.2. Validation of M3-specific dysregulome.

To validate the findings of the microarray analysis, we selected the 40 genes with the largest average fold changes (both up and down) between M3 and the other AML subtypes. Due to limited sample abundance, we used a high-throughput methodology for

gene validation that allowed us to perform triplicate measurements of expression of 46 genes (the 40 with the highest fold changes, plus 6 developmentally regulated myeloid genes for calibration) with only 100 ng of RNA per replicate. Based on an average RNA yield of 25 μg per 10^7 cells from the bone marrow aspirate samples used in this study, we estimated that 100 ng corresponded to approximately 40,000 cells. The NanoString nCounter Analysis System uses digital technology based on direct multiplexed measurement of gene expression and offers high levels of sensitivity (500 attomolar, i.e., <1 copy per cell), precision, and reproducibility (1). The technology uses molecular barcodes and single-molecule imaging to detect and count hundreds of unique mRNAs in a single reaction (See Methods) (1). In this study the full capacity of the nCounter system was not utilized; up to 500 genes can be assayed in 1 multiplex reaction (1). To confirm the performance of this technology, we selected 6 "calibration" genes known to be differentially expressed in each myeloid cell fraction and in M3 samples. A total of 28 AML (11 M3 and 17 other AML subtypes), 2 CD34+, 5 promyelocyte, and 2 neutrophil samples were analyzed. The NanoString results showed the expected pattern of expression for all 6 calibration genes (compare Figure 2-4, A–C with Figure 2-1C). As shown in Table 2-4, 37 of the 40 M3-specific dysregulome genes were also assayed. The remaining 3 genes, *SYNE1, FUT4*, and *PGDB5*, could not be analyzed due to either inaccurate (*SYNE1* and *FUT4*) or ambiguous (*PGDB5*) mapping of Affymetrix probe set target sequences to the human genome (See footnote in Table 2-3). Data from both methods are plotted for 2 examples each of up- or downregulated genes (*HGF* and *FAM19A5*, *NRIP1* and *TNFRSF1B*, respectively) in Figure 2-5. Data from nCounter and

microarray analyses demonstrate similar patterns of expression in M3 samples relative to other AML subtypes and normal promyelocytes (See Table 2-4 and 2-5).

To more directly compare the nCounter and microarray methods, which have different units of measurement, we transformed each AML data point as a proportion of maximum signal for each probe set (microarray) or probe (nCounter) for all samples. These proportions were then plotted on a graph. As depicted in Figure 2-6, A and B, and Table 2-4, the correlation coefficients between the results of the 2 methods were $r > 0.7$ and statistically significant ($P < 0.05$) for all but 1 gene, CD300A, which may be due to differential targeting of the microarray and nCounter probes (middle and 5′, respectively) to an mRNA with 3 isoforms. Three other genes (*AMICA1, SLC15A3,* and *HK3*) demonstrated similar fold change values and high correlation coefficients compared with the microarray data but did not achieve significance when comparing expression in M3 with other AML subtypes in the nCounter assay. This result may be due to the low overall expression signals shown by both methods (Table 2-5). We also compared fold change ratio measurements (M3/other FAB subtypes) of all genes assayed by both microarray and NanoString. As demonstrated in Figure 2-6C, the correlation between the 2 platforms was very high ($r = 0.963$, $P < 0.05$). Based on the stringent criteria of a significantly high correlation coefficient, similar fold change values, and significant difference in expression (M3 vs. other subtypes and promyelocytes), 33 genes were validated by the nCounter system.

We also performed qRT-PCR for 9 of the 40 M3-specific dysregulome genes in parallel with the nCounter method. For 7 of the 9 genes, qRT-PCR confirmed the significant fold change expression differences among M3, other FAB subtypes, and

normal promyelocytes, as determined by the NanoString and microarray datasets (Table 2-4). Due to the limited abundance of many of our samples, we were unable to perform qRT-PCR assays on all 40 M3-specific dysregulome genes. However, the nCounter method has previously demonstrated strong correlation with qRT-PCR for 21 genes whose expression was measured in quadruplicate at 7 time points (1).

To determine whether the 33 validated genes are similarly dysregulated in AML samples from other studies, we used GSEA (19, 20) to evaluate a published dataset (18) (GSE6891). Expression in this set of 325 primary AML samples demonstrated a highly significant enrichment of the validated 33-gene set (FDR q value = 0.0; Figure 2-7A). In addition, GSEA analysis of expression in one of our mouse models of APL (5) demonstrated significant enrichment (FDR q value = 0.034; Figure 2-7B) of the murine orthologs of the validated genes. Finally, we tested expression of these validated genes in the PR-9 cell line (21), a commonly-used model of M3 AML. Zn2+ treatment massively increased expression of the PML-RARA fusion gene (see Figure 2-8). GSEA analysis failed to demonstrate significant enrichment of the validated gene set in PR-9 cells expressing high levels of PML-RARA (FDR q value = 0.956; Figure 2-7C).

2.3.3. Classification of M3 samples using the NanoString-validated gene set.

We next tested the ability of the 33 validated genes to identify M3 samples using unsupervised principle component analysis (PCA; ref. 26). In our dataset, all M3 samples positive for the PML-RARA rearrangement separated from the other samples (Figure 2-9). Notably, 1 sample diagnosed morphologically as M3 AML, but with normal cytogenetics and negative FISH, did not cluster with those positive for the PML-RARA

fusion gene (Figure 2-9A). The patient from whom this sample was taken also failed all-trans retinoic acid (ATRA) therapy and died 2 months after induction. PCA of the primary NanoString expression data also clearly separated 11/11 M3 t(15;17)-positive samples from other FAB subtypes, as expected (Figure 2-9B). We next tested the validated gene set on a set of 325 M0–M4 AML samples (18) that contained several potentially ambiguous diagnoses. The PCA plot from this analysis shows that all 20 M3 t(15;17)-positive samples clustered separately from the other FAB subtypes, as expected (Figure 2-9C). In addition, 4 morphologically diagnosed M3 samples, in which the t(15;17) was missed by routine cytogenetics, clustered appropriately. Another sample in which morphological diagnosis (M2) conflicted with routine cytogenetics [t(15;17)] was also appropriately identified. Figure 2-9D demonstrates the ability of the validated gene set to separate all but 1 of the M3 t(15;17)-positive samples from other FAB subtypes; 19 of 20 M3 samples were appropriately identified in a dataset of 93 AML M0–M4 samples obtained from CALGB and analyzed in our microarray facility (see Methods).

2.4. Discussion

We have demonstrated the use of an innovative high-throughput methodology, the NanoString nCounter Analysis System, to quantify the mRNA abundance of a large number of genes from an expression signature using very small amounts of clinical material. Through the use of a large number of clinical samples and normal, primary myeloid cells, we defined the unique expression signature of M3 AML, which is distinct from other subtypes of AML and from normal promyelocytes. We then validated the M3-specific signature using the NanoString nCounter Analysis System, which enabled us to

quantitate the relative expression of 46 genes with only 300 ng of total RNA, using multiplexed reactions. We determined that the validated genes were also significantly dysregulated in M3 AML samples from another large clinical study and from a mouse model of APL, but not from a commonly used tissue culture model of PML-RARA function. Finally, the validated genes reliably identify bona fide t(15;17)-positive M3 samples, separating them from other FAB subtypes in 3 independent AML datasets.

The findings presented here demonstrate the power of including a large number of de novo AML samples and normal human myeloid samples to define malignancy-specific expression signatures. Comparison of 14 M3 samples with 62 samples of other AML subtypes and 15 samples of normal primary myeloid cells allowed us to identify expression patterns that were both unique and highly reproducible for M3 AML. Comparison with normal enriched promyelocyte samples enabled us to filter out genes that were simply markers of the promyelocyte stage of myeloid development. Although a previous study (7) compared M3 and promyelocyte expression patterns, these were derived from CD34+ PBMCs cultured for 7 days with G-CSF, IL-3, and GM-CSF. Our analysis showed that the majority of the genes reported in that study (7) were filtered out by our comparison of M3 with CD34+ cells, primary promyelocytes, neutrophils, and other AML subtypes.

The NanoString nCounter system allowed us to quantify and validate (in triplicate) the expression of 42 of 46 genes in 28 AML and 11 normal myeloid samples, using approximately 1/10th of the RNA that qRT-PCR would have required. The nCounter system performed with a high level of precision and reproducibility, using only 100 ng of RNA (the RNA content of ~40,000 AML cells) per replicate. Expression signal

values demonstrated significant correlation with microarray expression data. The coefficient of variation, a ratio of the standard deviation to the mean and a measure of reproducibility, was consistent with that of conventional qRT-PCR (data not shown).

We have shown that the validated M3 gene set was significantly enriched in M3 samples in another large clinical study. Experimental and in silico validation of the signature allowed us to examine 2 models of APL, one a knockin mouse model of the disease, the other a myeloid cell line with inducible expression of PML-RARA. Analysis of expression in APL cells derived from mCG-PML-RARA mice (27) demonstrated that the validated gene set was significantly dysregulated when compared with wild-type promyelocytes. Our previous work with this mouse model demonstrated that only 3 of 116 genes in the murine APL dysregulome were dysregulated in PML-RARA–expressing preleukemic promyelocytes, suggesting that in mice the genes that are dysregulated in APL are not downstream targets of the transgene (27). Similarly, the validated gene set identified in the current study was not altered in PR-9 cells, suggesting that many of the dysregulated genes in primary M3 AML samples are not direct targets of PML-RARA.

We have further demonstrated that the validated 33-gene set identifies M3 samples from within AML microarray expression datasets from other large studies, reliably separating those with t(15;17) and/or the PML-RARA fusion gene from those that were morphologically ambiguous. Only 1 of 60 M3 samples analyzed by PCA failed to segregate with the other M3s. Unsupervised hierarchical clustering of global expression analysis using the CALGB samples demonstrated that this outlier M3 sample segregated with a large mixed group of FAB subtypes and not with the other M3s (data not shown). There was no difference between the survival of the patient from whom this

sample was taken and the survival of other M3 patients in the CALGB group. This evidence suggests that in a small number of patients there may be secondary mutations that can modify expression phenotypes without altering response to ATRA.

Importantly, the NanoString dataset itself was sufficient in reliably identifying all M3 samples in an unsupervised PCA of the 33-gene validated set. In both our study and one other that we analyzed (18), the results of routine cytogenetics conflicted with the morphologic diagnosis in several samples, but all PML-RARA+ samples were appropriately clustered by PCA. This conflict is important since ATRA is critical for the proper treatment of M3 AML patients. When treated with ATRA, patients with M3 AML have a significantly higher survival rate than those with other FAB subtypes (28). Moreover, due to the risk of disseminated intravascular coagulation in M3 AML, rapid, highly accurate diagnosis and initiation of therapy are crucial for optimal patient outcomes. Although most cases of M3 AML can be diagnosed using routine methods, a substantial number present atypically (i.e., without evidence for the reciprocal translocation [ref. 29], with atypical morphology, or with normal cytogenetics [ref. 18]).

The findings of this study may have implications for other types of cancer as well. For example, the diagnosis of solid tumors is often made from fine needle biopsies, which retrieve a small amount of tissue containing relatively few tumor cells. Depending upon the type of needle used and the ratio of tumor cells to stroma, a few hundred thousand to one million cells are typically extracted (30). Given the typical RNA yield of a metabolically active tumor cell, fine needle biopsies from solid tumors would likely provide sufficient RNA for nCounter assays of hundreds of genes.

In summary, we have identified and validated a set of genes that is significantly and specifically dysregulated in M3 relative to other subtypes of AML and normal myeloid cells, including promyelocytes. The nCounter method used to validate this signature is precise, sensitive, and automated and requires only 300 ng of RNA to assay up to several hundred genes in triplicate. The manufacturer provides custom probes, and the assay can be performed on site in a research or clinical lab. With the advent of this innovative technology, a more extensive validation of microarray-based signatures in precious clinical samples is now attainable. Extensive validation of dysregulated genes from clinical samples will allow us to more confidently assess the gene expression profiles of parallel studies performed in different laboratories and to more precisely evaluate model systems for human cancers. Furthermore, use of the nCounter method to assay the M3-specific signature provides a valuable diagnostic tool and offers the potential to assay the expression of hundreds of genes in very small clinical samples.

2.5. Methods

2.5.1. Human AML and normal sorted bone marrow samples.

Seventy-seven de novo adult AML bone marrow aspirates, including 14 M3 samples, were analyzed. Patient selection has been described previously (23); patient characteristics are summarized in Table 2-1. Bone marrow aspirates were also obtained from healthy adult donors. This study was approved by the Human Research Protection Office at Washington University School of Medicine after patients and donors provided informed consent in accordance with the Declaration of Helsinki. Isolation of normal promyelocytes and neutrophils was performed as described previously (22). Briefly,

high-speed cell sorting isolated CD9–, CD14–, CD15hi, and CD16lo promyelocytes and CD9–, CD14–, CD15hi, and CD16hi neutrophils (Figure 1, A and B). MACS sorting was performed to isolate normal CD34+ cells according to the manufacturer's instructions (Miltenyi Biotec). For all samples, sufficient cells were collected to perform the standard 1-cycle in vitro transcription protocol; this strategy avoids the bias introduced by linear amplification (2-cycle) required for small amounts of RNA. Sorted cells were lysed in Trizol reagent (Invitrogen) and stored at –80°C until RNA purification. RNA from AML bone marrow aspirates was prepared from unfractionated snap-frozen cell pellets using Trizol reagent. RNA from all samples was quantified using UV spectroscopy (Nanodrop Technologies) and qualitatively assessed using a BioAnalyzer 2100 and RNA NanoChip assay (Agilent Technologies). An additional 93 de novo AML bone marrow samples, described previously (23), were obtained from C. Bloomfield and M. Caligiuri, both of The Ohio State University Comprehensive Cancer Center and James Cancer Hospital & Solove Research Institute, Columbus, Ohio, USA; J. Vardiman of the University of Chicago, Chicago, Illinois, USA; and the Cancer and Leukemia Group B Tumor Bank, Chicago, Illinois and processed using the same methods as the samples from Washington University School of Medicine. Samples were labeled and hybridized to Affymetrix Human Genome U133 Plus 2.0 Array GeneChip microarrays (Affymetrix) using standard protocols from the Laboratory for Clinical Genomics (http://www.pathology.wustl.edu/research/lcgoverview.php; ref. 27). Profiling data for all samples have been deposited on the Gene Expression Omnibus (GEO; http://www.ncbi.nlm.nih.gov/geo/; accession no. GSE12662).

2.5.2. Analysis of AML and normal myeloid datasets.

To find genes that are differentially expressed in M3 in comparison with M0, M1, M2, and M4 subtypes, all probe sets with fewer than 10% present calls in both groups and less than 0.5 coefficient of variation across all samples were eliminated from further analysis. The remaining probe sets were analyzed using significance analysis of microarrays, 2-class analysis; 3,787 probe sets were significant at an FDR of 0.05. The normal myeloid developmental signature was defined by probe sets that were significantly different among CD34+, promyelocytes, and neutrophils at an ANOVA-adjusted $P < 0.05$ after multiple test correction. Probe sets specific to each developmental class were defined as having a significantly higher average expression in one class relative to both other classes (adjusted $P < 0.05$), yielding 2,622 CD34+-specific, 371 promyelocyte-specific, and 601 neutrophil-specific probe sets.

2.5.3. Cell lines

NB-4 cells were obtained from ATCC. PR-9 cells were a gift of P. Pelicci of the European Institute of Oncology, Milan, Italy (21). All cell lines were maintained in RPMI 1640 with 10% fetal calf serum. PR-9 cells were induced in 100 μM $ZnSO_4$ diluted in medium. Cell lysates were collected at 0, 2, 4, 8, 16, and 24 hours after induction. RNA was isolated, quantified, and hybridized to microarrays as described above.

2.5.4. Western blots

Prior to lysis, 2 × 106 cells were incubated in the presence of 100 μM diisopropyl-fluorophosphate (Sigma-Aldrich), then lysed in 100 μl 2% SDS/PBS. Total protein (20 μg) was electrophoresed and Western blotting performed as previously described (5).

2.5.5. NanoString nCounter assay

Details of the nCounter Analysis System (NanoString Technologies) were reported previously (1). In brief, 2 sequence-specific probes were constructed for each gene of interest (Table 2-6). The probes were complementary to a 100-base region of the target mRNA. One probe was covalently linked to an oligonucleotide containing biotin (the capture probe), and the other was linked to a color-coded molecular tag that provided the signal (the reporter probe; see ref. 1). The nCounter CodeSet for these studies contained probe pairs for 73 test and control genes. Forty-six probe pairs were specific for Homo sapiens genes, and 28 corresponded to various nCounter system controls, including a standard curve. Detailed sequence information for the capture probes and reporter probes is listed in Table 2-6. Each sample was hybridized in triplicate with 100 ng of total RNA in each reaction. All 46 genes and controls were assayed simultaneously in multiplexed reactions (for details, see ref. 1). To account for slight differences in hybridization and purification efficiency, the raw data were normalized to the standard curve generated via the nCounter system spike-in controls present in all reactions.

2.5.6. qRT-PCR

One-step qRT-PCR was performed on 20 ng total RNA using the QuantiTect SYBR Green RT-PCR kit and QuantiTect Primer assays (Qiagen) on a Prism 7300 real-

time PCR system (Applied Biosystems) according to the manufacturer's instructions. All reactions were performed in triplicate. Expression was normalized to GAPDH using the ΔCt method.

2.5.7. Analysis software

For a significance analysis of microarrays, depending on the sample set, 2-class or multi-class analysis was performed. An FDR cutoff of 0.05 was used (http://www-stat.stanford.edu/~tibs/SAM/) (25). For GSEA, depending on the sample size, phenotype or gene set permutation analysis with ratio-of-classes or signal-to-noise gene ranking were performed using GSEA (http://www.broad.mit.edu/gsea) (19, 20). Spotfire DecisionSite 8.2 software (TIBCO) was used in PCA and Wards hierarchical clustering.

2.5.8. Statistics

P values for NanoString nCounter and qRT-PCR data were calculated using a Student's 2-tailed t test and were considered significant when $P < 0.05$. Correlation coefficients for comparison of nCounter and microarray data were calculated as follows: each patient data point was transformed to a percentile of the maximum value for that particular probe set (microarray) or probe (nCounter). Microarray and nCounter percentiles were plotted against each other (see Figure 5) and the Pearson's correlation coefficient R calculated. Correlation coefficients were considered significant if greater than 0.374, which corresponds to $P < 0.05$.

Note that the T statistic for R is calculated by the formula $T = R\sqrt{(n - 2)} / \sqrt{(1 - R2)}$. $T = 2.056$ when $P = 0.05$ with a 2-tailed distribution. Using $T = 2.056$ and $n = 28$

(the total number of AML samples assayed by both Affymetrix microarrays and nCounter), the equation was solved for R ($R = 0.374$), meaning that any R value greater than 0.374 was statistically significant ($P < 0.05$).

2.6. Acknowledgements

This work was supported by grants from the NIH (RO1 CA083962 and PO1 CA0101937) and the Barnes-Jewish Hospital Foundation (to T.J. Ley). The authors thank Clara Bloomfield, Michael Caligiuri, and James Vardiman, and the Cancer and Leukemia Group B (CALBG) Tumor Bank for providing the CALBG AML samples used in this study. The authors are grateful to the High Speed Cell Sorter Core, the Laboratory for Clinical Genomics, the Tissue Procurement Core, and the Bioinformatics Core of the Siteman Cancer Center for their invaluable support. Nancy Reidelberger provided expert editorial assistance. Richard Perrin provided expert microscopy assistance. Matthew Walter critically read the paper and provided helpful advice.

2.7. References

1. Geiss, G.K., et al. 2008. Direct multiplexed measurement of gene expression with color-coded probe pairs. Nat. Biotechnol. 26:317–325.

2. Grisolano, J.L., Wesselschmidt, R.L., Pelicci, P.G., and Ley, T.J. 1997. Altered myeloid development and acute leukemia in transgenic mice expressing PML-RAR alpha under control of cathepsin G regulatory sequences. Blood. 89:376–387.

3. Brown, D., et al. 1997. A PMLRARalpha transgene initiates murine acute promyelocytic leukemia. Proc. Natl. Acad. Sci. U. S. A. 94:2551–2556.

4. He, L.Z., et al. 1997. Acute leukemia with promyelocytic features in PML/RARalpha transgenic mice. Proc. Natl. Acad. Sci. U. S. A. 94:5302–5307.

5. Westervelt, P., et al. 2003. High-penetrance mouse model of acute promyelocytic leukemia with very low levels of PML-RARalpha expression. Blood. 102:1857–1865.

6. Bullinger, L., et al. 2004. Use of gene-expression profiling to identify prognostic subclasses in adult acute myeloid leukemia. N. Engl. J. Med. 350:1605–1616.

7. Casorelli, I., et al. 2006. Identification of a molecular signature for leukemic promyelocytes and their normal counterparts: Focus on DNA repair genes. Leukemia. 20:1978–1988.

8. Debernardi, S., et al. 2003. Genome-wide analysis of acute myeloid leukemia with normal karyotype reveals a unique pattern of homeobox gene expression distinct from those with translocation-mediated fusion events. Genes Chromosomes Cancer. 37:149–158.

9. Gutierrez, N.C., et al. 2005. Gene expression profile reveals deregulation of genes with relevant functions in the different subclasses of acute myeloid leukemia. Leukemia. 19:402–409.

10. Haferlach, T., et al. 2005. Global approach to the diagnosis of leukemia using gene expression profiling. Blood. 106:1189–1198.

11. Haferlach, T., et al. 2005. AML M3 and AML M3 variant each have a distinct gene expression signature but also share patterns different from other genetically defined AML subtypes. Genes Chromosomes Cancer. 43:113–127.

12. Kohlmann, A., et al. 2003. Molecular characterization of acute leukemias by use of microarray technology.Genes Chromosomes Cancer. 37:396–405.

13. Lee, S., et al. 2006. Gene expression profiles in acute myeloid leukemia with common translocations using SAGE. Proc. Natl. Acad. Sci. U. S. A. 103:1030–1035.

14. Valk, P.J., et al. 2004. Prognostically useful gene expression profiles in acute myeloid leukemia. N. Engl. J. Med. 350:1617–1628.

15. Ross, M.E., et al. 2004. Gene expression profiling of pediatric acute myelogenous leukemia. Blood.104:3679–3687.

16. Schoch, C., et al. 2002. Acute myeloid leukemias with reciprocal rearrangements can be distinguished by specific gene expression profiles. Proc. Natl. Acad. Sci. U. S. A. 99:10008–10013.

17. Wilson, C.S., et al. 2006. Gene expression profiling of adult acute myeloid leukemia identifies novel biologic clusters for risk classification and outcome prediction. Blood. 108:685–696.

18. Verhaak, R.G., et al. 2009. Prediction of molecular subtypes in acute myeloid leukemia based on gene expression profiling. Haematologica. 94:131–134.

19. Mootha, V.K., et al. 2003. PGC-1alpha-responsive genes involved in oxidative phosphorylation are coordinately downregulated in human diabetes. Nat. Genet. 34:267–273.

20. Subramanian, A., et al. 2005. Gene set enrichment analysis: a knowledge-based approach for interpreting genome-wide expression profiles. Proc. Natl. Acad. Sci. U. S. A. 102:15545–15550.

21. Grignani, F., et al. 1993. The acute promyelocytic leukemia-specific PML-RAR[alpha] fusion protein inhibits differentiation and promotes survival of myeloid precursor cells. Cell. 74:423–431.

22. Grenda, D.S., et al. 2007. Mutations of the ELA2 gene found in patients with severe congenital neutropenia induce the unfolded protein response and cellular apoptosis. Blood. 110:4179–4187.

23. Link, D.C., et al. 2007. Distinct patterns of mutations occurring in de novo AML versus AML arising in the setting of severe congenital neutropenia. Blood. 110:1648–1655.

24. Jaffe, E.S., Harris, N.L., Stein, H., and Vardiman, J.W. 2001. Pathology and genetics of tumours of haematopoietic and lymphoid tissues. IARC Press. Lyon, France. 352 pp.

25. Tusher, V.G., Tibshirani, R., and Chu, G. 2001. Significance analysis of microarrays applied to the ionizing radiation response. Proc. Natl. Acad. Sci. U. S. A. 98:5116–5121.

26. Jolliffe, I.T. 2002. Principal component analysis. 2nd edition. Springer. New York, New York, USA. 502 pp.

27. Yuan, W., et al. 2007. Commonly dysregulated genes in murine APL cells. Blood. 109:961–970.

28. Mrozek, K., Heerema, N.A., and Bloomfield, C.D. 2004. Cytogenetics in acute leukemia. Blood Rev.18:115–136.

29. Lafage-Pochitaloff, M., et al. 1995. Acute promyelocytic leukemia cases with nonreciprocal PML/RARa or RARa/PML fusion genes. Blood. 85:1169–1174.

30. Welker, L., Akkan, R., Holz, O., Schultz, H., and Magnussen, H. 2007. Diagnostic outcome of two different CT-guided fine needle biopsy procedures. Diagn. Pathol. 2:31.

2.8. Figure Legends

Figure 2-1. Isolation and expression profiling of myeloid cells.

(A) High-speed cell sorting of bone marrow aspirates from healthy donors. FSC, forward scatter; PMNs, polymorphonuclear cells; Pros, promyelocytes; SSC, side scatter. (B) May Grunwald/Giemsa–stained cytospins of sorted promyelocytes (left; average purity, 80% promyelocytes, 11% myelocytes) and neutrophils (right; average purity, 74% mature granulocytes with segmented nuclei, 21% bands [immediate precursor stage prior to the mature granulocyte, characterized by horseshoe-shaped nuclei]). Original magnification, ×100. (C) Microarray signal intensity data demonstrate the expected stage-specific expression of early, middle, and late developmental myeloid genes in each fraction, with minimal expression in other fractions. Data are mean ± SD. (D) Heat map of microarray data demonstrates a progression of expression from less differentiated to terminally differentiated myeloid cells. Red indicates relatively upregulated expression. Green indicates relatively downregulated expression.

Figure 2-2. Identification of the M3-specific dysregulome: genes with significantly different expression in M3 compared with other AML subtypes and normal promyelocytes.

(A) Heat map of microarray data demonstrates clear separation of 2,023 significantly up- or downregulated genes in M3 samples compared with other AML subtypes, although some genes were expressed at similar levels in normal and malignant (M3) promyelocytes (markers of promyelocyte differentiation). (B) The genes from A were

filtered, by comparison with normal myeloid cells (including normal promyelocytes), to retain only those genes with M3-specific expression (510 genes).

Figure 2-3. Identification of genes with significantly different expression in M3 compared to normal myeloid cell fractions.

(A) Heatmap of microarray data shows genes that are normally expressed only in CD34+ cells, but are aberrantly expressed in M3 cells. (B) Heatmap of microarray data shows genes that are normally expressed in promyelocytes, but not expressed in M3 AML cells. (C) Heatmap of microarray data shows genes with very high expression levels in M3 cells, but little or no expression in any normal myeloid fraction.

Figure 2-4. Validation of NanoString nCounter system performance by comparison with microarray results for calibration genes.

A total of 28 AML (11 M3, 17 other AML subtypes), 2 CD34+, 5 promyelocyte, and 2 neutrophil samples were analyzed. Expression is plotted as a percentage ([sample signal/signal of index group] × 100) because the microarray and nCounter system data were expressed in different units. Asterisks indicate the signal index group for each graph. The NanoString results showed the expected pattern of expression for all 6 genes. (A) Expression of early myeloid-specific hematopoietic genes in CD34+ cells, promyelocytes, neutrophils, M3 AML, and other FAB subtypes (oAML) as measured by the Affymetrix microarray (red) and NanoString nCounter system (green). (B) Promyelocyte-specific genes. (C) Late myeloid–specific genes.

Figure 2-5. Validation of the M3-specific signature by the NanoString nCounter system.

(A–D) Expression of (A) *HGF*, (B) *FAM19A5*, (C) *NRIP1*, and (D) *TNFRSF1B* as measured by the Affymetrix Hu133+2 microarray (left panels) and the nCounter system (right panels). The same samples are plotted as in Figure 3. Each data point represents 1 patient sample. The horizontal line indicates the mean of each group. For microarray plots, each data point represents 1 sample (either patient or sorted normal cells) and indicates signal intensity for a single probe set on 1 microarray. For nCounter plots, each data point represents the mean normalized counts for 3 technical replicate measurements of 1 sample (either patient or sorted normal cells).

Figure 2-6. Comparison plots of NanoString nCounter with Affymetrix GeneChip data for M3-specific genes.

(A and B) Scatter plots show the percentage of maximum expression per probe/probe set in all samples for microarray data versus that for nCounter data. Correlation coefficients demonstrate significant correlation between the microarray and nCounter data. (A) Upregulated genes (*HGF* and *FAM19A5*), (B) downregulated genes (*NRIP1* and *TNFRSF1B*), and (C) log2 (M3/other AML) fold change ratios as measured by Affymetrix arrays (x axis) and NanoString assay (y axis) for 37 highly dysregulated genes. The linear fit of the ratios in both assays yielded a correlation coefficient of 0.963.

Figure 2-7. The validated 33-gene M3-specific signature is consistently dysregulated in other AML datasets and a mouse model of APL, but not in a PML-RARA+ cell line.

The top portion of each GSEA plot shows the running enrichment score for the validated M3-specific genes as the analysis moves down the ranked list. The peak score for each plot is the enrichment score for the gene set. The bottom portion of each plot shows the value of the ranking metric as it moves down the list of ranked genes. The FDR is an expression of the significance level of the enrichment, after multiple test correction. (A) GSEA plot of 325 M0–M4 AML samples (GSE6891), comparing M3 with other FAB subtypes, demonstrates significant enrichment. (B) GSEA plot of mCG-PML-RARA murine APL cells (20, 24) compared with day 2 wild-type murine myeloid cells (mostly promyelocytes) demonstrates significant enrichment. (C) GSEA plot of uninduced versus PML-RARA–induced PR-9 cells demonstrates no enrichment of the M3-specific genes at any time point.

Figure 2-8. Zn2+ treatment induces PML-RARA expression and up-regulation of known downstream targets in PR-9 cells.

(A) Western blot showing PML-RARA and actin protein levels at 0, 2, 4, 8, 16 and 24 hours post Zn2+-induction. NB4 cells, which express PML-RARA, serve as a positive control in lane 1. (B) Expression of *PML*, *RARA*, *PU.1* and *CCNA1* in other AML (oAML) subtypes, M3, and PR-9 cells 0-24 hours post Zn2+-induction. All are upregulated after PML-RARA induction, as expected. Inset: *MTX1*, a known Zn-responsive gene, is also upregulated after Zn2+ treatment.

Figure 2-9. The NanoString-validated, 33-gene M3-specific signature reliably identifies M3 samples, including those with normal cytogenetics and/or ambiguous morphology.

PCA plots of the validated gene expression data demonstrate a clear separation of M3 t(15;17)-positive samples (red) from other FAB subtypes (gray). (A) Data from the Washington University AML discovery set, including 15 M3 and 62 M0, M1, M2, and M4 AML samples (1). The PCA plot shows clustering of all M3 samples with the PML-RARA rearrangement, but not of 1 sample with an M3 morphological diagnosis, normal cytogenetics, and negative FISH that did not respond to ATRA therapy (blue). (B) NanoString nCounter expression data were sufficiently robust to separate 11/11 of M3 t(15;17)-positive samples from other FAB subtypes. (C) M3 samples from a published dataset (GSE6891) formed a distinct cluster separate from other FAB subtypes (total of 325). M3s with t(15;17) that were missed by routine cytogenetics (yellow) and a t(15;17)-positive sample morphologically classified as M2 (green) were also assigned appropriately to the M3 cluster. (D) A total of 19/20 M3s with t(15;17) from a CALGB sample set clustered separately from 73 other FAB subtypes.

Table 2-1: Clinical characteristics of patients and de novo AML samples

Parameter	No.	%[A]
Cytogenetic subgroup		
Normal	28	36
t(15;17) only	12	16
t(15;17) + other	2	3
t(8;21) only	1	1
inv(16) only	2	3
Trisomy 8 only	4	5
5q–/–5 only	1	1
7q–/–7 only	1	1
Complex karyotype	7	9
Other	19	25
FAB subtype		
M0	6	8
M1	18	23
M2	20	26
M3	15	19
M4	18	23
Sex		
Male	47	61
Female	30	39
Ethnicity		
Asian	1	1
African-American	8	10
White	67	87
Hispanic	1	1
Other	0	0

Median age of patients was 54 years (range, 18–81). [A]Percentages are from all samples (n = 77) or all patients (n = 77).

Table 2-2. The M3 specific dysregulome

Figure 2-2B Probeset	Gene Symbol
215409_at	AGPAT7
228264_at	ACCS
200862_at	DHCR24
218043_s_at	AZI2
218051_s_at	NT5DC2
201790_s_at	DHCR7
215483_at	AKAP9
225098_at	ABI2
49452_at	ACACB
200974_at	ACTA2
208002_s_at	ACOT7
204497_at	ADCY9
225342_at	AK3L1
226718_at	AMIGO1
228094_at	AMICA1
209122_at	ADFP
201792_at	AEBP1
212285_s_at	AGRN
232810_at	AIG1
223092_at	ANKH
213035_at	ANKRD28
201590_x_at	ANXA2
203074_at	ANXA8 /// ANXA8L1 /// ANXA8L2
219366_at	AVEN
39248_at	AQP3
207076_s_at	ASS1
218694_at	ARMCX1
230244_at	UNQ830
205047_s_at	ASNS
210192_at	ATP8A1
219660_s_at	ATP8A2
201242_s_at	ATP1B1
203505_at	ABCA1
1554918_a_at	ABCC4
212599_at	AUTS2
214575_s_at	AZU1
218792_s_at	BSPRY
205681_at	BCL2A1
205839_s_at	BZRAP1
207693_at	CACNB4
221042_s_at	CLMN
221879_at	CALML4
212586_at	CAST
200935_at	CALR
211031_s_at	CLIP2
201850_at	CAPG
227522_at	CMBL

205624_at	CPA3
209790_s_at	CASP6
205653_at	CTSG
214450_at	CTSW
203323_at	CAV2
214523_at	CEBPE
217078_s_at	CD300A
218529_at	CD320
213539_at	CD3D
200663_at	CD63
201005_at	CD9
206761_at	CD96
221556_at	CDC14B /// CDC14C
217849_s_at	CDC42BPB
232355_at	---
233422_at	---
236787_at	---
243937_x_at	BMS1P5 /// CTGLF1 /// CTGLF6 /// CT
223513_at	CENPJ
224794_s_at	CERCAM
229958_at	CLN8
213385_at	CHN2
226473_at	CBX2
218829_s_at	CHD7
205944_s_at	CLTCL1
208792_s_at	CLU
205229_s_at	COCH
204363_at	F3
201161_s_at	CSDA
229168_at	COL23A1
205382_s_at	CFD
213800_at	CFH
225129_at	CPNE2
202119_s_at	CPNE3
211709_s_at	CLEC11A
232466_at	CUL4A
205899_at	CCNA1
200953_s_at	CCND2
224851_at	CDK6
213348_at	CDKN1C
209644_x_at	CDKN2A
205518_s_at	CMAH
217889_s_at	CYBRD1
209975_at	CYP2E1
223377_x_at	CISH
219837_s_at	CYTL1
222101_s_at	DCHS1
239648_at	DCUN1D3
224215_s_at	DLL1

228293_at	DEPDC7
218854_at	DSE
226817_at	DSC2
201681_s_at	DLG5
215102_at	DPY19L1P1
238784_at	DPY19L2
215116_s_at	DNM1
212838_at	DNMBP
233850_s_at	EBF4
201693_s_at	EGR1
204160_s_at	ENPP4
206580_s_at	EFEMP2
206871_at	ELA2
204163_at	EMILIN1
213779_at	EMID1
204503_at	EVPL
223253_at	EPDR1
231944_at	ERO1LB
236700_at	EIF3C
209365_s_at	ECM1
231846_at	FOXRED2
229459_at	FAM19A5
1568865_at	FNTB
210933_s_at	FSCN1
216080_s_at	FADS3
227222_at	FBXO10
224162_s_at	FBXO31
1560031_at	FRMD4A
205110_s_at	FGF13
211535_s_at	FGFR1
204379_s_at	FGFR3
223321_s_at	FGFRL1
218618_s_at	FNDC3B
202995_s_at	FBLN1
210220_at	FZD2
202862_at	FAH
234192_s_at	GKAP1
228770_at	GPR146
64942_at	GPR153
204537_s_at	GABRE
208438_s_at	FGR
215659_at	GSDML
223319_at	GPHN
224839_s_at	GPT2
205164_at	GCAT
208798_x_at	GOLGA8A
210425_x_at	GOLGA8A /// GOLGA8B
238002_at	GOLIM4
217771_at	GOLM1

31874_at	GAS2L1
216860_s_at	GDF11
215248_at	GRB10
229377_at	GRTP1
219777_at	GIMAP6
213766_x_at	GNA11
207124_s_at	GNB5
226840_at	H2AFY
211936_at	HSPA5
227361_at	HS3ST3B1
201655_s_at	HSPG2
203821_at	HBEGF
209960_at	HGF
235500_at	HNRNPC
235468_at	HRNBP3 /// LOC100130312
205936_s_at	HK3
225601_at	HMGB3
222126_at	HRBL
226651_at	HOMER1
231050_at	HRASLS5
211728_s_at	HYAL3 /// NAT6
200825_s_at	HYOU1
1554452_a_at	HIG2
202660_at	ITPR2
202718_at	IGFBP2
211959_at	IGFBP5
201163_s_at	IGFBP7
202746_at	ITM2A
1555349_a_at	ITGB2
226535_at	ITGB6
224514_x_at	IL17RC
212195_at	IL6ST
213392_at	IQCK
230472_at	IRX1
229638_at	IRX3
210239_at	IRX5
209099_x_at	JAG1
211202_s_at	JARID1B
201466_s_at	JUN
212813_at	JAM3 /// LOC100133502
220010_at	KCNE1L
243428_at	KCNQ1OT1
212236_x_at	KRT17
201596_x_at	KRT18
234307_s_at	KIF26A
216264_s_at	LAMB2
200771_at	LAMC1
244881_at	LMLN
205381_at	LRRC17

206076_at	LRRC23
1559502_s_at	LRRC25
239471_at	LRRC28
235359_at	LRRC33
210784_x_at	LILRA6 /// LILRB3
207106_s_at	LTK
208771_s_at	LTA4H
206480_at	LTC4S
218656_s_at	LHFP
212658_at	LHFPL2
204381_at	LRP3
209468_at	LRP5
207734_at	LAX1
206960_at	LPAR4
227145_at	LOXL4
216320_x_at	MST1
213380_x_at	MSTP9
209823_x_at	HLA-DQB1
206111_at	hCG_1998957 /// HLA-DQB1
204059_s_at	ME1
37408_at	MRC2
221713_s_at	MAP6D1
210794_s_at	MEG3
201069_at	MMP2
212509_s_at	MXRA7
235409_at	MGA
35147_at	MCF2L
210254_at	MS4A3
224356_x_at	MS4A6A
211456_x_at	MT1P2
213629_x_at	MT1F
208581_x_at	MT1X
212185_x_at	MT2A
226852_at	MTA3
1554127_s_at	MSRB3
201761_at	MTHFD2
224918_x_at	MGST1
203151_at	MAP1A
203208_s_at	MTFR1
35617_at	MAPK7
205447_s_at	MAP3K12
225997_at	MOBKL1A
226844_at	MOBKL2B
221636_s_at	MOSC2
234224_at	---
225185_at	MRAS
207895_at	NAALADL1
228523_at	NANOS1
220429_at	NDST3

224802_at	NDFIP2
227870_at	NOPE
223638_at	NBPF3
218888_s_at	NETO2
209949_at	NCF2
212803_at	NAB2
202237_at	NNMT
1552553_a_at	NLRC4
231798_at	NOG
227556_at	NME7
202599_s_at	NRIP1
219557_s_at	NRIP3
203920_at	NR1H3
207202_s_at	NR1I2
1559139_at	NOC2L
212775_at	OBSL1
213125_at	OLFML2B
213825_at	OLIG2
228170_at	OLIG1
225105_at	OCC-1
223464_at	OSBPL5
226435_at	PAPLN
227204_at	PARD6G
209815_at	PTCH1
210139_s_at	PMP22
212012_at	PXDN
208510_s_at	PPARG
204604_at	PFTK1
226150_at	PPAPDC1B
207621_s_at	PEMT
208591_s_at	PDE3B
201481_s_at	PYGB
222688_at	PHCA
235411_at	PGBD1
219225_at	LOC100134440 /// PGBD5
220798_x_at	PRG2
205463_s_at	PDGFA
220952_s_at	PLEKHA5
228171_s_at	PLEKHG4
1553139_s_at	PLXNA3
241742_at	PRAM1
212662_at	PVR
203688_at	PKD2
226245_at	KCTD1
212192_at	KCTD12
222668_at	KCTD15
239763_at	LOC100129965 /// PRDM11
226065_at	PRICKLE1
200656_s_at	P4HB

226423_at	PAQR8
214203_s_at	PRODH
205618_at	PRRG1
211748_x_at	PTGDS
207650_x_at	PTGER1
213933_at	PTGER3
231323_at	PSMB2
208658_at	PDIA4
226101_at	PRKCE
225203_at	PPP1R16A
204944_at	PTPRG
1555579_s_at	PTPRM
219654_at	PTPLA
232473_at	PRPF18
220005_at	P2RY13
206277_at	P2RY2
235634_at	PURG
222087_at	PVT1
201251_at	PKM2
201482_at	QSOX1
202252_at	RAB13
219412_at	RAB38
230266_at	RAB7B
222810_s_at	RASAL2
215620_at	RREB1
219167_at	RASL12
226597_at	REEP6
212589_at	RRAS2
220570_at	RETN
228550_at	RTN4R
226638_at	ARHGAP23
202975_s_at	RHOBTB3
212912_at	RPS6KA2
205228_at	RBMS2
228802_at	RBPMS2
218394_at	ROGDI
213939_s_at	RUFY3
202917_s_at	S100A8
203535_at	S100A9
209686_at	S100B
201825_s_at	SCCPDH
206671_at	SAG
215641_at	SEC24D
209875_s_at	SPP1
203021_at	SLPI
219689_at	SEMA3G
221696_s_at	STYK1
202628_s_at	SERPINE1
200986_at	SERPING1

207714_s_at	SERPINH1
212921_at	SMYD2
224817_at	SH3PXD2A
1554343_a_at	STAP1
244889_at	LOC388210
204900_x_at	SAP30
203787_at	SSBP2
221562_s_at	SIRT3
206634_at	SIX3
232636_at	SLITRK4
232020_at	SMURF2
219480_at	SNAI1
219593_at	SLC15A3
207057_at	SLC16A7
204430_s_at	SLC2A5
219090_at	SLC24A3
232280_at	SLC25A29
205097_at	SLC26A2
220475_at	SLC28A3
238418_at	SLC35B4
234976_x_at	SLC4A5
201195_s_at	SLC7A5
228654_at	SPIN4
224995_at	SPIRE1
218638_s_at	SPON2
225639_at	SKAP2
210942_s_at	ST3GAL6
204150_at	STAB1
231891_at	STAMBPL1
204548_at	STAR
201061_s_at	STOM
202260_s_at	STXBP1
214708_at	SNTB1
233719_s_at	TASP1
222116_s_at	TBC1D16
227632_at	TBC1D24
206301_at	TEC
218872_at	TESC
220623_s_at	TSGA10
219587_at	TTC12
219838_at	TTC23
215146_s_at	TTC28
225308_s_at	TANC1
203313_s_at	TGIF1
229253_at	THEM4
220384_at	TXNDC3
201666_at	TIMP1
204043_at	TCN2
226197_at	---

230408_at	---
230684_at	---
237945_at	---
238024_at	---
244352_at	---
1555348_at	TFAP2E
238520_at	TRERF1
228284_at	TLE1
244716_x_at	TMIGD2
1554077_a_at	TMEM53
235245_at	TMEM92
203476_at	TPBG
209344_at	TPM4
239742_at	TULP4
209191_at	TUBB6
228285_at	TDRD9
207113_s_at	TNF
203508_at	TNFRSF1B
214228_x_at	TNFRSF4
202286_s_at	TACSTD2
213943_at	TWIST1
206828_at	TXK
238057_at	USP45
232621_at	USP48
236597_at	UGT3A1
203188_at	B3GNT1
205844_at	VNN1
235818_at	VSTM1
219251_s_at	WDR60
243526_at	WDR86
206067_s_at	WT1
218775_s_at	WWC2
228788_at	YPEL1
226137_at	ZFHX3
205739_x_at	ZNF107
234394_at	ZNF124
235728_at	ZFP3
222016_s_at	ZNF323
205514_at	ZNF415
205964_at	ZNF426
1555793_a_at	ZNF545
223680_at	ZNF607
228864_at	ZNF653
227080_at	ZNF697
228988_at	ZNF711
206059_at	ZNF91
1562303_at	ZKSCAN3
219247_s_at	ZDHHC14
219628_at	ZMAT3
210282_at	ZMYM2

Table 2-3: M3-specific signature's most dysregulated genes: average microarray expression, fold change and FDR

Probe set	Gene symbol	Gene name	M3 average	oAML average	M3/oAML FC	FDR	Pros average	M3/Pros FC	FDR
204537_s_at	*GABRE*	γ-Aminobutyric acid (GABA) A receptor, ε	7,663	216	35.4	0	423	18.1	0.02
205110_s_at	*FGF13*	Fibroblast growth factor 13	8,086	330	24.5	0	4,471	1.8	0.02
210997_at	*HGF*	Hepatocyte growth factor	22,667	1,066	21.3	0	406	55.9	<0.01
203074_at	*ANXA8*	Annexin A8	14,843	698	21.3	0	2,231	6.7	<0.01
219225_at	*PGBD5*[A]	PiggyBac transposable element derived 5	1,266	68	18.7	0	252	5.0	<0.01
234224_at	*PTPRG*	Protein tyrosine phosphatase, receptor type, G	1,267	75	16.9	0	359	3.5	<0.01
206634_at	*SIX3*	SIX homeobox 3	4,143	256	16.2	0	294	14.1	<0.01
209686_at	*S100B*	S100 calcium binding protein B	4,686	336	14.0	0	36	132.0	<0.01
202237_at	*NNMT*	Nicotinamide N-methyltransferase	5,814	425	13.7	0	927	6.3	0.03
212187_x_at	*PTGDS*	Prostaglandin D2 synthase 21 kDa	20,218	1,666	12.1	0	548	36.9	<0.01
229459_at	*FAM19A5*	Family with sequence similarity 19 (chemokine-like), member A5	1,434	118	12.1	0	145	9.9	<0.01
214228_x_at	*TNFRSF4*	Tumor necrosis factor receptor superfamily, member 4	2,476	206	12.0	0	78	31.9	<0.01
202718_at	*IGFBP2*	Insulin-like growth factor binding protein 2	20,887	1,840	11.4	0	701	29.8	<0.01
236787_at	*SYNE1*[A]	Spectrin repeat containing, nuclear envelope 1/CDNA FLJ35091 fis	3,848	345	11.1	0	1,118	3.4	<0.01
208510_s_at	*PPARG*	Peroxisome proliferator activated receptor γ	1,616	145	11.1	0	32	49.8	<0.01
213943_at	*TWIST1*	Twist homolog 1	3,424	309	11.1	0	157	21.8	<0.01
38487_at	*STAB1*	Stabilin 1	39,862	4,080	9.8	0	301	132.6	<0.01
233422_at	*EBF3*	Early B cell factor 3	692	71	9.7	0	201	3.4	0.03
202994_s_at	*FBLN1*	Fibulin 1	837	91	9.2	0	107	7.8	<0.01
244889_at	*FUT4*[A]	Fucosyltransferase 4	3,658	411	8.9	0	967	3.8	0.02
1552553_a_at	*NLRC4*	NLR family, CARD domain containing 4	214	1,489	0.14	0.02	18,349	0.01	0
202917_s_at	*S100A8*	S100 calcium binding protein A8	17,142	130,368	0.13	<0.01	10^6	0.02	0
208438_s_at	*FGR*	V-fgr oncogene homolog	1,229	9,511	0.13	<0.01	77,507	0.02	0
203508_at	*TNFRSF1B*	Tumor necrosis factor receptor superfamily, member 1B	635	5,030	0.13	0.02	5,444	0.12	0
209949_at	*NCF2*	Neutrophil cytosolic factor 2	1,401	11,929	0.12	0.02	55,034	0.03	0
205681_at	*BCL2A1*	BCL2-related protein A1	766	6,680	0.11	0.02	27,417	0.03	0
1555349_a_at	*ITGB2*	Integrin, β2	2,158	19,282	0.11	<0.01	55,854	0.04	0
1559502_s_at	*LRRC25*	Leucine rich repeat containing 25	238	2,353	0.10	<0.01	2,507	0.09	0
228094_at	*AMICA1*	Adhesion molecule, interacts with CXADR antigen 1	373	3,714	0.10	0.01	10,562	0.04	0
225639_at	*SKAP2*	Src kinase associated phosphoprotein 2	947	9,550	0.10	<0.01	14,829	0.06	0
202599_s_at	*NRIP1*	Nuclear receptor interacting protein 1	1,153	12,784	0.09	<0.01	6,371	0.18	0
210784_x_at	LILRB2/B3/A6	Leukocyte immunoglobulin-like receptor, subfamily B2/B3/A6	177	2,021	0.09	0.01	9,711	0.02	0
219593_at	*SLC15A3*	Solute carrier family 15, member 3	76	998	0.08	0.02	3,179	0.02	0
217078_s_at	*CD300A*	CD300a molecule	151	2,125	0.07	<0.01	2,822	0.05	0
212192_at	*KCTD12*	Potassium channel tetramerisation domain-containing 12	973	13,842	0.07	0.02	9,173	0.11	0
203535_at	*S100A9*	S100 calcium binding protein A9	5,257	77,048	0.07	<0.01	821,839	0.01	0
205936_s_at	*HK3*	Hexokinase 3 (white cell)	138	2,424	0.06	0.04	60,843	0.00	0
220005_at	*P2RY13*	Purinergic receptor P2Y, G-protein coupled, 13	129	2,862	0.04	0.02	28,442	0.00	0
224356_x_at	*MS4A6A*	Membrane-spanning 4 domains, subfamily A, member 6A	609	14,977	0.04	<0.01	3,430	0.18	0
205844_at	*VNN1*	Vanin 1	130	4,219	0.03	0.02	12,620	0.01	0

oAML, other AML subtypes; FC, fold change. [A]Affymetrix annotations for these probe sets changed after microarray experiments were completed and before validation. ENSEMBL alignment of probe set target sequences showed that probe sets 236787_at and 244889_at did not map to the *SYNE1* or *FUT4* gene regions.

Table 2-4: M3-specific signature's most dysregulated genes: comparison of microarray and nCounter fold changes and nCounter average signal, and qRT-PCR validation.

Gene symbol	Gene name	Microarray	nCounter data					qRT-PCR data	
		M3/oAML FC	M3/oAML FC	M3 avg	oAML avg	*P*	*r*	Validated?	*P*
GABRE	γ-Aminobutyric acid (GABA) A receptor, ε	35.4	7.8	14.8	1.9	0.001	0.75	ND	ND
FGF13	Fibroblast growth factor 13	24.5	20.0	22.1	1.1	<0.001	0.94	No	0.206
HGF	Hepatocyte growth factor	21.3	24.4	1,311	53.7	0.001	0.93	Yes	<0.001
ANXA8	Annexin A8	21.3	39.0	100.4	2.6	0.003	0.96	Yes	<0.001
PTPRG	Protein tyrosine phosphatase, receptor type, G	16.9	11.4	14.3	1.3	<0.001	0.8	ND	ND
SIX3	SIX homeobox 3	16.2	12.0	36.7	3.1	0.003	0.98	ND	ND
S100B	S100 calcium binding protein B	14.0	17.9	123.3	6.9	0.003	0.97	ND	ND
NNMT	Nicotinamide N-methyltransferase	13.7	8.7	27.7	3.2	0.031	0.96	ND	ND
PTGDS	Prostaglandin D2 synthase 21 kDa	12.1	51.6	38.6	0.7	0.003	0.97	ND	ND
FAM19A5	Family with sequence similarity 19 (chemokine-like), member A5	12.1	19.3	17.9	0.9	0.005	0.97	ND	ND
TNFRSF4	Tumor necrosis factor receptor superfamily, member 4	12.0	17.0	27.1	1.6	0.01	0.92	Yes	<0.001
IGFBP2	Insulin-like growth factor binding protein 2	11.4	16.5	396.0	24.0	<0.001	0.97	Yes	<0.001
PPARG	Peroxisome proliferator activated receptor γ	11.1	8.1	25.7	3.2	<0.001	0.96	Yes	0.0033
TWIST1	Twist homolog 1	11.1	9.2	23.4	2.5	<0.001	0.9	ND	ND
STAB1	Stabilin 1	9.8	10.5	671.5	63.8	<0.001	0.85	Yes	<0.001
EBF3	Early B cell factor 3	9.7	9.3	33.0	3.5	0.005	0.72	ND	ND
FBLN1	Fibulin 1	9.2	6.8	4.1	0.6	0.012	0.86	ND	ND
NLRC4	NLR family, CARD domain containing 4	0.14	0.2	3.0	13.9	0.005	0.94	ND	ND
S100A8	S100 calcium binding protein A8	0.13	0.06	103.7	1,780	0.006	0.78	ND	ND
FGR	V-fgr oncogene homolog	0.13	0.06	17.0	268.3	0.017	0.94	ND	ND
TNFRSF1B	Tumor necrosis factor receptor superfamily, member 1B	0.13	0.06	8.5	139.1	0.02	0.99	ND	ND
NCF2	Neutrophil cytosolic factor 2	0.12	0.24	36.8	152.0	0.046	0.92	No	0.215
BCL2A1	BCL2-related protein A1	0.11	0.25	15.6	63.0	0.035	0.95	ND	ND
ITGB2	Integrin, β2	0.11	0.12	47.2	387.2	0.002	0.91	ND	ND
LRRC25	Leucine rich repeat containing 25	0.10	0.11	2.9	27.3	0.041	0.95	ND	ND
AMICA1	Adhesion molecule, interacts with CXADR antigen 1	0.10	0.63	0.6	0.9	0.203	0.8	ND	ND
SKAP2	Src kinase associated phosphoprotein 2	0.10	0.15	3.3	21.5	<0.001	0.86	ND	ND
NRIP1	Nuclear receptor interacting protein 1	0.09	0.14	4.7	32.9	<0.001	0.9	Yes	0.048
LILRB2/B3/A6	Leukocyte Ig-like receptor subfamily B2/B3/A6	0.09	0.13	14.2	111.7	0.014	0.9	ND	ND
SLC15A3	Solute carrier family 15, member 3	0.08	0.24	3.4	13.9	0.075	0.82	ND	ND
CD300A	CD300a molecule	0.07	0.69	6.6	9.5	0.303	0.19	ND	ND
KCTD12	Potassium channel tetramerisation domain-containing 12	0.07	0.13	4.5	35.7	0.042	0.92	ND	ND
S100A9	S100 calcium binding protein A9	0.07	0.05	50.1	992.5	0.012	0.8	ND	ND
HK3	Hexokinase 3 (white cell)	0.06	0.36	4.6	13.0	0.11	0.825	ND	ND
P2RY13	Purinergic receptor P2Y, G-protein coupled, 13	0.04	0.11	6.2	54.3	0.013	0.95	ND	ND
MS4A6A	Membrane-spanning 4 domains, subfamily A, member 6A	0.04	0.12	2.5	20.1	0.007	0.89	ND	ND
VNN1	Vanin 1	0.03	0.18	2.2	12.4	0.005	0.81	ND	ND

ND, not determined; avg, average. Pearson's correlation coefficient (*r*) comes from a comparison of NanoString and microarray results.

Table 2-5: Data from nCounter assays of AML samples and normal myeloid cells

		M0	M0	M0	M0	M0	M0	M0	M0	M0	M0	M0	M0	M1	M1	M1
Accession No.	**Gene Name/Sample ID**	**4528**	**4528**	**4528**	**4532**	**4532**	**4532**	**6742**	**6742**	**6742**	**17366**	**17366**	**17366**	**4534**	**4534**	**4534**
NM_002841.2	**PTPRG**	5	2	4	0	1	0	2	2	0	3	0	3	1	0	2
NM_145256.2	**LRRC25**	**176**	**175**	**165**	**2**	**1**	**3**	**3**	**3**	**2**	**9**	**10**	**8**	**23**	**22**	**21**
NM_001972.2	**ELA2**	5	2	2	0	4	0	2	2	1	24	23	22	174	188	150
NM_000597.2	**IGFBP2**	25	12	23	0	1	0	9	5	6	8	1	5	90	79	66
NM_005413.1	**SIX3**	5	17	0	7	1	1	2	1	1	8	4	3	3	0	2
NM_006272.1	**S100B**	7	3	8	1	0	6	6	4	6	14	20	11	3	4	3
NM_003327.2	**TNFRSF4**	5	3	0	0	1	1	0	3	1	3	0	4	1	2	3
NM_004049.2	**BCL2A1**	356	363	334	17	15	10	86	76	75	42	44	35	69	61	57
NM_001911.2	**CTSG**	7	5	4	1	0	3	0	1	1	45	30	42	456	481	469
NM_001557.2	**IL8RB**	36	47	36	6	1	1	3	1	4	9	10	11	15	9	14
NM_001066.2	**TNFRSF1B**	845	862	760	9	5	7	19	11	11	35	49	43	115	139	101
NM_002046.3	**GAPDH**	3533	3587	3208	1929	1762	1790	4100	3649	3447	2494	2367	2687	4885	5088	4813
NM_006169.2	**NNMT**	2	2	4	0	2	3	2	2	1	3	6	5	6	3	1
NM_015381.3	**FAM19A5**	2	0	0	4	0	1	1	1	1	1	0	1	2	0	0
NM_015136.2	**STAB1**	194	195	178	7	7	8	156	112	114	14	19	26	151	115	123
NM_002029.3	**FPR1**	282	255	283	4	1	3	5	8	5	10	19	15	38	29	19
NM_003930.3	**SCAP2**	52	45	32	21	19	25	12	15	15	14	10	14	19	32	21
NM_006486.2	**FBLN1**	2	2	0	0	0	1	0	0	0	1	1	0	0	0	1
NM_153206.1	**AMICA1**	2	5	2	0	0	0	1	1	0	3	0	1	1	1	0
NM_002965.2	**S100A9**	6135	6132	5334	11	6	3	290	231	214	873	809	849	895	792	794
NM_021209.3	**CARD12/NLRC4**	56	33	38	2	1	10	2	2	4	13	9	12	13	9	9
NM_000433.2	**NCF2**	933	1005	861	4	2	6	13	9	9	90	104	103	105	128	102
NM_003489.2	**NRIP1**	74	65	56	54	56	51	1	3	2	36	30	26	33	17	19
NM_001040084.1	**LOC653107/ANXA8**	2	2	4	0	1	0	2	1	1	3	0	1	2	0	0
NM_016582.1	**SLC15A3**	83	83	114	0	1	6	1	3	1	19	9	14	8	9	8
NM_000211.2	**ITGB2**	1710	1648	1340	109	85	117	147	134	129	196	151	174	418	427	382
NM_000601.4	**HGF**	56	35	53	31	29	32	31	41	30	9	13	15	2	2	4
NM_182961.1	**SYNE1**	41	35	11	17	13	13	12	19	18	33	36	37	17	12	8
NM_001042729.1	**FGR**	1649	1506	1370	9	1	8	90	86	67	101	87	124	339	306	270
NM_001614.2	**ACTG1**	4209	4072	3381	2051	1782	1754	2154	1778	1840	2854	2726	2720	4114	3423	3280
NM_138444.2	**KCTD12**	264	260	221	1	1	4	2	8	7	17	14	14	36	34	30
NM_002964.3	**S100A8**	9494	9373	8823	21	23	19	637	531	509	2010	2096	1911	1532	1347	1274
NM_001034996.1	**RPL14**	0	0	0	0	0	0	0	0	0	0	0	0	0	0	0
NM_001025109.1	**CD34**	18	17	11	131	123	128	159	151	116	22	20	20	2	2	1
NM_000474.3	**TWIST1**	2	3	6	1	0	0	2	0	1	0	3	3	3	4	2
NM_015869.3	**PPARG**	7	8	9	0	1	0	2	0	1	1	1	3	4	5	2
NM_004666.1	**VNN1**	9	12	11	4	2	4	3	1	3	1	3	0	17	12	21
NM_005874.1	**LILRB2**	509	516	490	39	44	39	37	34	27	32	49	37	98	77	86
NM_001005463.1	**EBF3**	2	5	4	6	2	1	5	3	2	0	3	3	3	5	2
NM_152852.1	**MS4A6A**	79	68	53	1	4	0	2	1	1	15	9	18	8	8	6
NM_000954.5	**PTGDS**	0	0	0	2	0	0	0	0	1	0	3	0	1	0	0
NM_000222.1	**KIT**	5	12	2	66	67	60	24	24	22	4	6	9	38	52	57
NM_004961.3	**GABRE**	0	2	2	2	0	3	2	1	0	1	0	1	3	2	1
NM_007261.2	**CD300A**	11	17	9	6	10	6	9	3	8	56	53	57	9	8	11
NM_002115.1	**HK3**	99	75	64	1	1	0	2	1	1	8	4	9	10	9	12
NM_023914.2	**P2RY13**	340	316	291	17	11	10	6	16	8	18	11	11	55	52	44
NM_033642.1	**FGF13**	0	2	0	1	1	1	1	1	1	1	1	0	1	1	0
AF324996.2	**Athal_Spike_S23**	1829	1841	1822	1853	1765	1800	1846	1855	1837	1832	1873	1858	1806	1871	1823
AF325027.2	**Athal_Spike_S14**	692	759	762	726	775	755	730	728	715	746	759	738	731	729	716
AF325042.2	**Athal_Spike_S19**	527	479	505	518	546	533	532	518	519	497	493	502	548	504	569
AY058560.1	**DrosSpike8**	194	158	189	179	158	202	171	165	184	195	181	180	181	183	175
AF325027.2	**Athal_Spike_S13**	95	72	58	79	94	68	69	87	78	82	64	78	66	80	71
AF324998.2	**Athal_Spike_S22**	81	98	96	77	100	88	84	83	91	88	67	73	87	72	76
AY058658.1	**DrosSpike7**	32	37	23	33	27	14	31	27	36	21	24	30	42	23	28
AF325032.2	**Athal_Spike_S17**	34	40	28	25	23	24	26	23	27	24	27	28	26	26	31
DQ412624	**SarsSpike3**	7	15	13	5	7	11	7	6	6	8	3	7	10	8	6
AY058658.1	**DrosSpike6**	9	0	4	4	4	6	2	6	6	5	7	4	1	3	3
AY058560.1	**DrosSpike10**	2	2	2	0	2	0	2	0	1	4	0	1	2	0	1
AY058658.1	***DrosSpike11***	*2*	*0*	*2*	*1*	*5*	*0*	*0*	*2*	*0*	*0*	*0*	*3*	*2*	*3*	*0*
AF325014.2	***Athal_Spike_S12***	*2*	*3*	*0*	*4*	*6*	*3*	*3*	*2*	*5*	*4*	*1*	*9*	*5*	*3*	*3*
AF325016.2	***Athal_Spike_S15***	*5*	*2*	*0*	*6*	*1*	*8*	*4*	*2*	*3*	*3*	*3*	*3*	*3*	*2*	*3*
AF325016.2	***Athal_Spike_S16***	*2*	*5*	*8*	*2*	*1*	*3*	*2*	*2*	*1*	*5*	*1*	*0*	*3*	*4*	*3*
AF325032.2	***Athal_Spike_S18***	*7*	*5*	*2*	*2*	*1*	*0*	*3*	*2*	*0*	*3*	*1*	*1*	*2*	*2*	*2*
AF324998.2	***Athal_Spike_S20***	*2*	*2*	*2*	*0*	*4*	*6*	*0*	*2*	*3*	*9*	*1*	*3*	*4*	*2*	*2*
AF324998.2	***Athal_Spike_S21***	*0*	*5*	*0*	*2*	*2*	*4*	*3*	*3*	*3*	*8*	*6*	*1*	*4*	*2*	*2*
AF324998.2	***Athal_Spike_S24***	*0*	*10*	*6*	*2*	*2*	*6*	*0*	*1*	*1*	*4*	*4*	*3*	*4*	*2*	*5*
DQ412624	***SarsSpike4***	*5*	*3*	*0*	*2*	*0*	*1*	*7*	*1*	*4*	*5*	*6*	*1*	*3*	*2*	*6*
AY058560.1	***DrosSpike9***	*5*	*2*	*0*	*2*	*2*	*1*	*2*	*1*	*1*	*0*	*0*	*0*	*3*	*1*	*0*

		M1	M1	M1	M1	M1	M1	M1	M1	M1	M1	M1	M1	M2	M2	M2
Accession No.	**Gene Name/Sample ID**	**6747**	**6747**	**6747**	**15599**	**15599**	**15599**	**16066**	**16066**	**16066**	**20900**	**20900**	**20900**	**4530**	**4530**	**4530**
NM_002841.2	**PTPRG**	2	0	2	1	0	0	0	2	3	0	0	1	1	1	3
NM_145256.2	**LRRC25**	**8**	**3**	**0**	**63**	**29**	**38**	**5**	**3**	**4**	**2**	**3**	**2**	**4**	**5**	7
NM_001972.2	**ELA2**	38	33	40	25	15	7	3	2	2	3	1	3	49	58	64
NM_000597.2	**IGFBP2**	131	98	125	39	18	22	11	3	11	11	30	18	2	2	7
NM_005413.1	**SIX3**	2	0	0	0	0	4	1	0	2	0	5	2	2	1	2
NM_006272.1	**S100B**	2	0	0	7	3	4	7	2	1	0	2	5	5	6	4
NM_003327.2	**TNFRSF4**	2	5	0	0	2	0	2	0	1	1	2	1	2	0	2
NM_004049.2	**BCL2A1**	17	20	35	14	21	18	8	12	5	9	13	8	26	46	19
NM_001911.2	**CTSG**	29	45	38	524	549	469	408	414	363	54	22	37	10	14	16
NM_001557.2	**IL8RB**	0	3	5	10	11	5	1	2	0	1	0	1	7	6	3
NM_001066.2	**TNFRSF1B**	38	30	24	310	252	264	111	101	92	29	40	35	28	29	35
NM_002046.3	**GAPDH**	5798	5066	6083	5419	5985	4994	4404	4284	4310	3726	3595	3359	3401	3593	3512
NM_006169.2	**NNMT**	12	10	12	1	2	2	1	2	2	7	3	2	1	1	2
NM_015381.3	**FAM19A5**	0	0	0	1	0	2	1	0	0	0	0	1	0	0	0
NM_015136.2	**STAB1**	21	18	24	34	30	25	9	3	4	3	1	1	35	39	22
NM_002029.3	**FPR1**	27	8	12	1	15	9	4	3	3	3	2	3	10	19	16
NM_003930.3	**SCAP2**	33	25	40	22	33	24	31	26	15	20	23	22	19	11	14
NM_006486.2	**FBLN1**	0	0	0	1	2	2	0	0	1	0	0	0	2	0	0
NM_153206.1	**AMICA1**	0	0	0	1	6	2	0	0	0	0	0	0	1	0	0
NM_002965.2	**S100A9**	602	684	654	654	665	529	140	120	108	2	2	3	319	365	375
NM_021209.3	**CARD12/NLRC4**	4	5	2	35	41	36	10	9	11	5	5	2	9	5	7
NM_000433.2	**NCF2**	27	20	19	353	309	306	118	122	115	3	4	5	50	59	51
NM_003489.2	**NRIP1**	35	28	59	21	20	29	57	56	54	59	52	50	26	41	36
NM_001040084.1	**LOC653107/ANXA8**	4	0	5	1	8	2	4	5	6	2	3	2	3	10	6
NM_016582.1	**SLC15A3**	8	5	0	18	12	13	2	0	1	3	2	3	4	5	7
NM_000211.2	**ITGB2**	346	298	391	1030	1175	900	666	585	660	132	135	123	90	106	94
NM_000601.4	**HGF**	62	78	75	186	154	186	9	16	11	56	59	49	203	214	233
NM_182961.1	**SYNE1**	2	8	5	25	21	14	21	17	11	8	18	22	3	4	10
NM_001042729.1	**FGR**	44	35	38	601	616	561	47	40	63	11	6	5	63	78	83
NM_001614.2	**ACTG1**	2949	3035	3403	5348	4840	4460	5820	5376	5246	3142	3097	3123	2513	2689	2595
NM_138444.2	**KCTD12**	8	13	9	34	23	9	4	7	2	3	9	7	22	17	22
NM_002964.3	**S100A8**	1121	1165	1426	1091	916	934	246	310	272	4	2	1	645	670	656
NM_001034996.1	**RPL14**	0	0	0	0	0	0	0	0	0	0	0	0	0	0	0
NM_001025109.1	**CD34**	17	13	31	7	9	2	21	10	13	3	5	2	125	128	134
NM_000474.3	**TWIST1**	2	5	0	4	0	2	0	3	4	4	2	4	3	3	5
NM_015869.3	**PPARG**	0	10	0	1	14	13	2	0	1	1	1	1	1	2	0
NM_004666.1	**VNN1**	2	8	2	13	11	9	5	9	10	2	0	1	23	20	22
NM_005874.1	**LILRB2**	12	15	16	159	142	165	142	125	139	46	55	55	57	56	52
NM_001005463.1	**EBF3**	8	0	5	9	2	4	3	3	3	3	5	3	5	0	5
NM_152852.1	**MS4A6A**	0	0	2	73	78	63	5	9	2	1	6	3	12	17	20
NM_000954.5	**PTGDS**	2	8	2	0	0	0	0	0	0	1	0	1	0	0	0
NM_000222.1	**KIT**	60	83	99	22	18	11	15	12	5	59	74	71	41	54	40
NM_004961.3	**GABRE**	2	0	7	3	2	0	2	0	1	2	3	3	0	1	0
NM_007261.2	**CD300A**	4	8	7	10	14	11	13	12	8	0	7	9	4	4	1
NM_002115.1	**HK3**	2	3	5	24	14	36	4	2	5	1	1	1	5	8	2
NM_023914.2	**P2RY13**	40	35	40	148	121	100	42	47	29	5	3	1	28	28	20
NM_033642.1	**FGF13**	2	5	2	1	0	2	0	0	4	0	1	0	0	0	1
AF324996.2	**Athal_Spike_S23**	1924	1796	1859	1856	1870	1841	1840	1893	1875	1850	1803	1804	1824	1862	1825
AF325027.2	**Athal_Spike_S14**	667	739	772	727	738	746	678	675	727	752	752	775	740	693	746
AF325042.2	**Athal_Spike_S19**	506	510	482	500	523	527	566	501	512	496	519	505	528	506	525
AY058560.1	**DrosSpike8**	175	219	174	185	155	183	198	188	180	173	204	188	180	185	163
AF325027.2	**Athal_Spike_S13**	92	78	85	66	63	67	72	77	67	70	60	71	79	73	73
AF324998.2	**Athal_Spike_S22**	79	91	71	97	72	80	88	108	64	91	94	82	83	97	102
AY058658.1	**DrosSpike7**	29	33	24	29	36	22	28	23	32	32	21	29	35	38	30
AF325032.2	**Athal_Spike_S17**	21	25	21	29	29	25	20	26	31	25	27	28	20	27	27
DQ412624	**SarsSpike3**	4	5	7	9	9	7	7	5	9	5	13	10	7	14	6
AY058658.1	**DrosSpike6**	2	3	5	1	3	2	3	3	2	3	6	5	2	5	4
AY058560.1	**DrosSpike10**	4	3	2	1	3	0	1	0	3	2	1	1	2	3	1
AY058658.1	***DrosSpike11***	*2*	*0*	*2*	*0*	*0*	*0*	*3*	*2*	*0*	*0*	*3*	*1*	*0*	*1*	*1*
AF325014.2	***Athal_Spike_S12***	*2*	*0*	*0*	*1*	*5*	*2*	*6*	*5*	*4*	*2*	*6*	*6*	*5*	*3*	*1*
AF325016.2	***Athal_Spike_S15***	*2*	*5*	*2*	*7*	*5*	*2*	*3*	*2*	*10*	*5*	*5*	*4*	*4*	*5*	*7*
AF325016.2	***Athal_Spike_S16***	*0*	*0*	*0*	*1*	*2*	*5*	*4*	*2*	*1*	*0*	*1*	*3*	*4*	*2*	*2*
AF325032.2	***Athal_Spike_S18***	*2*	*0*	*0*	*0*	*2*	*0*	*1*	*2*	*4*	*1*	*3*	*2*	*2*	*3*	*3*
AF324998.2	***Athal_Spike_S20***	*8*	*5*	*2*	*3*	*5*	*2*	*2*	*2*	*3*	*3*	*3*	*3*	*2*	*3*	*6*
AF324998.2	***Athal_Spike_S21***	*2*	*3*	*0*	*5*	*5*	*4*	*5*	*2*	*1*	*2*	*2*	*4*	*0*	*2*	*2*
AF324998.2	***Athal_Spike_S24***	*6*	*3*	*2*	*1*	*3*	*0*	*5*	*2*	*4*	*0*	*2*	*5*	*0*	*3*	*2*
DQ412624	***SarsSpike4***	*0*	*0*	*2*	*3*	*0*	*2*	*5*	*2*	*1*	*6*	*4*	*5*	*2*	*6*	*3*
AY058560.1	***DrosSpike9***	*2*	*3*	*0*	*3*	*2*	*7*	*1*	*0*	*1*	*0*	*0*	*0*	*0*	*4*	*1*

		M2	M2	M2	M2	M2	M2	M2	M2	M2	M3	M3	M3	M3	M3	M3
Accession No.	**Gene Name/Sample ID**	**4983**	**4983**	**4983**	**6744**	**6744**	**6744**	**6746**	**6746**	**6746**	**3038**	**3038**	**3038**	**4537**	**4537**	**4537**
NM_002841.2	**PTPRG**	2	2	2	2	0	0	1	0	1	9	15	10	13	13	9
NM_145256.2	**LRRC25**	**23**	**18**	**19**	**2**	**5**	**3**	**6**	**7**	**4**	**12**	**8**	**15**	**1**	**3**	**2**
NM_001972.2	**ELA2**	124	75	96	3	4	2	95	107	87	239	263	283	109	91	101
NM_000597.2	**IGFBP2**	4	7	7	23	24	22	13	16	9	115	95	106	319	350	341
NM_005413.1	**SIX3**	2	4	3	3	7	7	7	8	4	16	16	12	24	27	27
NM_006272.1	**S100B**	2	2	3	3	19	14	8	19	7	23	32	25	134	126	135
NM_003327.2	**TNFRSF4**	0	3	1	0	1	3	1	0	1	0	5	0	20	17	18
NM_004049.2	**BCL2A1**	78	78	83	35	50	35	37	35	28	13	16	10	9	8	11
NM_001911.2	**CTSG**	223	182	248	107	103	108	6	5	7	671	707	634	156	144	163
NM_001557.2	**IL8RB**	21	15	23	6	7	3	4	6	4	1	5	5	5	5	2
NM_001066.2	**TNFRSF1B**	90	60	93	11	18	11	20	12	13	14	11	7	5	4	6
NM_002046.3	**GAPDH**	2823	1890	2450	2778	3455	3297	2787	2900	1919	4007	4085	3661	3195	2812	2996
NM_006169.2	**NNMT**	1	1	2	2	1	1	0	1	1	10	5	4	13	19	15
NM_015381.3	**FAM19A5**	2	0	1	0	1	0	1	0	1	2	3	2	12	7	11
NM_015136.2	**STAB1**	73	52	65	47	83	70	11	12	7	529	611	518	245	195	255
NM_002029.3	**FPR1**	86	63	69	2	3	4	11	4	5	3	9	4	2	4	2
NM_003930.3	**SCAP2**	25	7	21	16	25	24	12	16	7	1	3	1	3	3	7
NM_006486.2	**FBLN1**	0	0	1	1	3	0	0	0	0	0	0	2	10	6	6
NM_153206.1	**AMICA1**	2	0	5	0	0	1	0	0	1	0	0	0	2	0	0
NM_002965.2	**S100A9**	1814	1322	1642	57	53	39	243	238	165	44	63	54	30	20	23
NM_021209.3	**CARD12/NLRC4**	9	8	12	2	3	3	4	3	4	1	3	2	5	3	2
NM_000433.2	**NCF2**	156	121	156	19	22	32	31	32	21	29	27	29	21	26	19
NM_003489.2	**NRIP1**	14	10	12	73	79	63	19	26	15	4	3	4	3	1	2
NM_001040084.1	**LOC653107/ANXA8**	2	0	2	1	3	0	1	4	0	60	55	72	33	39	62
NM_016582.1	**SLC15A3**	11	6	8	2	2	1	1	2	2	1	5	2	1	3	3
NM_000211.2	**ITGB2**	414	275	400	106	141	126	51	55	37	215	223	175	32	28	28
NM_000601.4	**HGF**	5	3	8	27	24	19	37	40	21	621	778	666	612	606	574
NM_182961.1	**SYNE1**	5	9	11	6	8	11	15	3	12	8	8	0	8	5	4
NM_001042729.1	**FGR**	331	267	310	39	35	35	17	12	14	67	54	48	12	7	5
NM_001614.2	**ACTG1**	2029	1559	1813	1849	2445	2162	2086	2190	1507	3295	3953	3430	1900	1984	1935
NM_138444.2	**KCTD12**	16	19	25	3	10	4	2	1	4	5	3	4	2	1	2
NM_002964.3	**S100A8**	3456	2593	3002	100	111	99	662	662	416	119	203	128	31	47	44
NM_001034996.1	**RPL14**	0	0	0	0	0	0	0	0	0	0	0	0	0	0	0
NM_001025109.1	**CD34**	2	4	2	157	167	205	288	274	202	3	5	4	2	0	2
NM_000474.3	**TWIST1**	1	2	1	0	1	1	9	6	4	11	7	13	7	10	11
NM_015869.3	**PPARG**	4	8	5	2	0	2	1	2	2	17	16	12	24	30	30
NM_004666.1	**VNN1**	14	12	13	15	29	19	1	2	4	1	3	0	1	1	1
NM_005874.1	**LILRB2**	62	48	59	17	29	24	19	22	12	21	26	17	10	11	10
NM_001005463.1	**EBF3**	5	6	5	3	2	2	5	0	2	15	14	13	8	6	7
NM_152852.1	**MS4A6A**	10	5	5	6	3	3	2	3	2	1	1	2	0	5	3
NM_000954.5	**PTGDS**	3	2	4	0	0	0	1	0	0	114	119	116	12	11	13
NM_000222.1	**KIT**	12	6	9	43	59	60	70	76	49	28	38	39	28	24	29
NM_004961.3	**GABRE**	2	3	5	1	1	1	0	3	1	21	31	17	2	7	3
NM_007261.2	**CD300A**	7	7	5	5	5	6	4	2	0	4	3	5	3	4	2
NM_002115.1	**HK3**	17	8	6	0	3	1	4	5	1	4	8	6	2	2	5
NM_023914.2	**P2RY13**	74	49	63	5	3	6	31	25	21	4	4	6	2	6	3
NM_033642.1	**FGF13**	1	1	1	0	2	2	1	3	5	22	15	11	9	16	9
AF324996.2	**Athal_Spike_S23**	1897	1764	1772	1800	1810	1818	1792	1814	1808	1784	1759	1759	1820	1806	1800
AF325027.2	**Athal_Spike_S14**	729	749	785	760	783	776	794	754	757	782	812	803	729	753	782
AF325042.2	**Athal_Spike_S19**	493	579	513	530	516	504	512	507	524	512	484	490	533	517	512
AY058560.1	**DrosSpike8**	161	172	190	201	175	194	171	189	179	166	195	211	181	165	174
AF325027.2	**Athal_Spike_S13**	77	82	80	70	66	63	79	77	65	64	80	65	87	85	75
AF324998.2	**Athal_Spike_S22**	71	90	87	70	90	86	98	84	87	112	112	96	92	93	80
AY058658.1	**DrosSpike7**	37	27	32	28	26	23	22	31	39	34	30	32	25	32	27
AF325032.2	**Athal_Spike_S17**	19	22	25	29	26	23	21	32	32	38	24	29	22	35	33
DQ412624	**SarsSpike3**	8	12	8	7	4	7	9	9	4	3	1	10	6	9	11
AY058658.1	**DrosSpike6**	7	3	8	4	3	3	2	4	3	2	3	3	4	4	6
AY058560.1	**DrosSpike10**	1	0	2	1	0	2	1	1	1	0	1	6	1	0	2
AY058658.1	***DrosSpike11***	*2*	*2*	*1*	*1*	*0*	*2*	*1*	*1*	*3*	*3*	*1*	*2*	*2*	*2*	*4*
AF325014.2	***Athal_Spike_S12***	*2*	*3*	*3*	*3*	*3*	*3*	*6*	*4*	*3*	*2*	*1*	*6*	*1*	*7*	*2*
AF325016.2	***Athal_Spike_S15***	*3*	*4*	*3*	*4*	*3*	*8*	*2*	*5*	*4*	*8*	*5*	*9*	*2*	*4*	*5*
AF325016.2	***Athal_Spike_S16***	*3*	*0*	*2*	*3*	*3*	*2*	*2*	*2*	*4*	*4*	*4*	*2*	*7*	*4*	*3*
AF325032.2	***Athal_Spike_S18***	*6*	*6*	*1*	*5*	*0*	*1*	*3*	*1*	*4*	*0*	*3*	*3*	*3*	*2*	*2*
AF324998.2	***Athal_Spike_S20***	*4*	*4*	*4*	*4*	*4*	*6*	*4*	*5*	*3*	*7*	*4*	*2*	*3*	*4*	*2*
AF324998.2	***Athal_Spike_S21***	*5*	*5*	*5*	*4*	*1*	*0*	*5*	*4*	*2*	*2*	*3*	*8*	*2*	*6*	*5*
AF324998.2	***Athal_Spike_S24***	*2*	*3*	*3*	*3*	*1*	*2*	*3*	*4*	*1*	*5*	*3*	*7*	*6*	*2*	*2*
DQ412624	***SarsSpike4***	*5*	*6*	*5*	*2*	*3*	*2*	*5*	*4*	*6*	*5*	*4*	*6*	*2*	*4*	*7*
AY058560.1	***DrosSpike9***	*5*	*2*	*1*	*2*	*2*	*1*	*1*	*1*	*1*	*1*	*0*	*3*	*2*	*0*	*0*

		M3	M3	M3	M3	M3	M3	M3	M3	M3	M3	M3	M3	M3	M3	M3
Accession No.	**Gene Name/Sample ID**	**6947**	**6947**	**6947**	**9062**	**9062**	**9062**	**15590**	**15590**	**15590**	**15591**	**15591**	**15591**	**15605**	**15605**	**15605**
NM_002841.2	**PTPRG**	24	19	34	8	10	12	5	5	3	9	15	10	29	16	28
NM_145256.2	**LRRC25**	**2**	**0**	**2**	**3**	**4**	**4**	**1**	**2**	**1**	**1**	**2**	**0**	**3**	**1**	**1**
NM_001972.2	**ELA2**	325	245	353	438	351	372	388	408	352	183	192	186	213	215	319
NM_000597.2	**IGFBP2**	435	336	516	525	491	537	269	302	261	268	264	255	369	376	550
NM_005413.1	**SIX3**	4	4	9	21	22	18	34	22	18	15	14	13	78	71	133
NM_006272.1	**S100B**	43	26	43	196	165	213	108	113	122	44	36	39	86	86	116
NM_003327.2	**TNFRSF4**	16	12	16	16	11	8	16	18	23	11	6	3	73	50	87
NM_004049.2	**BCL2A1**	11	11	11	20	12	20	13	23	10	7	7	16	22	16	23
NM_001911.2	**CTSG**	534	434	617	2104	2089	2080	829	976	939	610	646	613	1207	1252	1899
NM_001557.2	**IL8RB**	2	0	2	1	4	8	5	3	4	2	1	2	6	4	7
NM_001066.2	**TNFRSF1B**	6	8	4	5	6	6	3	6	0	5	3	2	11	3	9
NM_002046.3	**GAPDH**	4026	3047	4763	5197	5040	5239	5816	6194	5803	2568	2787	2293	5517	5467	8500
NM_006169.2	**NNMT**	5	5	5	13	15	9	12	23	24	5	4	2	9	19	15
NM_015381.3	**FAM19A5**	2	5	5	17	17	17	17	23	21	21	20	15	29	42	65
NM_015136.2	**STAB1**	546	510	721	667	681	697	550	530	569	796	891	693	998	842	1295
NM_002029.3	**FPR1**	6	4	7	14	8	3	5	6	4	4	4	3	9	8	6
NM_003930.3	**SCAP2**	1	0	2	3	3	5	0	4	2	2	4	1	9	9	20
NM_006486.2	**FBLN1**	0	2	1	4	6	10	1	4	1	2	1	3	3	6	4
NM_153206.1	**AMICA1**	2	0	0	1	1	0	0	2	0	0	0	0	0	1	1
NM_002965.2	**S100A9**	28	28	48	96	84	107	16	25	20	9	4	10	5	5	4
NM_021209.3	**CARD12/NLRC4**	0	1	2	2	1	3	3	4	4	2	0	2	0	3	5
NM_000433.2	**NCF2**	28	20	43	38	27	37	26	22	23	18	26	14	31	17	20
NM_003489.2	**NRIP1**	2	3	1	4	6	4	16	6	8	3	3	2	6	7	14
NM_001040084.1	**LOC653107/ANXA8**	243	201	301	45	37	41	81	103	80	98	99	73	56	83	114
NM_016582.1	**SLC15A3**	1	1	2	8	2	1	1	5	4	2	2	1	1	2	6
NM_000211.2	**ITGB2**	21	13	21	33	33	41	16	21	23	11	7	22	29	27	54
NM_000601.4	**HGF**	962	719	1118	940	931	887	828	884	785	527	522	470	1096	1000	1504
NM_182961.1	**SYNE1**	7	2	14	9	13	15	8	5	8	3	7	5	13	11	13
NM_001042729.1	**FGR**	7	4	5	5	9	6	6	3	5	6	3	8	4	7	13
NM_001614.2	**ACTG1**	2937	2469	3799	4984	4897	4826	4636	4778	4599	2180	2432	2034	5431	4789	6845
NM_138444.2	**KCTD12**	5	0	1	5	5	4	5	2	6	2	0	1	5	3	4
NM_002964.3	**S100A8**	89	84	101	149	138	147	32	34	34	14	15	13	18	7	19
NM_001034996.1	**RPL14**	0	0	0	0	0	0	0	0	0	0	0	0	0	0	0
NM_001025109.1	**CD34**	0	3	3	12	10	10	3	5	4	2	2	2	5	7	9
NM_000474.3	**TWIST1**	17	15	24	44	45	41	48	47	37	15	13	14	11	24	27
NM_015869.3	**PPARG**	33	20	32	28	27	23	53	48	41	19	15	13	26	23	24
NM_004666.1	**VNN1**	3	0	0	3	1	1	3	2	4	2	1	1	4	3	6
NM_005874.1	**LILRB2**	13	6	9	18	23	15	5	12	14	5	6	2	5	9	16
NM_001005463.1	**EBF3**	11	12	6	8	23	14	61	65	55	20	29	16	11	21	29
NM_152852.1	**MS4A6A**	4	2	1	2	2	0	3	6	4	0	3	1	1	1	3
NM_000954.5	**PTGDS**	70	42	78	66	39	45	32	29	21	49	50	59	36	36	66
NM_000222.1	**KIT**	49	30	45	43	39	43	68	81	72	37	46	35	57	66	69
NM_004961.3	**GABRE**	24	28	26	11	8	8	5	6	15	5	13	7	29	22	23
NM_007261.2	**CD300A**	3	4	3	9	10	19	1	6	8	4	6	5	9	4	9
NM_002115.1	**HK3**	1	7	4	5	5	8	3	10	9	2	3	3	4	6	4
NM_023914.2	**P2RY13**	5	6	3	7	7	8	12	9	10	2	5	0	6	6	9
NM_033642.1	**FGF13**	29	20	25	25	24	20	26	32	28	12	13	18	24	12	23
AF324996.2	**Athal_Spike_S23**	1861	1772	1760	1810	1851	1792	1816	1849	1821	1795	1877	1782	1808	1839	1795
AF325027.2	**Athal_Spike_S14**	741	803	801	757	744	748	754	755	802	799	758	757	796	789	787
AF325042.2	**Athal_Spike_S19**	502	547	507	525	481	486	542	501	491	519	475	542	505	464	518
AY058560.1	**DrosSpike8**	167	177	208	174	179	194	162	170	154	154	185	186	152	164	184
AF325027.2	**Athal_Spike_S13**	85	69	76	66	87	86	69	62	72	78	76	75	70	88	82
AF324998.2	**Athal_Spike_S22**	90	79	83	90	96	110	94	90	99	90	69	83	89	90	61
AY058658.1	**DrosSpike7**	21	24	29	37	26	36	27	30	23	28	28	37	28	30	27
AF325032.2	**Athal_Spike_S17**	23	16	27	29	28	33	27	31	25	25	25	25	29	26	27
DQ412624	**SarsSpike3**	5	9	7	8	3	10	4	6	11	9	4	8	15	3	10
AY058658.1	**DrosSpike6**	4	4	1	2	6	4	4	4	3	2	2	3	6	5	7
AY058560.1	**DrosSpike10**	2	2	1	1	1	1	1	4	0	2	0	3	4	0	2
AY058658.1	***DrosSpike11***	*4*	*4*	*0*	*0*	*3*	*1*	*3*	*0*	*1*	*1*	*0*	*2*	*1*	*1*	*3*
AF325014.2	***Athal_Spike_S12***	*4*	*4*	*5*	*5*	*4*	*4*	*5*	*2*	*8*	*4*	*1*	*0*	*4*	*3*	*7*
AF325016.2	***Athal_Spike_S15***	*9*	*2*	*5*	*8*	*4*	*0*	*8*	*9*	*7*	*4*	*6*	*5*	*13*	*4*	*3*
AF325016.2	***Athal_Spike_S16***	*4*	*2*	*3*	*7*	*3*	*3*	*3*	*0*	*1*	*0*	*3*	*0*	*4*	*2*	*4*
AF325032.2	***Athal_Spike_S18***	*2*	*2*	*2*	*6*	*2*	*8*	*3*	*4*	*5*	*2*	*3*	*1*	*0*	*3*	*4*
AF324998.2	***Athal_Spike_S20***	*0*	*4*	*2*	*2*	*5*	*6*	*12*	*5*	*7*	*2*	*3*	*7*	*4*	*1*	*2*
AF324998.2	***Athal_Spike_S21***	*3*	*3*	*6*	*6*	*7*	*4*	*10*	*3*	*5*	*4*	*6*	*1*	*3*	*5*	*4*
AF324998.2	***Athal_Spike_S24***	*7*	*3*	*3*	*3*	*3*	*4*	*0*	*3*	*4*	*4*	*4*	*2*	*4*	*2*	*4*
DQ412624	***SarsSpike4***	*13*	*5*	*7*	*4*	*0*	*5*	*1*	*2*	*7*	*5*	*4*	*8*	*14*	*5*	*5*
AY058560.1	***DrosSpike9***	*2*	*2*	*0*	*2*	*2*	*1*	*1*	*0*	*1*	*0*	*1*	*1*	*0*	*1*	*2*

		M3	M3	M3	M3	M3	M3	M3	M3	M3	M3	M3	M3	M4	M4	M4
Accession No.	**Gene Name/Sample ID**	**16060**	**16060**	**16060**	**17932**	**17932**	**17932**	**20898**	**20898**	**20898**	**20899**	**20899**	**20899**	**6039**	**6039**	**6039**
NM_002841.2	**PTPRG**	12	12	12	15	16	13	12	12	7	27	19	19	1	2	2
NM_145256.2	**LRRC25**	**1**	**0**	**2**	**4**	**3**	**3**	**4**	**1**	**2**	**2**	**2**	**5**	**34**	**19**	**22**
NM_001972.2	**ELA2**	219	164	124	175	131	174	816	760	761	380	423	365	39	32	33
NM_000597.2	**IGFBP2**	327	329	294	327	342	285	280	236	223	1167	1011	1171	12	13	9
NM_005413.1	**SIX3**	46	37	32	30	29	18	76	70	73	70	67	65	0	4	9
NM_006272.1	**S100B**	92	101	93	66	87	78	179	189	149	362	356	406	2	0	1
NM_003327.2	**TNFRSF4**	29	32	49	7	4	6	39	26	28	79	79	87	0	4	0
NM_004049.2	**BCL2A1**	28	18	18	11	21	21	17	19	20	23	8	23	28	25	19
NM_001911.2	**CTSG**	1650	1378	1236	448	447	370	3320	3186	2917	714	790	754	6	10	8
NM_001557.2	**IL8RB**	2	4	6	1	1	3	8	3	3	2	2	4	2	4	4
NM_001066.2	**TNFRSF1B**	3	2	0	27	24	19	7	16	5	14	14	23	153	142	143
NM_002046.3	**GAPDH**	6921	6006	5285	7955	8067	6548	7659	6995	6260	7903	7728	8005	3409	3494	3539
NM_006169.2	**NNMT**	51	51	49	11	18	15	138	95	102	42	59	53	4	4	3
NM_015381.3	**FAM19A5**	7	8	10	48	54	43	9	6	6	14	14	15	1	3	1
NM_015136.2	**STAB1**	886	879	832	977	933	766	571	531	453	710	591	690	57	58	53
NM_002029.3	**FPR1**	19	15	10	11	10	7	6	6	2	10	5	7	28	40	32
NM_003930.3	**SCAP2**	0	0	0	0	9	1	2	2	1	0	3	5	19	25	13
NM_006486.2	**FBLN1**	8	1	4	0	1	0	19	13	7	2	2	4	0	4	1
NM_153206.1	**AMICA1**	3	2	0	0	1	0	0	0	0	1	0	1	1	1	3
NM_002965.2	**S100A9**	46	55	35	194	219	179	21	23	16	53	46	44	1589	1610	1490
NM_021209.3	**CARD12/NLRC4**	3	1	0	6	7	9	5	0	5	8	2	8	24	19	28
NM_000433.2	**NCF2**	31	18	12	82	84	65	37	37	40	88	79	101	179	185	173
NM_003489.2	**NRIP1**	8	9	2	10	3	9	1	0	5	2	3	1	18	31	23
NM_001040084.1	**LOC653107/ANXA8**	195	189	209	18	24	21	19	19	10	203	212	218	7	4	6
NM_016582.1	**SLC15A3**	2	1	6	7	6	9	1	6	2	6	5	4	11	24	25
NM_000211.2	**ITGB2**	13	15	6	84	90	72	28	13	19	45	63	35	362	360	329
NM_000601.4	**HGF**	2554	2173	2297	896	873	723	2321	2146	1725	3477	3564	3492	68	62	71
NM_182961.1	**SYNE1**	10	9	4	17	18	16	15	12	15	8	11	12	6	4	12
NM_001042729.1	**FGR**	6	7	0	55	41	58	15	8	3	21	29	35	275	267	252
NM_001614.2	**ACTG1**	3736	3420	3430	6033	5898	4910	5367	4817	4064	7911	7974	7995	2761	2655	2513
NM_138444.2	**KCTD12**	1	5	8	11	4	15	4	5	7	4	6	12	58	64	67
NM_002964.3	**S100A8**	74	65	83	483	435	419	50	38	30	107	87	87	2883	2798	2649
NM_001034996.1	**RPL14**	0	0	0	0	0	0	0	0	0	0	0	0	0	0	0
NM_001025109.1	**CD34**	0	2	4	4	1	3	5	8	7	14	14	11	6	12	18
NM_000474.3	**TWIST1**	18	18	20	46	31	38	31	19	24	18	11	18	4	3	2
NM_015869.3	**PPARG**	33	21	41	58	38	30	14	15	8	17	5	15	2	2	3
NM_004666.1	**VNN1**	3	4	2	1	6	3	4	2	1	1	3	3	23	19	23
NM_005874.1	**LILRB2**	10	16	10	39	25	25	9	5	3	16	25	27	100	112	118
NM_001005463.1	**EBF3**	70	69	49	92	103	69	11	18	12	45	59	49	1	2	2
NM_152852.1	**MS4A6A**	3	3	2	3	1	1	2	7	2	5	0	5	33	33	23
NM_000954.5	**PTGDS**	17	16	10	7	13	7	4	6	12	21	25	31	1	2	3
NM_000222.1	**KIT**	46	21	32	86	84	59	88	84	86	17	17	19	12	10	17
NM_004961.3	**GABRE**	27	25	20	24	25	19	0	1	2	12	10	11	2	2	4
NM_007261.2	**CD300A**	3	7	10	15	10	3	13	7	5	7	11	3	0	4	2
NM_002115.1	**HK3**	6	4	4	4	0	7	7	2	6	1	6	4	24	12	14
NM_023914.2	**P2RY13**	6	4	6	13	10	12	11	4	7	7	2	4	39	51	46
NM_033642.1	**FGF13**	25	20	16	34	22	19	37	40	27	28	32	18	2	2	1
AF324996.2	**Athal_Spike_S23**	1865	1797	1835	1801	1849	1889	1863	1832	1850	1875	1833	1819	1801	1816	1872
AF325027.2	**Athal_Spike_S14**	754	760	806	750	709	741	754	699	745	737	768	768	811	734	689
AF325042.2	**Athal_Spike_S19**	478	532	447	504	499	491	489	514	515	472	464	516	483	540	527
AY058560.1	**DrosSpike8**	161	191	203	197	194	167	155	201	168	174	208	195	190	183	183
AF325027.2	**Athal_Spike_S13**	97	68	55	66	79	65	67	92	71	60	62	60	66	69	66
AF324998.2	**Athal_Spike_S22**	85	85	87	103	97	100	79	91	89	97	79	76	84	88	93
AY058658.1	**DrosSpike7**	28	24	37	34	25	16	32	29	31	25	25	29	32	22	26
AF325032.2	**Athal_Spike_S17**	21	30	12	34	31	24	38	24	17	37	51	30	26	36	36
DQ412624	**SarsSpike3**	9	12	12	4	12	4	18	11	9	18	5	4	6	6	5
AY058658.1	**DrosSpike6**	1	0	6	6	3	1	5	6	5	4	5	3	2	5	2
AY058560.1	**DrosSpike10**	2	3	2	0	1	1	2	3	1	2	2	0	5	1	3
AY058658.1	***DrosSpike11***	*2*	*2*	*2*	*0*	*1*	*4*	*2*	*0*	*6*	*2*	*0*	*1*	*1*	*3*	*0*
AF325014.2	***Athal_Spike_S12***	*4*	*4*	*6*	*1*	*3*	*4*	*5*	*6*	*6*	*5*	*8*	*7*	*2*	*6*	*5*
AF325016.2	***Athal_Spike_S15***	*2*	*5*	*8*	*4*	*6*	*3*	*5*	*6*	*5*	*4*	*2*	*5*	*1*	*1*	*1*
AF325016.2	***Athal_Spike_S16***	*0*	*10*	*2*	*6*	*1*	*4*	*2*	*3*	*8*	*4*	*0*	*5*	*2*	*3*	*4*
AF325032.2	***Athal_Spike_S18***	*3*	*2*	*10*	*4*	*4*	*6*	*5*	*3*	*3*	*5*	*10*	*3*	*7*	*3*	*2*
AF324998.2	***Athal_Spike_S20***	*0*	*2*	*2*	*6*	*0*	*1*	*6*	*4*	*3*	*4*	*3*	*5*	*2*	*1*	*4*
AF324998.2	***Athal_Spike_S21***	*4*	*5*	*2*	*0*	*6*	*3*	*1*	*3*	*7*	*0*	*5*	*5*	*2*	*4*	*3*
AF324998.2	***Athal_Spike_S24***	*3*	*5*	*0*	*3*	*1*	*1*	*6*	*2*	*1*	*2*	*5*	*1*	*5*	*3*	*3*
DQ412624	***SarsSpike4***	*3*	*5*	*4*	*3*	*6*	*6*	*1*	*7*	*0*	*7*	*2*	*10*	*4*	*7*	*3*
AY058560.1	***DrosSpike9***	*1*	*1*	*0*	*0*	*1*	*0*	*0*	*1*	*0*	*4*	*2*	*3*	*0*	*2*	*0*

		M4	M4	M4	M4	M4	M4	M4	M4	M4	CD34	CD34	CD34	CD34	CD34	CD34
Accession No.	**Gene Name/Sample ID**	**15601**	**15601**	**15601**	**15602**	**15602**	**15602**	**20896**	**20896**	**20896**	**6**	**6**	**6**	**7**	**7**	**7**
NM_002841.2	**PTPRG**	0	1	4	2	2	2	1	1	0	1	1	1	0	0	7
NM_145256.2	**LRRC25**	**28**	**24**	**20**	**94**	**118**	**104**	**14**	**8**	**18**	**1**	**1**	**2**	**3**	**3**	**0**
NM_001972.2	**ELA2**	78	78	68	7	9	15	28	15	12	12	39	28	13	18	18
NM_000597.2	**IGFBP2**	57	55	48	33	28	30	7	13	12	14	21	12	15	18	22
NM_005413.1	**SIX3**	6	5	1	3	5	3	1	0	2	1	0	3	4	1	0
NM_006272.1	**S100B**	8	16	11	6	9	8	25	19	15	3	5	3	0	0	4
NM_003327.2	**TNFRSF4**	4	0	1	7	2	4	1	0	1	2	0	0	0	1	0
NM_004049.2	**BCL2A1**	47	46	35	180	199	180	39	34	24	23	34	41	35	49	49
NM_001911.2	**CTSG**	9	14	12	155	183	164	222	220	205	100	90	97	48	43	60
NM_001557.2	**IL8RB**	6	5	4	8	12	17	6	13	11	2	2	6	6	5	0
NM_001066.2	**TNFRSF1B**	126	106	92	440	460	432	90	58	78	17	16	12	9	11	9
NM_002046.3	**GAPDH**	4175	4256	3942	4328	4325	4464	5168	5296	5129	3824	4716	4995	3221	3288	3670
NM_006169.2	**NNMT**	10	8	8	1	3	2	3	2	4	3	0	1	4	5	7
NM_015381.3	**FAM19A5**	0	3	4	1	4	2	1	1	0	15	12	19	3	4	0
NM_015136.2	**STAB1**	23	34	24	214	223	218	54	72	58	4	5	3	5	4	7
NM_002029.3	**FPR1**	27	35	20	64	81	57	21	28	21	8	9	7	6	4	4
NM_003930.3	**SCAP2**	24	21	12	30	34	42	20	26	18	17	12	13	14	5	4
NM_006486.2	**FBLN1**	0	0	0	2	1	1	0	1	0	2	0	1	1	0	0
NM_153206.1	**AMICA1**	1	1	0	2	0	3	0	0	3	1	1	1	1	0	0
NM_002965.2	**S100A9**	2243	2078	1948	1550	1667	1472	619	642	542	60	90	98	107	123	116
NM_021209.3	**CARD12/NLRC4**	14	13	23	39	46	33	6	3	8	4	2	4	3	0	2
NM_000433.2	**NCF2**	114	115	110	317	324	344	120	151	154	14	12	33	18	34	24
NM_003489.2	**NRIP1**	34	21	18	34	41	38	22	28	19	130	146	149	70	86	109
NM_001040084.1	**LOC653107/ANXA8**	6	5	3	3	1	2	4	4	1	0	4	1	1	4	0
NM_016582.1	**SLC15A3**	13	17	14	31	36	36	7	8	4	4	6	0	5	4	2
NM_000211.2	**ITGB2**	259	233	269	754	706	775	283	247	216	67	72	83	39	32	44
NM_000601.4	**HGF**	139	104	108	28	30	28	78	68	87	23	44	39	18	23	18
NM_182961.1	**SYNE1**	12	7	6	10	19	16	10	8	8	16	20	18	11	16	13
NM_001042729.1	**FGR**	176	164	200	591	602	611	259	233	216	11	13	15	8	12	9
NM_001614.2	**ACTG1**	3267	2964	2951	3764	3904	3747	3575	3698	3542	3295	3986	4302	2823	3171	3121
NM_138444.2	**KCTD12**	84	72	60	74	73	70	24	9	12	9	16	10	9	9	18
NM_002964.3	**S100A8**	4377	3984	3749	3220	3314	3276	1046	1055	967	169	195	228	301	339	371
NM_001034996.1	**RPL14**	0	0	0	0	0	0	0	0	0	0	0	0	0	0	0
NM_001025109.1	**CD34**	55	68	76	8	8	5	39	23	29	112	118	149	54	61	62
NM_000474.3	**TWIST1**	3	2	2	8	2	4	4	1	3	4	5	10	1	4	4
NM_015869.3	**PPARG**	6	5	6	4	6	7	0	1	3	2	5	3	3	4	11
NM_004666.1	**VNN1**	3	3	3	54	56	47	17	18	15	3	2	3	3	5	0
NM_005874.1	**LILRB2**	75	69	74	487	473	440	39	54	48	35	34	33	42	31	42
NM_001005463.1	**EBF3**	10	5	4	3	3	2	6	4	4	2	8	3	3	3	7
NM_152852.1	**MS4A6A**	26	23	21	28	28	41	36	40	35	5	11	5	8	5	9
NM_000954.5	**PTGDS**	1	2	0	0	0	0	0	0	1	0	0	1	0	3	0
NM_000222.1	**KIT**	59	65	56	23	30	24	15	18	12	37	51	52	33	23	22
NM_004961.3	**GABRE**	2	7	3	4	4	2	0	2	4	1	4	3	0	0	2
NM_007261.2	**CD300A**	12	4	8	17	14	9	3	3	2	7	12	14	4	5	2
NM_002115.1	**HK3**	6	12	12	25	29	36	8	3	2	0	0	1	1	4	2
NM_023914.2	**P2RY13**	52	56	60	94	105	91	37	37	35	9	21	12	10	8	13
NM_033642.1	**FGF13**	2	0	3	2	1	1	1	1	0	4	0	3	3	0	2
AF324996.2	**Athal_Spike_S23**	1825	1866	1883	1858	1859	1909	1778	1871	1905	1838	1881	1839	1782	1827	1731
AF325027.2	**Athal_Spike_S14**	761	766	676	730	744	713	757	722	717	741	704	736	732	759	755
AF325042.2	**Athal_Spike_S19**	521	506	516	501	501	497	595	503	496	491	550	521	517	483	544
AY058560.1	**DrosSpike8**	166	165	196	190	187	173	155	170	165	190	145	178	187	167	202
AF325027.2	**Athal_Spike_S13**	76	69	77	84	74	61	69	69	79	72	64	85	89	77	73
AF324998.2	**Athal_Spike_S22**	90	65	81	84	81	89	85	100	87	82	90	81	117	101	98
AY058658.1	**DrosSpike7**	23	28	31	21	23	21	20	26	25	46	29	20	33	36	42
AF325032.2	**Athal_Spike_S17**	23	29	29	23	25	27	30	22	13	25	26	25	36	34	47
DQ412624	**SarsSpike3**	10	4	6	5	4	5	9	11	9	8	7	10	5	9	4
AY058658.1	**DrosSpike6**	5	3	4	4	0	4	1	4	3	6	4	3	0	4	2
AY058560.1	**DrosSpike10**	3	1	2	2	1	0	4	1	1	0	0	0	3	1	2
AY058658.1	***DrosSpike11***	*2*	*0*	*3*	*2*	*0*	*2*	*8*	*1*	*4*	*1*	*1*	*0*	*0*	*0*	*0*
AF325014.2	***Athal_Spike_S12***	*2*	*5*	*3*	*5*	*3*	*3*	*2*	*2*	*4*	*5*	*2*	*5*	*0*	*5*	*0*
AF325016.2	***Athal_Spike_S15***	*6*	*5*	*10*	*2*	*0*	*5*	*2*	*6*	*1*	*3*	*6*	*3*	*0*	*4*	*0*
AF325016.2	***Athal_Spike_S16***	*1*	*5*	*3*	*3*	*2*	*5*	*4*	*3*	*2*	*1*	*2*	*3*	*1*	*3*	*0*
AF325032.2	***Athal_Spike_S18***	*2*	*5*	*8*	*2*	*5*	*4*	*0*	*2*	*3*	*2*	*4*	*4*	*3*	*0*	*0*
AF324998.2	***Athal_Spike_S20***	*4*	*3*	*6*	*1*	*5*	*5*	*4*	*3*	*0*	*1*	*1*	*4*	*1*	*1*	*0*
AF324998.2	***Athal_Spike_S21***	*5*	*4*	*3*	*3*	*5*	*4*	*4*	*1*	*2*	*1*	*2*	*5*	*3*	*4*	*4*
AF324998.2	***Athal_Spike_S24***	*3*	*2*	*4*	*3*	*6*	*2*	*6*	*2*	*5*	*3*	*2*	*5*	*0*	*3*	*0*
DQ412624	***SarsSpike4***	*3*	*4*	*6*	*6*	*7*	*3*	*4*	*2*	*3*	*5*	*2*	*4*	*3*	*4*	*4*
AY058560.1	***DrosSpike9***	*4*	*1*	*1*	*0*	*1*	*2*	*1*	*1*	*1*	*2*	*0*	*0*	*0*	*0*	*2*

		Pros	Pros	Pros	Pros	Pros	Pros	Pros	Pros	Pros	Pros	Pros	Pros	Pros	Pros	Pros
Accession No.	**Gene Name/Sample ID**	**109055**	**109055**	**109055**	**109058**	**109058**	**109058**	**114099**	**114099**	**114099**	**114100**	**114100**	**114100**	**114101**	**114101**	**114101**
NM_002841.2	**PTPRG**	8	13	9	10	9	17	8	5	8	8	2	10	9	13	9
NM_145256.2	**LRRC25**	**17**	**15**	**10**	**28**	**25**	**28**	**6**	**11**	**5**	**9**	**2**	**7**	**13**	**15**	**13**
NM_001972.2	**ELA2**	1199	1075	1244	868	789	867	216	247	272	354	259	317	310	324	323
NM_000597.2	**IGFBP2**	26	21	18	74	73	55	7	11	9	27	4	21	13	15	15
NM_005413.1	**SIX3**	57	44	55	55	63	64	48	52	60	77	4	67	104	86	80
NM_006272.1	**S100B**	10	10	11	4	0	6	1	2	5	4	0	2	6	6	2
NM_003327.2	**TNFRSF4**	3	5	2	2	2	5	3	2	4	4	0	2	5	5	4
NM_004049.2	**BCL2A1**	88	74	78	124	147	125	44	56	65	74	50	74	135	122	121
NM_001911.2	**CTSG**	2067	1769	1995	1946	1977	1973	431	433	445	556	167	553	729	703	668
NM_001557.2	**IL8RB**	16	18	10	21	27	32	21	20	23	22	0	15	31	36	28
NM_001066.2	**TNFRSF1B**	44	44	37	63	86	65	75	69	69	75	59	59	115	111	104
NM_002046.3	**GAPDH**	7616	6498	7234	6988	7429	7887	2952	3264	3296	3723	1530	3410	5675	5553	5591
NM_006169.2	**NNMT**	13	12	12	6	11	11	15	14	11	14	2	10	15	17	17
NM_015381.3	**FAM19A5**	9	7	6	7	14	10	4	6	7	5	1	4	14	11	10
NM_015136.2	**STAB1**	9	7	10	14	11	14	4	8	8	6	1	7	12	10	10
NM_002029.3	**FPR1**	22	27	9	27	25	45	19	22	19	29	16	30	96	96	85
NM_003930.3	**SCAP2**	32	18	15	41	16	30	11	11	12	18	8	9	22	22	25
NM_006486.2	**FBLN1**	1	2	2	2	2	3	2	3	1	1	0	0	1	1	1
NM_153206.1	**AMICA1**	12	1	5	10	2	4	11	14	12	11	6	15	20	20	20
NM_002965.2	**S100A9**	12420	11305	11278	13705	14343	14743	3636	4143	4066	4738	520	4224	6612	6592	6666
NM_021209.3	**CARD12/NLRC4**	67	74	72	70	102	75	82	91	85	79	31	74	113	118	100
NM_000433.2	**NCF2**	271	260	227	334	358	374	167	153	171	198	93	199	288	319	267
NM_003489.2	**NRIP1**	40	27	32	35	48	42	13	19	24	25	2	31	37	33	33
NM_001040084.1	**LOC653107/ANXA8**	14	4	9	22	41	31	9	7	7	18	4	19	14	18	15
NM_016582.1	**SLC15A3**	28	18	21	33	23	34	18	12	18	19	3	18	32	24	17
NM_000211.2	**ITGB2**	554	450	499	658	655	763	294	322	344	386	143	339	513	504	500
NM_000601.4	**HGF**	21	10	15	31	20	30	10	11	8	13	4	11	20	11	15
NM_182961.1	**SYNE1**	49	51	56	78	68	79	33	42	40	53	17	54	72	76	73
NM_001042729.1	**FGR**	948	829	888	1172	1043	1256	968	990	1036	1004	1322	1018	1616	1601	1554
NM_001614.2	**ACTG1**	4404	3904	3926	5081	5345	5497	1856	2023	2143	2709	1644	2497	3200	3382	3364
NM_138444.2	**KCTD12**	30	21	23	37	23	42	13	13	12	13	2	21	26	20	17
NM_002964.3	**S100A8**	39038	34512	34841	42709	46190	47216	16732	18504	18732	20596	5219	18606	28528	28884	28963
NM_001034996.1	**RPL14**	0	0	0	0	0	0	0	0	0	0	0	0	0	0	0
NM_001025109.1	**CD34**	4	4	7	1	2	5	10	11	13	16	14	10	13	13	10
NM_000474.3	**TWIST1**	22	14	16	22	9	17	12	24	17	15	5	20	27	29	26
NM_015869.3	**PPARG**	41	30	28	51	50	49	27	34	33	41	2	26	40	43	51
NM_004666.1	**VNN1**	14	17	16	12	9	13	11	9	8	11	1	9	31	35	30
NM_005874.1	**LILRB2**	177	162	155	189	177	183	45	62	63	105	19	78	135	136	132
NM_001005463.1	**EBF3**	12	7	10	11	11	9	12	19	16	16	12	15	31	22	23
NM_152852.1	**MS4A6A**	6	5	4	7	11	11	4	2	1	3	1	2	5	6	4
NM_000954.5	**PTGDS**	2	1	0	2	0	3	2	1	1	1	1	0	2	2	1
NM_000222.1	**KIT**	7	4	5	4	14	6	5	1	5	4	1	2	6	9	3
NM_004961.3	**GABRE**	12	23	17	25	18	18	17	17	22	16	2	17	22	26	24
NM_007261.2	**CD300A**	12	4	7	6	5	10	3	5	5	5	2	5	10	10	9
NM_002115.1	**HK3**	40	42	37	51	70	57	22	28	27	23	3	22	34	40	36
NM_023914.2	**P2RY13**	157	125	161	190	224	189	159	167	176	156	60	147	262	233	241
NM_033642.1	**FGF13**	15	25	27	4	7	9	5	4	5	9	1	7	13	11	11
AF324996.2	**Athal_Spike_S23**	1797	1875	1830	1825	1907	1837	1794	1783	1850	1774	1961	1746	1837	1833	1798
AF325027.2	**Athal_Spike_S14**	669	659	703	753	621	674	377	411	407	424	327	388	381	400	396
AF325042.2	**Athal_Spike_S19**	580	538	525	530	510	555	620	658	644	637	547	671	634	648	639
AY058560.1	**DrosSpike8**	195	166	197	150	163	173	184	187	174	164	162	180	173	169	181
AF325027.2	**Athal_Spike_S13**	75	83	71	75	86	71	208	161	162	182	178	187	152	157	153
AF324998.2	**Athal_Spike_S22**	98	88	94	89	98	101	155	183	154	161	202	153	136	160	202
AY058658.1	**DrosSpike7**	41	35	38	32	34	35	22	34	23	33	21	27	35	35	33
AF325032.2	**Athal_Spike_S17**	26	38	28	25	68	35	116	55	55	91	82	119	98	62	61
DQ412624	**SarsSpike3**	12	8	6	12	7	11	11	13	15	20	12	14	20	16	15
AY058658.1	**DrosSpike6**	6	8	7	7	5	8	13	15	15	14	7	13	32	18	20
AY058560.1	**DrosSpike10**	3	4	4	4	2	5	8	8	9	12	2	9	8	10	14
AY058658.1	***DrosSpike11***	*8*	*4*	*4*	*1*	*7*	*14*	*9*	*13*	*8*	*8*	*4*	*11*	*14*	*13*	*18*
AF325014.2	***Athal_Spike_S12***	*4*	*7*	*7*	*10*	*5*	*11*	*3*	*9*	*3*	*11*	*2*	*7*	*5*	*9*	*12*
AF325016.2	***Athal_Spike_S15***	*6*	*10*	*9*	*9*	*14*	*6*	*3*	*5*	*6*	*6*	*2*	*7*	*7*	*7*	*8*
AF325016.2	***Athal_Spike_S16***	*3*	*4*	*1*	*7*	*14*	*2*	*8*	*7*	*4*	*14*	*5*	*8*	*16*	*11*	*13*
AF325032.2	***Athal_Spike_S18***	*34*	*30*	*29*	*27*	*32*	*36*	*26*	*30*	*26*	*35*	*6*	*25*	*47*	*36*	*37*
AF324998.2	***Athal_Spike_S20***	*2*	*4*	*6*	*4*	*5*	*3*	*0*	*0*	*0*	*0*	*0*	*0*	*0*	*0*	*0*
AF324998.2	***Athal_Spike_S21***	*7*	*8*	*4*	*0*	*5*	*6*	*9*	*7*	*10*	*8*	*2*	*5*	*10*	*10*	*9*
AF324998.2	***Athal_Spike_S24***	*15*	*14*	*17*	*11*	*20*	*18*	*16*	*17*	*17*	*27*	*3*	*23*	*35*	*31*	*36*
DQ412624	***SarsSpike4***	*6*	*7*	*7*	*7*	*5*	*8*	*10*	*22*	*14*	*15*	*5*	*19*	*17*	*13*	*20*
AY058560.1	***DrosSpike9***	*5*	*1*	*4*	*5*	*0*	*8*	*5*	*11*	*9*	*10*	*1*	*6*	*15*	*6*	*12*

		PMNs	PMNs	PMNs	PMNs	PMNs	PMNs			
Accession No.	**Gene Name/Sample ID**	**109057**	**109057**	**109057**	**109583**	**109583**	**109583**	**SpikeOnly**	**SpikeOnly**	**SpikeOnly**
NM_002841.2	**PTPRG**	12	12	9	4	6	2	0	0	0
NM_145256.2	**LRRC25**	**249**	**266**	**208**	**198**	**159**	**180**	**1**	**0**	**0**
NM_001972.2	**ELA2**	47	35	38	19	21	7	3	1	2
NM_000597.2	**IGFBP2**	12	16	12	3	4	10	1	4	0
NM_005413.1	**SIX3**	61	43	40	26	35	22	0	0	1
NM_006272.1	**S100B**	5	8	6	1	6	0	1	2	1
NM_003327.2	**TNFRSF4**	5	9	5	3	2	8	1	0	1
NM_004049.2	**BCL2A1**	3264	2915	2420	1615	1554	1612	2	1	1
NM_001911.2	**CTSG**	73	65	49	46	38	35	0	0	0
NM_001557.2	**IL8RB**	2153	1982	1803	1273	1220	1311	1	1	1
NM_001066.2	**TNFRSF1B**	1273	1202	1257	768	788	720	3	5	1
NM_002046.3	**GAPDH**	3016	2697	2588	1269	1124	1213	1	1	0
NM_006169.2	**NNMT**	16	7	11	10	8	7	0	1	1
NM_015381.3	**FAM19A5**	12	3	4	6	4	3	0	1	0
NM_015136.2	**STAB1**	16	7	4	6	6	3	1	1	0
NM_002029.3	**FPR1**	2864	2610	2391	1342	1274	1345	0	2	1
NM_003930.3	**SCAP2**	56	60	43	82	43	66	0	0	0
NM_006486.2	**FBLN1**	2	0	2	4	2	0	0	0	0
NM_153206.1	**AMICA1**	17	14	20	7	5	20	1	1	1
NM_002965.2	**S100A9**	18402	16585	14408	10883	9845	10712	0	0	1
NM_021209.3	**CARD12/NLRC4**	21	43	37	22	19	22	1	0	1
NM_000433.2	**NCF2**	2950	2698	2364	1581	1531	1616	0	1	2
NM_003489.2	**NRIP1**	19	27	21	11	2	15	0	0	0
NM_001040084.1	**LOC653107/ANXA8**	12	15	12	8	7	5	1	0	0
NM_016582.1	**SLC15A3**	185	190	139	100	74	94	0	0	0
NM_000211.2	**ITGB2**	1534	1479	1466	753	687	670	1	1	0
NM_000601.4	**HGF**	16	18	14	8	12	19	0	0	1
NM_182961.1	**SYNE1**	66	65	60	35	46	32	0	0	0
NM_001042729.1	**FGR**	2959	2560	2483	1530	1615	1518	3	4	1
NM_001614.2	**ACTG1**	4005	3317	2889	1479	1383	1486	0	0	0
NM_138444.2	**KCTD12**	42	81	44	17	18	19	0	1	0
NM_002964.3	**S100A8**	38217	33320	29862	18679	17602	18700	1	0	0
NM_001034996.1	**RPL14**	0	0	0	0	0	0	0	0	0
NM_001025109.1	**CD34**	7	7	2	3	4	0	5	8	7
NM_000474.3	**TWIST1**	17	18	20	8	11	12	1	2	1
NM_015869.3	**PPARG**	33	31	31	11	11	17	0	0	0
NM_004666.1	**VNN1**	44	39	30	59	57	56	0	0	0
NM_005874.1	**LILRB2**	720	717	663	369	335	367	0	1	0
NM_001005463.1	**EBF3**	2	9	10	4	4	2	3	4	1
NM_152852.1	**MS4A6A**	0	4	2	6	8	3	1	0	0
NM_000954.5	**PTGDS**	2	1	0	0	1	0	0	0	0
NM_000222.1	**KIT**	5	4	1	0	0	0	1	1	0
NM_004961.3	**GABRE**	23	16	14	11	12	12	2	2	1
NM_007261.2	**CD300A**	21	19	23	46	34	62	0	1	0
NM_002115.1	**HK3**	44	43	41	46	33	22	0	0	1
NM_023914.2	**P2RY13**	887	726	736	488	437	456	3	4	3
NM_033642.1	**FGF13**	2	7	4	1	6	7	0	0	0
AF324996.2	**Athal_Spike_S23**	1881	1817	1874	1840	1847	1875	1815	1882	1863
AF325027.2	**Athal_Spike_S14**	657	688	694	707	694	677	380	428	405
AF325042.2	**Athal_Spike_S19**	528	535	500	513	522	518	653	650	683
AY058560.1	**DrosSpike8**	160	214	191	183	157	197	180	179	180
AF325027.2	**Athal_Spike_S13**	61	80	69	79	72	81	192	141	135
AF324998.2	**Athal_Spike_S22**	119	69	85	102	109	84	154	133	152
AY058658.1	**DrosSpike7**	31	35	37	24	47	20	26	19	22
AF325032.2	**Athal_Spike_S17**	47	46	33	26	33	37	85	56	48
DQ412624	**SarsSpike3**	9	14	11	18	13	8	9	7	9
AY058658.1	**DrosSpike6**	5	1	4	7	6	2	5	4	3
AY058560.1	**DrosSpike10**	2	4	7	0	2	3	2	2	2
AY058658.1	***DrosSpike11***	*2*	*5*	*2*	*1*	*1*	*3*	*3*	*4*	*3*
AF325014.2	***Athal_Spike_S12***	*12*	*8*	*9*	*3*	*4*	*3*	*3*	*4*	*5*
AF325016.2	***Athal_Spike_S15***	*9*	*5*	*10*	*3*	*1*	*3*	*3*	*2*	*1*
AF325016.2	***Athal_Spike_S16***	*9*	*14*	*2*	*3*	*2*	*0*	*8*	*7*	*5*
AF325032.2	***Athal_Spike_S18***	*23*	*33*	*19*	*12*	*15*	*8*	*2*	*2*	*1*
AF324998.2	***Athal_Spike_S20***	*5*	*7*	*2*	*0*	*6*	*3*	*0*	*0*	*0*
AF324998.2	***Athal_Spike_S21***	*9*	*5*	*4*	*1*	*5*	*8*	*4*	*2*	*2*
AF324998.2	***Athal_Spike_S24***	*7*	*23*	*8*	*3*	*9*	*15*	*1*	*1*	*0*
DQ412624	***SarsSpike4***	*5*	*5*	*6*	*8*	*7*	*2*	*10*	*8*	*3*
AY058560.1	***DrosSpike9***	*2*	*3*	*3*	*1*	*2*	*2*	*1*	*3*	*2*

Table 2-6: Detailed sequence information for nCounter CodeSet capture probes and reporter probes.

Target-NSID	Gene Symbol	Reporter Probe Sequence
NM_001614.2:1615	ACTG1	CCACGGTGTTCTGGCCAAAGACATCAGCTAAGAAAGGAAACTGGGTCCTA
NM_153206.1:125	AMICA1	CTTTGCCATCAGCTTTCCAGCCTCTAGGTGCTTCACACAGG
NM_001040084.1:775	ANXA8	GCAATTTTCTCATACTCTTCAAACACTCTCAGCAGGTGAGTGGCACTGCG
NM_004049.2:80	BCL2A1	CTGGTGGAGAGCAAAGTCTTGAGCTGGCTCACCTTGAAGCTGTTGA
NM_007261.2:0	CD300A	CTGCAGGTTCTTCGGCTATTTCTAGTGATGAGACCTCTCCC
NM_001025109.1:1580	CD34	AGCTTCTCCAGACCTTGGCTTTCCCCCGTCACACGTTTACCCAAAGAAGA
NM_001911.2:160	CTSG	CAGGGTGACATTTATATTGCTTCCCCAGCAATGAGCTGCTGTCAGCACA
NM_001005463.1:640	EBF3	CCAGCACGTGGCCGTCCACGTTGACTGTTGTCGATACAACAACCTGGA
NM_001972.2:195	ELA2	ACCACCCGCACCGCGCGGACGTTTACATTCGCCACGCAGTG
NM_015381.3:320	FAM19A5	CTCCAGACACGGAAGCATGTCACACCACTGCTTGGTC
NM_006486.2:1260	FBLN1	GCTGGCACTCGTTGACATCGACACACATCCTGCTGATGCCGTCAAAATAG
NM_033642.1:620	FGF13	TTCAACAGCACCTGGAGGTAAGGTTCTGTTACAGAGCCCTTCTTTTGCCC
NM_001042729.1:440	FGR	TATTGTTCAGGATGTGGAACTTCTCGCCCTTGGTGAAGGTGAGGTCATCC
NM_002029.3:350	FPR1	TGAGGGCGATCAGGAAGACACTTCCGAACAAGTTGATGTCCACTATGGTA
NM_004961.3:65	GABRE	GACAACATCACGGGAAGAGGCTTCATTCTTTGATTCAGTCTGAGGTCCCT
NM_002046.3:245	GAPDH	ATCTCGCTCCTGGAAGATGGTGATGGGATTTCCATTGATGACAAGCTTCC
NM_000601.4:550	HGF	AAGCTGTGTTCGTGTGGTATCATGGAACTCCAGGGCTGACATTTGATGCC
NM_002115.1:495	HK3	GTCTGGTGACAAGGGAAAGAGAAGCTGAAGCCAAGCTGCAGACCCTGTTT
NM_000597.2:675	IGFBP2	CAAGGTGATGCTTGCCACCCTTGCCCATCTGCCGG
NM_001557.2:2050	IL8RB	CTGAAGTTTTGAGGAAAGCTGCCATACTGTCTTCTGCAGTGGTCACACCA
NM_000211.2:520	ITGB2	CGGAGCAGGTCGCCACCTAGCTTCTTGACATTCCTGA
NM_138444.2:450	KCTD12	CTGCAAGTCCCGCAGGTAATCCAGGATGTAGCGGAAGAGGAA
NM_000222.1:5	KIT	AGATGGTTGAGAAGAGCCTGTCTGGACGCGAAGCAGTAGGAGCAGAACGC
NM_005874.1:595	LILRB2	GGCTGGGAGTTCAGGCATTGTGGGTGTTCATCTTCTCCTTCCTTACACAG
NM_145256.2:115	LRRC25	TCTGGTTTGCAGTCCCTGCACAGGTGCAAGTTCTAGAG
NM_152852.1:65	MS4A6A	TCTCAGTCCCATCAACGGTTTCTACTTACCTTCATCTTCTGAAAGTCATC
NM_000433.2:160	NCF2	AGGGACATGATTAGGTAGAAACTAGGAGGCCAAGAGAGCTGCCAGGAGAC
NM_021209.3:840	NLRC4	TGCCAGGTATATCCAGGAGTTGATCACAGAGGGTTTCAAAAAGTCCACCC
NM_006169.2:605	NNMT	AAGCCAGGGAGTGACCCTGCAGAAGTTGTCTTCCTGA
NM_003489.2:335	NRIP1	CCTGATCCCCCTGCTGCCTGATGCATTAGTAATCCTTCTAGGTAAGTTAA
NM_023914.2:2385	P2RY13	AGGTAAGGCCAGAAAGGTAGGCAAGTTCTAGGGCCTTTGAGGCCATGGAA
NM_015869.3:1035	PPARG	AAAACCAGGAATGCTTTTGGCATACTCTGTGATCTCCTGCACAGCCTCCA
NM_000954.5:180	PTGDS	TGGACAACGCCGCCTTCTTCTCCCGGAGCCAGCTC
NM_002841.2:0	PTPRG	CCTGAAAGTTGTGGCTCCGGCGCAGGCTGGGAAGGAAC
NM_002964.3:115	S100A8	AGACGTCTGCACCCTTTTTCCTGATATACTGAGGACACTCGGTCTCTAGC
NM_002965.2:75	S100A9	CTTTGAATTCCCCCTGGTTCAGGGTGTCTGGGTGC
NM_006272.1:40	S100B	CCCTCCCTTCCAGAATATTGGTGGAAAACGTCGATGAGGGCCACCATGGC
NM_003930.3:1270	SCAP2	AATATCATACATCTCCATTATGTAGGCTTTAGGCACCAAGCCAATGGCTC
NM_005413.1:1305	SIX3	GCGGCCTTGGCTATCATACATCACATTCCGAGTCGCTGG
NM_016582.1:820	SLC15A3	CAGCAGGAAGCTGATGTTCTGCTGAATAAACGCCACCACCAGCAGCGA
NM_015136.2:95	STAB1	GAGTGACAAACGTGGTTTTCACATCACAGCCTTTGAACAGCACCTGCCCC
NM_001066.2:835	TNFRSF1B	GACACAGTTCACCACTCCTATTATTAGTAGACCCAAGGCTGTCACACCCA
NM_003327.2:200	TNFRSF4	CACTCCCACTTCTGAGGTTACACCACGTGCAGGGC
NM_000474.3:35	TWIST1	AAAAAGAAAGCGCCCAACGGCTGGACGCACACCCCGCCAGGCC
NM_004666.1:195	VNN1	GGGTAGAGAGAGTCCCTGTTGAAGTTCCAGCCATAAATAGCATCTTCTGG

Target-NSID	Gene Symbol	Capture Probe Sequence
NM_001614.2:1615	ACTG1	CGGCTTGGACTTTCCAACCCTGACAGACCCGCAAGACAAAACAACTGGTT
NM_153206.1:125	AMICA1	GACCCCTGCCCATTATCTCTATGTTGCTCAAGCAATTTCGAGCGGTCACT
NM_001040084.1:775	ANXA8	CGTGCACAGGATGGTGATGAATTTCATCTCATCAGTCCCACGAATCTTCT
NM_004049.2:80	BCL2A1	GGCAATGTGCTGAGAATGCTCACTGAGCTTGACTGAGTTATGACACATGA
NM_007261.2:0	CD300A	TGTAGTGACTCCGTAGCTTGCAGGACTGATCCCCG
NM_001025109.1:1580	CD34	CCAGAGTCTGGCTCCAGGGAGCCGAATGTGTAAAGGACAGGAGTTTAC
NM_001911.2:160	CTSG	AAGTCTTCTCGCACCAGGAACCCTCCACATCTGCT
NM_001005463.1:640	EBF3	ATCTCCGCATATCTCGAGGGTTGCCTGCATTCTTCAAACAGTTCTGATTG
NM_001972.2:195	ELA2	CGCGGCCGACATGACGAAGTTGGGCGCAATCAGGGTGGCG
NM_015381.3:320	FAM19A5	TTGATGATTCTTGCGTCCACACAGGCGGGCCGGGCT
NM_006486.2:1260	FBLN1	TAACCCGTCTTGCATTCGCAGCGGAAACTGCCGGGAGAGTTCACGCAGCG
NM_033642.1:620	FGF13	TCACTGGCTACGTTGATTCATTGTGGCTCATGGATTTGCCTCCGTTCAGC
NM_001042729.1:440	FGR	TCAGTTCGAGCCTCATAGTCATACAGGGCAATGAACAGGGTCAC
NM_002029.3:350	FPR1	AAGACGAATTTGCACAGGAACCAGCCGAAAGGCCAATGTCCTCCCATGGC
NM_004961.3:65	GABRE	CGACCCTCGACTGGAGGATCAATAAGATGCCTAGGAGGACTGGAAGAACT
NM_002046.3:245	GAPDH	CGTTCTCAGCCTTGACGGTGCCATGGAATTTGCCATGGGTGGAATCATAT
NM_000601.4:550	HGF	ACTCTTAGTGATAGATACTGTTCCCTTGTAGCTGCGTCCTTTACCAATGA
NM_002115.1:495	HK3	GTTCACAGGCTGCGCATCCAGGAACTCAGACAGGC
NM_000597.2:675	IGFBP2	TGCTGCTCAGTGACCTTCTCCCGGAACACGGCCAG
NM_001557.2:2050	IL8RB	TTTTACAATCCCCCCCAGCAACGCTCGAGAGTTCCAGTTTCTCCTCTACA
NM_000211.2:520	ITGB2	GGTCATCAAGCATGGAGTAGGAGAGGTCCATCAGATAGTAC
NM_138444.2:450	KCTD12	GCCGTCCCGGTCCAGAAAGAAGCGGCCTTTGCTGT
NM_000222.1:5	KIT	AGAGAAAATCCCAGGCGCCGCGAGCGCCTCTCATCG
NM_005874.1:595	LILRB2	AATGAAGCCGCCAAATGCCACCTGTGACTCACACTGGAGGGTCACCCTTC
NM_145256.2:115	LRRC25	CCTCAGTCCTACCTTTTGGGTCCCACTGCCACGCTTTTG
NM_152852.1:65	MS4A6A	AGCCCTTCCTTATTCCAGTGTTTACAGCTATACAGGATGTGATACTCACA
NM_000433.2:160	NCF2	AGAGAGAAGACAGGTTGGAGCGTCTCCCCTAGCAG
NM_021209.3:840	NLRC4	TGGGCCCTGCTGAGACGGAGGAAGAAGACGAATTTGAACTTGGTCAGAGC
NM_006169.2:605	NNMT	GTCTCAGGCTAACAGCATTCCTTCCATCAGTTCAGCCCTTCTTTTAGAAC
NM_003489.2:335	NRIP1	AACAATAGAATCCTGGTGCACATCAGAGCCAAGCTCTTCTCCATGAGTCA
NM_023914.2:2385	P2RY13	GAAAACGTGGGCTTCACCCTACGATGGTCGTGTTGGAGCTCGTGG
NM_015869.3:1035	PPARG	CGGAGCGAAACTGGCAGCCCTGAAAGATGCGGATGGCCACCTCTTTG
NM_000954.5:180	PTGDS	GAGTTGGAGGCGAGGCCCGCGCTGAACCAGCGCCC
NM_002841.2:0	PTPRG	GAAGAGCGCGGCGCTGGAAACTGGCCATGCCTCCATACAGGAAGTAACAT
NM_002964.3:115	S100A8	AATTTCTTCAGGTCATCCCTGTAGACGGCATGGAAATTCCCCTTTATCAG
NM_002965.2:75	S100A9	CCCAGCTTCACAGAGTATTGGTGGAAGGTGTTGATGATGGTCTCTATGTT
NM_006272.1:40	S100B	CTTCTCCAGCTCAGACATCCTCTTCCTTGTCTCAC
NM_003930.3:1270	SCAP2	CCTTCATTTCTCCTACCCACCAGCCATATCTATTGTATTCCTTGCTAAGA
NM_005413.1:1305	SIX3	AGGTTACCGAGAGGATGGAGGTGCCGGTGTCCGCG
NM_016582.1:820	SLC15A3	CAGCACAGCACCCAGGTTGATGCTCCAGTAAAACCAGTTGAAGAAGCGGC
NM_015136.2:95	STAB1	CTGACGAAGCTGAAGCCTGCCAGGCAGAAGGCCAG
NM_001066.2:835	TNFRSF1B	CAATCAGTCCAACTGGAAGAGCGAAGTCGCCAGTGCTCCCTT
NM_003327.2:200	TNFRSF4	TTGCACGGCTTGGAGCTGACCACGTCGTTGTAGAAGCCCGG
NM_000474.3:35	TWIST1	TCCTGGAAACGGTGCCGGTGCTGCAGAGCCCGCGA
NM_004666.1:195	VNN1	AGTCACAATAATATGCGCACCCTGATCTGCTGCTGATGTGATCGCT

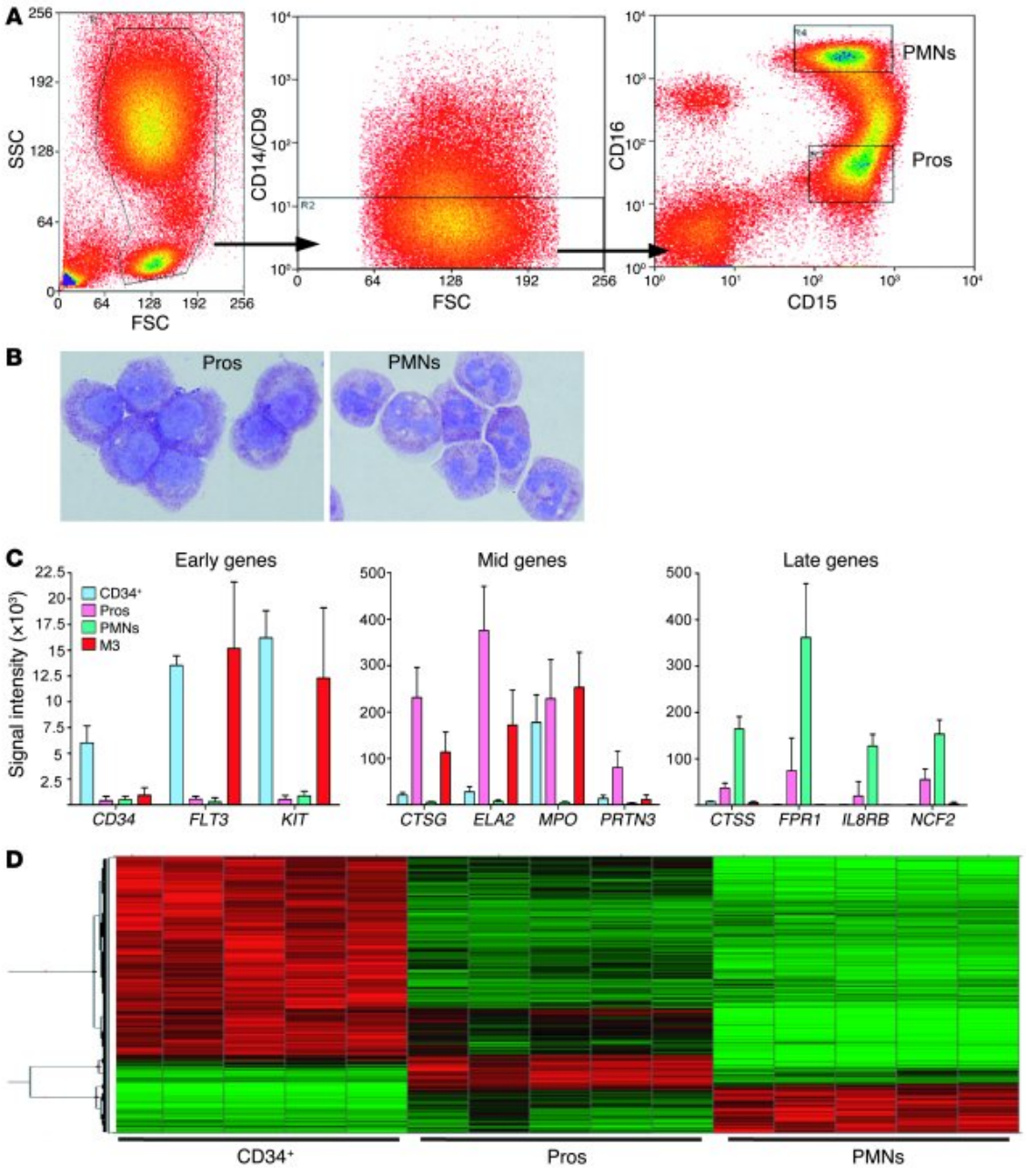
A
SSC
FSC
CD14/CD9
FSC
CD16
CD15
PMNs
Pros
B
Pros
PMNs
C
Early genes
Mid genes
Late genes
Signal intensity (×10³)
CD34⁺
Pros
PMNs
M3
CD34
FLT3
KIT
CTSG
ELA2
MPO
PRTN3
CTSS
FPR1
IL8RB
NCF2
D
CD34⁺
Pros
PMNs

Figure 2-1

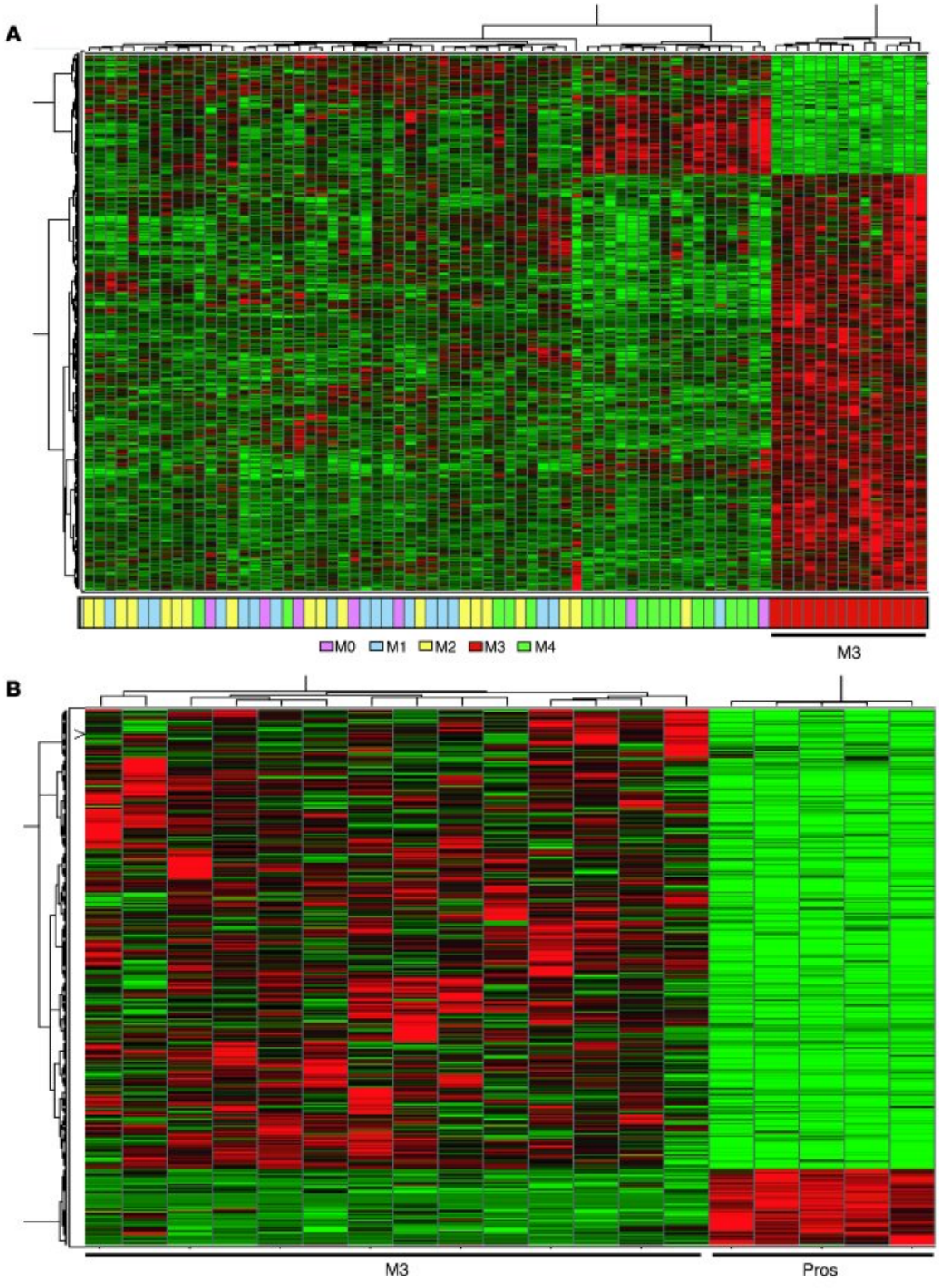

Figure 2-2

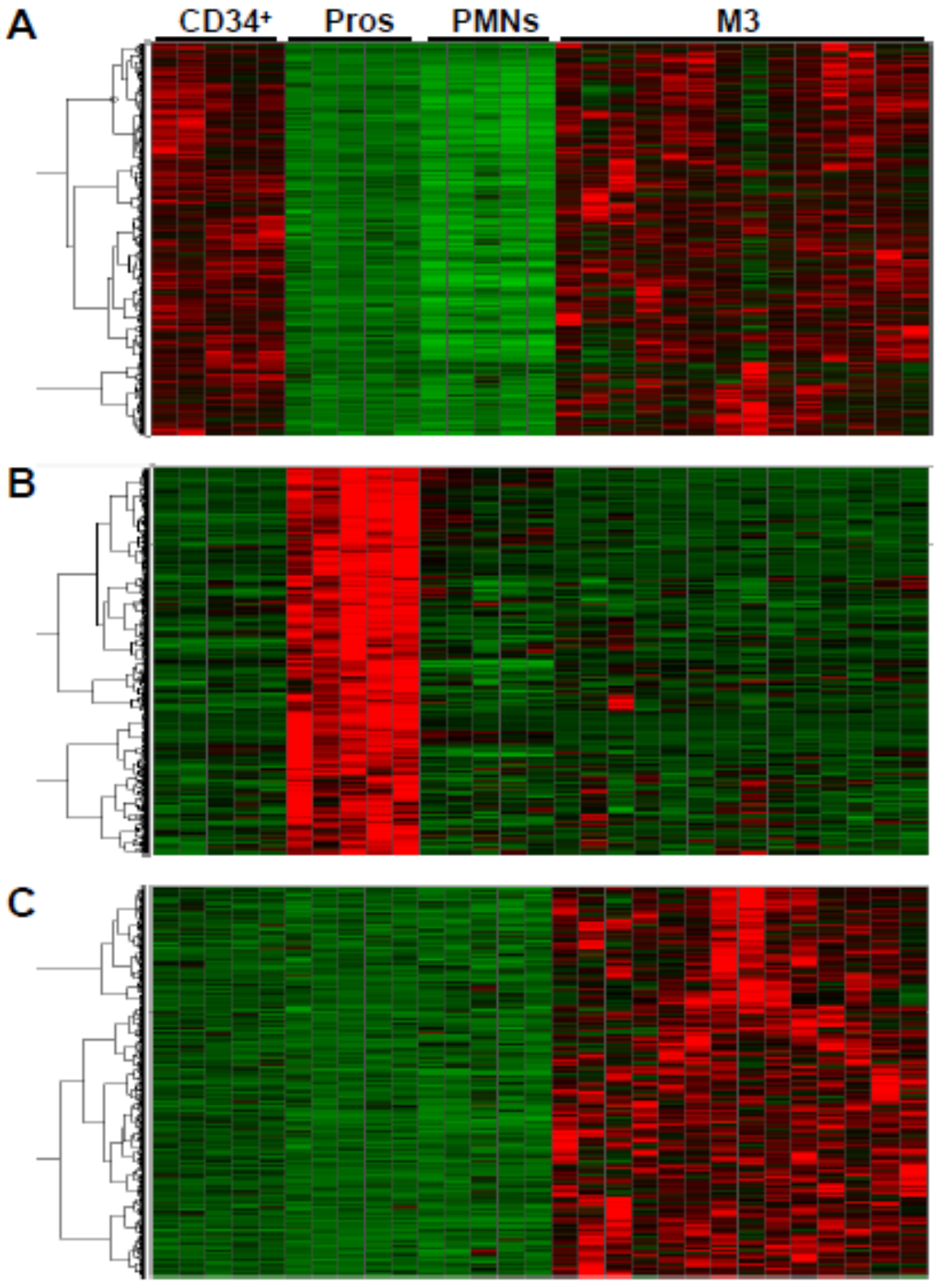

Figure 2-3

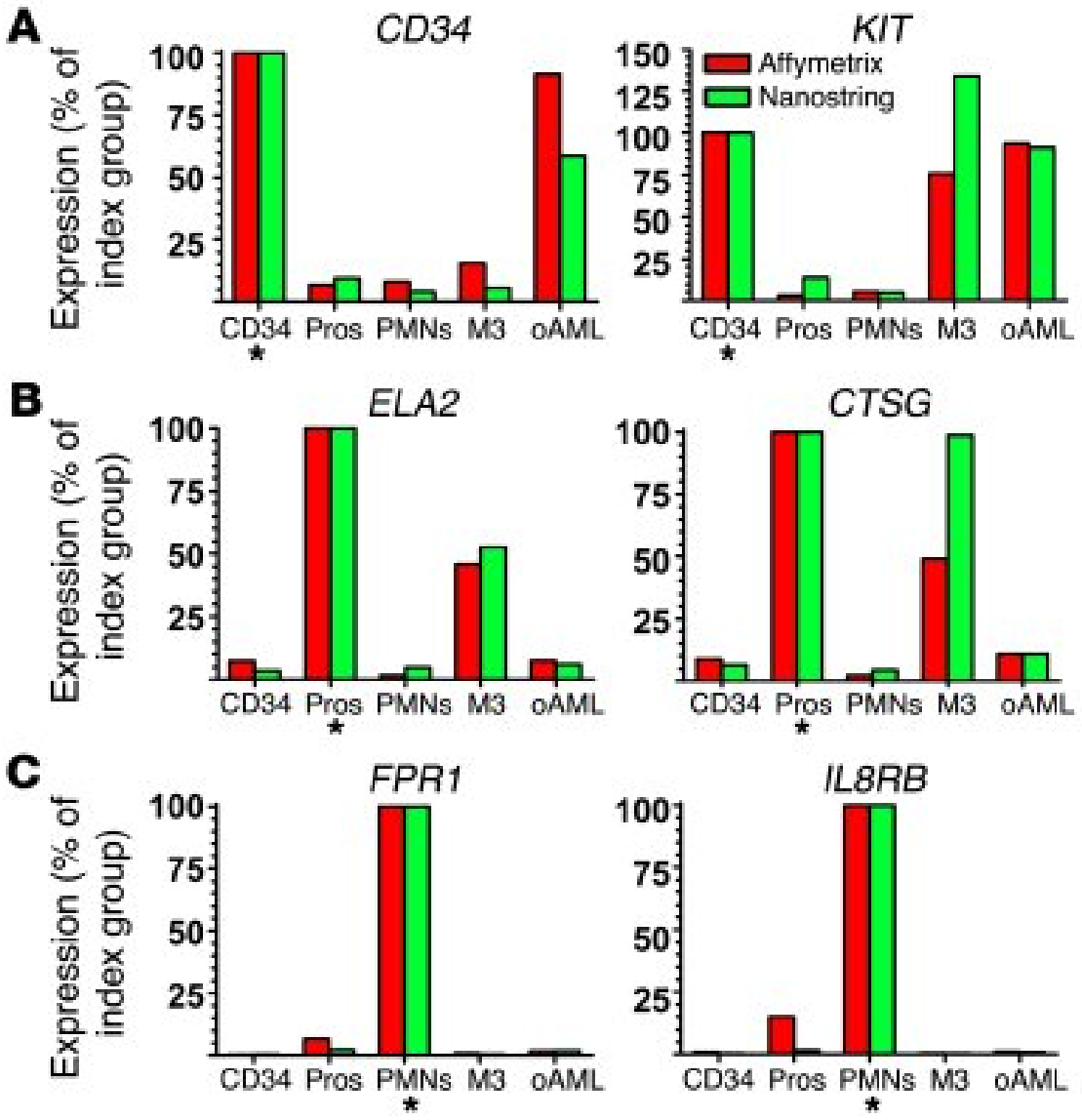
A
CD34
KIT
Affymetrix
Nanostring
Expression (% of index group)
100
75
50
25
150
125
CD34 Pros PMNs M3 oAML
*
B
ELA2
CTSG
C
FPR1
IL8RB

Figure 2-4

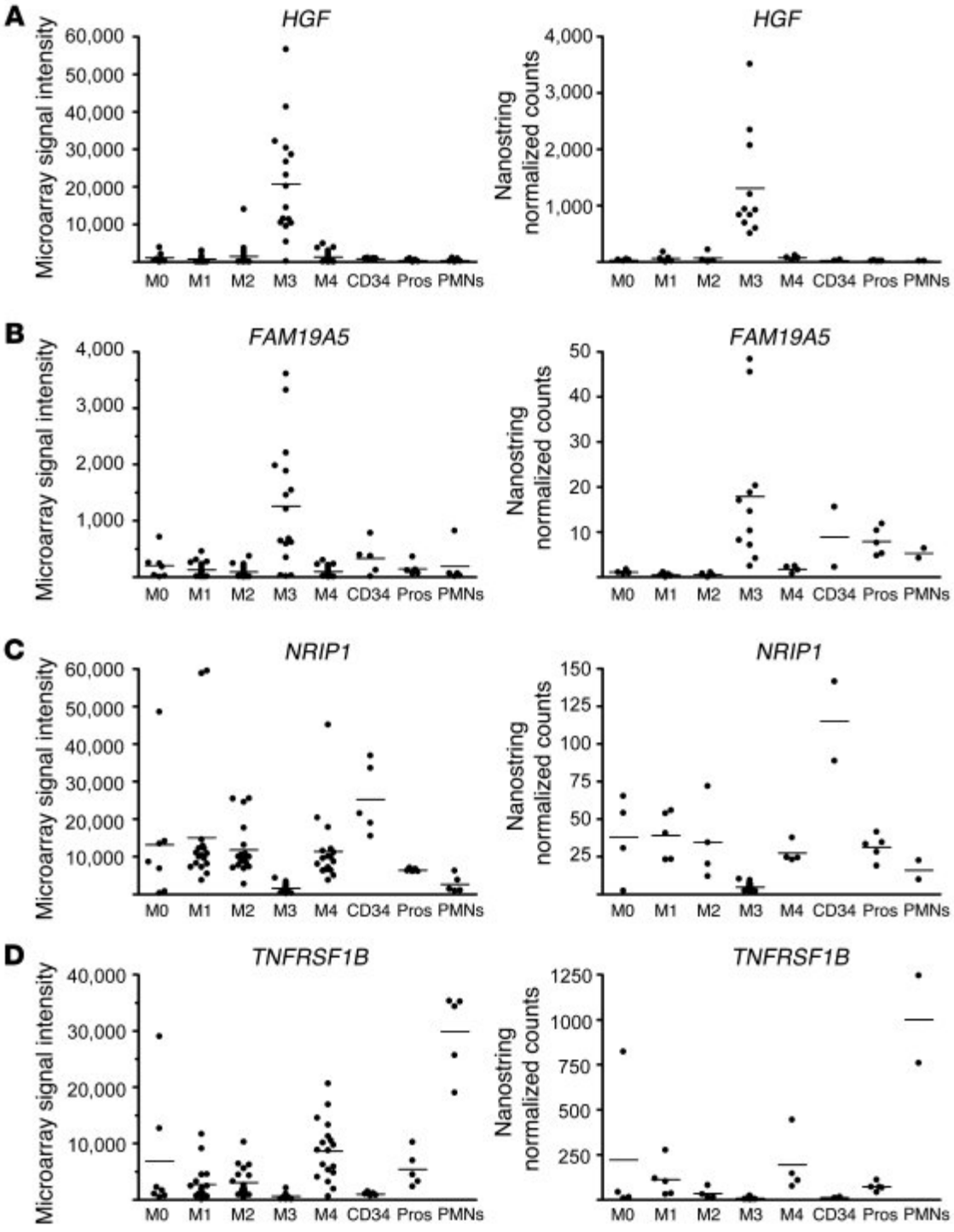
A
HGF
Microarray signal intensity
60,000
50,000
40,000
30,000
20,000
10,000
M0 M1 M2 M3 M4 CD34 Pros PMNs
HGF
Nanostring normalized counts
4,000
3,000
2,000
1,000
M0 M1 M2 M3 M4 CD34 Pros PMNs
B
FAM19A5
Microarray signal intensity
4,000
3,000
2,000
1,000
M0 M1 M2 M3 M4 CD34 Pros PMNs
FAM19A5
Nanostring normalized counts
50
40
30
20
10
M0 M1 M2 M3 M4 CD34 Pros PMNs
C
NRIP1
Microarray signal intensity
60,000
50,000
40,000
30,000
20,000
10,000
M0 M1 M2 M3 M4 CD34 Pros PMNs
NRIP1
Nanostring normalized counts
150
125
100
75
50
25
M0 M1 M2 M3 M4 CD34 Pros PMNs
D
TNFRSF1B
Microarray signal intensity
40,000
30,000
20,000
10,000
M0 M1 M2 M3 M4 CD34 Pros PMNs
TNFRSF1B
Nanostring normalized counts
1250
1000
750
500
250
M0 M1 M2 M3 M4 CD34 Pros PMNs

Figure 2-5

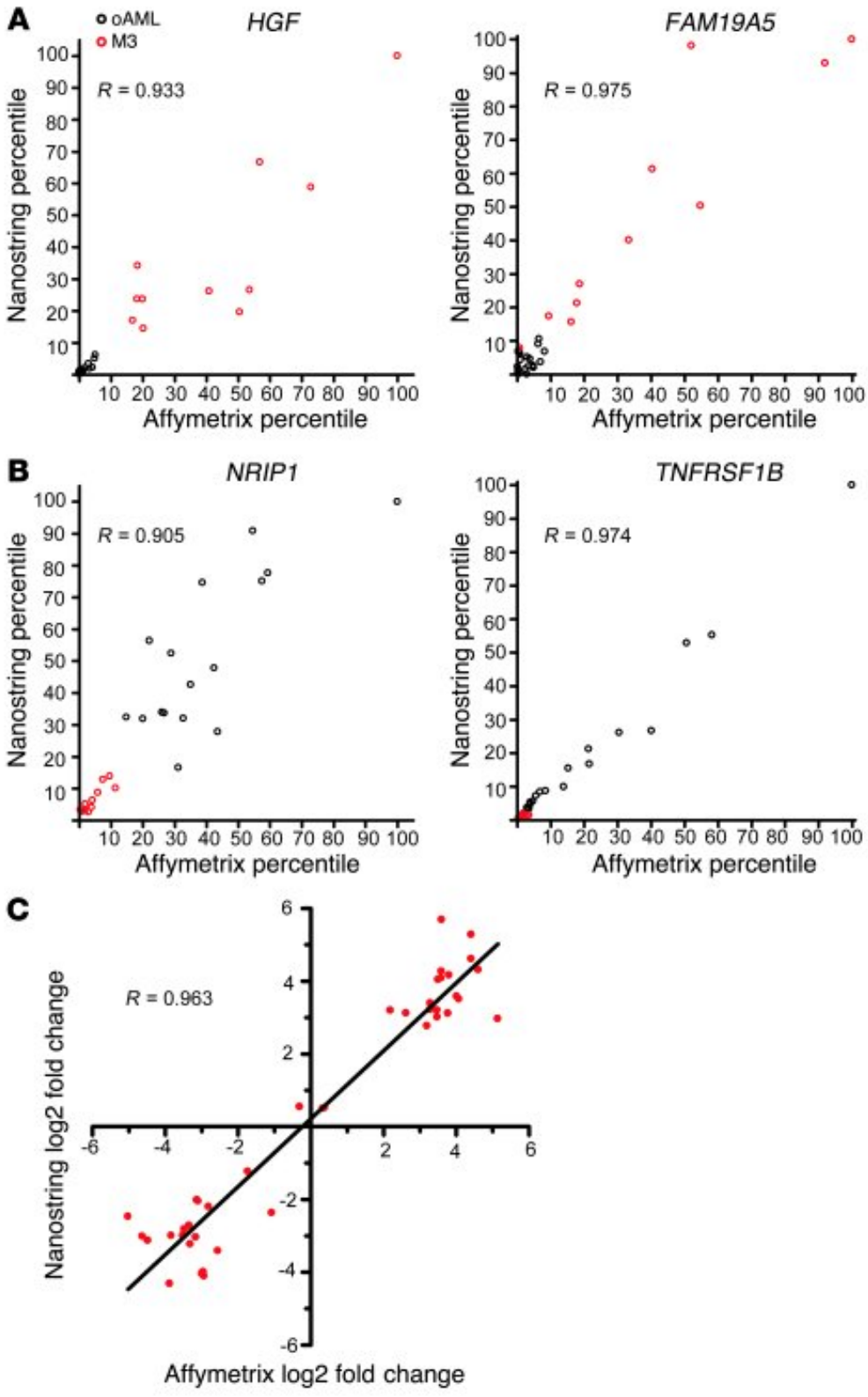
A
oAML
M3
HGF
R = 0.933
Nanostring percentile
Affymetrix percentile
FAM19A5
R = 0.975
Nanostring percentile
Affymetrix percentile
B
NRIP1
R = 0.905
Nanostring percentile
Affymetrix percentile
TNFRSF1B
R = 0.974
Nanostring percentile
Affymetrix percentile
C
R = 0.963
Nanostring log2 fold change
Affymetrix log2 fold change

Figure 2-6

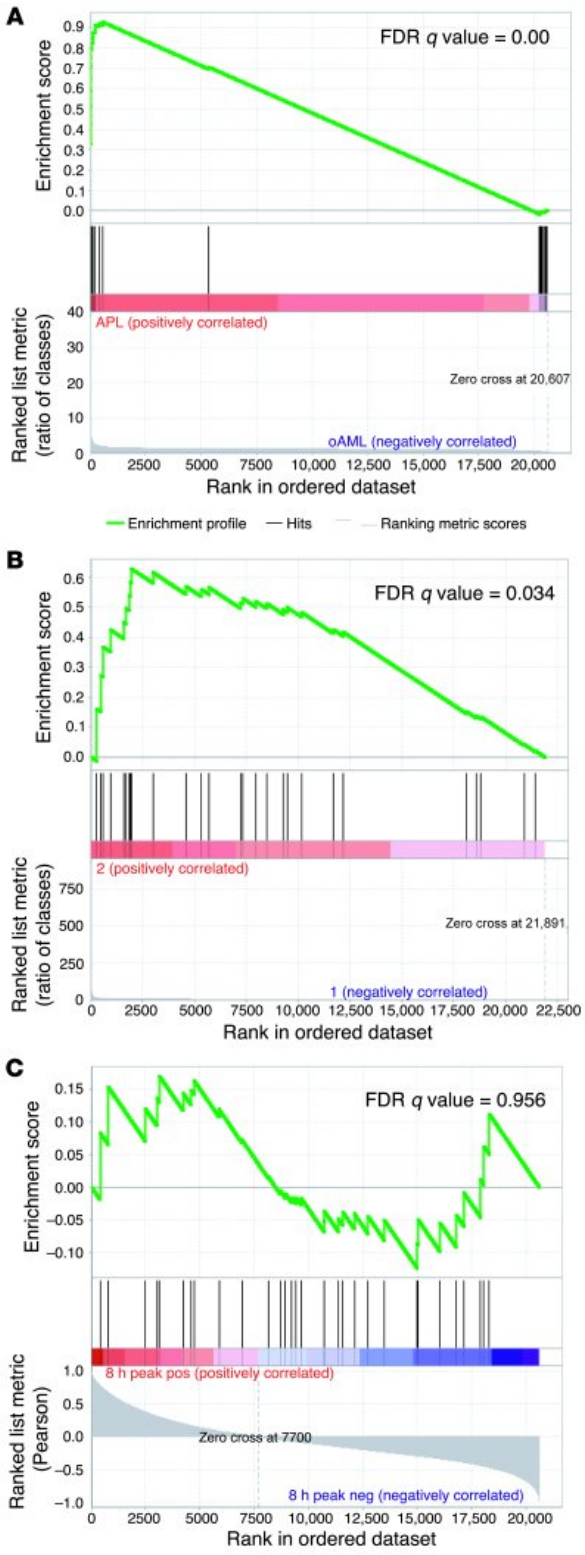
A
FDR q value = 0.00
Enrichment score
APL (positively correlated)
Zero cross at 20,607
oAML (negatively correlated)
Ranked list metric (ratio of classes)
Rank in ordered dataset
Enrichment profile
Hits
Ranking metric scores
B
FDR q value = 0.034
Enrichment score
2 (positively correlated)
Zero cross at 21,891
1 (negatively correlated)
Ranked list metric (ratio of classes)
Rank in ordered dataset
C
FDR q value = 0.956
Enrichment score
8 h peak pos (positively correlated)
Zero cross at 7700
8 h peak neg (negatively correlated)
Ranked list metric (Pearson)
Rank in ordered dataset

Figure 2-7

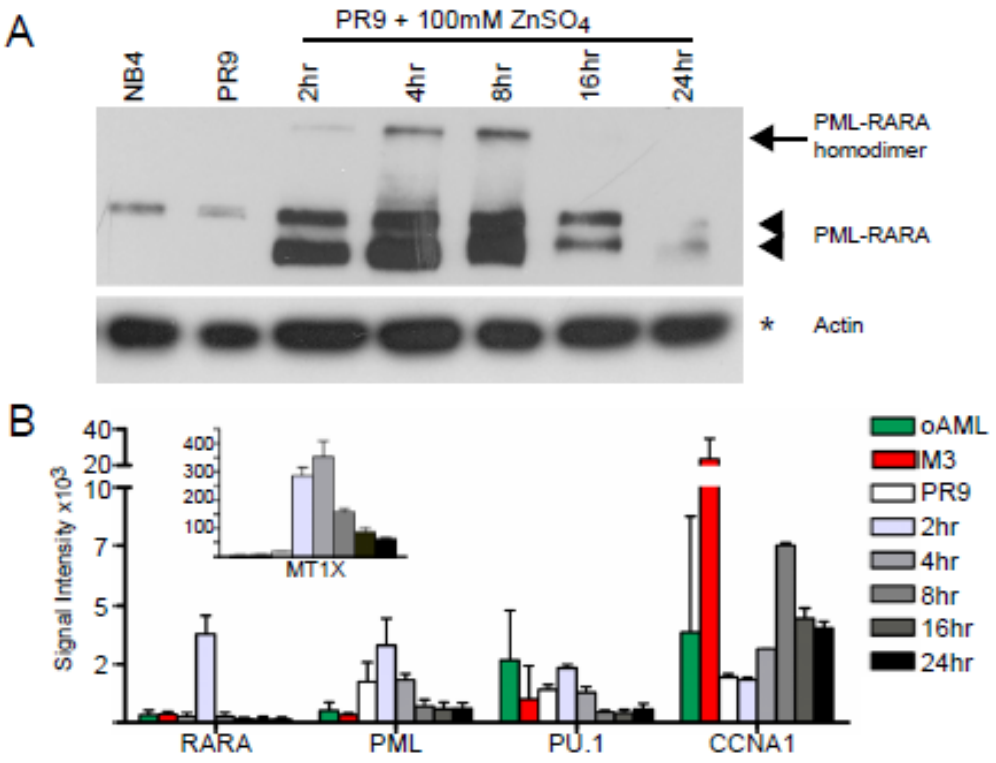
A
PR9 + 100mM ZnSO4
NB4
PR9
2hr
4hr
8hr
16hr
24hr
PML-RARA homodimer
PML-RARA
*
Actin
B
Signal Intensity x10^3
40
20
10
7
5
2
400
300
200
100
MT1X
RARA
PML
PU.1
CCNA1
oAML
M3
PR9
2hr
4hr
8hr
16hr
24hr

Figure 2-8

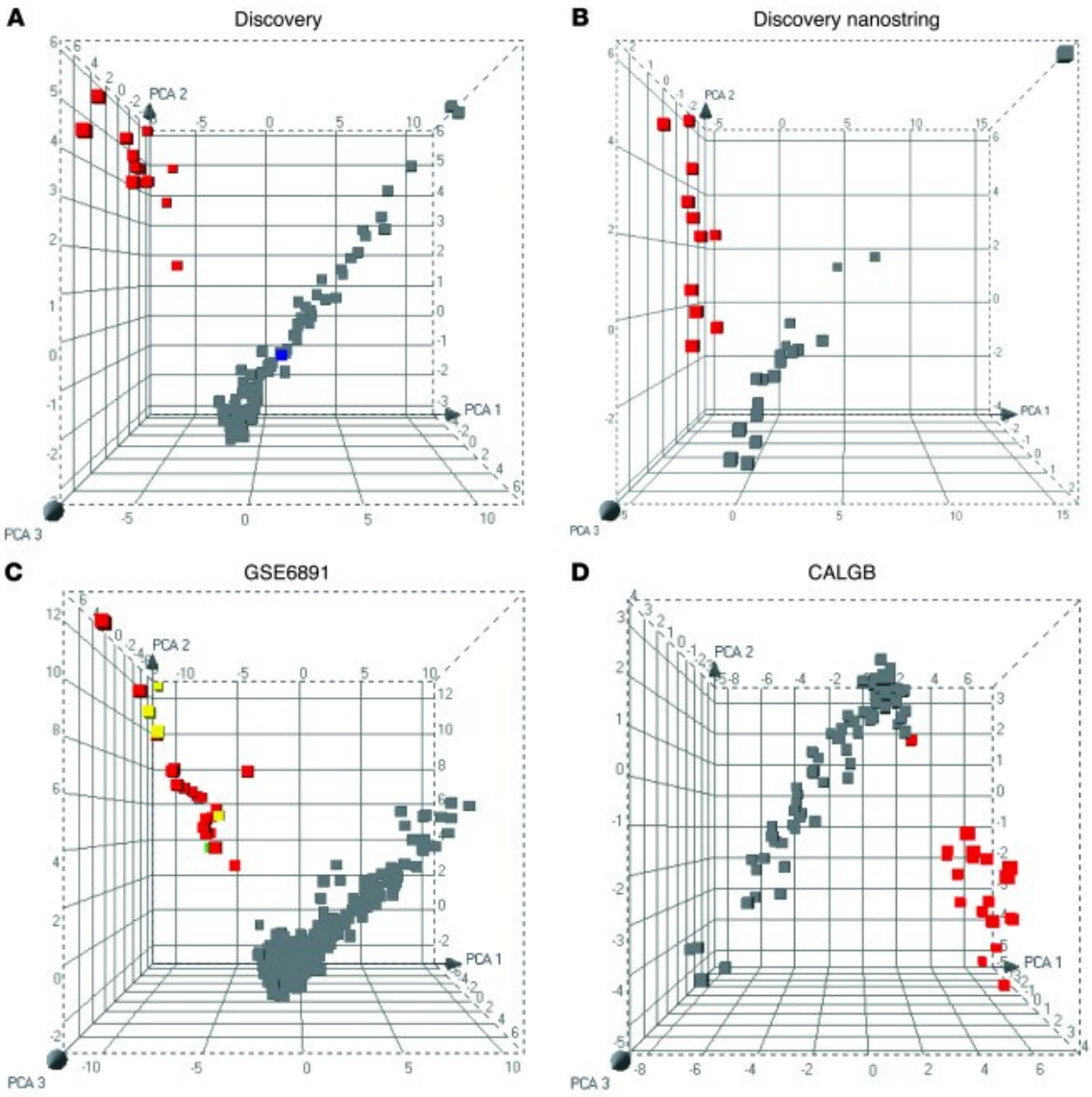
A
Discovery
PCA 1
PCA 2
PCA 3
B
Discovery nanostring
PCA 1
PCA 2
PCA 3
C
GSE6891
PCA 1
PCA 2
PCA 3
D
CALGB
PCA 1
PCA 2
PCA 3

Figure 2-9

Chapter 3

Notch signaling has a role in leukemogenesis in a mouse model of acute promyelocytic leukemia (APL).

Notch signaling has a role in leukemogenesis in a mouse model of acute promyelocytic leukemia (APL).

3.1. Abstract

The PML-RARA fusion protein is the initiating event in acute promyelocytic leukemia (APL), but the downstream pathways responsible for leukemogenesis are not yet completely understood. In this report, we show that Notch signaling, which has known roles in proliferation and survival, plays a role in PML-RARA mediated leukemogenesis. We demonstrate that human APL overexpresses the Notch ligand Jagged-1 (*JAG1*) compared to other AML subtypes, and normal promyelocytes. Overexpression of *JAG1* is also found in human APL cell lines and in murine APL tumors derived from mCG-PML-RARA knockin animals. Inhibition of Notch signaling by pharmacological and genetic approaches resulted in a loss of serial replating by marrow cells from young non-leukemic mCG-PML-RARA animals. In contrast, colony formation by wildtype marrow is unaffected by Notch inhibition, suggesting that PML-RARA expressing cells are uniquely dependent upon Notch signaling for increased self-renewal. Growth of primary murine APL cells *in vitro* was variably reduced by pharmacological inhibition of Notch signaling (6/9 samples), demonstrating that while Notch signaling is required for early events in leukemogenesis, in some cases it is dispensible for the fully transformed tumor. In conclusion, we have demonstrated a previously unappreciated role for the Notch signaling pathway in the development of acute promyelocytic leukemia.

3.2. Introduction

The t(15;17)(q22;q11.2) translocation, which is present in nearly 95% of acute promyelocytic leukemia (APL) cases, produces the PML-RARA fusion gene. Multiple transgenic and knockin mouse models have demonstrated that PML-RARA has a causative role in leukemogenesis (1-3). In all mouse models of APL, leukemogenesis proceeds slowly, presumably requiring secondary events for disease progression. However, there are subtle alterations in hematopoeisis that indicate that expression of PML-RARA *per se* alters hematopoeisis. Marrow cells from young, non-leukemic mCG-PR animals have increased colony forming ability, and will serially replate in methylcellulose cultures for up to one month, in contrast to wildtype cells, which do not form colonies after the second week in culture (4, 5). Serial replating is similarly observed in a conditional PML-RARA knockin animal, upon Cre-mediated activation of PML-RARA (John Welch and Tim Ley, unpublished data). In competitive repopulation assays with wildtype marrow, expansion of mCG-PR cells was observed not just in the Gr-1$^+$ myeloid cells, but also in the CD19$^+$ and CD3$^+$ lymphoid lineage cells (John Welch and Tim Ley, unpublished data). Collectively, these results suggest that PML-RARA acts in a multipotent progenitor cell to increase self renewal, and partially block myeloid differentiation. The molecular pathways that are activated or repressed to create these phenomena remain largely unknown, but remain an active area of investigation.

The Notch pathway is attractive candidate for further study. Several groups, including our group, have demonstrated that primary human APL samples characteristically overexpress the Notch ligand *JAG1* relative to other AML subtypes (6, 7), promyelocytes (7, 8) or CD34+ stem and progenitor cells (9). *JAG1* expression is

also found in two common cell line models of APL. When PML-RARA expression is induced in the PR-9 cell line, both JAG1 protein and mRNA increase (9). In addition, *JAG1* is highly expressed in NB-4 cells, and is rapidly downregulated upon ATRA treatment; similar results are observed in primary APL patient blasts (9, 10). Cotransfection of PML-RARA and a Hes1 promoter reporter construct resulted in increased luciferase expression, suggesting that PML-RARA expression leads to downstream activation of Notch signaling (9). Despite these reports, to date there has been no in depth investigation of the role of JAG1 and Notch signaling in APL pathogenesis.

Notch signaling is known to activate downstream targets involved in cellular survival, proliferation and self-renewal, as well as having major roles in the specification of several hematopoietic lineages (11). While Notch signaling is not required for maintenance of steady-state hematopoeisis in adult mice (12), alterations in Notch signaling are common in hematopoietic diseases. Most notably, Notch-1 itself is mutated in a majority of T-ALL cases (13) and in rare M0 AML cases (14), leading to constituitive activation of Notch signaling. In other cases of T-ALL, Fbxw3, an E3 ubiquitin ligase responsible for degradation of activated Notch, has inactivating mutations, allowing accumulation of intracellular Notch protein (15). Two AML fusion proteins, OTT-MAL and AML-ETO, disrupt the normal repression of Notch target genes, allowing activation of transcription in the absence of ligand engagement (16, 17). Increased Notch signaling, as evidenced by increased expression of the Notch target gene, *Hes1*, is also associated with progression of chronic phase CML to blast crisis (18). Additionally, it has been reported that human AML leukemic initiating cells (LICs)

express high levels of the Notch ligand *JAG2* and are susceptible to pharmacological inhibition of Notch signaling (19).

Understanding the role of Notch signaling in disease has clinical relevance because the Notch pathway is a druggable target. Multiples avenues of Notch inhibition are currently in pre-clinical development, including gamma secretase inhibitors (20), stapled peptide inhibitors (21), and Notch subtype specific antibodies (22). Some of these agents are currently being tested in phase 1 clinical trials (23).

In this report, we describe an in depth study of the functional role of Notch signaling in APL. In agreement with previous studies, we found that *JAG1* is highly expressed in APL cells. Furthermore, we demonstrate that the essential components of Notch signaling are expressed in human APL cells, and we provide bioinformatic evidence for activation of a known Notch signature in APL. Similar to the human disease, *Jag1* mRNA and protein are present in primary murine APL cells, allowing us to use the PML-RARA knockin mouse to model the role of Notch signaling in leukemogenesis. Using both pharmacologic and genetic approaches, we show that Notch signaling is a component of the increased self-renewal observed in preleukemic cells. In most fully transformed tumors, dependence on Notch signaling is retained *in vitro*. These findings suggest that Notch signaling is a key downstream effector of PML-RARA, with roles in both early leukemogenesis and the fully transformed state.

3.3. Results

3.3.1. Jagged-1 is dysregulated in acute promyelocytic leukemia.

We previously reported a signature of genes with altered expression specifically in APL; the Notch ligand Jagged-1 (*JAG1*) was among this set (7). Using gene expression profiling, we examined the expression of *JAG1* in bone marrow samples collected from a larger set of 180 de novo AML patients (see Table 3-1 for clinical characteristics of AML patients) and in sorted normal myeloid populations (CD34+ cells, promyelocytes and neutrophils) from 5 normal human bone marrow samples. *JAG1* was expressed at significantly higher levels in APL samples compared to all other FAB subtypes in 4/5 probesets on the Affymetrix 133+2 platform (see Figure 3-1A for 2 selected probesets). *JAG1* expression in APL was also significantly higher than in any normal myeloid population (Figure 3-1A). While *JAG1* expression in some other AML samples was similar to that seen in APL, it was consistently expressed at high levels only in APL. We validated the expression pattern of *JAG1* by comparing these results to those found in a second set of 93 de novo AML samples (M0-M4) obtained from the Cancer and Leukemia Group B (CALGB) Cooperative group. In this independent validation set, *JAG1* was also most highly expressed in APL samples (Figure 3-1B). We additionally performed quantitative RT-PCR for *JAG1* on 11 APL, 16 other AML and 4 normal promyelocyte RNA samples (Figure 3-1C) and confirmed that *JAG1* mRNA is present at significantly higher levels in APL compared to both other AML and normal promyeolocytes. These results are similar to several other AML gene expression profiling studies including our own, and strongly suggest that overexpression of *JAG1* is characteristic of APL. Because *JAG1* is a Notch ligand, we then decided to investigate the role of Notch signaling in APL.

3.3.2. Components of the Notch signaling pathway are expressed in APL.

We examined the expression of Notch pathway components in APL and normal promyelocytes. The *NOTCH1* and *NOTCH2* genes are expressed in APL cells at levels that do not differ significantly from normal promyelocytes, while *NOTCH3* and *NOTCH4* are not expressed in either group (Figure 3-2A). Of the Notch ligands, *JAG1*, as described above, and *DLL1* are overexpressed in APL samples relative to normal promyelocytes (Figure 3-2A). To determine whether APL cells express the necessary machinery for intact Notch signaling, we examined the expression of components of the gamma secretase complex (Figure 3-2B), enzymes involved in the S1 and S2 Notch cleavage events (Figure 3-2C), transcriptional cofactors of Notch (Figure 3-2D), Notch modifying enzymes (Figure 3-2E), and the Mindbomb and Fbxw7 E3 ubiquitin ligases involved in Notch endocytosis and degradation (Figure 3-2F). These genes were expressed at moderate to high levels in APL samples and promyelocytes, indicating that the essential components of Notch signaling are present in APL cells. For the majority of Notch pathway genes, expression did not differ significantly between APL and normal promyelocytes. However, 5 of these genes were previously reported as part of a signature of genes specifically dysregulated in APL relative to other AML and normal promyelocytes (7). *MIB1* and *MAML3* are expressed at higher levels in APL, while *CSL*, *PSEN1*, and *LFNG* were expressed at lower levels.

3.3.3. Bioinformatic evidence of Notch signaling in APL

Increased Notch signaling is a major component of T-ALL, due to activating mutations in *NOTCH1* (13). Several studies have reported signatures of genes whose

expression is controlled by Notch signaling in T-ALL cells. We used gene set enrichment analysis (GSEA) to determine whether these same pathways might be activated in APL. We selected two signatures, 'GSI-Notch', comprised of genes whose expression changes in T-ALL cells upon treatment with gamma secretase inhibitors (21) and 'Notch-Targets', comprised of genes previously reported to be transcriptional targets of NOTCH1, as defined by both ChIP-on-chip and microarrays (24). We then used GSEA to determine whether these signatures are enriched in APL compared to normal promyelocytes, and found that both the Notch-Targets (Figure 3-3A) and GSI-Notch (Figure 3-3B) gene sets are significantly enriched in human APL samples (FDR=0.00 for both comparisons). We then performed GSEA with a third signature derived from culturing murine KLS cells on OP9 stroma expressing *Dll1* (25). This signature, termed KLS-Notch, was also enriched in human APL samples (Figure 3-3C, FDR=0.013). These results provide bioinformatic evidence that Notch signaling is activated in APL cells.

3.3.4. Notch signaling is present in APL cell lines.

The PR-9 cell line, which contains a zinc inducible PML-RARA cassette, is frequently used as a model of APL and PML-RARA activities. As previously reported (9), *JAG1* mRNA and protein increase upon addition of $ZnSO_4$ to the culture media (Figure 3-4A-B). Both the mRNA and protein levels begin to rise at 8 hours post induction, peak at 16 hours, and remain elevated at 24 hours. JAG1 protein can also be detected in induced PR9 cells by intracellular flow cytometry (Figure 3-5). While staining non-permeabilized cells resulted in staining levels only slightly above the isotype

control background, incubating the antibody with fixed, permeabilized PR9 cells produced robust intracellular staining, indicating that the bulk of JAG1 protein is located within an intracellular compartment (Figure 3-5). Similarly, abundant intracellular JAG1 was detected in the NB-4 APL cell line, which possesses t(15;17) and expresses PML-RARA (Figure 3-6).

When PML-RARA expression is induced in PR-9 cells, cleaved Notch-1 protein also increases (Figure 3-4B) with the same kinetics as JAG1 protein. In addition, cleaved Notch-1 can be detected in NB4 cells by flow cytometry (Figure 3-6). These results demonstrate that *JAG1* expression and activation of Notch signaling are a common feature of two widely used cell line models of APL.

3.3.5. Jag1 and Notch signaling are found in a murine model of APL.

We next examined Notch signaling in a previously described murine model of APL, the mCG-PML-RARA knockin mouse (3), which develops AML with differentiation. Murine mCG-PR leukemia cells are morphologically promyelocytes and respond to ATRA both *in vitro* and *in vivo*. In addition, we have previously reported that a bona fide, validated human APL gene expression signature is present in the murine tumors (26). We examined the expression of *Jag1* using previously published gene expression profiles of 21 murine APL samples and wildtype $Lin^{-}Sca^{+}$ (LS) progenitor cells undergoing 7 days of G-CSF induced myeloid differentiation (Figure 3-7A). *Jag1* expression was detectable in a majority of tumors and was higher than that of either LS cells (d0) or promyelocytes (d2). We then used flow cytometry to assess the presence of Jag1 protein and cleaved Notch-1 in murine APL. Jag1 protein was readily detected by

intracellular staining but not by surface staining (see Figure 3-8 for 3 example tumors), similar to the results observed with PR-9 and NB-4 cells. We then examined Jag1 and cleaved Notch1 protein in 10 independent primary APL samples (see Table 3-2 for characteristics of murine APLs, Figure 3-7B for summarized results, Figure 3-7C for representative flow plots). Jag1 was detectable in all tumors assayed, with expression levels ranging from 19% to greater than 90% of the cells. Cleaved Notch-1 protein was detected in 6/10 tumors (range 0.32-71%). Notably, the abundance of intracellular Notch1 was significantly correlated with the level of Jag1 protein present (Pearson $R=0.9447$, $p<0.0001$). Therefore, like human APL and APL cell lines, murine APL cells both overexpress Jag1 and have activated Notch signaling, providing a rationale for utilizing the mCG-PR mouse as a model system in which to investigate the role of Notch signaling in leukemogenesis.

3.3.6. Inhibition of Notch signaling reduces colony formation by mCG-PR marrow.

Marrow cells from mCG-PR animals have increased colony forming ability and will serially replate in methylcellulose cultures for up to one month, in contrast to wildtype cells, which do not form colonies after a single round of replating. To examine the role of Notch signaling in early leukemogenesis, we cultured marrow cells from young (6-8 weeks) non-leukemic mCG-PR mice (or wildtype B6 mice) in methylcellulose media, and assessed colony formation in the presence of GSIs (compound E or compound IX) or DMSO control (Figure 3-9). Colony formation by marrow derived from young wildtype B6 animals was not affected by either compound (Figure 3-9A), as expected (12). In contrast, after 1 week in culture, colony formation by

PR+ marrow was significantly reduced (Figure 3-9B). After 2 rounds of replating, vehicle treated control cells had colony formation activity similar to that observed in the first week. In contrast, at weeks 2 and 3, GSI treated cells had significantly reduced colony forming activity. In some marrow samples, colony formation in GSI treated cultures was nearly abrogated by the third week of continuous drug exposure (Figure 3-9C). These data suggest that Notch signaling may be partially responsible for the replating phenotype observed in mCG-PR progenitor cells.

To further validate the role of Notch signaling in serial replating of mCG-PR marrow, we used a genetic approach to inactivate Notch signaling. We used a retrovirus containing a dominant-negative fragment of MAML1 fused to GFP (DNMAML-GFP) (27). DNMAML contains the domains necessary to interact with cleaved Notch, but lacks the domains needed to recruit transcriptional machinery. DNMAML therefore blocks Notch signaling at a transcriptional level, downstream of gamma secretase-mediated cleavage of Notch. We transduced wildtype B6 and mCG-PR marrow with either DNMAML-GFP or GFP control virus, sorted GFP+ cells to >95% purity, and plated them in methylcellulose media (Figure 3-10). As expected, genetic inhibition of Notch signaling did not impair colony formation by wildtype cells (Figure 3-10A). In contrast, DNMAML transduced mCG-PR marrow had significantly reduced colony forming activity at weeks 1, 2 and 3 (Figure 3-10B-C), similar to that observed with pharmacological inhibition of Notch signaling.

3.3.7. Inhibition of Notch signaling reduces colony formation in primary murine APL cells.

In order to investigate the role of Notch signaling in fully transformed tumors, we developed an assay to measure the effect of Notch inhibition on colony formation by murine APL cells (Figure 3-11A). Cryopreserved primary APL cells isolated from the spleens of moribund 129/B6 F1 mCG-PR mice were thawed, grown in liquid culture media supplemented with IL-6, IL-3 and SCF in the presence of ATRA, GSI (compound E or compound IX) or DMSO vehicle control for 48 hours, and then plated in methylcellulose without inhibitors. Colony formation was then scored after 7 days in methylcellulose. Both the liquid and methylcellulose cultures were conducted under hypoxic (3%) conditions, since a majority of primary APL tumors have poor colony formation under standard growth conditions (20% 02) (data not shown). As a control, 129/B6 F1 marrow was subjected to the same assay. Neither compound E nor compound IX significantly alters colony formation by wildtype marrow cells (Figure 3-11B). Of 13 tumors evaluated, 9 formed colonies under vehicle control conditions (Table 3-2), which allowed us to assess responses to drugs. As expected, ATRA exposure resulted in the formation of significantly fewer colonies in 9/9 tumors (Figure 3-11C), demonstrating that this assay is viable for testing drug activity. Six of the 9 assayed tumors formed significantly fewer colonies after exposure to GSIs (Table 3-2 and Figure 3-11C). In many of the GSI responsive tumors, the reduction in colony formation was similar to that observed with ATRA treatment. On average, exposure to compound E or compound IX resulted in colony formation that was 62.2% (SD 35.0%) and 45.2% (SD 24.4%) of the DMSO controls, respectively (Figure 3-11C). In addition, the degree of inhibition of colony formation was generally similar between compound E and compound IX treated plates for the same tumor. These results were statistically significant ($p<0.01$ for

compound E, and $p<0.001$ for compound IX), and suggest that Notch signaling plays a role in the survival or self-renewal of some fully transformed leukemic cells.

3.3.8. In vivo inhibition of Notch signaling in murine APL

To determine whether inhibition of Notch signaling reduces tumor growth *in vivo*, we utilized 2 indpendent murine APL cell lines derived from mCG-PR mice which express click beetle red luciferase (28). Both APL^{luc} cell lines express the myeloid marker Gr-1 and high levels of intracellular Jag1 protein (Figure 3-12). We injected 500,000 cells intraperitoneally into 129/B6 recipient animals. Animals received either no treatment, subcutaneous ATRA (20 mg as a sustained release pellet) or daily injections of 6 mg/kg compound E, and were imaged biweekly until clinical illness developed. As expected, ATRA treatment reduced tumor burden for both cell lines (Figure 3-13A and B). In contrast, the bioluminescence in GSI treated animals was not significantly different than that of untreated control animals (Figure 3-13).

Hypothesizing that immortalized cell lines may not retain the dependence on Notch signaling seen in primary APL, we transplanted two tumors that responded to GSIs *in vitro* (numbers 2894 and 3149) into sublethally irradiated syngeneic recipient animals and treated with the GSI compound E. Treated animals received intraperitoneal injections (3mg/kg) on a 5 days on, 2 days off dosing schedule, while control animals received no treatment. The lower dose and altered dosing schedule was selected in order to avoid the GI toxicity associated with continuous GSI exposure (29). At 4 weeks post-transplant, mice in both treated and control groups were anemic, thrombocytopenic and some animals had elevated WBCs (Figure 3-14A, B and C). There was no significant

difference in blood counts between GSI treated and control groups for either tumor. In addition, there was no decrease in spleen size or percentage of immature myeloid ($Gr1^+$, c-Kit^+) cells in the spleens with GSI treatment (Figure 3-14D). To determine whether drug treatment resulted in inhibition of gamma secretase-mediated cleavage of Notch, we examined protein extracts from the spleens of 3 treated and 3 untreated moribund animals. There was no decrease in cleaved Notch-1 in the GSI treated spleens, suggesting that the dose or delivery was not adequate to inhibit Notch cleavage (Figure 3-14E). Therefore whether Notch inhibition results in decreased disease burden *in vivo* remains an open question.

3.4. Discussion

In this report, we have shown that overexpression of *JAG1* and downstream activation of Notch signaling is important for the pathogenesis of APL. *JAG1* overexpression is found in human APL samples compared to other AML subtypes and to normal myeloid cells. Several groups, including our own, have previously reported that *JAG1* overexpression is associated with APL (6-8, 30). We extended these observations to a functional study of the role of Notch signaling in APL. APL cells express core components of the Notch pathway and are expected to be capable of transducing Notch signals. We have also provided bioinformatic data that two known Notch signatures are enriched in APL cells, suggesting that Notch signaling is activated. Like human APL samples, murine APL cells express abundant *Jag1* mRNA and protein, and have activated Notch signaling. This fact allowed us to use the mCG-PML-RARA knockin mouse as a model of Notch signaling *in vivo*. Pharmacological and genetic inhibition of Notch

signaling resulted in a loss of serial replating by mCG-PR progenitor cells, demonstrating that the Notch pathway is necessary for self-renewal. Most murine APL samples retain sensitivity to Notch inhibition *in vitro*, suggesting that Notch signaling is also relevant for fully transformed tumors.

JAG1 overexpression appears to be characteristic of APL, since nearly every APL sample has abundant *JAG1* mRNA. However, JAG1 expression is not restricted to only the M3 subtype of AML. Interestingly, in an unsupervised analysis of 285 AML patients, Valk et al. reported that high *JAG1* expression was associated with a cluster of patients in which the majority had either FLT3-ITD or FLT3-TKD mutations, and not with APL patients (31). Similarly, Verhaak et al. assigned JAG1 to a signature associated with overexpression in FLT3-ITD or TKD mutated AML (32). We also observed 30 other AML subtype samples with high JAG1 expression in our dataset, as defined by having signal intensity equal or greater to the APL sample with the lowest signal intensity for that probeset (see Table 3-3). While 12 cases did have either FLT3-ITD or FLT3-TKD mutations, we found that NPMc, IDH1, IDH2 and DNMT3A mutations were also present, either alone or in combination with FLT3 mutations. In addition, 4/9 patients with inv(16) alone had high JAG1 expression. It may be that there are multiple distinct pathways that lead to high JAG1 expression, and that Notch signaling has roles in pathogenesis for other AML subtypes as well.

While *JAG1* expression is induced upon PML-RARA expression in the PR-9 cell line, and is abrogated with ATRA treatment of NB-4 cells (9, 10), it is not clear how PML-RARA regulates *JAG1*. The proximal *JAG1* promoter has an everted repeat (10) and combined direct repeat-PU.1 motif sites similar to ones that PML-RARA has been

shown to bind (33). However, three independent whole genome chromatin immunoprecipitation studies failed to find evidence of PML-RARA binding in the *JAG1* promoter in either cell lines or primary APL cells (33-35). In addition, cotransfection of a *JAG1* promoter reporter construct (1.5 kb of 5' flanking sequence) with PML-RARA did not result in *JAG1* promoter activation (data not shown). These data suggest that *JAG1* is not a direct transcriptional target of PML-RARA.

In both cell lines and primary murine APL samples, Jag1 protein exists primarily within an intracellular compartment, since it can only be detected by flow cytometry if cells are fixed and permeabilized. While we cannot formally exclude the possibility that some Jag1 protein (below the limit of antibody detection) resides on the cell surface, this would be a minor portion compared to the intracellular fraction. If Jag1 is not present on the cell surface, how then is Notch signaling activated? One possible explanation is that autocrine activation of Notch signaling may occur intracellularly, within a membrane compartment shared by Jag1 and Notch. While Notch signals are generally thought to be transmitted from a ligand-bearing cell to an adjacent receptor-expressing cell, autocrine signaling has clearly been reported in primary human eosinophils (36). It is also possible that Jag1 reaches the cell surface, but is immediately encounters receptors and is endocytosed, so that under steady-state conditions, little surface Jag1 is present. Further studies are needed to distinguish between these mechanisms. Knowledge of the molecular details of Jag1 mediated signaling has clinical ramifications. For example, if Jag1 does not reach the cell surface, then antibodies targeting it are unlikely to be efficacious therapies.

Several groups have reported Notch independent effects of Jag1 mediated via binding of the cytoplasmic tail to PDZ-domain containing proteins, or via cleavage of Jag1 to release an intracellular fragment with transcriptional activation properties (37, 38). While we cannot exclude Notch independent activities of JAG1 in APL, we think that Notch-independent mechanisms are unlikely to be the primary mechanism for several reasons. First, Notch signaling is correlated with Jag1 expression in both cell lines and primary murine APL, suggesting that Notch cleavage is activated as a consequence of Jag1 expression. Second, pharmacologic inhibition of Notch signaling decreases colony formation by both preleukemic and leukemic cells. Similarly, genetic inhibition of Notch signaling through dominant negative mastermind-like (DNMAML) resulted in decreased colony formation by mCG-PR marrow. Neither GSIS nor DNMAML would be expected to affect expression of Jag1 or its potential interactions with cytoplasmic proteins. If these mechanisms were important components of Jag1 activity, GSIs and DNMAML would not be expected to decrease colony formation. . Finally, these Notch independent properties of Jag1 have primarily been studied in non-myeloid cell lines. No reports have yet demonstrated that these mechanisms have relevance *in vivo* or in primary myeloid cells.

We were unable to achieve inhibition of Notch signaling *in vivo* using a standing dosing protocol (39). Therefore, we do not yet know whether Notch inhibition will reduce tumor growth in this setting. Compound E is hydrophobic, and has been reported to have poor absorption when delivered intraperitoneally (40). Milano et al reported that increased doses resulted in a less than proportional increase in plasma concentration (40). In addition, the IC50 doses for compound E and other GSI used *in vivo* are commonly

reported as the dose necessary to reduce serum Aβ40, a cleavage product of amyloid precursor protein (APP) by 50% (40). There is evidence that gamma secretase cleavage of Notch is less susceptible to GSI mediated inhibition *in vitro*, requiring higher doses to achieve the same decrease in cleave as APP (41), and this may be true *in vivo* as well. We are currently considering other GSIs and dosing strategies, as well as alternative ways of demonstrating the role of Notch signaling *in vivo*, including determining whether APL cells treated with GSIs *ex vivo* are still capable of inducing disease in secondary recipients.

In summary, we have demonstrated a previously unappreciated role for Notch signaling in the pathogenesis of acute promyelocytic leukemia. The expression of *JAG1* and activation of Notch signaling is a common event in the development of both murine and human APL. Collectively, our results demonstrate that Notch signaling allowing for increased self-renewal is an early event in PML-RARA mediated leukemogenesis, and that dependence on Notch signaling is retained by some tumors *in vitro*. These results suggest that the Notch pathway is an attractive target for drug development, which may have clinical utility in treating some patients with relapsed or refractory APL.

3.5. Methods

3.5.1 AML and Normal Marrow Samples

One hundred eighty de novo adult AML bone marrow samples, including 22 APL samples, were collected as part of a study at Washington University to identify genetic factors associated with leukemogenesis. The study was approved by the Human Research Protection Office at Washington University School of Medicine and all patients

provided informed consent in accordance with the Declaration of Helsinki. Criteria for study inclusion were age greater than 18, more than 30% myeloblasts (or promyelocytes for M3 cases) in bone marrow aspirates. Patients with a history of myelodysplastic syndrome or prior chemotherapy or radiation therapy treatments were excluded. Patient characteristics are summarized in Table 3-1. An additional 93 de novo AML bone marrow samples were obtained from the Cancer and Leukemia Group B Tumor Bank and were processed using the same methods as the Washington University samples. Bone marrow aspirates from normal donors were also collected. The fractionation of normal marrow samples into CD34+ stem/progenitor cells, promyelocytes and neutrophils has been previously described (7).

3.5.2. RNA Processing, Microarray Hybridization and Data Analysis

The processing of RNA samples has been previously described (7) . In brief, RNA was isolated from unfractionated snap-frozen cell pellets using the Trizol reagent (Invitrogen). RNA was quantified using UV spectroscopy (Nanodrop Technologies) and assessed using a BioAnalyzer 2100 and RNA NanoChip assay (Agilent Technologies). RNA samples were labeled and hybridized to Affymetrix Human Genome 133 Plus 2.0 Array Gene Chip microarrays using standard protocols at the Laboratory for Clinical Genomics at Washington University (details availalable at http://www.pathology.wustl.edu/research/lcgoverview.php). Raw scan data was scaled to a target intensity of 1,500 using the Affymetrix GCOS 1.2 (MAS 5) statistical algorithm and then merged with current probeset annotations. Profiling data for all samples will be deposited online at the Gene Expression Omnibus.

3.5.3. Quantitative RT-PCR

One-step quantitative RT-PCR was performed with 20 ng RNA using the QuantiTect SYBR Green RT-PCR kit and QuantiTect Primer assays (Qiagen) on a Prism 7300 real-time PCR system (Applied Biosystems) according to the manufacturer's instructions. All reactions were performed in triplicate. Expression was normalized to GAPDH using the ΔCt method.

3.5.4. Gene Set Enrichment Analysis

Gene set enrichment analysis (GSEA) was performed using gene set permutation analysis with ratio-of-classes gene ranking (http://www.broad.mit.edu/gsea). Array data were pre-processed to remove probesets with average signal intensity < 500 in both comparison groups (APL and promyelocytes).

3.5.5. Cell lines

The PR-9 cell line was a kind gift of P. Pellicci of the European Institute of Oncology, Milan, Italy. NB-4 cells were obtained from the Deutsche Sammlung von Mikroorganismen und Zellkulturen (DSMZ). Cell lines were grown in RPMI supplemented with 10% fetal calf serum. PML-RARA expression was induced in PR9 cells using 100 μM $ZnSO_4$ diluted in media.

3.5.6. Western blots and antibodies

Prior to lysis, 2×10^6 cells were incubated in the presence of 100 μM diisopropyl-fluorophosphate (Sigma-Aldrich), then lysed in 100 μl 2% SDS/PBS. Total protein was

electrophoresed and transferred to Hybond-C membranes (Amersham) as described (3). Antibodies used include Rara (C-20, Santa Cruz), Jag1 (H-114, Santa Cruz), cleaved-Notch1 Val1744 (Cell Signal Technologies) and actin (C-4, Milipore). Blots were developed using the ECL Plus chemiluminescence system (Amersham).

3.5.7. Flow Cytometry

Cells were washed, RBC-lysed if necessary and pre-incubated with unlabeled anti-mouse CD16 (eBioscience) before surface staining against the following antigens: Jag1, Gr-1, and c-Kit (eBioscience). For intracellular staining, cells were fixed and permeabilized following surface staining using the FoxP3 Intracellular Staining Buffer Set (eBioscience) according to the manufacturer's recommendations. In experiments comparing the presence of Jag1 on the cell surface versus with intracellular compartments, equal amounts of antibody were used for surface and intracellular staining. Intracellular cleaved Notch-1 was detected using the mN1A Notch antibody (eBioscience). Data were collected on a FacSCAN (BD) and analyzed using FlowJo (Treestar).

3.5.8. Mice

The mCG-PML-RARA mice have been previously described (3), and have been fully back-crossed to the C57/B6 strain (Jackson Laboratory) for at least 10 generations. 129SvJ/B6 F1 hybrid animals were generated by mating 129SvJ males with C57/B6 females (both parental strains obtained from Jackson Laboratory). Animal care and

experimental protocols were approved by the Animal Studies Committee of Washington University School of Medicine.

3.5.9. Drugs

The gamma secretase inhibitors (GSIs) compound E and compound IX (Calbiochem) were dissolved in DMSO at concentrations of 2mM and 25mM, respectively. These solutions were used as 1000X stocks in liquid and semi-solid culture experiments. All-trans retinoic acid (ATRA, Sigma) was dissolved in 100% ethanol to make a 10mM stock solution. This stock was then diluted in DMSO to make a 1mM 1000X working stock solution for liquid and methylcellulose culture experiments. For *in vivo* experiments compound E (Axon Med Chem) was diluted in DMSO to make a 6 mg/mL stock solution. DMSO stock was diluted into a 1:1 mixture of PBS and propylene glycol (Sigma) immediately prior to intraperitoneal injections.

3.5.10. Methylcellulose assays

Marrow was harvested from the tibias and femurs of 6-8 week mCG-PR or C57/B6 animals and subjected to a 10 minute incubation in ammonium chloride lysis buffer on ice. After washing, 35,000 cells were added to 3.5 mL of methylcellulose media containing IL-3, IL-6 and stem cell factor (M3534 media, Stem Cell Technologies). Following thorough mixing to evenly distribute cells into the media, 1 mL was plated in 3 replicate dishes. After 1 week, colony formation was scored using the 40X objective on a light microscope. For replating experiments, cells were harvested from methylcellulose

cultures by dissolving in 37°C RPMI, and were then replated in fresh methylcellulose media as described above.

3.5.11. Retroviral transductions

The MSCV-DNMAML-GFP plasmid has been previously described (27) and was a kind gift of Rafael Kopan. Retrovirus production was performed as described (42). Viral stocks were titered based upon GFP expression in 3T3 cells. Viral transductions were done as follows: after harvest and red cell lysis, marrow cells were grown in 6 well plates overnight in 3mL RPMI media supplemented with 10% FBS, 6 ng/mL IL-3, 10 ng/mL IL-6 and 100 ng/mL SCF. On day 1, 0.5-1mL of viral supernatant, 3 μg/mL polybrene, and 100 mM Hepes buffer were added to the culture media. Plates were spun for 90 minutes at 1,500 rpm. After 3 hours, the cells were transferred to fresh media. The transduction was repeated on day 2. On day 3, GFP+ cells were sorted into media using an iCyte Reflection sorter at the High Speed Cell Sorting Core of the Siteman Cancer Center, Washington University. Cells were plated in methylcellulose media as described above.

3.5.12. Cryopreserved murine APL samples

Cryopreserved murine APL samples were collected and frozen as described previously (43). Vials containing 1 mL of cells were rapidly thawed in a 37°C water bath. An equal volume of fetal calf serum was added to the cryovial, and the 2mL of cells/FBS were immediately diluted in 8mL of cold recovery media (30%FBS in RPMI), which was then further diluted in 40 mL of recovery media. After centrifugation, the cell pellet was

resuspended in 20 mL recovery media and incubated at 37°C for 1-2 hours. APL cells were then centrifuged and resuspended in 10 mL RPMI media supplemented with 10% FBS, 6 ng/mL IL-3 (Peprotech), 10 ng/mL IL-6 (Peprotech) and 100 ng/mL SCF (Peprotech). Viable cell counts were performed using trypan blue exclusion. Viability typically exceeded 75%. Two mL of media containing approximately 200,000 live cells were plated into each well of a 12 well plate. Inhibitors were added to the wells at concentrations as described above and the plate was incubated at 37°C at 3% O2 for 48 hours. After 2 days in liquid culture, cells were plated in methylcellulose media as described above and grown in 3% O2 for 7 days. Colony formation was scored as described above.

3.5.13. Secondary transplantation of primary murine APL

Murine APL cells were thawed as described above, washed and resuspended in PBS. $5x10^5$ cells were injected retro-orbitally into sub-lethally irradiated (300cGy) 129/B6 F1 recipient animals. Treated animals received IP injections of 3 mg/kg compound E on a 5 days on/2 days off dosing schedule beginning the day immediately after transplant. Disease progression was assessed with weekly CBCs performed on retro-orbital eye bleeds beginning 3 weeks post injection. Upon the appearance of clinical illness, animals were humanely sacrificed and spleen cells were harvested and banked as described.

3.5.14. Murine APL Cell Lines and Bioluminescent Imaging

Click beetle red labeled APL^{luc} cell lines derived from mCG-PR mice on a 129/B6 F1 background have been described previously (28). Two independent clones, 42c5 and

62c5, were used in our experiments. 129/B6 recipient animals were injected intraperitoneally with 500,000 cells diluted in PBS. Some animals received two 21-day release 10 mg subcutaneous ATRA pellets (Innovative Research of America). Compound E treated animals were injected daily with 6mg/kg compound E. Bioluminescent imaging was performed using an IVIS 50 CCD camera (Xenogen). Mice were shaved ventrally to reduce signal attenuation, and injected intraperitoneally with D-luciferin (150 µg/g in PBS) and anesthetized using isoflurane. Images were collected 10 minutes after D-luciferin injection. Photons/second were measured using a rectangular region of interest drawn around the head, thorax, abdomen and hind limbs of the animal. Imaging was performed biweekly until animals exhibited clinical signs of illness.

3.5.15. Statistics

Data shown are mean +/- standard deviation. P-values were calculated using a Student's two tailed t-test and were considered significant when $P < 0.05$. Statistical analysis and graphing were performed using Prism5 (GraphPad).

3.6. Acknowledgments

We thank Drs. Raphael Kopan, Dan Link, Matt Walter, Lukas Wartman, Jackie Payton, and John Welch for helpful discussions. Mieke Hoock, Dan George, and Nick Protopsaltis provided invaluable animal husbandry assistance and Erin Wehmeyer provided excellent technical support. We appreciate the High Speed Cell Sorter Core, the Laboratory of Clinical Genomics, the Tissue Procurement Core, and the Bioinformatics Core of the Siteman Cancer Center at Washington University for their assistance with this study. We also thank Lynne Collins, Erin Smith and the Molecular Imaging Core for help with bioluminescent imaging experiments. This work was supported by the following grants: NIH R01 CA083962 (T.JL.), NIH PO1 CA101937 (T.J.L), and NIH 5T32 HL007088-35 (N.R.G.).

3.7. References

1. Brown D, Kogan S, Lagasse E, et al. A PMLRARalpha transgene initiates murine acute promyelocytic leukemia. *Proceedings of the National Academy of Sciences of the United States of America*. 1997;94:2551-2556.

2. Grisolano JL, Wesselschmidt RL, Pelicci PG, Ley TJ. Altered myeloid development and acute leukemia in transgenic mice expressing PML-RARa under control of cathepsin G regulatory sequences. *Blood*. 1997;89:376-387.

3. Westervelt P, Lane AA, Pollock JL, et al. High-penetrance mouse model of acute promyelocytic leukemia with very low levels of PML-RARa expression. *Blood*. 2003;102:1857-1865.

4. Uy GL, Payton JE, Ley TJ. Multilineage Expansion of Lymphoid and Myeloid Cells in Mice Expressing PML-RAR under the Control of the Murine Cathepsin G Locus. *Blood*. 2006;108:2051.

5. Wojiski S, Guibal FC, Kindler T, et al. PML-RARalpha initiates leukemia by conferring properties of self-renewal to committed promyelocytic progenitors. *Leukemia : official journal of the Leukemia Society of America, Leukemia Research Fund, U.K*. 2009;23(8):1462-71.

6. Ross ME, Mahfouz R, Onciu M, et al. Gene expression profiling of pediatric acute myelogenous leukemia. *Blood*. 2004;104:3679-3687.

7. Payton JE, Grieselhuber NR, Chang L, et al. High throughput digital quantification of mRNA abundance in primary human acute myeloid leukemia samples. *The Journal of clinical investigation*. 2009;119(6):1714-26.

8. Casorelli I, Tenedini E, Tagliafico E, et al. Identification of a molecular signature for leukemic promyelocytes and their normal counterparts: focus on DNA repair genes. *Leukemia*. 2006;20:1978–1988.

9. Alcalay M, Meani N, Gelmetti V, et al. Acute myeloid leukemia fusion proteins deregulate genes involved in stem cell maintenance and DNA repair. *The Journal of clinical investigation*. 2003;112(11):1751-61.

10. Meani N, Minardi S, Licciulli S, et al. Molecular signature of retinoic acid treatment in acute promyelocytic leukemia. *Oncogene*. 2005;24:3358-3368.

11. Radtke F, Fasnacht N, Macdonald HR. Notch signaling in the immune system. *Immunity*. 2010;32(1):14-27.

12. Maillard I, Koch U, Dumortier A, et al. Canonical notch signaling is dispensable for the maintenance of adult hematopoietic stem cells. *Cell stem cell*. 2008;2(4):356-66.

13. Weng AP, Ferrando AA, Lee W, et al. Activating mutations of NOTCH1 in human T cell acute lymphoblastic leukemia. *Science (New York, N.Y.)*. 2004;306(5694):269-71.

14. Palomero T, McKenna K, O-Neil J, et al. Activating mutations in NOTCH1 in acute myeloid leukemia and lineage switch leukemias. *Leukemia : official journal of the Leukemia Society of America, Leukemia Research Fund, U.K*. 2006;20(11):1963-6.

15. O'Neil J, Grim J, Strack P, et al. FBW7 mutations in leukemic cells mediate NOTCH pathway activation and resistance to gamma-secretase inhibitors. *The Journal of experimental medicine*. 2007;204(8):1813-24.

16. Salat D, Liefke R, Wiedenmann J, Borggrefe T, Oswald F. ETO, but not leukemogenic fusion protein AML1/ETO, augments RBP-Jkappa/SHARP-mediated repression of notch target genes. *Molecular and cellular biology*. 2008;28(10):3502-12.

17. Mercher T, Raffel GD, Moore SA, et al. The OTT-MAL fusion oncogene activates RBPJ-mediated transcription and induces acute megakaryoblastic leukemia in a knockin mouse model. *The Journal of clinical investigation*. 2009;119(4):852-64.

18. Nakahara F, Sakata-Yanagimoto M, Komeno Y, et al. Hes1 immortalizes committed progenitors and plays a role in blast crisis transition in chronic myelogenous leukemia. *Blood*. 2010;115(14):2872-81.

19. Gal H, Amariglio N, Trakhtenbrot L, et al. Gene expression profiles of AML derived stem cells; similarity to hematopoietic stem cells. *Leukemia : official journal of the Leukemia Society of America, Leukemia Research Fund, U.K*. 2006;20(12):2147-54.

20. Cullion K, Draheim KM, Hermance N, et al. Targeting the Notch1 and mTOR pathways in a mouse T-ALL model. *Blood*. 2009;113(24):6172-81.

21. Moellering RE, Cornejo M, Davis TN, et al. Direct inhibition of the NOTCH transcription factor complex. *Nature*. 2009;462(7270):182-8.

22. Wu Y, Cain-Hom C, Choy L, et al. Therapeutic antibody targeting of individual Notch receptors. *Nature*. 2010;464(7291):1052-1057.

23. Deangelo DJ, Stone RM, Silverman LB, et al. A phase I clinical trial of the notch inhibitor MK-0752 in patients with T-cell acute lymphoblastic leukemia/lymphoma (T-ALL) and other leukemias. *Journal of Clincal Oncology*. 2006;24(18S):6585.

24. Palomero T, Lim WK, Odom DT, et al. NOTCH1 directly regulates c-MYC and activates a feed-forward-loop transcriptional network promoting leukemic cell growth.

Proceedings of the National Academy of Sciences of the United States of America. 2006;103(48):18261-6.

25. Mercher T, Cornejo MG, Sears C, et al. Notch signaling specifies megakaryocyte development from hematopoietic stem cells. *Cell stem cell*. 2008;3(3):314-26.

26. Yuan W, Payton JE, Holt MS, et al. Commonly dysregulated genes in murine APL cells. *Blood*. 2007;109(3):961-70.

27. Weng AP, Nam Y, Wolfe MS, et al. Growth suppression of pre-T acute lymphoblastic leukemia cells by inhibition of notch signaling. *Molecular and cellular biology*. 2003;23(2):655-64.

28. Nervi B, Ramirez P, Rettig MP, et al. Chemosensitization of acute myeloid leukemia (AML) following mobilization by the CXCR4 antagonist AMD3100. *Blood*. 2009;113(24):6206-14.

29. Real PJ, Tosello V, Palomero T, et al. γ-secretase inhibitors reverse glucocorticoid resistance in T cell acute lymphoblastic leukemia. *Nature Medicine*. 2008;15(1):50-58.

30. Alcalay M, Tiacci E, Bergomas R, et al. Acute myeloid leukemia bearing cytoplasmic nucleophosmin (NPMc+ AML) shows a distinct gene expression profile characterized by up-regulation of genes involved in stem-cell maintenance. *Blood*. 2005;106(3):899-902.

31. Valk PJ, Verhaak RG, Beijen MA, et al. Prognostically useful gene-expression profiles in acute myeloid leukemia. *New England Journal of Medicine*. 2004;350(1617-1628).

32. Verhaak RG, Wouters BJ, Erpelinck CA, et al. Prediction of molecular subtypes in acute myeloid leukemia based on gene expression profiling. *Haematologica*. 2009;94(1):131-4.

33. Wang K, Wang P, Shi J, et al. PML/RARalpha targets promoter regions containing PU.1 consensus and RARE half sites in acute promyelocytic leukemia. *Cancer cell*. 2010;17(2):186-97.

34. Martens JH, Brinkman AB, Simmer F, et al. PML-RARalpha/RXR Alters the Epigenetic Landscape in Acute Promyelocytic Leukemia. *Cancer cell*. 2010;17(2):173-85.

35. Hoemme C, Peerzada A, Behre G, et al. Chromatin modifications induced by PML-RARalpha repress critical targets in leukemogenesis as analyzed by ChIP-Chip. *Blood*. 2008;111(5):2887-95.

36. Radke AL, Reynolds LE, Melo RC, et al. Mature human eosinophils express functional Notch ligands mediating eosinophil autocrine regulation. *Blood*. 2009;113(13):3092-101.

37. Pintar A, De Biasio A, Popovic M, Ivanova N, Pongor S. The intracellular region of Notch ligands: does the tail make the difference? *Biology direct*. 2007;2:19.

38. Ascano JM, Beverly LJ, Capobianco AJ. The C-terminal PDZ-ligand of JAGGED1 is essential for cellular transformation. *The Journal of biological chemistry*. 2003;278(10):8771-9.

39. Yan P, Bero AW, Cirrito JR, et al. Characterizing the appearance and growth of amyloid plaques in APP/PS1 mice. *The Journal of neuroscience : the official journal of the Society for Neuroscience*. 2009;29(34):10706-14.

40. Milano J, McKay J, Dagenais C, et al. Modulation of notch processing by gamma-secretase inhibitors causes intestinal goblet cell metaplasia and induction of genes known to specify gut secretory lineage differentiation. *Toxicological sciences : an official journal of the Society of Toxicology*. 2004;82(1):341-58.

41. Yang T, Arslanova D, Gu Y, Augelli-Szafran C, Xia W. Quantification of gamma-secretase modulation differentiates inhibitor compound selectivity between two substrates Notch and amyloid precursor protein. *Molecular brain*. 2008;1(1):15.

42. Luo H, Li Q, O'Neal J, et al. c-Myc rapidly induces acute myeloid leukemia in mice without evidence of lymphoma-associated antiapoptotic mutations. *Blood*. 2005;106(7):2452-61.

43. Pollock JL, Westervelt P, Kurichety AK, et al. A bcr-3 isoform of RARa-PML potentiates the development of PML-RARa-driven acute promyelocytic leukemia. *Proceedings of the National Academy of Sciences of the United States of America*. 1999;96:11508-15103.

3.7. Figure Legends

Figure 3-1: *JAG1* is overexpressed in human APL.

A). Gene expression profile data for Jagged-1 (*JAG1*) in a set of 180 de novo AML and sorted normal CD34+ cells, promyelocytes, and neutrophils. Two probesets, 209099 and 216286, are shown. B). *JAG1* expression in the CALGB set of 93 de novo AML samples, showing the same probesets as in A. Each data point in A and B represents one patient sample or one normal sample. C). Validation of *JAG1* expression by qRT-PCR in 11 APL, 12 other AML (4 samples each of M0, M1, M2, and M4 FAB subtypes) and 4 flow-sorted normal promyelocyte samples. Data are normalized to GAPDH expression.

Figure 3-2: Human APL cells express the necessary components of Notch signaling.

A). Expression of Notch receptors and ligands in APL (closed bars) and normal promeylocytes (open bars). Data shown are the mean +/- standard deviation of the probeset with the highest average signal intensity for 22 APL and 5 normal promyelocyte samples present in the Washington University *de novo* AML set. B). Expression of gamma secretase components in APL cells and promyelocytes C). Expression of enzymes involved in the S1 and S2 cleavage of Notch. D). Expression of transcriptional cofactors of cleaved Notch. E). Expression of enzymes that modify Notch receptors. F). Expression of E3 ubiquitin ligases involved in Notch signaling. Genes present in the APL dysregulome are marked with an asterisk.

Figure 3-3: Notch target gene signatures are enriched in human APL cells

A). GSEA plot (top) and heat map (bottom) of 22 APL samples compared to 5 normal promyelocyte samples demonstrates significant enrichment in APL of a previously described set of Notch transcriptional targets in T-ALL (21). B). GSEA plot (top) and heat map (bottom) of the same APL and promyelocyte samples as in A, showing significant enrichment in APL of a previously published set of genes downregulated in T-ALL by gamma secretase inhibitor treatment (24).

Figure 3-4: Increased *JAG1* expression and activation of Notch signaling are found in induced PR-9 cells.

A). Microarray expression data for *JAG1* in PR-9 cells after Zn^{2+} induction of PML-RARA expression. Each data point represents a single sample. B). Western blots showing protein levels of PML-RARA, JAG1, cleaved Notch-1 and actin in PR-9 cells at 4, 8, 16 and 24 hours after Zn^{2+} induction.

Figure 3-5: JAG1 protein is found in an intracellular compartment in PR-9 cells.

Flow cytometry plots showing: A). staining of PR-9 cells with an isotype control antibody, B) detection of JAG1 protein by flow cytometry in PR-9 cells by surface staining or C) intracellular staining following fixation and permeabilization.

Figure 3-6: NB-4 cells express JAG1 protein and have activated Notch signaling.

Flow cytometry plots showing: A). staining of NB-4 cells with an isotype control antibody, B). intracellular staining of NB-4 cells with a PE conjugated anti-JAG1 antibody or C) intracellular staining of NB-4 cells with a PE conjugated anti-Notch1

antibody. This antibody recognizes only cleaved isoforms of Notch1 and not uncleaved surface Notch1.

Figure 3-7: Jag1 and activated Notch signaling are found in murine APL samples.

A). Microarray expression data for *Jag1* from *in vitro* differentiation of LS cells with G-CSF and 22 murine APL samples. B). Summarized data showing percent of Jag1 and intracellular Notch-1 (ICN1) positive cells present in 10 independent murine APL tumors. C). Intracellular flow cytometry detection of Jag1 and ICN1 in a representative murine APL (tumor number 13355).

Figure 3-8: Comparison of extracellular and intracellular Jag1 in murine APL samples.

Flow cytometry staining of 3 murine APL tumors (numbers 13441, 13843 and 3430 from top row to bottom row) stained with either isotype control (left column), extracellular staining for Jag1 and Gr-1 (center column), or extracellular staining for Gr-1 and intracellular staining for Jag1 (right column).

Figure 3-9: Pharmacological inhibition of Notch signaling in mCG-PR marrow

A). Relative colony formation for 3 wildtype marrow samples plated in Methocult (3534) containing DMSO, 2 μM compound E, or 25 μM compound IX. Data shown are mean value +/- standard deviation. Data are normalized to the week 1 DMSO treated control colony counts. Cells from each animal were plated in triplicate for all treatment conditions. B). Relative colony formation for 5 independent mCG-PR marrow samples

plated in Methocult (3534) under the same conditions and normalized as described in A. C). Representative data from a single mCG-PR animal. Each data point is mean +/- SD of 3 replicate platings. In all graphs, one asterisk (*) indicates $p<0.05$, two asterisks (**) indicates $p<0.01$ and three asterisks (***) indicates $p<0.001$.

Figure 3-10: Genetic inhibition of Notch signaling via DNMAML in mCG-PR marrow

A). Relative colony formation for 3 wildtype B6 marrow samples transduced with either MSCV-GFP-DNMAML or GFP control, sorted for GFP+ cells and plated in Methocult (3534). Data shown are mean +/- standard deviation. Data are normalized to the GFP control. Cells from each animal were plated in triplicate for all treatment conditions. B). Relative colony formation for 2 independent mCG-PR marrow samples plated in Methocult (3534) under the same conditions and normalized as in A. C). Representative data from a single PR+ animal. Each data point is mean +/- SD of 3 replicate platings. In all graphs, one asterisk (*) indicates $p<0.05$, two asterisks (**) indicates $p<0.01$ and three asterisks (***) indicates $p<0.001$.

Figure 3-11: Pharmacological inhibition of Notch signaling in murine APL cells *in vitro*

A). Schematic diagram of experimental setup. B). Summarized data for 3 wildtype marrow samples treated for 48 hours with 1 μM ATRA, 2 μM compound E, 25 μM compound IX or DMSO control, and then plated in Methocult in triplicate, as described in A. Each data point represents the average of 3 plates for a single animal. Data were

normalized to the average colony formation for DMSO controls for each tumor. C). Summarized data for 9 independent tumors treated for 48 hours with 1 μM ATRA, 2 μM compound E, 25 μM compound IX or DMSO control and then plated in Methocult in triplicate. Each data point represents the average of three plates for a single tumor. Data were normalized to the average colony formation for DMSO controls for each tumor. Tumor numbers 2894 and 3149 are highlighted in red and blue, respectively. D. Representative data from 3 tumors. In all graphs, one asterisk (*) indicates $p<0.05$, two asterisks (**) indicates $p<0.01$ and three asterisks (***) indicates $p<0.001$.

Figure 3-12: Detection of Jag1 protein in murine APL^{luc} cell lines

A) Staining of murine APL cell lines with an isotype control antibody. B). Intracellular staining of murine APL cell line 42c5 with a PE conjugated anti-Jag1 antibody. C). Intracellular staining of murine APL cell line 62c5 with a PE conjugated anti-Jag1 antibody. Both cell lines were surface stained with an APC-conjugated anti-Gr1 antibody.

Figure 3-13: *In vivo* treatment of APL^{luc} cell lines with compound E

A). Bioluminescence (photons/sec) detected in mice injected intraperitoneally with 500,000 42c5 cells, and then treated with no drug, 20 mg subcutaneous ATRA or daily IP injections of 6mg/kg compound E. Mice were imaged on post-injection days 1, 4, 7 and 11. B). As in A, except the 62c5 cell line was used. C). Representative images from mice in B.

Figure 3-14: *In vivo* treatment of primary murine APL with compound E

Sub-lethally irradiated 129/B6 mice were injected retro-orbitally with 500,000 tumor cells, either tumor 2894 or 3149, and received either no treatment or IP injections of 3 mg/kg compound E on a "5 days on, 2 days off" dosing schedule. A) WBC counts 4 weeks after injections with tumor 2894 or 3149. Compound E treated animals are indicated in red. B). Platelet counts for animals in A. C). RBC counts for animals in A. D). Spleen weights for animals in A. E) Percentage of Gr-1+, c-Kit+ cells in the spleens. F) Western blot showing the presence of cleaved Notch-1 in spleen cell lysates from 3 untreated (left) or 3 compound E treated (right) animals.

Table 3-1: Clinical characteristics of patients and de novo AML samples

Parameter	No.	%
Cytogenetic subgroup		
Normal	77	42.78
t(15;17) only	13	7.22
t(15;17) + other	6	3.33
t(8;21) only	4	2.22
inv(16) only	9	5.00
Trisomy 8 only	6	3.33
5q-/-5 only	1	0.56
7q-/-7 only	4	2.22
Complex karyotype	20	11.11
Other	36	17.22
Unknown	4	2.22
Mutation		
FLT3 ITD	31	17.22
FLT3 D835	11	6.11
IDH1	16	8.89
IDH2	15	8.33
NPM1	46	25.56
DNMT3A	44	24.44
PML-RARA	22	12.22
FAB subtype		
M0	13	7.22
M1	40	22.22
M2	42	23.33
M3	22	12.22
M4	36	20.00
M5	21	11.67
M6	3	1.67
M7	3	1.67
Sex		
Male	96	53.33
Female	84	46.67
Age		
18-29	18	10.00
30-39	22	12.22
40-49	25	13.89
50-59	40	22.22
60-69	45	25.00
70-79	27	15.00
80-89	3	1.67
Ethnicity		
Asian	1	0.56
African-American	16	8.89
Caucasian	159	88.33
Hispanic	2	1.11
Other	2	1.11

Table 3-2: Characteristics of mCG-PR mice and murine APL samples

Mouse	Strain	Sex	DOB	Age (mo)	Spleen (g)	WBC	% Jag1+	GSI responsive
3842	129/B6	M	1/17/2003	5	1.14	11.3	34.5	ND
13441	129/B6	F	1/11/2000	11.5	1.21	115	51.5	ND
13487	129/B6	M	2/8/2000	8	1.15	25.8	92.8	ND
13843	129/B6	M	5/6/2000	5	1.03	45.2	46.8	ND
2894	129/B6	M	10/1/2002	7	2.29	109.5	19.3	yes
2972	129/B6	F	10/13/2002	11	1.02	94.4	19.3	no
3149	129/B6	F	11/5/2002	8	1.55	35.5	ND	yes
3430	129/B6	M	12/12/2002	8	1.61	182.3	29.9	yes
3673	129/B6	M	1/4/2003	5	0.97	224	ND	no
13346	129/B6	F	12/10/1999	8	1.7	17	36.1	no
13355	129/B6	M	1/2/2000	9	0.93	18.8	90.7	yes
13499	129/B6	M	2/18/2003	6	1.23	69	ND	yes
13659	129/B6	M	3/24/2000	7.5	0.75	29.8	15.5	yes

Table 3-3: Characteristics of other AML samples with high *JAG1* expression

UPN	JAG1 209099	JAG1 216268	FAB	Cytogenetics	DNMT3A	FLT3 ITD	FLT3 D835	IDH1	IDH2	NPM1
146218	8,733	7,038	M1	inv(16)						W288fs
224143	21,169	17,406	M1	normal	F909C	ITD				
322110	12,800	8,877	M1	9qh+		ITD			R140Q	W288fs
329614	8,674	6,709	M1	normal		ITD				W288fs
431799	9,711	9,067	M1	normal	R882H			R132H		W288fs
548327	7,279	6,518	M1	normal				R132G		W288fs
721214	6,444	6,227	M1	failed	R882H	ITD				W288fs
804168	21,776	17,443	M1	normal		ITD				W288fs
809653	8,215	6,508	M1	complex						
851929	8,014	6,634	M1	+8	R792H/F827fs				R172K	
933124	7,231	8,515	M1	normal	L723fs	ITD				W288fs
982009	9,965	8,705	M1	normal			D835Y			W288fs
104851	9,586	9,069	M2	normal		ITD				
141273	10,470	7,886	M2	normal						
208027	11,564	9,096	M2	1 cell +7	R803S		D835Y			W288fs
237983	8,373	6,419	M2	-7 only					R140Q	
254137	6,372	6,893	M2	normal		ITD				W288fs
258135	12,242	10,132	M2	inv(16), t(3;3)						
753374	7,214	6,094	M2	normal						W288fs
817156	10,072	8,404	M2	normal	R882H					
104	7,122	5,818	M4	normal	R882C			R132H		
311636	9,225	10,726	M4	normal					R140Q	W288fs
507696	12,039	9,842	M4	inv(16)						
595704	6,559	5,887	M4	inv(16)		ITD				
671473	7,077	5,796	M4	inv(16)						
708512	21,956	16,860	M4	complex	R882H		D835E	R132H		W288fs
862507	7,514	6,758	M4	del(16),+22						
180168	8,895	6,265	M5	normal	R882H					
737451	7,299	6,859	M5	normal	R882H					W288fs
923966	6,461	4,941	M5	t(9;11)						

A

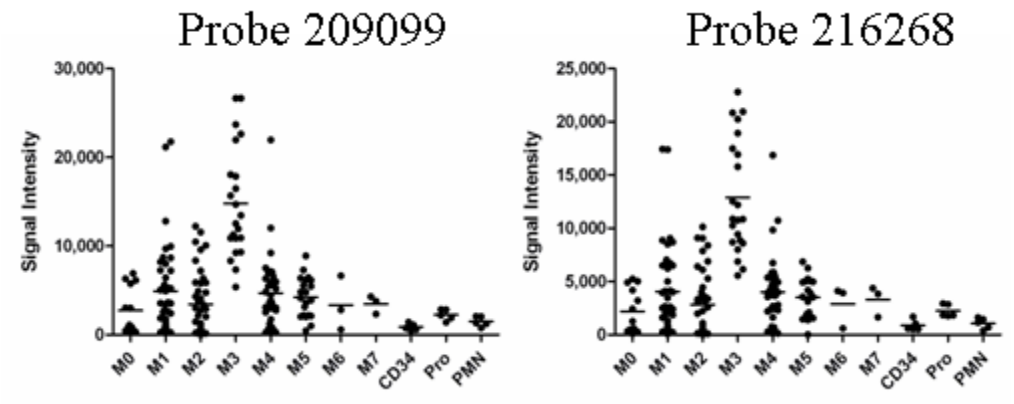

B

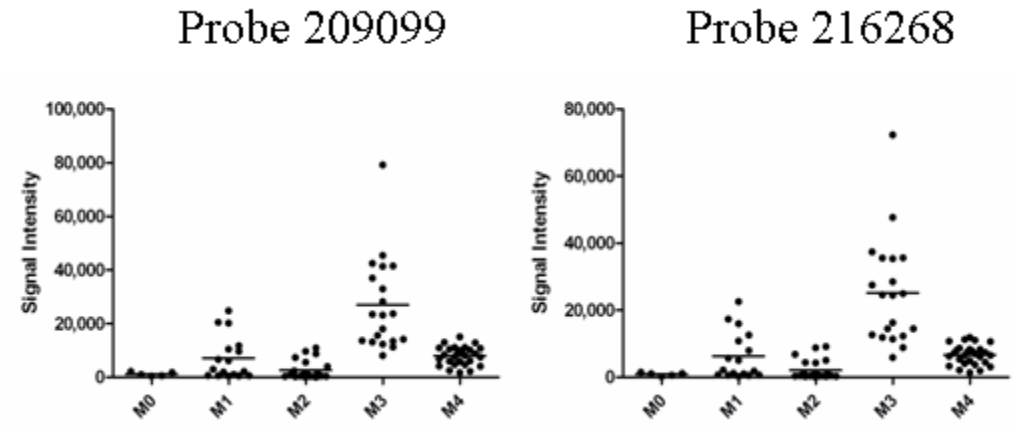

C

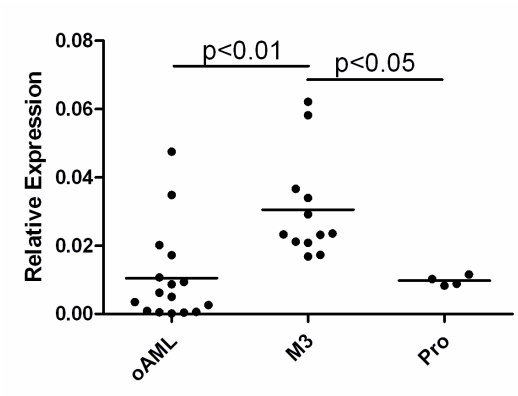

Figure 3-1

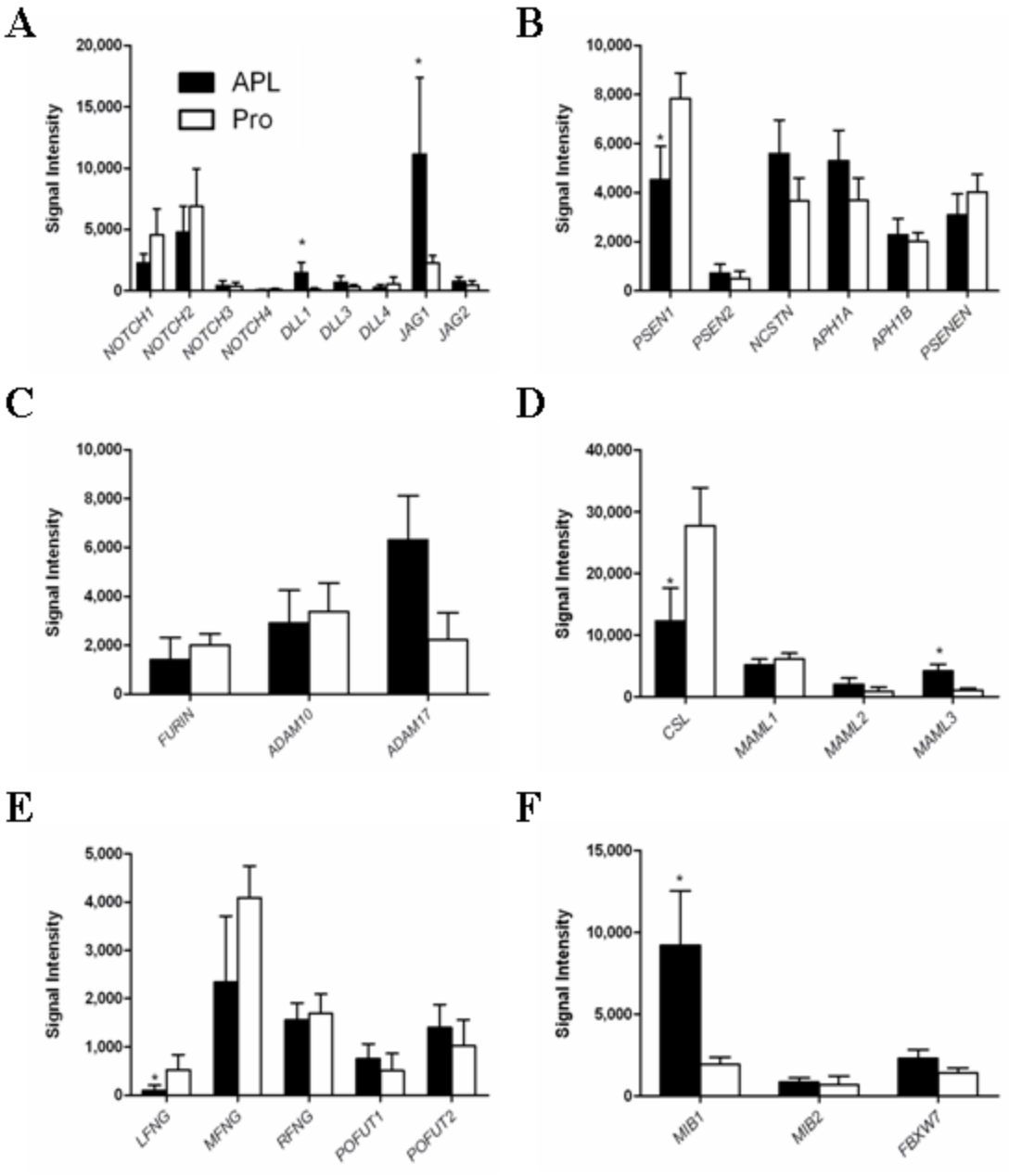
A
B
C
D
E
F
APL
Pro
Signal Intensity
NOTCH1
NOTCH2
NOTCH3
NOTCH4
DLL1
DLL3
DLL4
JAG1
JAG2
PSEN1
PSEN2
NCSTN
APH1A
APH1B
PSENEN
FURIN
ADAM10
ADAM17
CSL
MAML1
MAML2
MAML3
LFNG
MFNG
RFNG
POFUT1
POFUT2
MIB1
MIB2
FBXW7

Figure 3-2

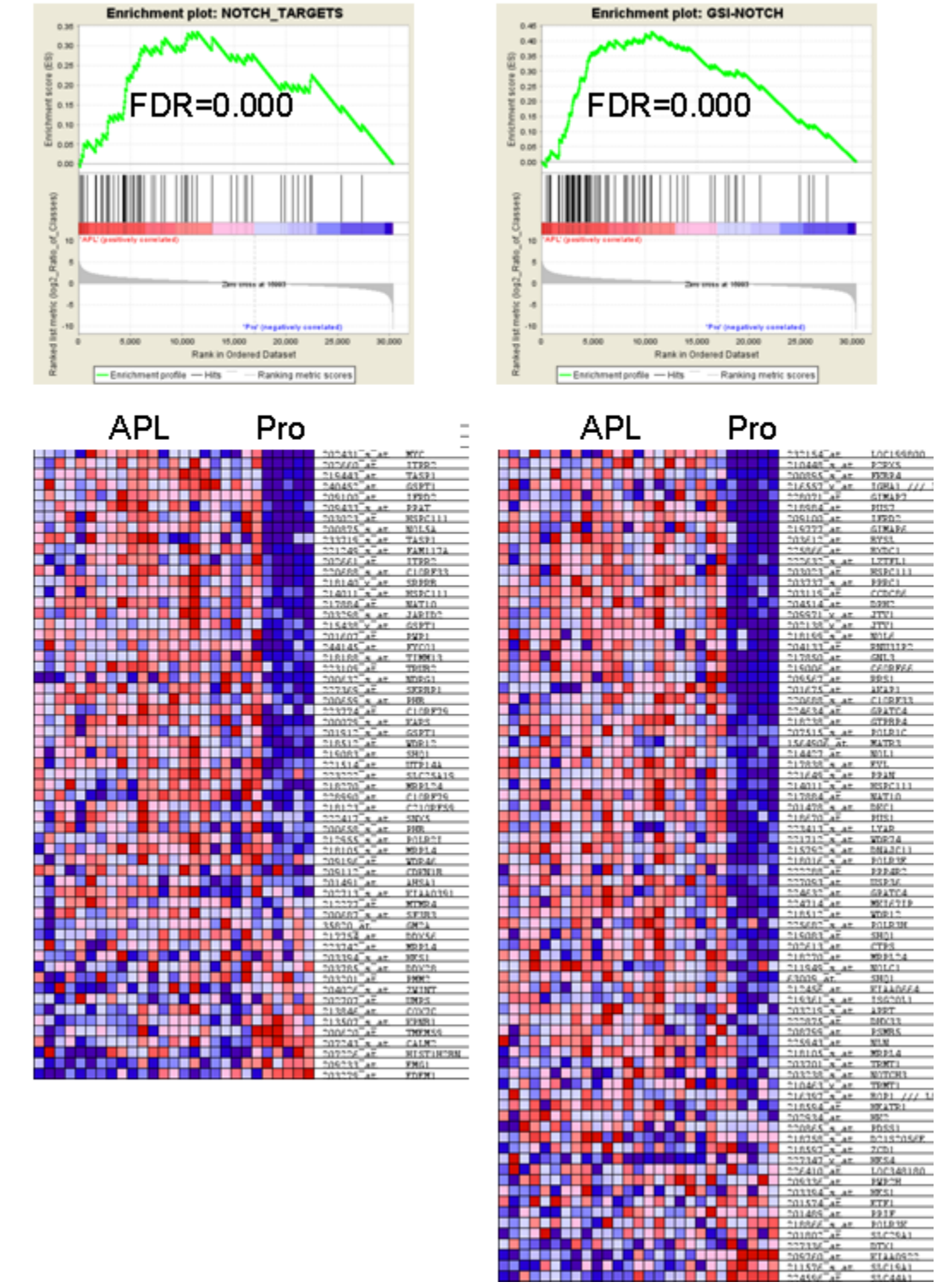

Figure 3-3A and 3-3B

C

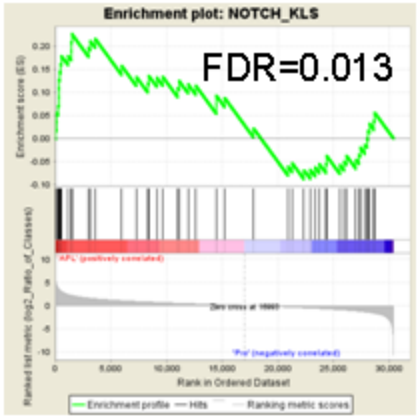
Enrichment plot: NOTCH_KLS
FDR=0.013
Enrichment score (ES)
Ranked list metric (log2_Ratio_of_Classes)
Rank in Ordered Dataset
Enrichment profile
Hits
Ranking metric scores

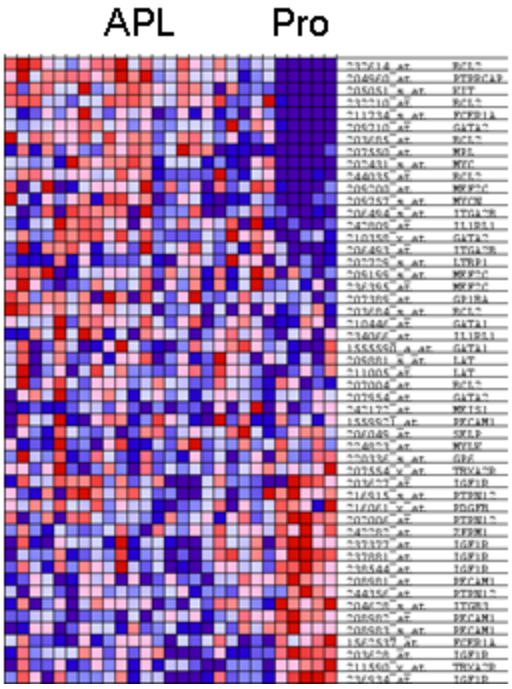
APL
Pro

Figure 3-3C

A

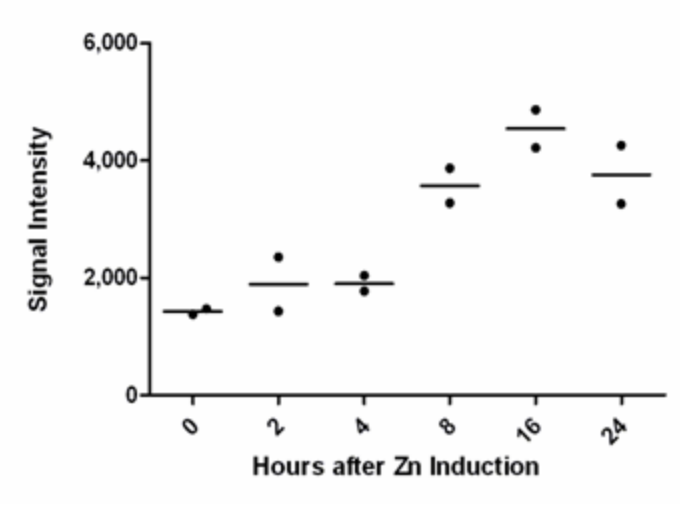
6,000
4,000
2,000
0
Signal Intensity
0
2
4
8
16
24
Hours after Zn Induction

B

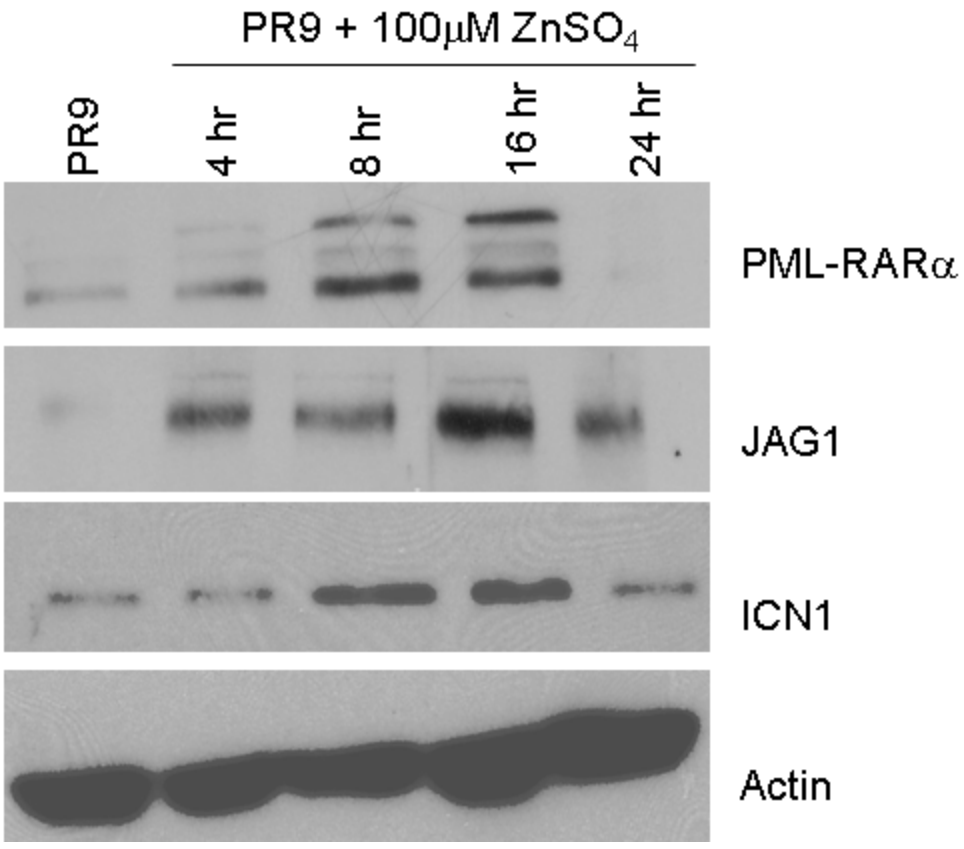
PR9 + 100μM ZnSO4
PR9
4 hr
8 hr
16 hr
24 hr
PML-RARα
JAG1
ICN1
Actin

Figure 3-4

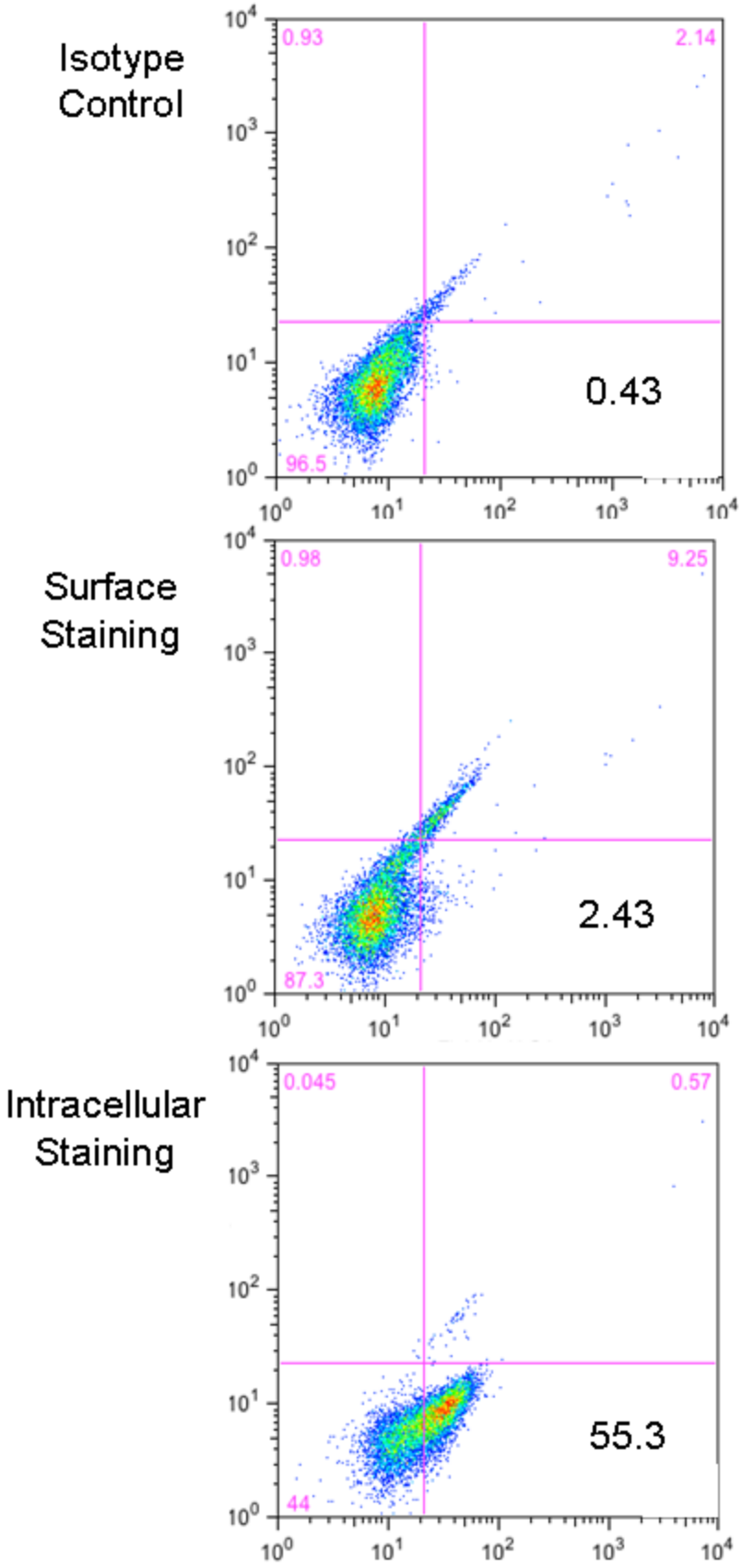
Isotype Control
0.93
2.14
0.43
96.5
Surface Staining
0.98
9.25
2.43
87.3
Intracellular Staining
0.045
0.57
55.3
44

Figure 3-5

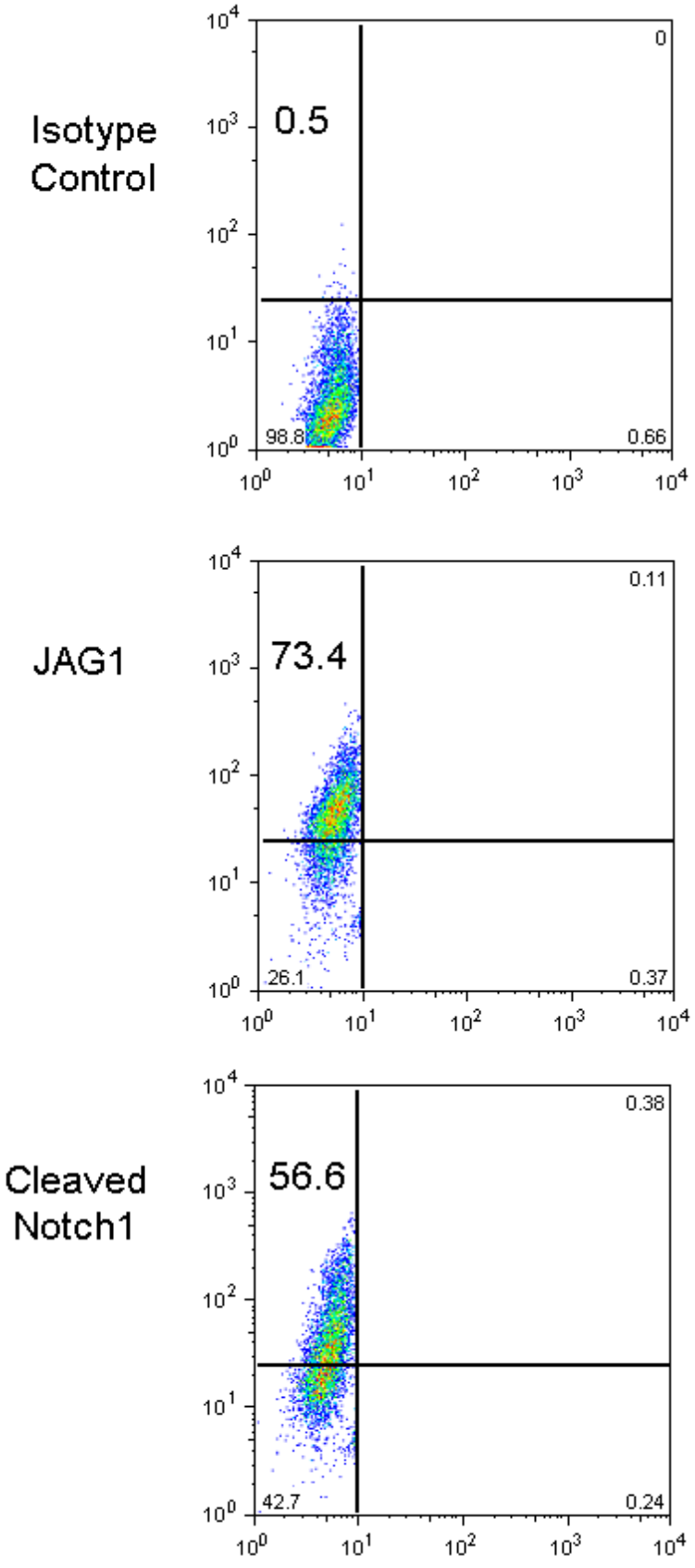
Isotype Control
0.5
0
98.8
0.66
JAG1
73.4
0.11
26.1
0.37
Cleaved Notch1
56.6
0.38
42.7
0.24

Figure 3-6

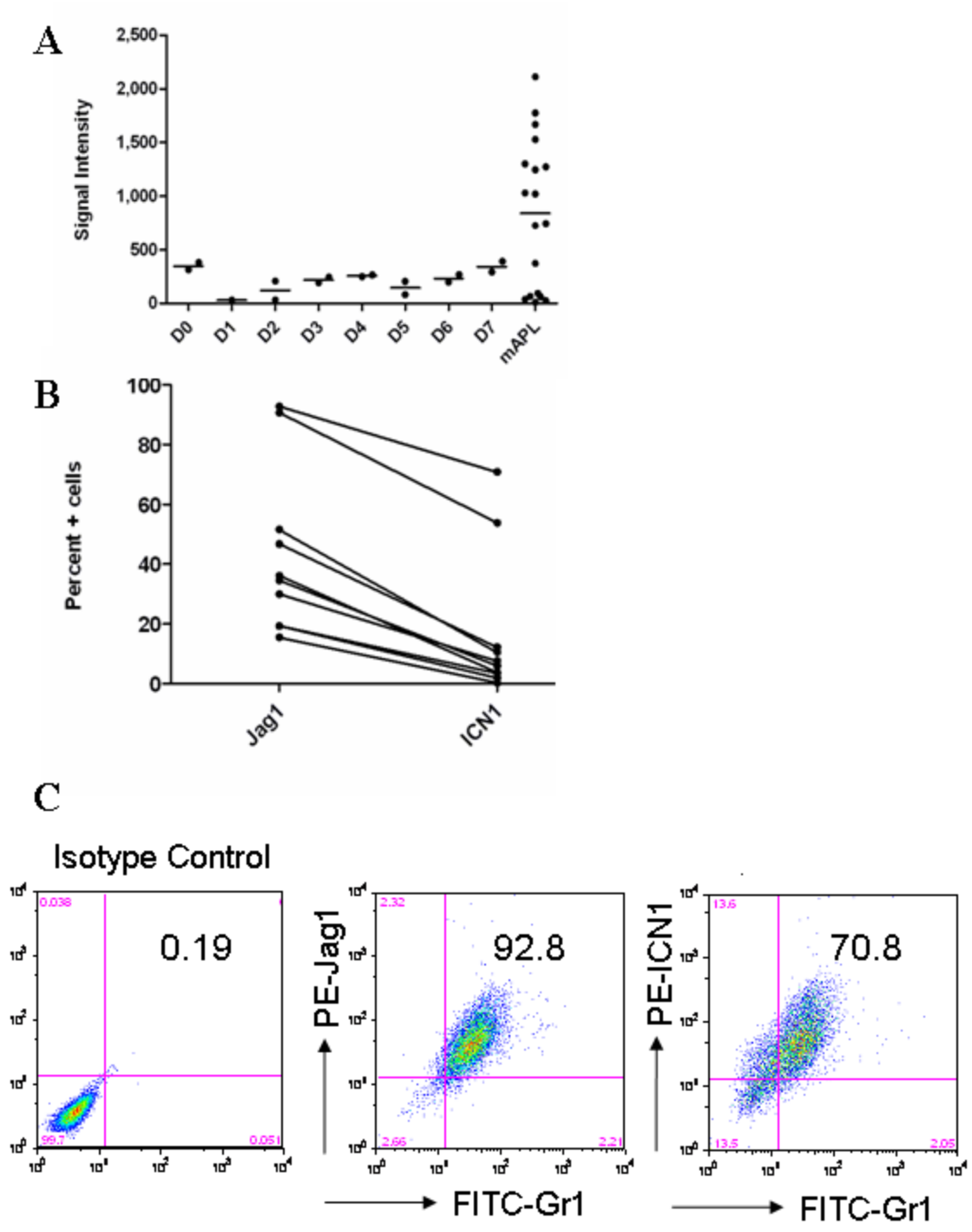
A
Signal Intensity
2,500
2,000
1,500
1,000
500
0
D0
D1
D2
D3
D4
D5
D6
D7
mAPL
B
Percent + cells
100
80
60
40
20
0
Jag1
ICN1
C
Isotype Control
0.19
92.8
70.8
PE-Jag1
PE-ICN1
FITC-Gr1
FITC-Gr1

Figure 3-7

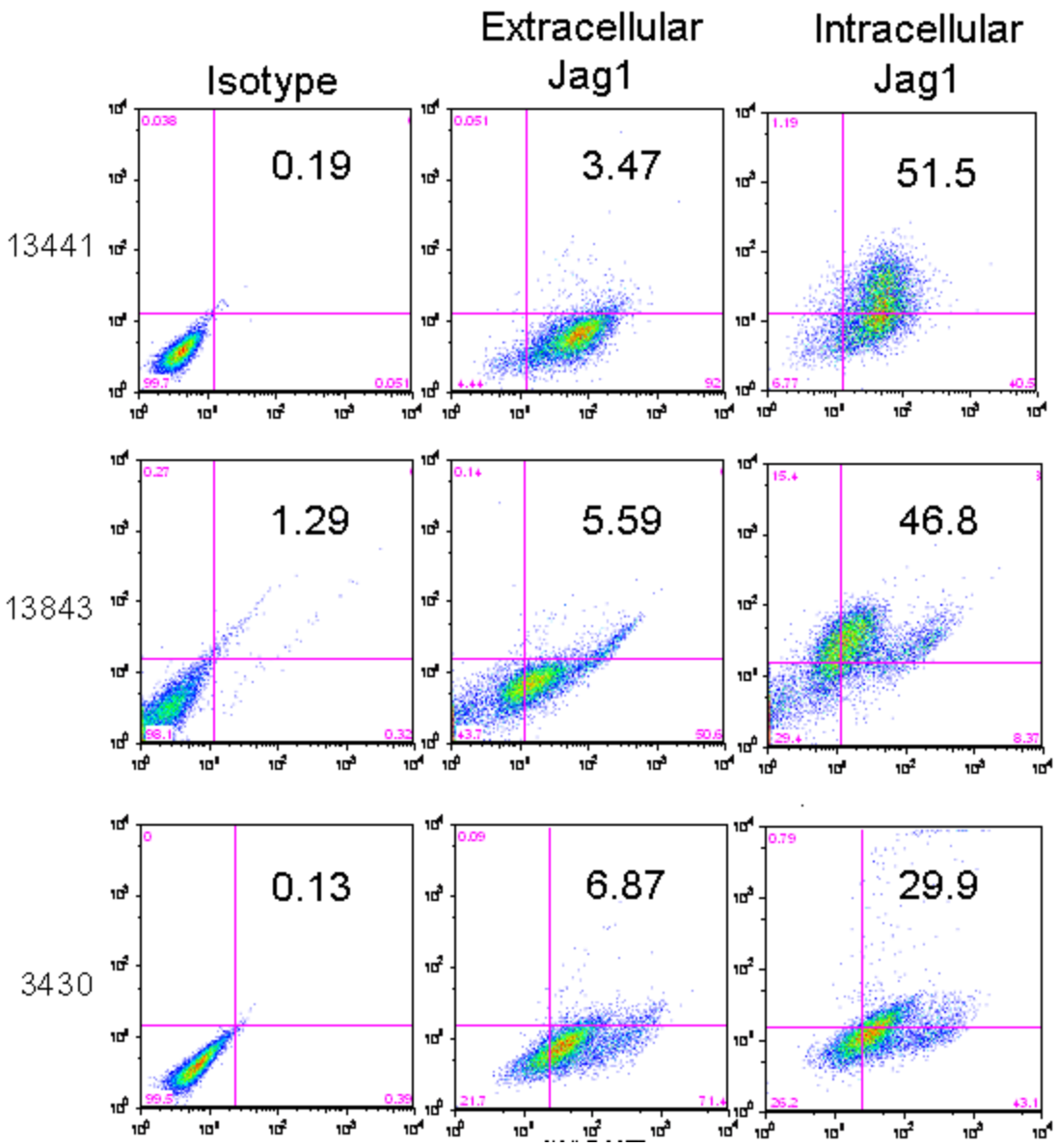
Isotype
Extracellular Jag1
Intracellular Jag1
13441
13843
3430
0.19
3.47
51.5
1.29
5.59
46.8
0.13
6.87
29.9

Figure 3-8

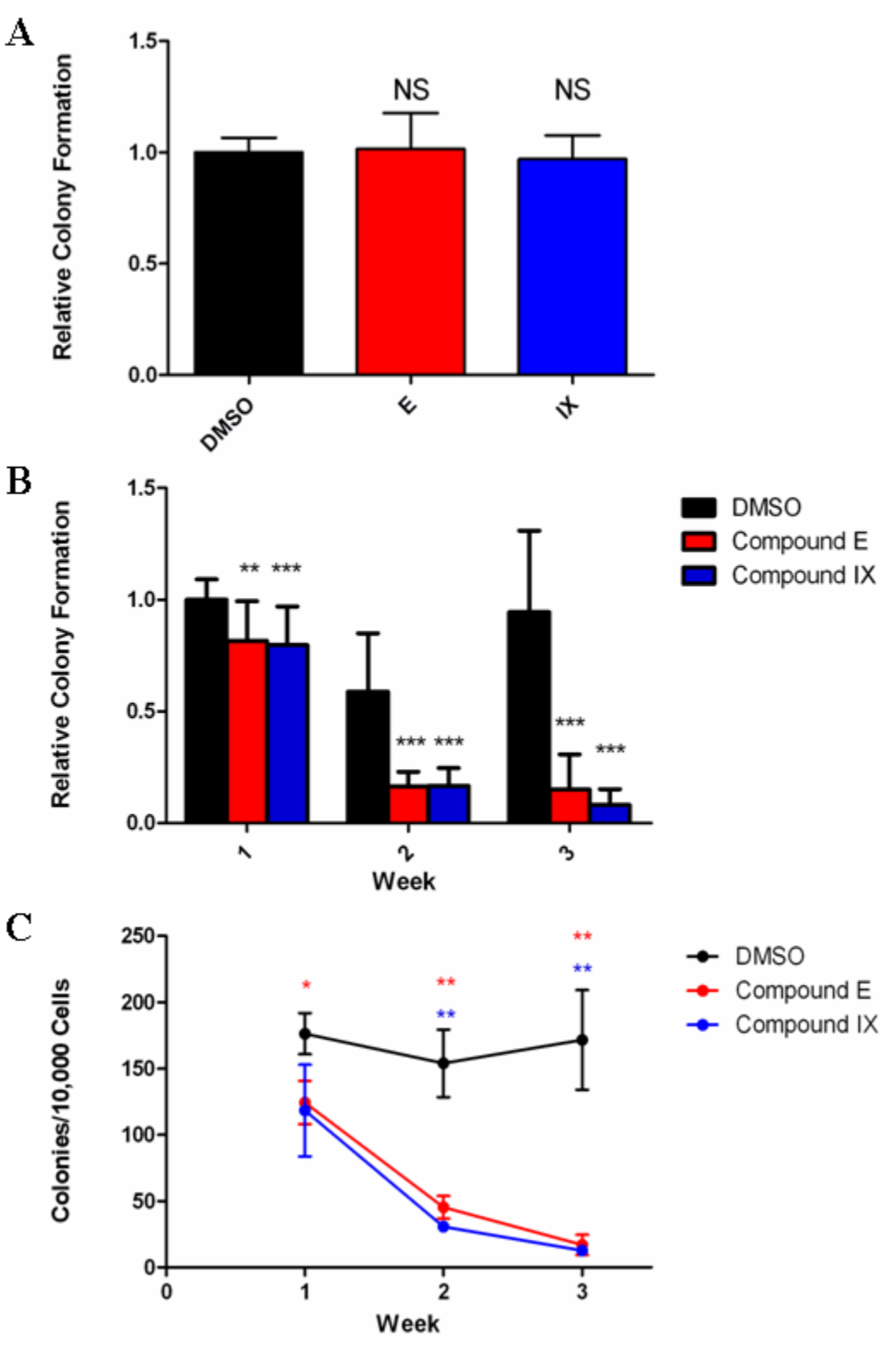
A
Relative Colony Formation
1.5
1.0
0.5
0.0
NS
NS
DMSO
E
IX
B
Relative Colony Formation
1.5
1.0
0.5
0.0
** ***
*** ***
***
***
1
2
3
Week
DMSO
Compound E
Compound IX
C
Colonies/10,000 Cells
250
200
150
100
50
0
*
**
**
**
**
0
1
2
3
Week
DMSO
Compound E
Compound IX

Figure 3-9

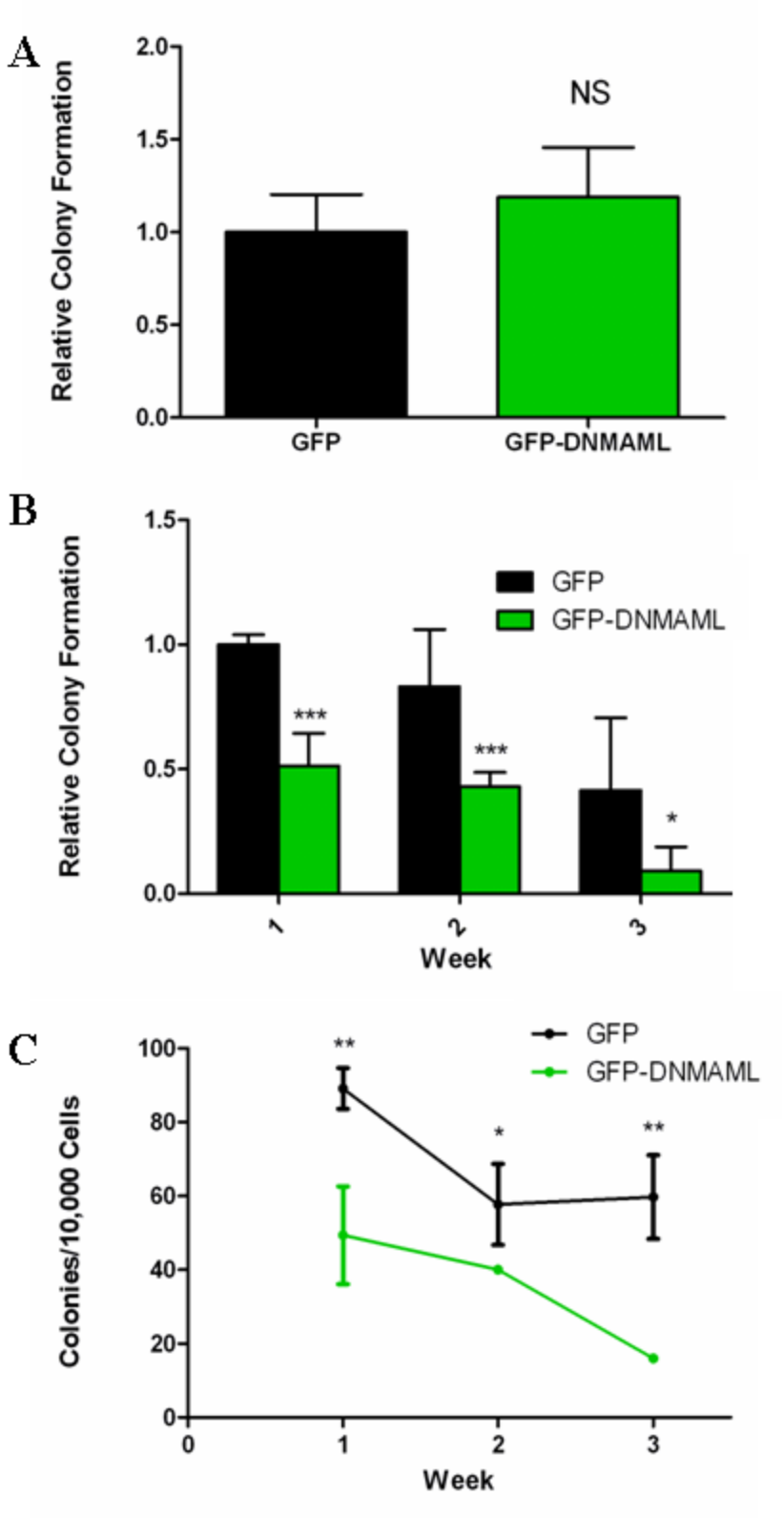
A
Relative Colony Formation
2.0
1.5
1.0
0.5
0.0
NS
GFP
GFP-DNMAML
B
Relative Colony Formation
1.5
1.0
0.5
0.0
GFP
GFP-DNMAML
***
***
*
1
2
3
Week
C
Colonies/10,000 Cells
100
80
60
40
20
0
**
*
**
GFP
GFP-DNMAML
0
1
2
3
Week

Figure 3-10

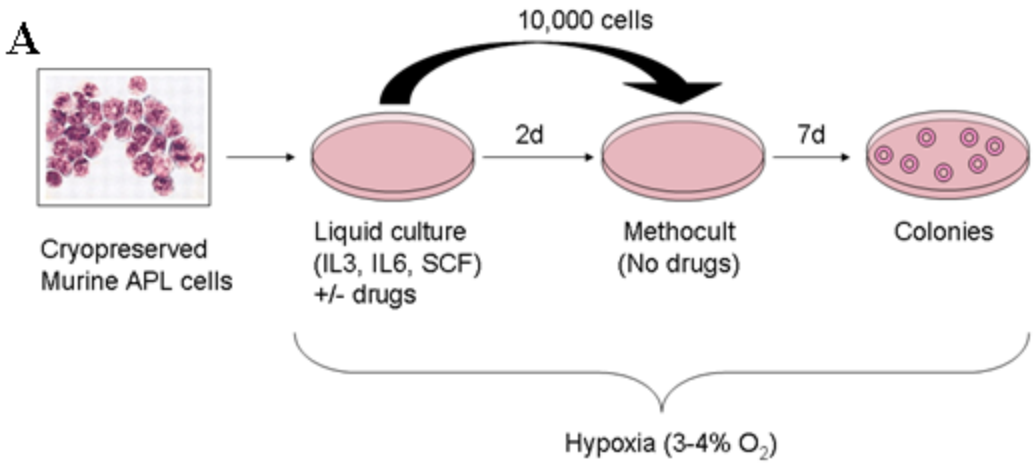

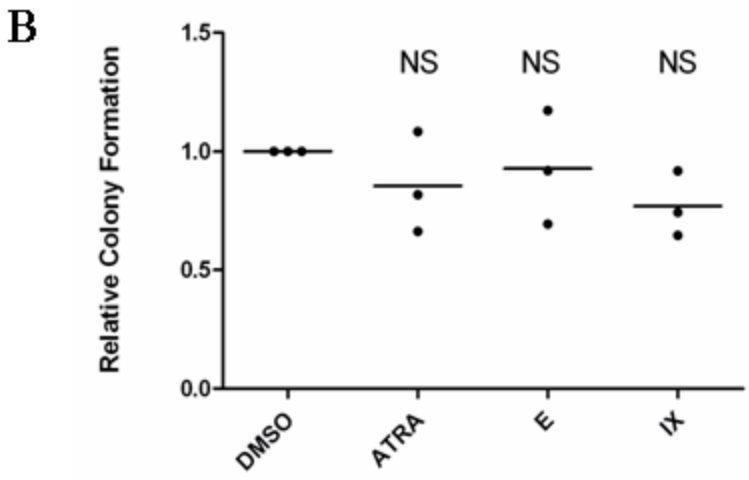

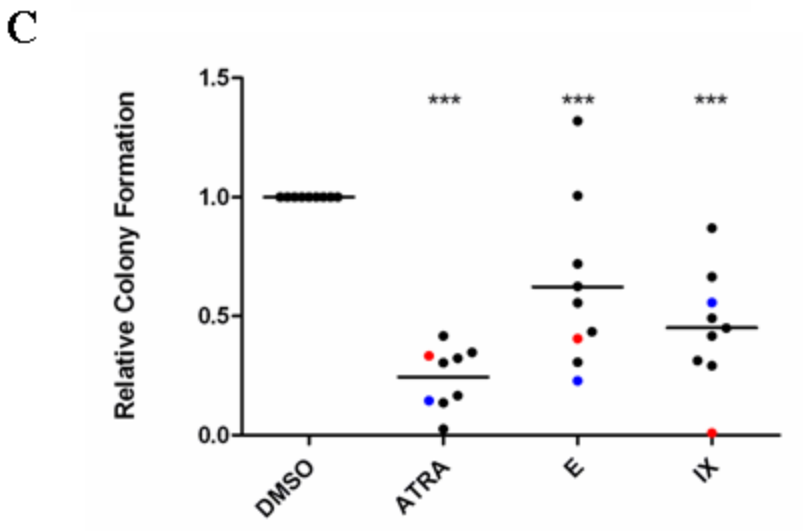

Figure 3-11A-C

D

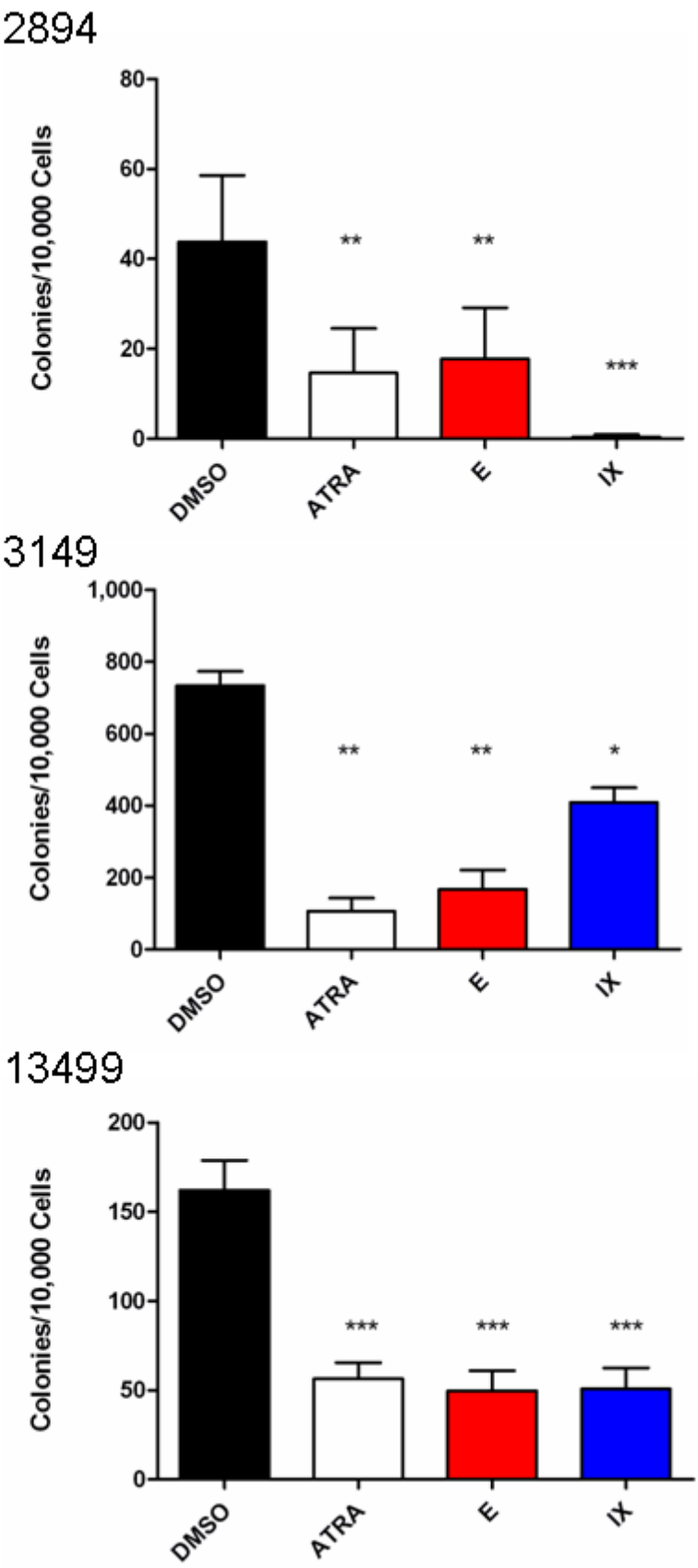

Figure 3-11D

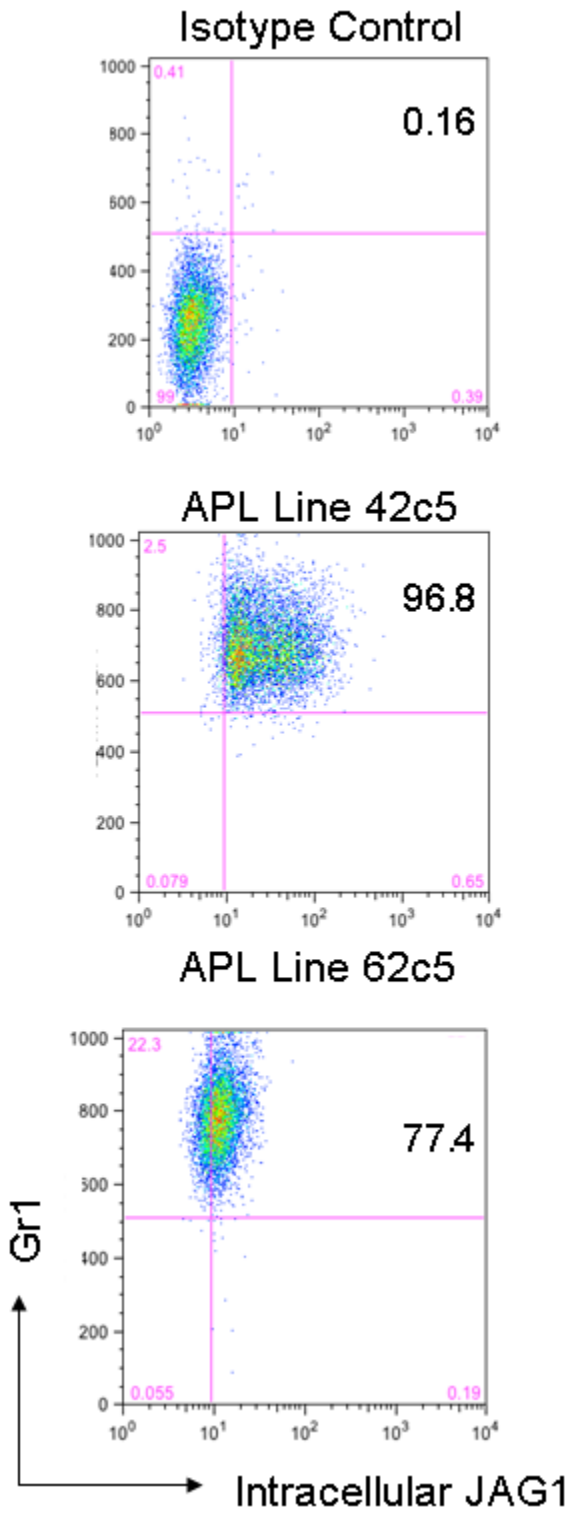
Isotype Control
0.16
0.41
99
0.39
APL Line 42c5
96.8
2.5
0.079
0.65
APL Line 62c5
77.4
22.3
0.055
0.19
Gr1
Intracellular JAG1

Figure 3-12

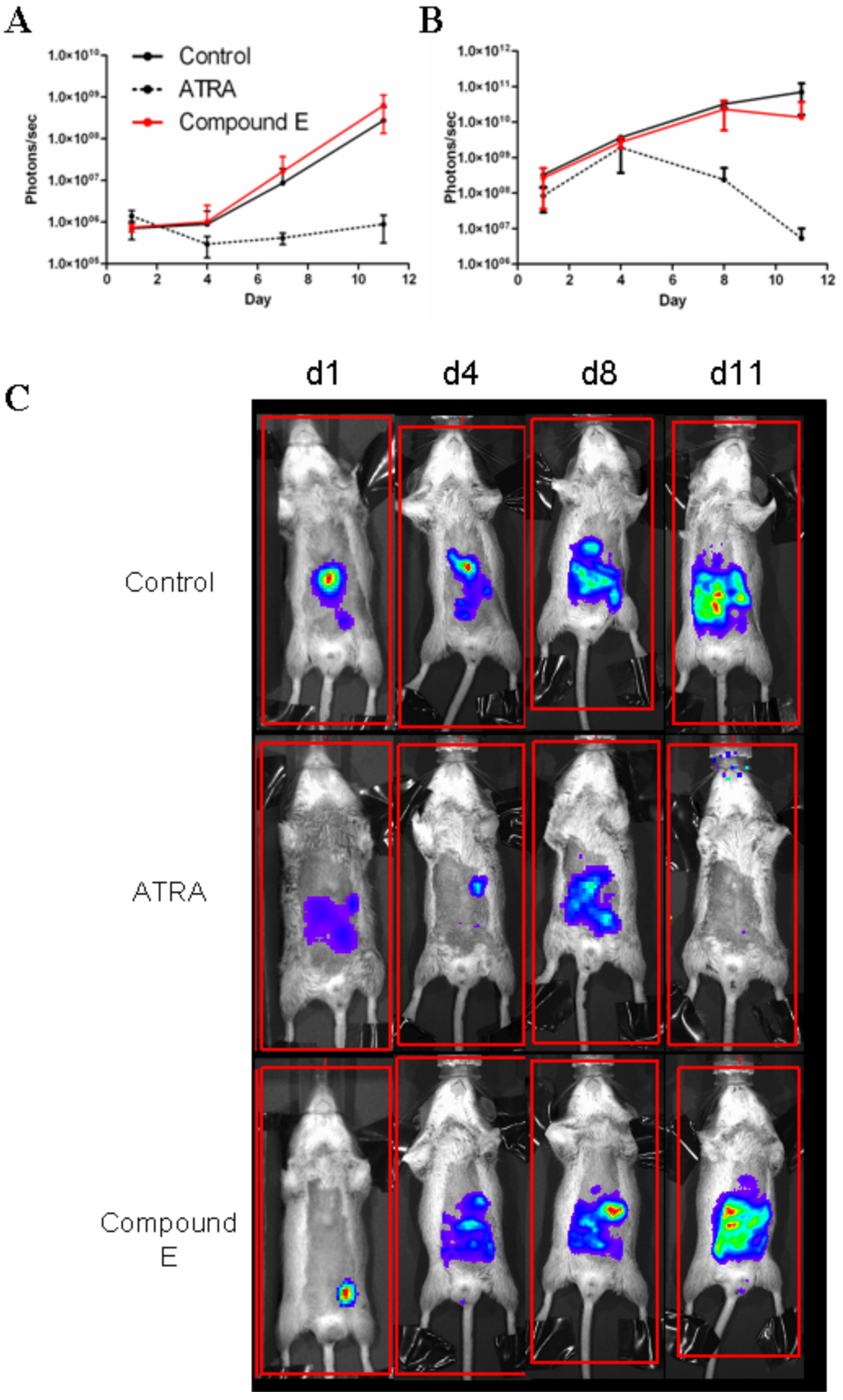
A
B
C
Control
ATRA
Compound E
Photons/sec
Day
d1
d4
d8
d11
Control
ATRA
Compound
E

Figure 3-13

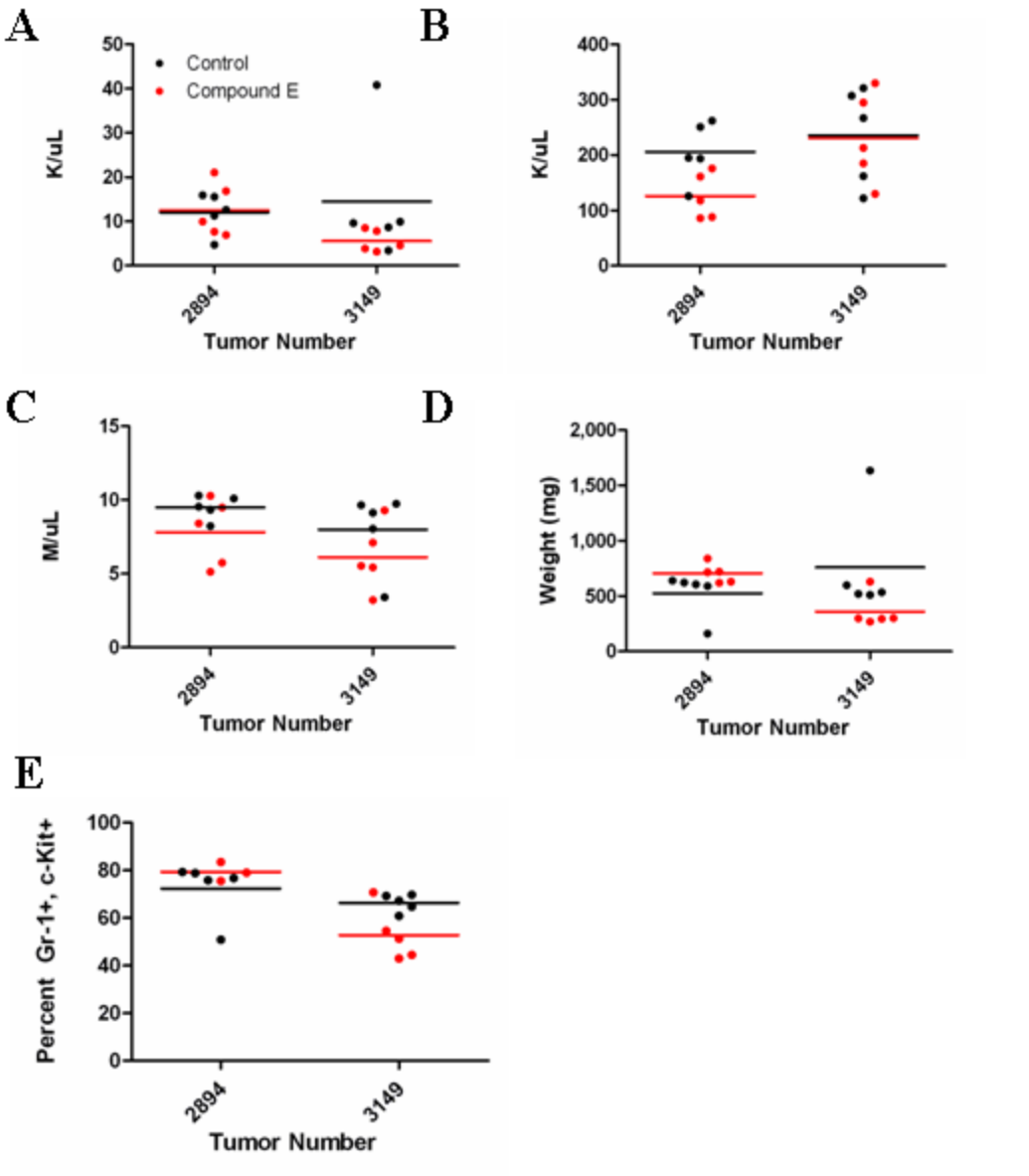
A
B
Control
Compound E
K/uL
Tumor Number
2894
3149
C
D
M/uL
Weight (mg)
E
Percent Gr-1+, c-Kit+
F
Control
GSI
Cleaved Notch1
Actin

Figure 3-14

Chapter 4

Summary and Future Directions

4.1. Summary

In this thesis, we present an analysis of factors involved in the pathogenesis of acute promyelocytic leukemia. In **Chapter 2**, we described a signature of genes with expression specifically altered in APL compared to other subtypes of AML and normal myeloid cells. This signature is not retained in two common cell line models of APL, PR-9 and NB-4 cells, suggesting that the presence of PML-RARA alone is insufficient to produce most of the gene expression changes seen in APL, and that most dysregulome genes are not immediate targets of PML-RARA. In contrast, the APL specific signature is enriched in a murine model of APL, demonstrating that common pathways for APL development exist in humans and mice. In **Chapter 3**, we focused on the Notch ligand JAG1, an APL signature gene that is expressed in APL cell lines and is also found in murine APL cells. We then showed that activated Notch signaling is found in human APL, APL cell lines and murine APL. We then demonstrated that Notch signaling is required for the serial replating phenotype of hematopoietic progenitor cells derived from young mCG-PR mice, and that most murine APL tumors retain dependence on Notch signaling for growth in vitro. In **Chapter 4**, we will examine the unresolved issues raised by these results, and how future experiments might be designed to further elucidate the role of Notch signaling in APL.

4.2. Regulation of JAG1 in APL

Although *JAG1* expression is induced upon PML-RARA expression in cells lines and abrogated with ATRA treatment, it is not clear how PML-RARA regulates *JAG1*. The proximal JAG1 promoter has an everted repeat (1) and combined direct repeat-PU.1

motif sites that PML-RARA is known to bind (2). However, three independent whole genome chromatin immunoprecipitation studies failed to find evidence of PML-RARA binding in the *JAG1* promoter in either cell lines or primary APL cells (2-4). In addition, cotransfection of a *JAG1* promoter (1.5 kb of upstream sequences) reporter construct with PML-RARA did not result in promoter activation (data not shown). These data suggest that JAG1 is not a direct transcriptional target of PML-RARA. How, then, is JAG1 expression such a reproducible characteristic of PML-RARA expressing cells? Clearly, some intermediary is required. JAG1 is a known target of the Wnt/β–Catenin (5) and TGF-βpathways (6). While PML-RARA is thought to inhibit TGF-β signaling (7), it is known to activate expression of γ–catenin/plakoglobin (8). It is possible that plakoglobin is the unknown intermediary. This hypothesis could be tested via examining whether overexpression of plakoglobin in either myeloid cell lines or primary hematopoetic cells results in increased expression of *JAG1*.

In addition, *JAG1* mRNA translation is repressed by several microRNAs, including mir34a and mir21 (9) in addition to mir335 and mir153 (10). PML-RARA represses several miR genes, though not any associated with JAG1 regulation (11). *JAG1* mRNA has a 3' UTR over 1.5 kb in length. It is possible that PML-RARA represses a microRNA, relieving JAG1 repression. Alternatively, PML-RARA may drive the expression of a microRNA which downregulates a repressor of JAG1 expression. A comprehensive screen of microRNAs with altered expression upon PML-RARA induction in PR-9 cells using microRNA arrays could be employed. First tier candidate mIRs selected for further study would include those with decreased expression upon PML-RARA induction, predicted binding to the JAG1 3'UTR, and either altered

expression in APL or known regulation by PML-RARA. These mIRs would then be validated by cotransfection with luciferase-JAG1 3'UTR reporters. Any mIR that represses the luciferase JAG1 3' UTR reporter would be further confirmed via repeating the experiment using a reporter with a mutated mIR binding site. Second tier mIRs would include those that increase upon PML-RARA induction and repress transcription factors thought to repress JAG1 expression. These candidates would be assessed in a similar manner to tier1 mIRs, except that the 3' UTR assessed in the reporter assay would be a JAG1 repressor.

4.3. Cellular location of JAG1 and the mechanism of signaling

In both cell lines and primary murine APL samples, Jag1 protein exists primarily within an intracellular compartment, since it can be detected by flow cytometry only if cells are fixed and permeabilized. While we cannot formally exclude the possibility that some Jag1 protein below the limit of antibody detection resides on the cell surface, this would be a minor portion compared to the intracellular fraction. If Jag1 is not present on the cell surface, how then is Notch signaling activated? One possible explanation is that autocrine activation of Notch signaling may occur intracellularly, within a membrane compartment shared by Jag1 and Notch. While Notch signals are generally thought to be transmitted from a ligand-bearing cell to an adjacent receptor-expressing cell, autocrine signaling has been reported in primary human eosinophils (12). It is also possible that Jag1 reaches the cell surface, but is immediately encounters receptors and is endocytosed, so that under steady-state conditions, little surface Jag1 is present.

Further studies are needed to distinguish between these mechanisms. Immunoelectron microscopy could demonstrate the specific subcellular localization of Jag1. The question of whether JAG1 reaches the cell surface could be answered by treating of NB-4 cells with pharmacological inhibitors of endocytosis. If Jag1 concentration on the cell surface is kept low by endocytosis, inhibition should result in an increase in surface Jag1, so that it could be detected by surface staining and flow cytometry. Knowledge of the molecular details of Jag1-mediated signaling has clinical ramifications. For example, if Jag1 does not reach the cell surface, then antibodies targeting it are unlikely to be efficacious therapies.

4.4. Consequences of JAG1 overexpression in hematopoietic cells

The consequences of JAG1 overexpression in hematopoietic cells are not yet known. Retroviral mediated expression of *Dll4* result in lymphoproliferation with progression to T cell leukemia/lymphoma in mice (13). There is reason to believe that overexpression of Jagged would result in myeloproliferation or myeloid leukemia, not lymphoid lineage alterations. Secondary Jag1 overexpression results in myeloproliferation in several mouse models, and none of these mice exhibit lymphoproliferation (14-17). In Ikba -/- mice, overexpression of Jag1 in the fetal liver and bone marrow stroma results in myeloproliferation not lymphoid alterations (16). In the Lck-Jag1 KI mouse, Jag1 is overexpressed in the T cell precursors, resulting in loss of thymic epithelial cells without cell autonomous effects on the T cell lineages themselves (14). Transgenic mice expressing activated parathyroid hormone receptor on osteoblasts have increased stem cells due to secondary to PTHR/adenylate cyclase-activated

overexpression of JAG1 on osteoblasts (15, 17). It should be noted that in the Ikba -/- and Pthr transgenic animals, the Notch ligand is expressed on a stromal cell, not the hematopoietic cell, and in the Lck-Jag1 mice, the cells affected by Jag1 overexpression are stromal cells.

Because Jag1 overexpression is found in many non-M3 AML cases, understanding its effects have importance for the understanding of AML pathogenesis in general. We have obtained *Dll1* and *Jag1* retroviruses from Raphael Kopan and are currently examining whether transduction with Jag1 results in serial replating of wildtype marrow progenitors or the development of leukemia/MPD after transplantation into syngeneic hosts. In addition, it is possible that Jag1 may cooperate with PML-RARA, and that Jag1 overexpression in the context of PML-RARA expression may result in a different phenotype than Jag1 overexpression alone. Repeating the experiments described above with marrow from mCG-PR mice will allow us to answer these questions. Finally, the target genes of Jag1-mediated Notch signaling in hematopoetic stem and progenitor cells are currently unknown. In contrast, the target genes of Dll1 mediated Notch signaling in KLS cells are known from experiments in which KLS cells were grown on OP9 stroma expressing either Dll1 or GFP control (18). Evidence suggests that different Notch ligands have differing biologic activities, and that activation of Notch signaling by different ligands may result in differential activation of target genes (19, 20). We plan to repeat these experiments using OP9-Jag1 cells to determine the gene expression changes activated by Jag1-mediated Notch signaling in hematopoietic precursor cells, and to learn whether they are different than those induced by Dll1.

A transgenic mouse could also be developed to model the role of Jag1 in AML; for example, Jag1 could be expressed under the control of cathepsin G regulatory sequences (21). It is possible that these animals would have a different phenotype than that observed with retroviral overexpression of Jag1. In addition to characterizing the hematopoietic phenotype of Jag1 overexpression by itself, hCG-Jag1 mice could be useful in examining the broader role of Jag1 in AML pathogenesis. The marrow from these animals could be transduced with other AML-associated oncogenes such as FLT3-ITD, DNMT3A, IDH1, and/or NPMc to examine possible cooperation between Jag1 and other AML associated oncogenes. Since increased JAG1 expression is found in non-M3 AML, particularly those with FLT3 mutations (22, 23), these mice could provide insights into the role of Notch signaling in AML.

4.5. *In vivo* targeting of Notch signaling in APL

As described in **Chapter 3, we** were unable to achieve inhibition of Notch signaling in vivo using a standing dosing protocol (24). Therefore, we do not yet know whether Notch inhibition will reduce tumor growth in this setting, something that is important to know for clinical translation. Why were we unable to achieve inhibition of Notch cleavage? There are several possible reasons. Compound E is hydrophobic, and has been reported to have poor absorption when delivered intraperitoneally (25). Milano et al reported that increased doses resulted in a less than proportional increase in plasma concentration. In addition, the IC50 doses for compound E and other GSI used in vivo are commonly reported as the dose necessary to reduce serum Aβ40, a cleavage product of amyloid precursor protein (APP) by 50%. There is evidence that gamma secretase

cleavage of Notch is less susceptible to GSI mediated inhibition in vitro, requiring higher doses to achieve the same decrease in cleave as APP (26), and this may be true in vivo as well.

It may be possible to alter our current dose or delivery method of compound E to produce Notch inhibition in vivo. There are several aspects of our system that could be altered besides simply increasing the dose. For example, compound E can be given by oral gavage and is effective against breast cancer xenografts in nude mice when administered in this manner (Loren Michel, personal communication). Furthermore, we dissolved compound E in a 1:1 mix of PBS and propylene glycol, while other groups have used 0.5% (w/v) hydroxypropyl methylcellulose and 0.1% (w/v) Tween 80 in water or 6% (v/v) ethanol/94% (v/v) Labrafil M 1944 CS (25). Labrafil M 1944 CS is an emulsifier known to increase bioavailability. It is possible that the differences in the diluent used altered the absorption of the drug, and that a different method of dissolving compound E would yield improved results. To test these approaches, wildtype mice would be dosed daily for 2 weeks, and assessed for signs of Notch inhibition, including development of GI toxicity and reduction in the CD4/CD8 double positive thymocyte population (27). Upon finding a dose and delivery system that produces consistent Notch inhibition, the in vivo experiments described in **Chapter 3** could be repeated.

In addition, there are other pharmacological means to inhibit Notch signaling which have been used in *in vivo* mouse models, including the GSI compound IX (28), the experimental GSI MRK003 (29), MK0752, a GSI produced by Merck that is currently in phase I clinical trials (30), and stapled peptide inhibitors of the Notch/Csl/Maml complex (31). It is possible that these drugs may prove superior to compound E; they could be

tested as described above. Finally, we are currently determining whether APL cells treated with GSIs *ex vivo* are still capable of inducing disease in secondary recipients. While these experiments still do not directly address the question of whether Notch inhibition has clinical efficacy in vivo, they will serve as a useful proof of principle as well as helping to determine if GSI treatment reduces the leukemia initiating cell (LIC) population.

4.6. Leukemia development in PML-RARA knockin x transgenic Notch Reporter mice.

The true extent of Notch signaling in leukemic and preleukemic mCG-PR mice cannot be ascertained using currently available methodology. Measurement of Notch signaling by flow cytometry detects only Notch-1 signaling due to limitations in available antibodies. Some of the murine APLs have little detectable cleaved Notch-1, yet respond to GSIs. Transgenic Notch Reporter (TNR) mice have a GFP transgene under the control of 4 tandem copies of the Notch/CSL consensus site, so GFP expression is known to be a faithful reporter of Notch signaling (32). Furthermore, the GFP expression in TNR mice integrates signals from all four Notch receptors, and will allow for a more accurate readout of the presence of Notch signaling. Do the TNR+PR+ mice develop leukemia, and if so, are their tumors inevitably GFP+, indicating active Notch signaling? How does the number of GFP+ cells in the marrow and spleen change over time as mice progress from a preleukemic state to frank leukemia? The establishment of a tumor watch using TNRxPR mice and collection of resulting APL tumors will allow for these questions to be answered. This reagent will allow us to determine at what point in leukemogenesis

Notch signaling is most active. In addition, TNR+/PR+ tumors could be a valuable tool for screening drugs and drug dosages that inhibit Notch signaling in vivo, since GFP expression would be a convenient read out of efficacy.

One potential caveat is that the TNR mice are currently on a mixed B6/SJL background. SJL mice are considered to be a tumor-prone strain; they develop AML after radiation exposure (33), and lymphoma after ENU exposure (34). Without exposure to carcinogenic agents, SJL mice develop a B cell lymphoma resembling Hodgkin's lymphoma with 90% penetrance by 1 year of age (35), and 40% of B6/SJL F2 animals retain this phenotype (36). It is possible that strain related B cell neoplasms will complicate our analysis of APL in TNR+PR+ mice, and any tumors resulting in these animals will have to be carefully screened for myeloid lineage markers and PML-RARA expression. If our analysis of APL is hampered by lymphoma development, we could backcross the TNR mice to the B6 strain and repeat the TNRxPR cross.

4.7. The requirement for Notch signaling in leukemia development

Are Jag1 expression and Notch signaling required for leukemogenesis in mCG-PR mice? These questions are addressable using knockout and conditional knockout mice that have already been reported in the literature. Because of the complexity of the Notch pathway (4 receptors and 5 ligands), fully dissecting the requirement for Jag1 and Notch signaling in leukemogenesis would necessitate breeding our mCG-PR mice with animals carrying multiple other targeted mutations.

Mice with conditional alleles of Jag1 (37) and CSL (38) are available, as are mice with a conditional DNMAML transgene (38). Jag1 conditional knockout mice have no

detectable hematopoietic phenotype (37), while Csl conditional knockout and conditional DNMAML expression (both of which inhibit all Notch signaling) results in phenotypes in the lymphoid lineages only (38). These mice could be intercrossed with mCG-PR mice and Mx-Cre animals (39) to generate $mCG^{PR/+}Jag1^{f/f}$Mx-Cre, $mCG^{PR/+}Csl^{f/f}$Mx-Cre and $mCG^{PR/+}DNMAML^{f/f}$Mx-Cre, and the corresponding controls that have either 1 or no floxed alleles. Young animals would be treated with pIpC to induce Cre-mediated excision, and the mice would be followed for the development of leukemia. If Jag1 or Notch signaling are necessary for leukemogenesis, we would expect to see decreased penetrance or increased latency in the conditional knockout mice. It would be particularly interesting to see whether there is a unique requirement for Jag1, or if it has redundant functions with the other Notch ligands in the setting of PML-RARA-mediated leukemogenesis. In the second scenario, conditional loss of Jag1 would have no effect on the development of APL, but CSL loss or DNMAML expression (both of which would block all Notch signaling) would result in impaired leukemogenesis. Any leukemias resulting from conditional ablation of Jag1 or Notch signaling would then be fully characterized using lineage marker analysis, secondary transplantation, and gene expression profiling, with results compared to tumors derived from mCG-PR controls.

These mice could also be used to investigate the requirement for Jag1 and Notch signaling in early stages of leukemia development. Marrow from pIpC treated $mCG^{PR/+}Jag1^{f/f}$Mx-Cre, $mCG^{PR/+}Csl^{f/f}$Mx-Cre and $mCG^{PR/+}DNMAML^{f/f}$Mx-Cre mice or untreated controls would be subjected to the serial replating assay as described in **Chapter 3**. We would expect that conditional loss of Csl or expression of DNMAML would result in loss of serial replating. If conditional loss of Jag1 abrogated replating,

those results would indicate that Jag1 is non-redundantly required for the replating phenotype of mCG-PR progenitor cells. However, if conditional Jag1 knockout mCG-PR marrow replates, this would indicate that other Notch ligands may have redundant functions with Jag1.

In addition, the marrow from the conditional knockout animals could be used for competitive repopulation experiments. While inhibition of Notch signaling decreases colony formation and serial replating *in vitro*, the role of Notch signaling in the early events of leukemogenesis *in vivo* is not known. In competitive repopulation assays with wildtype marrow, expansion of mCG-PR cells was observed not just in the Gr-1^{+} myeloid cells, but also in the $CD19^{+}$ and $CD3^{+}$ lymphoid lineage cells (John Welch and Timothy Ley, unpublished observation). Collectively, these results suggest that PML-RARA acts in a multipotent progenitor cell to increase self renewal, and partially block myeloid differentiation. To determine whether Jag1 and Notch signaling are necessary for competitive expansion *in vivo*, marrow from pIpC treated $mCG^{PR/+}Jag1^{f/f}$Mx-Cre, $mCG^{PR/+}Csl^{f/f}$Mx-Cre and $mCG^{PR/+}DNMAML^{f/f}$Mx-Cre mice (or controls with 1 or no floxed alleles) would be transplanted into lethally irradiated syngeneic CD45.1/45.2 hosts with WT CD45.1 competitor marrow at WT:PR ratios of 1:9, 1:1, and 9:1. Expansion would be followed by flow cytometry of CD45.2+Gr-1+ and CD45.2+CD19+ cells. Note that CD3+ T cells cannot be used to follow expansion, because the presence of DNMAML by itself results in the loss of T cells.

These experiments would be very time and labor intensive. A shorter approach would be to utilize haploinsufficent Jag1 and CSL animals, which are viable and fertile (40,41), to generate $mCG^{PR/+}Jag1^{+/-}$ and $mCG^{PR/+}CSL^{+/-}$ animals, and determine whether

a reduction in gene dosage affects the penetrance of leukemia, serial replating or competitive repopulation. This approach should be performed in parallel with the conditional knockouts, since it is possible that a phenotype exists only with loss of both Jag1 or Csl alleles.

Finally, in the short term, the requirement for Notch signaling in vivo could be tested via use of the DNMAML-GFP retrovirus (42), concurrent with breeding mCG-PR mice to the conditional knockouts. Marrow from mCG-PR animals would be transduced with DNMAML-GFP or GFP control, and GFP+ cells would be transplanted into recipient animals; we would determine whether DNMAML expression reduces penetrance or extends APL latency, compared to GFP controls. It is possible that the retroviral construct could undergo silencing, allowing Notch signaling to resume. Measurement of GFP expression by flow cytometry would allow us to determine whether leukemias arising in DNMAML-GFP/PR animals are derived from cells that developed alternate pathways to compensate for inhibited Notch signaling (GFP+ tumors), or from cells in which DNMAML-GFP was silenced (GFP-), allowing for re-activation of the normal Notch-mediated pathway. In addition, to determine whether Notch signaling is necessary for competitive expansion *in vivo*, competitive repopulation experiments with DNMAML-GFP or GFP-transduced mCG-PR marrow could be performed as described above, except that expansion would be followed GFP expression instead of CD45.2.

4.8. Roles of Notch1 versus Notch2 in leukemogenesis

If Notch signaling is necessary for leukemogenesis, which specific Notch genes are necessary? Both human and murine APL cells express Notch1 and Notch2 (with little

or no expression of Notch3 and Notch4) but it is not known whether there is a unique requirement for Notch1 or Notch2. This question has important clinical ramifications. Inhibition of signaling by both Notch1 and Notch2 results in gastrointestinal toxicity in mice, causing significant mortality (43, 44). However, inhibiting only Notch1 in T-ALL models spares the GI tract while preserving anti-leukemic effects (44). Notch subtype antibodies are currently in development, and the stapled peptide inhibitor reported by Moellering et al appears to be specific for the Notch1/CSL/MAML complex without affecting Notch2/CSL/MAML (31). Knowing whether Notch1 or Notch2 are most important for APL pathogenesis could guide drug development and influence the design of clinical trials. Conditional alleles of Notch1 and Notch2 are available (37, 45), as are haploinsufficient animals (46, 47). These could be crossed with mCG-PR mice and analyzed for development of leukemia, serial replating, and competitive repopulation, as described above.

It is possible that neither Notch1 nor Notch2 alone are sufficient for leukemogenesis, and acquisition of leukemia will be unaffected by conditional loss of either Notch1 or Notch2. In this case, we could investigate the outcome when both Notch1 and Notch2 are deleted. Notch2 haploinsufficient mice are viable and fertile but Notch2 null animals die during the perinatal period (48). It would be possible to generate mCG-PR$^{+/-}$Notch2$^{-/-}$Notch1$^{f/f}$ animals and harvest marrow from neonatal pups. Marrow from these mice could be transduced with Cre-expressing retrovirus or adenovirus ex vivo, and transplanted into recipient animals to determine whether loss of both Notch1 and Notch2 affects leukemia development or competitive repopulation.

4.9. Target genes of Notch signaling in APL and their roles in leukemogenesis

The transcriptional target genes of Notch are highly dependent upon the cellular context. Indeed, one study found significant differences between the genes activated by Notch signaling in embryonic stem cells, ectoderm, and mesoderm (49). The targets of Notch1 in T-ALL include genes such as cold shock domain protein A (CSDA), c-myc, cyclin D2 and Taspase-1 (50). While these genes are overexpressed in APL compared to normal promyelocytes, it is not known whether they are directly activated by Notch signaling. Identification of Notch target genes in APL would help to identify the mechanism of Notch signaling in leukemogenesis. ChIP grade antibodies against Notch1 and Notch2 are available (50, 51) and ChIP on chip studies could be performed in order to define the promoters that are bound by Notch1 and Notch2. Correlation of ChIP results with gene expression profiles of APL cells and normal promyelocytes would then be used to filter genes without detectable changes in gene expression resulting from intracellular Notch binding. Notch binding to the promoters of candidate target genes would then be validated by ChIP-QPCR. These experiments would be useful for determining the mechanism(s) by which Notch signaling promotes the growth and survival of APL cells, and how it compares to the mechanism of Notch signaling in other malignancies.

Several putative target genes of Notch are currently being investigated. The role of cold shock domain proteins (including *Ybx1* and *CSDA/Msy4*) in leukemogenesis is currently under active investigation in the Ley laboratory. Myc and Taspase-1 haploinsufficient mice have been generated by other groups (52, 53) and could potentially be intercrossed with mCG-PR animals to assess their roles in APL. Assuming

that these genes are in fact targets of Notch signaling in APL, these studies would shed further light on the downstream effectors of Notch signaling and their roles in leukemogenesis.

4.10. Roles of other Notch pathway components in leukemogenesis

In **Chapter 3**, we demonstrated that expression of several other components of the Notch pathway besides JAG1 are altered in APL. These include the fringe family glycosylase lunatic fringe (*LFNG*), which is repressed in APL, and Mindbomb-1 (*MIB1*) and Mastermindlike-3 (*MAML3*), which have increased expression in APL. The role of these genes in leukemogenesis is not known, nor is it understood how they interact with JAG1 overexpression in APL. It is possible that any MPD or leukemia resulting from Jag1 overexpression requires cooperation with other Notch pathway members.

PML-RARA downregulates the fringe family glycosylase lunatic fringe (*LFNG*) (54). Fringe modified Notch receptors preferentially bind delta-like family ligands at the expense of Jagged ligands (55). Therefore, downregulation of *LFNG* would be expected to increase JAG1 mediated signaling. The role of *LFNG* in leukemogenesis has not yet been investigated. *LFNG* null mice have been generated and while there is some embryonic lethality, some mice do survive to adulthood (56, 57). LFNG null mice could be crossed with mCG-PR mice to generate $mCG^{PR/+}Lfng^{+/-}$ and $mCG^{PR/+}Lfng^{-/-}$ animals. We predict that due to increased Jag1 mediated signaling, Lfng loss would cooperate with PML-RARA, and that $mCG^{PR/+}Lfng^{+/-}$ and $mCG^{PR/+}Lfng^{-/-}$ mice will have shorter latencies than $mCG^{PR/+}Lfng^{+/+}$ controls. In addition, we hypothesize that $Lfng^{+/-}$ and

Lfng$^{-/-}$ marrow would be more susceptible to the effects of Jag1 overexpression than wildtype marrow.

MIB1 and *MAML3* are overexpressed in human APL samples compared to normal promyelocytes. The effect of overexpression of these genes in hematopoietic cells has not yet been reported. This could be investigated by creating MSCV-MIB1 and MSCV-MAML3 retroviruses to transduce WT marrow. MIB1 and MAML3 transduced marrow would be assessed for increased colony formation, acquisition of replating, and ability to cause leukemia after transplantation. In addition, possible cooperation of MIB1 and MAML3 with PML-RARA would be investigated by repeating the above experiments using marrow from mCG-PR mice. Finally, cooperation of MIB1 and MAML3 with Jag1 could be assessed using three different approaches. The Ley laboratory is currently generating MSCV-based retroviruses that express mCherry or YFP in place of the typical Ires-EGFP marker, and these additional markers would be critical for implementation of these experiments. Wildtype marrow would be co-transduced with Jag1-Ires-GFP and either Mib1-Ires-mCherry or Maml3-Ires-mCherry, and GFP+mCherry- and GFP+mCherry+ cells sorted and transplanted into secondary recipients. If there is cooperation between Jag1 and either Mib1 or Maml3, the double positive marrow would be expected to have accelerated disease progression or a more severe disease phenotype (for example, AML instead of a non-transplantable MPD) than marrow transduced with Jag1 alone. In the second approach, marrow from hCG-Jag1 animals would be transduced with Mib1, Maml3 or vector control, transplanted into secondary hosts and followed for leukemia development, with similar results to the co-transduction experiments described above. In the third approach, conditional Mib1 and Maml3

animals could be crossed with Mx-Cre and hCG-Jag1 mice to generate hCG-Jag1, Mx-Cre, Mib1$^{f/f}$ and hCG-Jag1, Mx-Cre, Maml3$^{f/f}$ mice. Mib1 conditional knockout animals have previously been reported (58), but Maml3 conditional knockout mice would have to be generated using gene targeting and homologous recombination. After pIpC-induced Cre-mediated excision, the mice would be followed to determine if Mib1 or Maml3 loss alters the hematopoietic phenotype of hCG-Jag1 mice.

4.11. Final remarks

In conclusion, we have described a set of genes whose expression is specifically altered in APL and demonstrated a previously unappreciated role for Notch signaling in the development of APL. These results underscore the complexity involved in leukemogenesis. Oncogenes may have indirect effects that are nonetheless important in disease development. Overexpression of JAG1 and activation of Notch signaling are indirect consequences of PML-RARA expression, yet they appear to have an important role in leukemogenesis. In addition, pathways may be necessary for early events in tumorigenesis, but dispensible for later stages. Notch signaling was necessary for serial replating in every young mCG-PR animal tested, yet not all fully transformed tumors retain dependence on Notch signaling. While our results have clinical relevance for the treatment of relapsed or refractory APL, it is clear that there is still much to learn about the role of Notch signaling in myeloid leukemogenesis.

4.12. References

1. Meani N, Minardi S, Licciulli S, et al. Molecular signature of retinoic acid treatment in acute promyelocytic leukemia. *Oncogene*. 2005;24:3358-3368.

2. Wang K, Wang P, Shi J, et al. PML/RARalpha targets promoter regions containing PU.1 consensus and RARE half sites in acute promyelocytic leukemia. *Cancer cell*. 2010;17(2):186-97.

3. Martens JH, Brinkman AB, Simmer F, et al. PML-RARalpha/RXR Alters the Epigenetic Landscape in Acute Promyelocytic Leukemia. *Cancer cell*. 2010;17(2):173-85.

4. Hoemme C, Peerzada A, Behre G, et al. Chromatin modifications induced by PML-RARalpha repress critical targets in leukemogenesis as analyzed by ChIP-Chip. *Blood*. 2008;111(5):2887-95.

5. Estrach S, Ambler CA, Lo Celso C, Hozumi K, Watt FM. Jagged 1 is a beta-catenin target gene required for ectopic hair follicle formation in adult epidermis. *Development (Cambridge, England)*. 2006;133(22):4427-38.

6. Morrissey J, Guo G, Moridaira K, et al. Transforming growth factor-beta induces renal epithelial jagged-1 expression in fibrotic disease. *Journal of the American Society of Nephrology : JASN*. 2002;13(6):1499-508.

7. Lin H, Bergmann S, Pandolfi PP. Cytoplasmic PML function in TGF-beta signalling. *Nature*. 2004;431(7005):205-11.

8. Müller-Tidow C, Steffen B, Cauvet T, et al. Translocation products in acute myeloid leukemia activate the Wnt signaling pathway in hematopoietic cells. *Molecular and cellular biology*. 2004;24(7):2890-904.

9. Hashimi ST, Fulcher JA, Chang MH, et al. MicroRNA profiling identifies miR-34a and miR-21 and their target genes JAG1 and WNT1 in the coordinate regulation of dendritic cell differentiation. *Blood*. 2009;114(2):404-14.

10. Sathyan P, Golden HB, Miranda RC. Competing interactions between micro-RNAs determine neural progenitor survival and proliferation after ethanol exposure: evidence from an ex vivo model of the fetal cerebral cortical neuroepithelium. *The Journal of neuroscience : the official journal of the Society for Neuroscience*. 2007;27(32):8546-57.

11. Saumet A, Vetter G, Bouttier M, et al. Transcriptional repression of microRNA genes by PML-RARA increases expression of key cancer proteins in acute promyelocytic leukemia. *Blood*. 2009;113(2):412-21.

12. Radke AL, Reynolds LE, Melo RC, et al. Mature human eosinophils express functional Notch ligands mediating eosinophil autocrine regulation. *Blood*. 2009;113(13):3092-101.

13. Yan XQ, Sarmiento U, Sun Y, et al. A novel Notch ligand, Dll4, induces T-cell leukemia/lymphoma when overexpressed in mice by retroviral-mediated gene transfer. *Blood*. 2001;98(13):3793-9.

14. Beverly LJ, Ascano JM, Capobianco AJ. Expression of JAGGED1 in T-lymphocytes results in thymic involution by inducing apoptosis of thymic stromal epithelial cells. *Genes and immunity*. 2006;7(6):476-86.

15. Calvi LM, Adams GB, Weibrecht KW, et al. Osteoblastic cells regulate the haematopoietic stem cell niche. *Nature*. 2003;425(6960):841-6.

16. Rupec RA, Jundt F, Rebholz B, et al. Stroma-mediated dysregulation of myelopoiesis in mice lacking I kappa B alpha. *Immunity*. 2005;22(4):479-91.

17. Weber JM, Forsythe SR, Christianson CA, et al. Parathyroid hormone stimulates expression of the Notch ligand Jagged1 in osteoblastic cells. *Bone*. 2006;39(3):485-93.

18. Mercher T, Cornejo MG, Sears C, et al. Notch signaling specifies megakaryocyte development from hematopoietic stem cells. *Cell stem cell*. 2008;3(3):314-26.

19. Choi K, Ahn Y, Gibbons DL, et al. Distinct biological roles for the notch ligands Jagged-1 and Jagged-2. *The Journal of biological chemistry*. 2009;284(26):17766-74.

20. Abe N, Hozumi K, Hirano K, Yagita H, Habu S. Notch ligands transduce different magnitudes of signaling critical for determination of T-cell fate. *European journal of immunology*. 2010.

21. Grisolano JL, Sclar GM, Ley TJ. Early myeloid cell-specific expression of the human cathepsin G gene in transgenic mice. *Proceedings of the National Academy of Sciences of the United States of America*. 1994;91(19):8989-93.

22. Valk PJ, Verhaak RG, Beijen MA, et al. Prognostically useful gene-expression profiles in acute myeloid leukemia. *New England Journal of Medicine*. 2004;350(1617-1628).

23. Verhaak RG, Wouters BJ, Erpelinck CA, et al. Prediction of molecular subtypes in acute myeloid leukemia based on gene expression profiling. *Haematologica*. 2009;94(1):131-4.

24. Yan P, Bero AW, Cirrito JR, et al. Characterizing the appearance and growth of amyloid plaques in APP/PS1 mice. *The Journal of neuroscience : the official journal of the Society for Neuroscience*. 2009;29(34):10706-14.

25. Milano J, McKay J, Dagenais C, et al. Modulation of notch processing by gamma-secretase inhibitors causes intestinal goblet cell metaplasia and induction of genes known to specify gut secretory lineage differentiation. *Toxicological sciences : an official journal of the Society of Toxicology*. 2004;82(1):341-58.

26. Yang T, Arslanova D, Gu Y, Augelli-Szafran C, Xia W. Quantification of gamma-secretase modulation differentiates inhibitor compound selectivity between two substrates Notch and amyloid precursor protein. *Molecular brain*. 2008;1(1):15.

27. Real PJ, Tosello V, Palomero T, et al. γ-secretase inhibitors reverse glucocorticoid resistance in T cell acute lymphoblastic leukemia. *Nature Medicine*. 2008;15(1):50-58.

28. Yustein JT, Liu YC, Gao P, et al. Induction of ectopic Myc target gene JAG2 augments hypoxic growth and tumorigenesis in a human B-cell model. *Proceedings of the National Academy of Sciences, USA*. 2010;107(8):3534-3539.

29. Cullion K, Draheim KM, Hermance N, et al. Targeting the Notch1 and mTOR pathways in a mouse T-ALL model. *Blood*. 2009;113(24):6172-81.

30. Deangelo DJ, Stone RM, Silverman LB, et al. A phase I clinical trial of the notch inhibitor MK-0752 in patients with T-cell acute lymphoblastic leukemia/lymphoma (T-ALL) and other leukemias. *Journal of Clincal Oncology*. 2006;24(18S):6585.

31. Moellering RE, Cornejo M, Davis TN, et al. Direct inhibition of the NOTCH transcription factor complex. *Nature*. 2009;462(7270):182-8.

32. Duncan AW, Rattis FM, DiMascio LN, et al. Integration of Notch and Wnt signaling in hematopoietic stem cell maintenance. *Nature immunology*. 2005;6(3):314-22.

33. Resnitzky P, Estrov Z, Haran-Ghera N. High incidence of acute myeloid leukemia in SJL/J mice after X-irradiation and corticosteroids. *Leukemia research*. 1985;9(12):1519-28.

34. Fenske TS, McMahon C, Edwin D, et al. Identification of candidate alkylator-induced cancer susceptibility genes by whole genome scanning in mice. *Cancer research*. 2006;66(10):5029-38.

35. Kumar RK. Hodgkin's disease. SJL/J murine lymphoma. *The American journal of pathology*. 1983;110(3):393-6.

36. Harris AW, Pinkert CA, Crawford M, et al. The E mu-myc transgenic mouse. A model for high-incidence spontaneous lymphoma and leukemia of early B cells. *The Journal of experimental medicine*. 1988;167(2):353-71.

37. Mancini SJ, Mantei N, Dumortier A, et al. Jagged1-dependent Notch signaling is dispensable for hematopoietic stem cell self-renewal and differentiation. *Blood*. 2005;105(6):2340-2.

38. Maillard I, Koch U, Dumortier A, et al. Canonical notch signaling is dispensable for the maintenance of adult hematopoietic stem cells. *Cell stem cell*. 2008;2(4):356-66.

39. Kühn R, Schwenk F, Aguet M, Rajewsky K. Inducible gene targeting in mice. *Science (New York, N.Y.)*. 1995;269(5229):1427-9.

40. Xue Y, Gao X, Lindsell CE, et al. Embryonic lethality and vascular defects in mice lacking the Notch ligand Jagged1. *Human molecular genetics*. 1999;8(5):723-30.

41. Oka C, Nakano T, Wakeham A, et al. Disruption of the mouse RBP-J kappa gene results in early embryonic death. *Development (Cambridge, England)*. 1995;121(10):3291-301.

42. Weng AP, Nam Y, Wolfe MS, et al. Growth suppression of pre-T acute lymphoblastic leukemia cells by inhibition of notch signaling. *Molecular and cellular biology*. 2003;23(2):655-64.

43. Riccio O, van Gijn ME, Bezdek AC, et al. Loss of intestinal crypt progenitor cells owing to inactivation of both Notch1 and Notch2 is accompanied by derepression of CDK inhibitors p27Kip1 and p57Kip2. *EMBO reports*. 2008;9(4):377-83.

44. Wu Y, Cain-Hom C, Choy L, et al. Therapeutic antibody targeting of individual Notch receptors. *Nature*. 2010;464(7291):1052-1057.

45. Saito T, Chiba S, Hirai H. Notch2 deficient bone marrow cells can reconstitute both to lymphoid and myeloid lineages. *Blood*. 2001;98:68a.

46. Krebs LT, Xue Y, Norton CR, et al. Notch signaling is essential for vascular morphogenesis in mice. *Genes & development*. 2000;14(11):1343-52.

47. McCright B, Lozier J, Gridley T. Generation of new Notch2 mutant alleles. *Genesis (New York, N.Y. : 2000)*. 2006;44(1):29-33.

48. McCright B, Gao X, Shen L, et al. Defects in development of the kidney, heart and eye vasculature in mice homozygous for a hypomorphic Notch2 mutation. *Development (Cambridge, England)*. 2001;128(4):491-502.

49. Meier-Stiegen F, Schwanbeck R, Bernoth K, et al. Activated Notch1 target genes during embryonic cell differentiation depend on the cellular context and include lineage determinants and inhibitors. *PloS one*. 2010;5(7):e11481.

50. Palomero T, Lim WK, Odom DT, et al. NOTCH1 directly regulates c-MYC and activates a feed-forward-loop transcriptional network promoting leukemic cell growth. *Proceedings of the National Academy of Sciences of the United States of America*. 2006;103(48):18261-6.

51. Mazur PK, Einwachter H, Lee M, et al. Notch2 is required for progression of pancreatic intraepithelial neoplasia and development of pancreatic ductal adenocarcinoma. *Proceedings of the National Academy of Sciences*. 2010;107(30):13438-43.

52. Hsieh JJ, Cheng EH, Korsmeyer SJ. Taspase1: a threonine aspartase required for cleavage of MLL and proper HOX gene expression. *Cell*. 2003;115(3):293-303.

53. Trumpp A, Refaeli Y, Oskarsson T, et al. c-Myc regulates mammalian body size by controlling cell number but not cell size. *Nature*. 2001;414(6865):768-73.

54. Alcalay M, Meani N, Gelmetti V, et al. Acute myeloid leukemia fusion proteins deregulate genes involved in stem cell maintenance and DNA repair. *The Journal of clinical investigation*. 2003;112(11):1751-61.

55. Visan I, Tan JB, Yuan JS, et al. Regulation of T lymphopoiesis by Notch1 and Lunatic fringe-mediated competition for intrathymic niches. *Nature immunology*. 2006;7(6):634-43.

56. Zhang N, Gridley T. Defects in somite formation in lunatic fringe-deficient mice. *Nature*. 1998;394(6691):374-7.

57. Xu J, Norton CR, Gridley T. Not all lunatic fringe null female mice are infertile. *Development (Cambridge, England)*. 2006;133(4):579; author reply 579-80.

58. Kim Y, Koo B, Jeong H, et al. Defective Notch activation in microenvironment leads to myeloproliferative disease. *Blood*. 2008;112(12):4628-38.